

**N-Heterocyclic Carbene and its Derivative “Zwitterion” Supported  
Magnesium and Zinc Complexes: Synthesis, Characterization,  
Reactivity Studies and Catalytic Applications**

*By*

**ASHIM BAISHYA**

**CHEM11201004012**

**National Institute of Science Education and Research (NISER), Bhubaneswar**

*A thesis submitted to the*

*Board of Studies in Chemical Sciences*

*In partial fulfillment of requirements*

*for the Degree of*

**DOCTOR OF PHILOSOPHY**

*of*

**HOMI BHABHA NATIONAL INSTITUTE**



**November, 2016**

---

## **STATEMENT BY AUTHOR**

This dissertation has been submitted in partial fulfillment of requirements for an advanced degree at Homi Bhabha National Institute (HBNI) and is deposited in the Library to be made available to borrowers under rules of the HBNI.

Brief quotations from this dissertation are allowable without special permission, provided that accurate acknowledgement of source is made. Requests for permission for extended quotation from or reproduction of this manuscript in whole or in part may be granted by the Competent Authority of HBNI when in his or her judgment the proposed use of the material is in the interests of scholarship. In all other instances, however, permission must be obtained from the author.

Ashim Baishya

## **DECLARATION**

I, hereby declare that the investigation presented in the thesis has been carried out by me. The work is original and has not been submitted earlier as a whole or in part for a degree / diploma at this or any other Institution / University.

Ashim Baishya

## List of Publications arising from the thesis

### Journal

1. “Structure, bonding and energetics of N-heterocyclic carbene (NHC) stabilized low oxidation state Group 2 (Be, Mg, Ca, Sr and Ba) metal complexes: A theoretical study”, **Ashim Baishya**, V Rao Mundlapati, Sharanappa Nembenna\* and Himansu S Biswal\*, *J. Chem. Sci.*, **2014**, *126*, 6, 1781-1788.
2. “Catalytic C–N bond formation in guanylation reaction by N-heterocyclic carbene supported magnesium(II) and zinc(II) amide complexes”, **Ashim Baishya**, Milan Kr. Barman, Thota Peddarao, Sharanappa Nembenna\*, *J. Organomet. Chem.*, **2014**, *769*, 112-118.
3. “Catalyst free C–N bond formation by the reaction of amines with diimides: bulky guanidines”, **Ashim Baishya**, Thota Peddarao, Milan Kr. Barman and Sharanappa Nembenna\*, *New J. Chem.*, **2015**, *39*, 7503-7510.
4. “Air stable N-heterocyclic carbene-carbodiimide (“NHC-CDI”) adducts: bulky amidinates”, **Ashim Baishya**, Lokesh Kumar, Milan Kr. Barman, Thota Peddarao, and Sharanappa Nembenna\*, *ChemistrySelect*, **2016**, *3*, 498-503.

### Manuscript submitted or in preparation:

5. “NHC-CDI adduct or Zwitterionic type neutral amidinate supported Mg(II) and Zn(II) complexes” (*manuscript submitted*), **Ashim Baishya**, Lokesh Kumar and Sharanappa Nembenna\*.
6. “Reduction of N-heterocyclic carbene (NHC) supported aryl magnesium bromide complexes: Intramolecular (sp<sup>3</sup>)C–H bond activation” (*manuscript in preparation*), **Ashim Baishya**, Himansu S Biswal, and Sharanappa Nembenna\*.

7. “Organo Magnesium Amide as Pre-catalysts for Cross Dehydrogenative Coupling Reactions of Silanes with Amines (*manuscript in preparation*), **Ashim Baishya**, Thota Peddarao and Sharanappa Nembenna\*.
8. “Reaction of NHCs with PhZnI: Abnormal and normal N-heterocyclic carbene supported Zn(II) complexes” (*manuscript in preparation*), **Ashim Baishya** and Sharanappa Nembenna\*.

### **Conferences**

1. Attended ‘**13<sup>th</sup> CRSI National Symposium** in Chemistry & **5<sup>th</sup> CRSI-RSC Symposium**’ in Chemistry held at KIIT, Bhubaneswar (02-06 February 2011).
2. Attended ‘**Indo-European Symposium on Frontiers in Chemistry**’ held at NISER, Bhubaneswar (12-16 February 2012).
3. Presented poster in ‘**Indo-French Symposium on Functional Metal-Organics**’ held at NISER, Bhubaneswar (24-26 February 2014).

Ashim Baishya

DEDICATED TO .....

.....MY PARENTS & GRANDFATHER

## ACKNOWLEDGMENTS

First of all, I would like to express my sincere gratitude to Dr. Sharanappa Nembenna for giving me the opportunity to work on his esteemed group. The work described in this doctoral thesis has been carried out under the guidance and supervision of Dr. Sharanappa Nembenna at National Institute of Science Education and Research (NISER) in Bhubaneswar between January 2011 and August 2016.

My grateful thanks to

### **Dr. Sharanappa Nembenna**

for his constant advice, guidance, motivation, suggestions, and discussions throughout this work. I would like to thank him for his personal attention and the freedom I enjoyed during my stay in NISER, Bhubaneswar.

And also I am grateful to Prof. V. Chandrasekhar, director and Prof. T. K. Chandrashekar, former director, NISER and the faculty members of the School of Chemical Sciences (SCS), NISER.

I would like to thank my thesis monitoring committee members Dr. Sanjib Kar and Dr. J. N. Behera for their kind support.

My sincere thank goes to Prof. A. Srinivasan, chairperson and Dr. M. Sarkar, former chairperson in SCS, NISER.

I would like to convey my heartfelt thanks to Dr. C. S. Purohit and Dr. Rudresh Acharya for their kind help in X-ray crystallographic studies. I am grateful to Dr. H. S. Biswal for the theoretical studies. My special thanks to Dr. A. Kumar for his support and kind help.

I am also thankful to Dr. A. K. Singh and Mr. Sayed Mukter, IIT Bhubaneswar for Elemental Analysis.

I could not have finished my research work without the help from technical and non-technical staff from our institute. I thank Mr. Dipak Kr. Behera (X-ray studies), Mr. Sanjay Mishra (NMR studies), and Ms. Anuradha (IR spectral measurements) of analytical division for

their timely help. I am also thankful to non-technical staff members Ashutosh and Bhabani of SCS NISER for their co-operation.

I wish to offer my sincere thanks to the members of our group starting with my fellow lab mates Milan Kr. Barman, Thota Pedda Rao and my junior lab members Lokesh, Vineet, Ashish and Ajay for their cooperation and help during the course of this work.

I wish to acknowledge the University Grant Commission (UGC) for my fellowship and National Institute of Science Education and Research (NISER) for infrastructure and funding.

I am also greatly indebted to many teachers and seniors in the past and present, starting from school education till the completion of the studies in the university.

Finally, I would like to thank all my friends for their support and fun time I had with them. And of course, I am greatly thankful to my family members especially, my father, mother and brother for their motivation and continuous support. Lastly, I would like to acknowledge them, whose names are unintentionally missed out despite of their unconditional help for accomplishing this work.

I will be always indebted to the beautiful city Bhubaneswar, for obtaining my PhD and making my stay here peaceful and happy.

I bow down in front of THE ALMIGHTY GOD for providing me the health, strength, and this opportunity in my life.



## CONTENTS

	Page No.
Synopsis -----	1-11
List of Schemes -----	12
List of Figures -----	12
List of Tables -----	14
List of Abbreviations -----	16
<b>Chapter 1</b> Introduction -----	18-39
<b>1.1</b> N-Heterocyclic carbene (NHC) as neutral ligand -----	19
<b>1.2</b> Complexes of NHCs with magnesium and zinc element -----	20
<b>1.3</b> NHC supported low oxidation state main group metal complexes	
<b>1.3.1</b> Literature reports -----	21
<b>1.3.2</b> Theoretical studies -----	22
<b>1.4</b> NHC stabilized main group metal complexes: Catalytic applications -----	23
<b>1.4.1</b> C–N bond formation in guanylation reaction of amines to diimides -----	24
<b>1.4.2</b> Cross dehydrogenative coupling of silanes with amines -----	26
<b>1.5</b> NHC adducts of heteroallenes	
<b>1.5.1</b> “NHC-CDI” Adducts or Zwitterions -----	27
<b>1.5.2</b> Coordination chemistry of zwitterions (NHC-CDI adducts) -----	28
<b>1.6</b> Aim, scope and objective of the present work -----	30
<b>1.7</b> References -----	31
<b>Chapter 2</b> N-Heterocyclic carbene supported magnesium and zinc bis(amide) complexes: Catalytic and catalyst free C–N bond formation reactions -----	40-59
<b>Part A:</b> Catalytic C–N bond formation in guanylation reaction by NHC supported magnesium and zinc(II) amide complexes -----	40-50
<b>2A.1.</b> Reaction of <i>t</i> Bu with M[N(SiMe <sub>3</sub> ) <sub>2</sub> ] <sub>2</sub> : Synthesis and characterization -----	42

**2A.2.** Catalytic activity: Guanylation reaction of primary aromatic and cyclic secondary amines with carbodiimides ----- 45

**Part B:** Catalyst-free C–N bond formation by the reaction of amines with diimides: Synthesis of bulky guanidines ----- 50-59

**2B.1** Addition reaction of aromatic carbodiimides

to cyclic secondary amines ----- 51

**2B.2** Spectroscopic characterization ----- 54

Conclusion ----- 56

Crystal data and structural refinement details ----- 57

References----- 59

**Chapter 3** N-Heterocyclic carbene adducts of magnesium(II) and zinc(II) complexes: Synthesis, reactivity and theoretical studies----- 60-93

**Part A:** Structure, bonding and energetics of NHC stabilized low oxidation state Group 2 (Be, Mg, Ca, Sr and Ba) metal complexes: A theoretical study ----- 61-76

**3A.1** Structure ----- 61

**3A.2** Bonding -----64

**3A.3** Energetics ----- 66

**Part B:** IMes adducts of organo-magnesium(II) complexes: Synthesis, characterization and reactivity studies----- 61-83

**3B.1** Reactions of IMes with ArMgBr, (Ar = Ph, Xyl & Mes) ----- 71

**3B.1.1** Synthesis -----71

**3B.1.2** Spectroscopic characterization ----- 72

**3B.1.3** Crystallographic characterization ----- 74

**3B.2** Reduction of IMes supported aryl magnesium bromide complexes: Intramolecular (sp<sup>3</sup>)C–H bond activation----- 77

**3B.2.1** Synthesis of [IMesMgAr(IMes<sup>+</sup>)] ----- 77

<b>3B.2.2</b> Spectroscopic analysis of [IMesMgAr( <i>IMes</i> ')]-----	79
<b>3B.2.3</b> X-ray diffraction studies of [IMesMgAr( <i>IMes</i> ')]-----	80
<b>Part C:</b> Reaction of NHCs with PhZnI:	
NHC supported organo-zinc(II) complexes-----	84-93
<b>3C.1</b> Synthetic aspects -----	84
<b>3C.2</b> Spectroscopic characterization -----	85
<b>3C.3</b> Crystallographic characterization -----	86
Conclusion -----	88
Crystal data and structural refinement details -----	90
References -----	93
<b>Chapter 4</b> IMes supported organo-magnesium(II) amide complexes as pre-catalysts for cross dehydro-coupling of silanes with amines -----	94-104
Abstract -----	95
<b>4.1</b> Synthesis of IMes supported organo-magnesium(II) amide complexes -----	95
<b>4.2</b> Spectroscopic characterization -----	96
<b>4.3</b> Crystallographic characterization -----	97
<b>4.4</b> Catalytic application of organo-magnesium(II) amide complexes -----	98
Conclusion -----	102
Crystal data and structural refinement details -----	103
References -----	104
<b>Chapter 5</b> Reaction of N-Heterocyclic carbenes with aromatic carbodiimides (NHC-CDI adducts); air stable zwitterions and their co-ordination chemistry -----	105-131
<b>Part A:</b> Air stable “NHC-CDI” adducts: Zwitterionic type bulky amidinates -----	106-114
<b>5A.1</b> Synthesis and characterization of air stable bulky amidinates -----	106
<b>Part B:</b> “NHC-CDI” adducts or zwitterionic type neutral amidinate supported Mg(II) and Zn(II) complexes -----	115-130
<b>5B.1</b> Coordination of zwitterions (“NHC-CDI”adducts) to magnesium and zinc elements -----	116

<b>5B.2</b> Characterization of zwitterionic amidinate metal complexes -----	120
<b>5B.3</b> X-Ray crystallographic studies of zwitterionic amidinate complexes -----	121
Conclusion -----	125
Crystal data and structural refinement details -----	127
References -----	131
<b>Chapter 6</b> Summary and future directions -----	132-138
<b>Chapter 7</b> Experimental section -----	139-191

## **Synopsis**

1. Name of the Student: **Ashim Baishya**
2. Name of the Constituent Institution: **National Institute of Science Education and Research (NISER), Bhubaneswar**
3. Enrolment No.: **CHEM11201004012**
4. Title of the Thesis: **N-Heterocyclic carbene and its derivative “zwitterion” supported magnesium and zinc complexes: Synthesis, characterization reactivity studies and catalytic applications**
5. Board of Studies: **Chemical Sciences**

N-Heterocyclic carbenes (NHCs) have received much attention in recent years both in main group synthesis and catalysis, due to their strong  $\sigma$ -donating properties. Here, in the present work we have demonstrated the synthesis of NHC supported magnesium and zinc(II) bis(amide) complexes and their catalytic activity towards various organic reactions such as C–N bond formation reaction of amines with carbodiimides and cross dehydrogenative coupling of silanes with amines have been studied.

Further, a series of NHC stabilized organo-magnesium and -zinc(II) halide complexes are synthesized and structurally characterized. Furthermore, IMes supported organo-magnesium(II) halide complexes are reduced with excess sodium metal in toluene for 3 days to obtain cyclo-metalated compounds of organo-magnesium(II), stabilized by IMes and (*IMes'*) ligands. Theoretical calculations have been carried out on support of the low oxidation state Group 2 metal complexes with M–M bond stabilized by NHC.

Apart from being used as an excellent neutral ligand system for stabilization of unusual molecules across the periodic table, the strong nucleophilicity of NHC makes its own place as a reagent, in synthesizing varieties of organic molecules. Here, we have presented a synthetic way to zwitterions or “NHC-CDI” adducts. Continuing the synthesis of ligand system, a library of “NHC-CDI” adducts have been synthesized and their coordination behavior with main group elements, especially with magnesium and zinc has been studied.

The thesis has been organized into five chapters.

## **Chapter 1 Introduction**

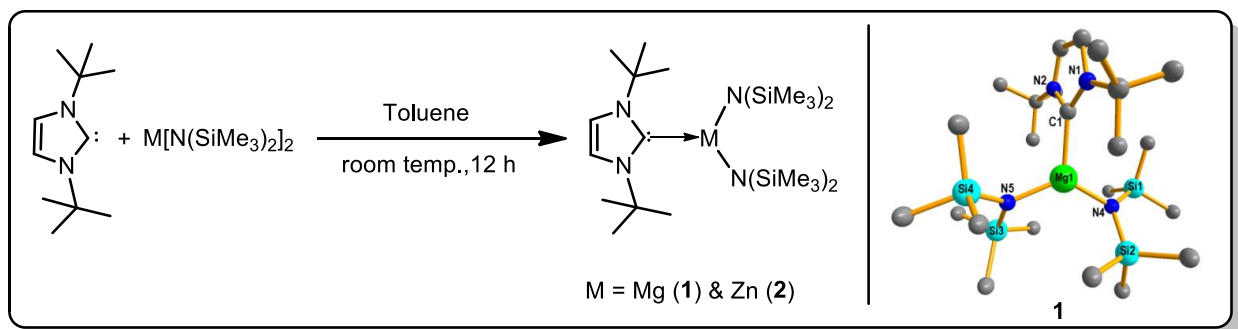
Chapter 1 introduces a brief outline of literature reports related to the work carried out throughout the thesis. This chapter comprises a concise description about the ligands used, their synthesis and metalation chemistry with main group elements, namely magnesium and zinc. A brief discussion on the catalytic applications using these complexes is also presented. Furthermore, a summary of literature review on low oxidation state main group metals have been discussed. Finally, on the basis of literature reports, we have designed the aim, scope and objectives of the present work.

## **Chapter 2 N-heterocyclic carbene supported magnesium and zinc bis(amide) complexes: Catalytic and catalyst free C–N bond formation reactions**

**Part A:** Catalytic C–N bond formation in guanylation reaction by NHC supported magnesium and zinc(II) amide complexes

### **2A.1** Reaction of *t*Bu with $M[N(\text{SiMe}_3)_2]_2$ : Synthesis and characterization

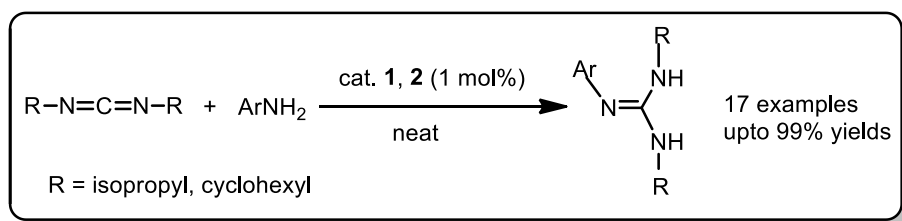
Treatment of the free carbene 1,3-di-*tert*-butylimidazol-2-ylidene (*t*Bu) with  $M[N(SiMe_3)_2]_2$ ,  $M = Mg$  or  $Zn$  in toluene led to the formation of  $tBu:M[N(SiMe_3)_2]_2$ ,  $M = Mg$  (**1**) or  $Zn$  (**2**) compounds, respectively.



**Scheme 1** Synthesis of compounds **1** & **2**; molecular structure of  $tBu:Mg[N(SiMe_3)_2]_2$  (**1**)

**2A.2** Catalytic activity: Guanylation of aromatic primary and cyclic secondary amines with carbodiimides

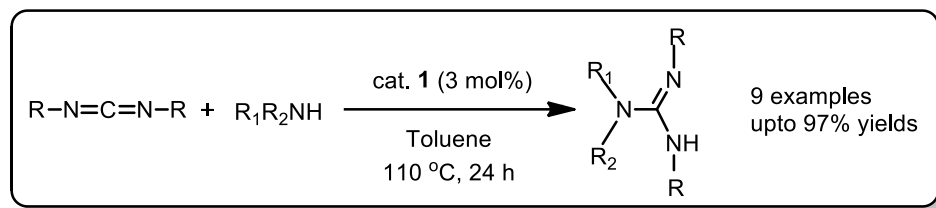
The catalytic activity of compounds **1** & **2** towards the addition of N–H bond of amines to carbodiimides was studied. Upon addition of primary amines to alkyl carbodiimides in the presence of 1 mol % of catalyst at room temperature without solvent, immediate formation of the  $N,N',N''$ -trisubstituted guanidine products in good to excellent yields was observed.



**Scheme 2** Synthesis of  $N,N',N''$ -trisubstituted guanidines

Furthermore, we examined the catalytic activity of compound **1** for the addition of various cyclic secondary amines with carbodiimides to obtain the  $N,N',N'',N''$ -tetra substituted guanidines in

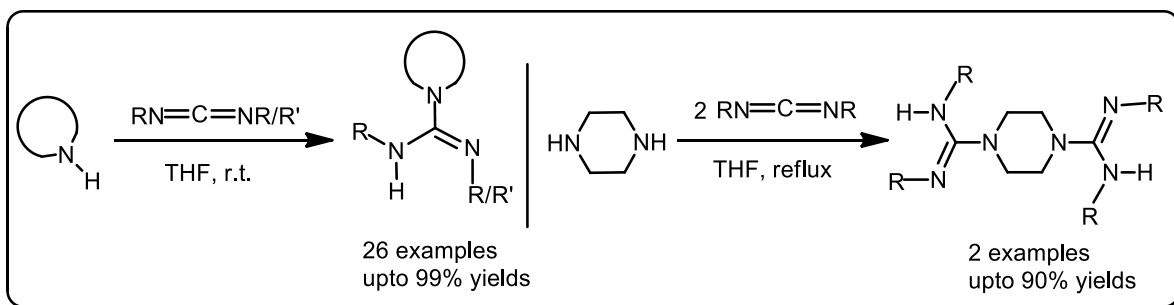
good to excellent yields. However, the reaction generally requires a higher temperature 110 °C and longer reaction period of 24 h for completion.



**Scheme 3** Synthesis of *N,N',N'',N'''*-tetra substituted guanidines

**Part B:** Catalyst-free C–N bond formation by the reaction of amines with diimides: Synthesis of bulky guanidines

Taking the advantages of metal free & facile access of bulky aryl symmetrical & unsymmetrical carbodiimides (CDIs) and high electrophilicity of sp hybridized carbon atom in CDI in comparison to aliphatic CDI, we have shown an atom economical and catalyst-free addition of cyclic secondary amines to various carbodiimides to afford *N,N',N'',N'''*-tetra-substituted guanidines (26 examples) in quantitative yield at ambient reaction conditions. Furthermore, it was established that the addition of diamines to bulky aryl symmetrical carbodiimides (2 equiv.) led to the formation of bulky aryl biguanidines (2 examples).



**Scheme 4** Synthesis of bulky *N,N',N'',N'''*-tetra-substituted guanidines and biguanidines



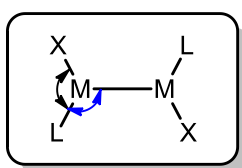
### Chapter 3 NHC adducts of magnesium(II) and zinc(II) complexes: Synthesis, reactivity and theoretical studies

#### Part A: Structure, bonding and energetics of NHC stabilized low oxidation state Group 2

(Be, Mg, Ca, Sr and Ba) metal complexes: A theoretical study

Schematic representation of  $[LM(X)-M(X)L]$ , where,  $X = H$  or  $Cl$ ,

$L = \text{NHC } [(CHNH)_2C:]$ ,  $M = \text{Be, Mg, Ca, Sr \& Ba}$ .



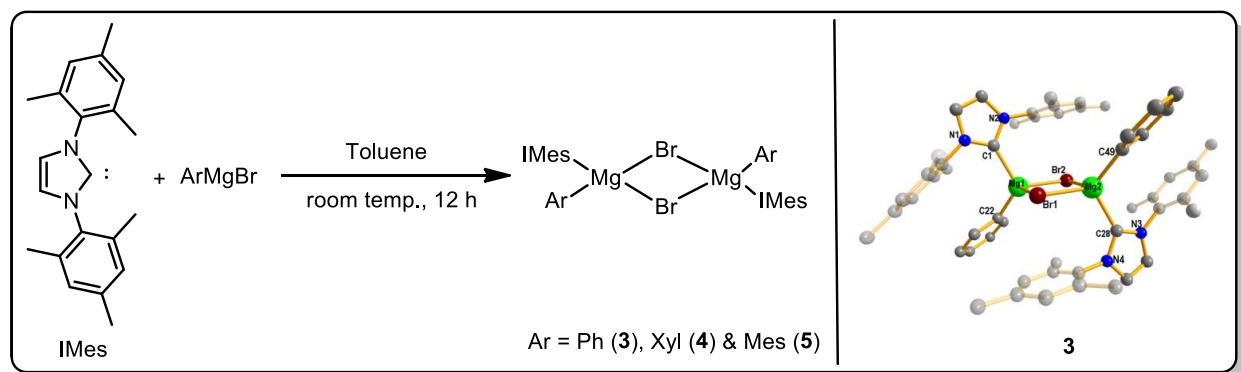
The homolytic M–M Bond Dissociation Energy (BDE) calculations (Table 1), Natural Bond Orbital (NBO) and Energy Decomposition Analyses (EDA) using density functional theory (DFT) reveal the stability of  $[LM(X)-M(X)L]$  complexes. Further, the bond order analyses, Wiberg Bond Indices (WBI) and Fuzzi Bond Order (FBO) confirm the existence of single covalent bond between two metal atoms.

**Table 1**  $\omega$ -B97X-D/def2-TZVP-calculated BDE in kJ/mol, enthalpy ( $\Delta H$  in kJ/mol) and free energies ( $\Delta G$  in kJ/mol) of the fragmentation of the complex  $[(X)(L)M-M(L)(X)] \rightarrow 2[(X)(L)M]$

Species	X = H, L = NHC			X=Cl, L=NHC		
	BDE	$\Delta H$	$\Delta G$	BDE	$\Delta H$	$\Delta G$
$[(X)(L)Be-Be(L)(X)]$	-189.1	-193.8	-138.6	-296.7	-295.6	-247.8
$[(X)(L)Mg-Mg(L)(X)]$	-193.3	-191.7	-149.2	-211.8	-209.5	-166.1
$[(X)(L)Ca-Ca(L)(X)]$	-144.2	-141.0	-108.6	-152.5	-149.0	-113.4
$[(X)(L)Sr-Sr(L)(X)]$	-126.7	-123.8	-84.6	-136.1	-132.1	-98.0
$[(X)(L)Ba-Ba(L)(X)]$	-120.4	-117.7	-75.6	-127.3	-124.0	-83.2

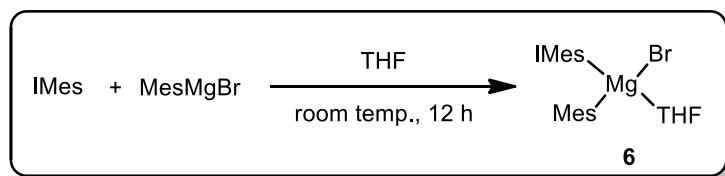
**Part B:** NHC adducts of organo-magnesium(II) complexes: Synthesis, characterization and reactivity studies

**3B.1** Reaction of IMes with ArMgBr (Ar = Ph, Xyl & Mes): IMes stabilized organo-magnesium(II) bromide complexes  $\{\text{IMesMg}(\text{Ar})\text{Br}\}_2$  are synthesized by direct treatment of IMes with aryl magnesium bromide solution in toluene. Synthesized compounds are characterized by NMR and X-ray crystal structural analyses. Solid state structures reveal the dimeric nature of IMes supported organo-magnesium bromides, where the two magnesium atoms are bridged by bromine atoms and are in distorted tetrahedral environments.



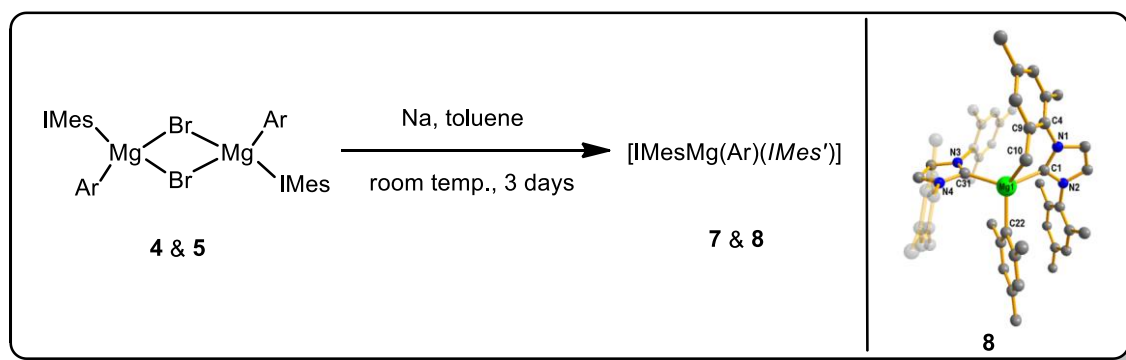
**Scheme 5** Synthesis of **3**, **4** and **5**; molecular structure of  $\{\text{IMesMg}(\text{Ph})\text{Br}\}_2$  (**3**)

Further, reaction of IMes with mesityl magnesium bromide in ethereal solvents gives the monomeric compound of IMes supported organo-magnesium(II) bromide complex, where the THF molecule occupies to the fourth vacant site of the Mg atom, fulfilling its tetra-coordination.



**Scheme 6** Synthesis of  $[\text{IMesMg}(\text{Mes})\text{Br}(\text{THF})]$ , (**6**)

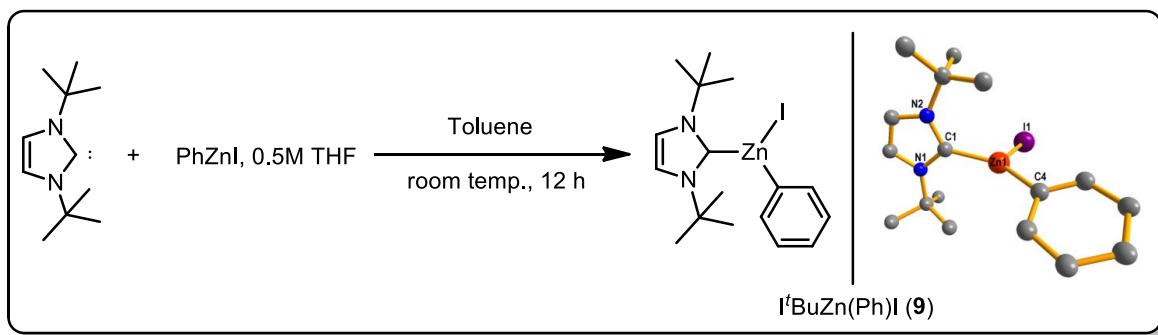
**3B.2** Reduction of NHC supported aryl magnesium bromide complexes: IMes supported organo-magnesium(II) bromide complexes,  $\{\text{IMesMg}(\text{Ar})\text{Br}\}_2$  upon reaction with excess sodium at room temperature in 3 days yields six membered cyclometalated compounds of magnesium  $[\text{IMesMg}(\text{Ar})(\text{IMes}^*)]$ , where the intermediate organo-magnesium(I) radical generated during reduction possibly activates the ortho-methyl mesityl  $\text{sp}^3(\text{C}-\text{H})$  bond near to it.



**Scheme 7** Synthesis of  $[\text{IMesMg}(\text{Ar})(\text{IMes}^*)]$ , Ar = Xyl (**7**) & Mes (**8**)

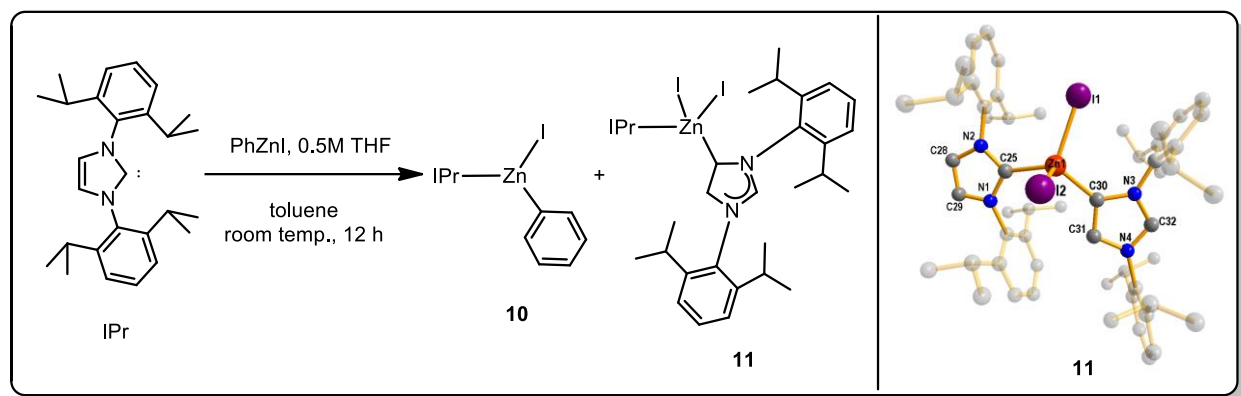
**Part C:** Reaction of NHCs with PhZnI: NHC supported organo-zinc(II) complexes

The commercial solution of phenyl zinc iodide in 0.5 M THF was treated with NHCs in toluene at room temperature with constant stirring for 12 h. *t*Bu formed a stoichiometric adduct with PhZnI which was characterized by  $^1\text{H}/^{13}\text{C}$  NMR and single crystal X-ray structural analysis.



**Scheme 8** Synthesis and molecular structure of *t*BuZnPhI (**9**)

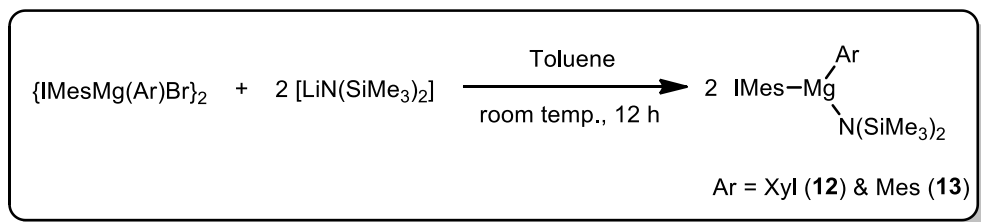
During the course of the reaction between IPr and PhZnI, we have isolated the novel abnormal carbene stabilized zinc diiodide IPr(ZnI<sub>2</sub>)aIPr (**11**) complex along with the normal PhZnI adduct of IPr, IPrZn(Ph)I (**10**). The identity of compound **10** was confirmed by NMR data whereas, **11** has been characterized by single crystal x-ray diffraction.



**Scheme 9** Synthesis of **10** & **11**; molecular structure of IPrZnI<sub>2</sub>aIPr (**11**)

**Chapter 4 IMes supported organo-magnesium(II) amide complexes as pre-catalysts for cross dehydrogenative coupling reactions of silanes with amines.**

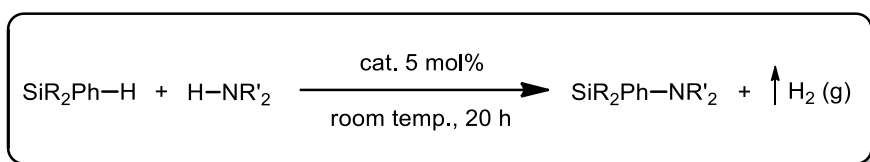
**4.1** Synthesis of IMes supported organo-magnesium(II) amide complexes: The synthesis of IMes stabilized organo-magnesium(II) amide complexes, [IMesMg(Ar)N(SiMe<sub>3</sub>)<sub>2</sub>] has been achieved from the salt metathesis reaction of {IMesMg(Ar)Br}<sub>2</sub> with non-nucleophilic base, [LiN(TMS)<sub>2</sub>] in toluene. The structures of thus synthesized compounds have been confirmed by single crystal X-ray structural analysis.



**Scheme 10** Synthesis of [IMesMg(Ar){N(SiMe<sub>3</sub>)<sub>2</sub>}] ; Ar = Xyl (**12**) & Mes (**13**)

## 4.2 Catalytic application of organo-magnesium(II) amide complexes: Cross dehydrogenative coupling reactions of silanes with amines

The formation of Si–N bond from the reaction of silanes with amines has been investigated in the presence of catalytic amount of compounds [IMesMg(Ar){N(TMS)<sub>2</sub>}]. The catalytic reactions were carried out using 5 mol % loading of catalyst in benzene at room temperature for 20 h.



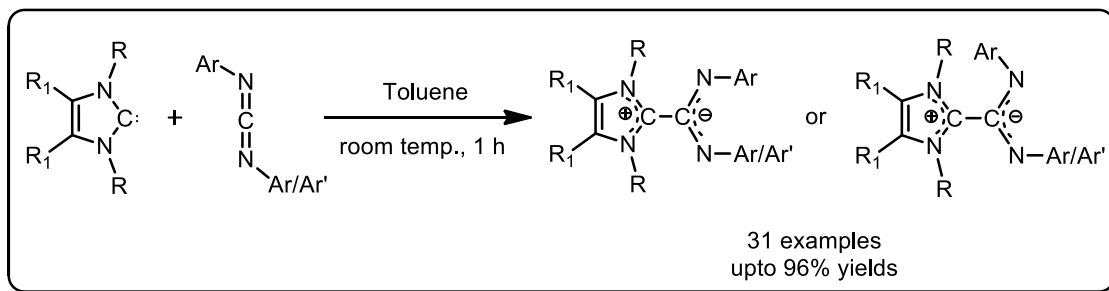
**Scheme 11** Catalytic Si–N bond formation reactions

Further, the catalytic activity of compound **13** has been explored for the reaction of silanes (1° & 2°) with various primary aliphatic, acyclic and cyclic secondary and aromatic amines to isolate the aminosilane products in good to excellent yields.

## **Chapter 5** Reaction of NHCs with aromatic carbodiimides (NHC–CDI adducts); air stable zwitterions and their co-ordination chemistry

### **Part A:** Air stable “NHC-CDI” adducts: Zwitterionic type bulky amidinates

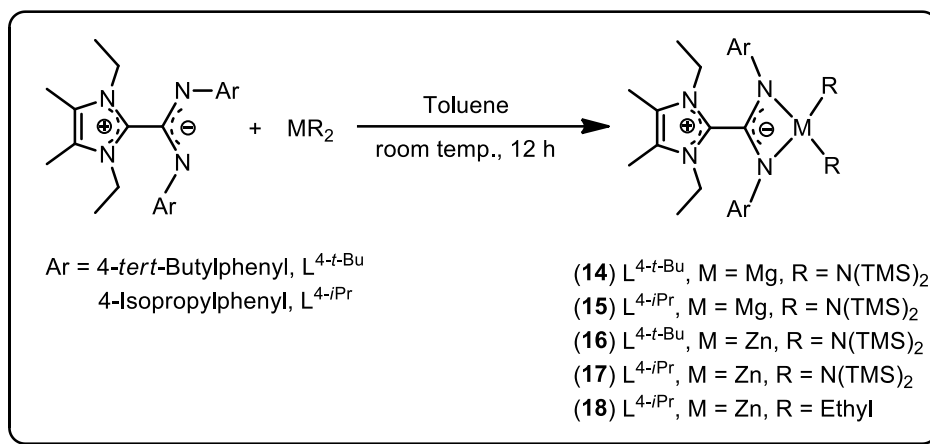
A library of N-heterocyclic carbene-carbodiimide (“NHC-CDI”) adducts *i.e.* zwitterionic type amidinates, have been synthesized from the reaction between *N,N'*-diaryl substituted symmetrical or unsymmetrical carbodiimides and NHCs at room temperature conditions. In contrast to normal amidinates, these new zwitterionic type bulky amidinate compounds are neutral and stable in the presence of air.



**Scheme 12** Synthesis of zwitterionic type amidinates

**Part B:** “NHC-CDI” adducts or zwitterionic type neutral amidinate supported Mg(II) and Zn(II) complexes

Stoichiometric amounts of NHC-CDI adducts *i.e.*  $L^{4-t-Bu}$  or  $L^{4-iPr}$  and  $[M\{N(TMS)_2\}_2]$  or  $MEt_2$ , are mixed together to yield the corresponding zwitterion supported metal amide and alkyl complexes. Solid state structures reveal the tetra-coordinated geometry around the metal centers with the neutral zwitterionic ligand bonded to metal in  $N,N'$ -chelated fashion.



**Scheme 13** Zwitterion chelated Mg(II) & Zn(II) complexes

## Summary of the work:

- In summary, we have synthesized *t*Bu stabilized magnesium and zinc bis(amide) complexes and studied their catalytic activity towards guanylation reaction.
- Taking advantage of bulky aromatic carbodiimide, a large number of bulky guanidines and biguanidines are synthesized by direct treatment of secondary amines with carbodiimides.
- Theoretical studies have been carried out to know the stability of NHC supported low oxidation state Group 2 metal complexes with M–M bond.
- IMes stabilized organo-magnesium and zinc(II) halide complexes are synthesized and characterized by X-ray diffraction. Further, cyclometalated compounds of magnesium, formed by intramolecular  $sp^3(C-H)$  bond activation of ortho-methyl mesityl group, have been isolated.
- Heteroleptic magnesium(II) amide complexes supported by IMes ligand are synthesized and their catalytic activity aimed at cross dehydrogenative coupling reactions of silanes with amines has been described.
- A library of “NHC-CDI” adducts or zwitterions have been synthesized and their coordination chemistry with magnesium and zinc elements has been studied.

List of Schemes			Page No.
1	<b>Scheme 1.1.1</b>	Synthesis of NHC; a) salt elimination reaction of imidazolium salts, b) reduction reaction of cyclic thioureas	20
2	<b>Scheme 1.4.1.1</b>	Synthesis of substituted guanidine	25
3	<b>Scheme 1.4.2.1</b>	Cross-dehydrocoupling of organosilanes with amines	26
4	<b>Scheme 1.5.1.1</b>	Synthesis of NHC-CDI adduct	28
5	<b>Scheme 2A.1.1</b>	Synthesis of $t\text{Bu:M}[\text{N}(\text{SiMe}_3)_2]_2$ , <b>1</b> and <b>2</b>	42
6	<b>Scheme 3B.1.1.1</b>	Synthesis of $[\text{IMesMg}(\text{Ar})\text{Br}]_2$ ; Ar = Ph ( <b>3</b> ), Xyl ( <b>4</b> ) & Mes ( <b>5</b> )	72
7	<b>Scheme 3B.1.1.2</b>	Synthesis of $[\text{IMesMg}(\text{Mes})\text{Br}(\text{THF})]$ ( <b>6</b> )	72
8	<b>Scheme 3B.2.1.1</b>	Synthesis of $[\text{IMesMgAr}(\text{IMes}^*)]$ ; Ar = Xyl ( <b>7</b> ) and Mes ( <b>8</b> )	77
9	<b>Scheme 3C.1.1</b>	Synthesis of $t\text{BuZn}(\text{Ph})\text{I}$ ( <b>9</b> )	84
10	<b>Scheme 3C.1.2</b>	Reaction of IPr with $\text{PhZnI}$ ; Synthesis of <b>10</b> and <b>11</b>	85
11	<b>Scheme 4.1.1</b>	Synthesis of $[\text{IMesMg}(\text{Ar})\text{N}(\text{TMS})_2]$ ; Ar = Xyl ( <b>12</b> ) & Mes ( <b>13</b> )	95
12	<b>Scheme 5A.1.1</b>	Direct addition of NHC to symmetrical $N,N'$ -diaryl carbodiimides	106
14	<b>Scheme 5A.1.2</b>	Direct addition of NHC to unsymmetrical $N,N'$ -diaryl carbodiimides	107
15	<b>Scheme 5B.1.1</b>	Synthesis of zwitterionic complexes of metal bis(amide) & dialkyl	117
16	<b>Scheme 5B.1.2</b>	Synthesis of a) $^{\text{Me}}\text{IEt}\{\text{LiN}(\text{TMS})_2\}_2$ ( <b>19</b> ); & b) $^{\text{Me}}\text{IEtMg}\{-\text{N}(\text{TMS})_2\}_2$ ( <b>20</b> )	118
17	<b>Scheme 5B.1.3</b>	Direct synthesis of <b>19, 20</b>	119

List of Figures			Page No.
1	<b>Figure 1.1.1</b>	Five membered N-heterocyclic carbene	19
2	<b>Figure 1.4.1.1</b>	Conformational isomers	26
3	<b>Figure 1.5.1.1</b>	“NHC-CDI” adducts or zwitterions	28
4	<b>Figure 1.5.2.1</b>	Bonding modes in zwitterionic type amidinates (top) and their metal complexes (bottom)	29
5	<b>Figure 2A.1.1</b>	Molecular structures of <b>1</b> and <b>2</b>	44
6	<b>Figure 2A.2.1</b>	Proposed mechanism for the guanylation reaction catalyzed by the	50



		$t\text{Bu:Mg}[\text{N}(\text{SiMe}_3)_2]_2$ ( <b>1</b> )	
7	<b>Figure 2B.2.1</b>	Molecular structures of a) <b>1c</b> , b) <b>22c</b> and c) <b>27c</b>	55
8	<b>Figure 3A.1.1</b>	Schematic representation of $[\text{L}(\text{X})\text{M}-\text{M}(\text{X})\text{L}]$ complex	61
9	<b>Figure 3A.1.2</b>	$\omega$ -B97X-D/def2-TZVP-optimized geometries of $[(\text{Cl})(\text{NHC})\text{Mg}-\text{Mg}(\text{Cl})(\text{NHC})]$ & $[(\text{H})(\text{NHC})\text{Mg}-\text{Mg}(\text{H})(\text{NHC})]$	62
10	<b>Figure 3A.3.1</b>	Different energy components as obtained from LMO-EDA calculation at the $\omega$ -B97X-D/def2-TZVP level of theory for $[(\text{Cl})(\text{NHC})\text{Mg}-\text{Mg}(\text{Cl})(\text{NHC})]$ & $[(\text{H})(\text{NHC})\text{Mg}-\text{Mg}(\text{H})(\text{NHC})]$	69
11	<b>Figure 3B.1.2.1</b>	Isomeric forms of $[\text{IMesMg}(\text{Mes})\text{Br}(\text{THF})]$	71
12	<b>Figure 3B.1.3.1</b>	Molecular structures of a) $[\text{IMesMg}(\text{Ph})\text{Br}]_2$ ( <b>3</b> ), b) $[\text{IMesMg}(\text{Xyl})\text{Br}]_2$ ( <b>4</b> ), c) $[\text{IMesMg}(\text{Mes})\text{Br}]_2$ ( <b>5</b> ) and d) $[\text{IMesMg}(\text{Mes})\text{Br}(\text{THF})]$ ( <b>6</b> )	74
13	<b>Figure 3B.2.3.1</b>	Molecular structure of $[\text{IMesMg}(\text{Xyl})(\text{IMes}^*)]$ ( <b>7</b> ) and $[\text{IMesMg}(\text{Mes})(\text{IMes}^*)]$ ( <b>8</b> )	81
14	<b>Figure 3B.2.3.2</b>	Proposed mechanism for intramolecular ( $\text{sp}^3$ )C–H bond activation of magnesium	83
15	<b>Figure 3C.3.1</b>	Molecular structure of $t\text{BuZn}(\text{Ph})\text{I}$ ( <b>9</b> )	87
16	<b>Figure 3C.3.2</b>	Molecular structure of $\text{IPr}(\text{ZnI}_2)\text{aIPr}$ ( <b>11</b> )	88
17	<b>Figure 4.3.1</b>	Molecular structures of $[\text{IMesMg}(\text{Ar})\text{N}(\text{TMS})_2]$ ; Ar = Xyl ( <b>12</b> ) & Mes ( <b>13</b> )	97
18	<b>Figure 4.4.1</b>	Proposed mechanism for $[\text{IMesMg}(\text{Ar})\text{N}(\text{TMS})_2]$ catalyzed dehydrogenative coupling reactions of amine with silane	102
19	<b>Figure 5A.1.1</b>	NHC-CDI adducts or zwitterion type bulky amidinates ( <b>1e-26e</b> )	108
20	<b>Figure 5A.1.2</b>	NHC-CDI (unsymmetrical) zwitterion type bulky amidinates ( <b>27e-31e</b> )	109
21	<b>Figure 5A.1.3</b>	a) Normal amidinates vs b) Zwitterion type amidinates	110
20	<b>Figure 5A.1.4</b>	Molecular structures of <b>1e</b> , <b>8e</b> , <b>12e</b> , <b>13e</b> , <b>16e</b> , <b>25e</b> , <b>26e</b> & <b>29e</b>	112
21	<b>Figure 5B.1.1</b>	Zwitterionic amidinates with NCN bond angles	116
22	<b>Figure 5B.3.1</b>	Molecular structures of <b>14</b> , <b>15</b> , <b>16</b> , <b>17</b> & <b>18</b>	122
23	<b>Figure 5B.3.2</b>	Molecular structures <b>19</b> & <b>20</b>	125

List of Tables			Page No.
1	<b>Table 2A.2.1</b>	Metal catalyzed reaction of aniline with <i>N,N'</i> -diisopropyl carbodiimides	45
2	<b>Table 2A.2.2</b>	Results of reaction of various anilines with <i>N,N'</i> -dialkyl carbodiimides catalyzed by <i>t</i> Bu:Mg[N(SiMe <sub>3</sub> ) <sub>2</sub> ] <sub>2</sub> ( <b>1</b> )	46
3	<b>Table 2A.2.3</b>	Results of reaction of various cyclic secondary amines with <i>N,N'</i> -dialkyl carbodiimide catalyzed by <b>1</b>	48
4	<b>Table 2B.1.1</b>	Addition of cyclic secondary amines to symmetrical aryl carbodiimides	52
5	<b>Table 2B.1.2</b>	Addition of cyclic secondary amines to un-symmetrical aryl carbodiimides	53
6	<b>Table 2B.1.3</b>	Synthesis of bulky aryl biguanidines	54
7	<b>Table 2B.2.1</b>	Selected bond lengths (Å) and bond angles (°) of compound <b>1c</b> , <b>22c</b> & <b>27c</b>	55
8	<b>Table 2S.1</b>	Crystal data and structural refinement summary for complexes <b>1</b> and <b>2</b>	57
9	<b>Table 2S.2</b>	Crystal data and structural refinement summary for compounds <b>1c</b> , <b>22c</b> & <b>27c</b>	57
10	<b>Table 3A.1.1</b>	Selected bond lengths, angles and dihedral angles in [(H)(NHC)M–M(H)(NHC)] as obtained from the ω-B97X-D/def2-TZVP-optimized structures	62
11	<b>Table 3A.1.2</b>	Selected bond lengths, angles and dihedral angles in [(Cl)(NHC)M–M(Cl)(NHC)] as obtained from the ω-B97X-D/def2-TZVP optimized structures	63
12	<b>Table 3A.1.3</b>	Selected bond lengths and angles in K <sub>2</sub> [(CHNH) <sub>2</sub> Mg–Mg(CHNH) <sub>2</sub> ] and compared with the corresponding crystallographic data [K(THF) <sub>3</sub> ] <sub>2</sub> [LMg–MgL]	64
13	<b>Table 3A.2.1</b>	The Wiberg Bond Index (WBI) of metal-metal bond (M–M) and natural charge of metal (q <sub>M</sub> ) in [(X)(L)M–M(L)(X)] complexes	65
14	<b>Table 3A.3.1</b>	ω-B97X-D/def2-TZVP calculated BDE, enthalpy and free energies of the fragmentation of the complex [(X)(L)M–M(L)(X)] ---->2[(X)(L)M]	66

15	<b>Table 3A.3.2</b>	Comparison of the $\omega$ -B97X-D/def2-TZVP-estimation of BDE, enthalpy, free energy with disproportionation energy, enthalpy, free energy	68
16	<b>Table 3A.3.3</b>	Comparison of the $\omega$ -B97X-D/def2-TZVP estimation of BDE, WBI and bond length of Mg–Mg bond with those in the related Mg(I)–Mg(I) systems reported in the literature	70
17	<b>Table 3B.1.3.1</b>	Selected bond lengths (Å) and angles (°) for compounds <b>3-6</b>	76
18	<b>Table 3B.2.3.1</b>	Selected bond distances (Å) and angles (°) for compounds <b>7 &amp; 8</b>	82
19	<b>Table 3S.1</b>	Crystal data and structure refinement details for compounds <b>3-6</b>	90
20	<b>Table 3S.2</b>	Crystal data and structure refinement details for compounds <b>7 &amp; 8</b>	91
21	<b>Table 3S.3</b>	Crystal data & structure refinement details for compounds <b>9 &amp; 11</b>	92
22	<b>Table 4.4.1</b>	Metal catalyzed reactions of <i>t</i> -BuNH <sub>2</sub> with PhSiH <sub>3</sub>	99
23	<b>Table 4.4.2</b>	Compound <b>13</b> catalyzed dehydrogenative coupling reactions of amines with silanes	100
24	<b>Table 4S.1</b>	Crystal data and structure refinement details for compounds <b>12 &amp; 13</b>	103
25	<b>Table 5A.1.1</b>	Comparisons of carbenic carbon peak (NCN) of free NHCs with “NHC-CDI” adducts in <sup>13</sup> C{ <sup>1</sup> H} NMR	110
26	<b>Table 5A.1.2</b>	Selected bond lengths (Å) and angles (°) for compounds <b>1e, 8e, 12e, 13e, 16e, 25e, 26e &amp; 29e</b>	113
27	<b>Table 5B.3.1</b>	Selected bond distances (Å) and angles (°) for compounds <b>14-18,</b>	123
28	<b>Table 5S.1</b>	Crystallographic data and structure refinement summary of compounds <b>1e, 8e, 12e, &amp; 13e</b>	127
29	<b>Table 5S.2</b>	Crystallographic data and structure refinement summary of compounds <b>16e, 25e, 26e &amp; 29e</b>	128
30	<b>Table 5S.3</b>	Crystallographic data and structure refinement summary of compounds <b>14-18</b>	129
31	<b>Table 5S.4</b>	Crystallographic data and structure refinement summary of compounds <b>19 &amp; 20</b>	130

## Abbreviations

$\delta$	chemical shift
$\lambda$	wavelength
$\mu$	bridging
$\tilde{\nu}$	wave number
Ar	aryl
av	average
b	broad
°C	Celsius
calcd.	calculated
Cp*	pentamethylcyclopentadienyl
d	doublet
dd	doublet of doublet
decomp.	decomposition
EI	electron impact ionization
equiv/eq.	equivalents
Et	ethyl
eV	electron volt
g	grams
h	hours
Hz	Hertz
<i>i</i> Pr	<i>iso</i> -propyl
IR	infrared
<i>J</i>	coupling constant
K	Kelvin

m	multiplet
M	metal
<i>m/z</i>	mass/charge
Mp	melting point
M <sup>+</sup>	molecular ion
Me	methyl
MS	mass spectrometry, mass spectra
NHC	N-heterocyclic carbene
NMR	nuclear magnetic resonance
Ph	phenyl
ppm	parts per million
q	quartet
quant.	quantitative
<sup>t</sup> Bu	<i>tert</i> -butyl
s	singlet
sept	septet
t	triplet
THF	tetrahydrofuran
V	volume
w	weak
XRD	X-ray diffraction
Z	number of molecules in the unit cell

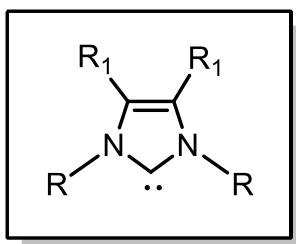
# **INTRODUCTION**

## Chapter 1 Introduction

This section of the thesis gives the background and an overview of the area in several sections before the work is presented.

### 1.1 N-Heterocyclic carbene (NHC) as neutral ligand

N-Heterocyclic carbenes (NHCs) have received much attention in recent years due to their strong  $\sigma$ -donating properties, which offer stabilities to the reactive molecules across the periodic table.<sup>1</sup> NHCs are neutral ligands and for the first time one of them has been isolated as a crystalline solid by A. J. Arduengo, III in the year 1991.<sup>2</sup> General structure of a five membered NHC is shown below (Figure 1.1.1).

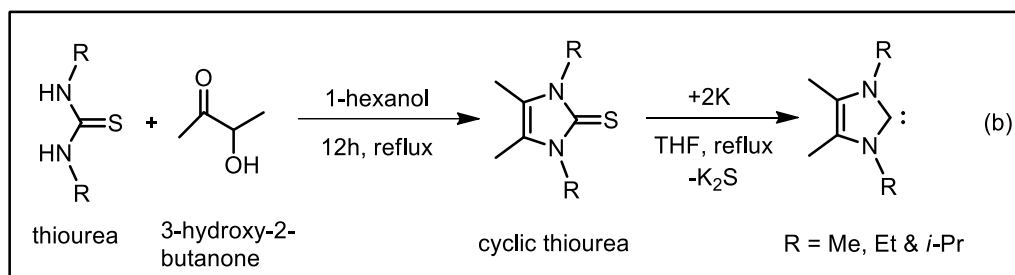
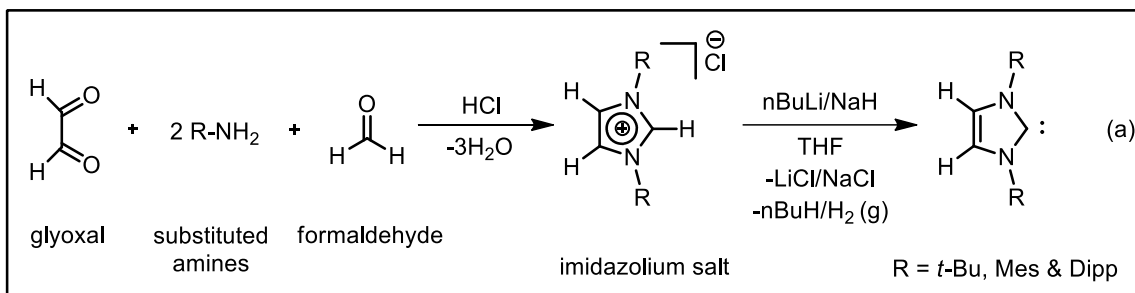


$R_1 = \text{H or Me}$

$R = \text{aliphatic or aromatic group}$

**Figure 1.1.1** Five membered N-heterocyclic carbene

A number of synthetic methods for preparation of NHCs are known in the literature. General synthetic route comprises the preparation of NHCs from their corresponding imidazolium salts using bases.<sup>3</sup> Here we are presenting the ones that used in our laboratory for the preparation of NHC ligands (Scheme 1.1.1).



**Scheme 1.1.1** Synthesis of NHC; a) salt elimination reaction of imidazolium salts, b) reduction reaction of cyclic thioureas.

Besides the use of NHCs as ligand in organometallic synthesis<sup>4</sup> and catalysis,<sup>5</sup> NHCs themselves have been investigated as nucleophilic reagents<sup>6</sup> and potential organocatalysts.<sup>7</sup> The reactivity of NHCs is adjusted by tuning the steric and electronic properties, and extensive studies have been carried out regarding quantifying and understanding their properties.<sup>8</sup> The chemistry of NHCs as ligands for organometallic catalysts to mediate an exciting range of organic reactions has been well-studied.<sup>9-11</sup> The uses of NHCs as ligands to stabilize low oxidation state main group molecules<sup>12</sup> has been very recently established.

## 1.2 Complexes of NHCs with magnesium and zinc element

NHC stabilized main group metal complexes have significant roles in stabilizing reactive metal complexes, which provides a unique platform for novel main group molecules. Despite the widely developed coordination chemistry of NHC's with p-block elements,<sup>13</sup> especially NHC



supported unusual main group molecules, the chemistry of NHC as ligand to s-block elements<sup>14</sup> is less widely considered. The reactions of NHC to magnesium and zinc reagents are already known in literature.<sup>15</sup> For the first time, Hill & co-workers reported the IPr {1,3-bis-(2,6-diisopropylphenyl)imidazole-2-ylidene} stabilized soluble magnesium hydride cluster<sup>16</sup>  $[\text{Mg}_4\text{H}_6]$ , by starting with NHC supported magnesium bis(amide),  $[\text{IPrMg}\{\text{N}(\text{TMS})_2\}_2]$  and phenylsilane. Very recently, using NHC zinc bis(amide) as a precursor, mixed amide-hydrido zinc complexes  $[\text{Zn}_4(\text{HMDS})_2\text{H}_6 \cdot 2\text{IPr}]$  and  $[\text{IPrZnH}(\text{HMDS})]$ , {HMDS =  $\text{N}(\text{SiMe}_3)_2$ } have been synthesized with two alternative hydride sources namely dimethylamine borane (DMAB) and phenylsilane ( $\text{PhSiH}_3$ ) respectively.<sup>17</sup> On the other hand, research groups of Okuda and Rivard independently reported the isolation of NHC supported dimeric zinc dihydride compounds.<sup>18</sup> Further mixed zinc alkyl-hydrido complexes stabilized by NHC have been synthesized by the reaction of dimeric zinc hydride  $[\{(\text{NHC})\text{ZnH}_2\}_2]$  with 2 equiv. of  $[(\text{NHC})\text{ZnEt}_2]$  in an alkyl-hydride exchange reaction.<sup>19</sup> In a very recent report, Stephan and co-workers have described the synthesis of monomeric species of NHC stabilized zinc mono hydride compounds,  $[(\text{NHC})\text{Cp}^*\text{Zn}(\text{H})]$  from the reaction of NHC adducts of decamethylzincocene  $[(\text{NHC})\text{ZnCp}^*_2]$  with  $\text{H}_2(\text{g})$  at high pressure reaction condition.<sup>20</sup>

### 1.3 NHC supported low oxidation state main group metal complexes

**1.3.1 Literature reports:** The chemistry of sub-valent metal complexes with metal-metal bond is of great importance in organometallic synthesis<sup>21</sup> and catalysis.<sup>22</sup> NHC as a neutral ligand, supported the synthesis of low oxidation state molecules both in main group and transition metal chemistry. Notable works in p-block chemistry starts with the Robinson's silicon(0) compound with Si=Si double bond from the potassium graphite reduction of the neutral hyper-valent carbene silicon  $[\text{IPr}:\text{SiCl}_4]$  compound.<sup>23</sup> In contrast to commercially available Group 14 heavier

## Introduction

metal halides (e.g.  $\text{PbCl}_2$ ,  $\text{SnCl}_2$  &  $\text{GeCl}_2$ .dioxane), the lighter congeners are not stable at room temperature. In 2009, Roesky and co-workers have isolated the NHC stabilized silicon dichloride ( $\text{IPrSiCl}_2$ ), where silicon atom is tricoordinated with +2 oxidation state.<sup>24</sup> It was formed by reductive elimination of HCl from trichlorosilane in the presence of IPr. In the same year, Filippou et al. accessed the NHC adduct of dibromosilylene.<sup>25</sup> Furthermore, NHCs have been used in the stabilization of highly reactive main group molecules such as metal dihydrides<sup>26</sup> ( $\text{SiH}_2$ ,  $\text{GeH}_2$  &  $\text{SnH}_2$ ) and diatomic allotropes ( $\text{Ge-Ge}$  &  $\text{Sn-Sn}$ ) of heavier Group 14 elements<sup>12a,27</sup>. The NHC supported metal hydrides are accessed using donor-acceptor strategy,<sup>28</sup> whereas the diatomic allotropes are synthesized by reduction from their corresponding hypervalent metal halides. Recently, Braunschweig and co-workers isolated a boron-boron triple ( $\text{B}\equiv\text{B}$ )<sup>29</sup> bonded compound in the presence of NHC at ambient temperature. Due to their excellent  $\sigma$ -donating ability and steric bulk, NHCs have been utilized in the stabilization of reactive molecules of Group 13 elements such as diborene,<sup>30</sup> dialane,<sup>31</sup> gallium octahedron<sup>32</sup> and indium trihydride.<sup>33</sup> Similarly, there are reports where NHCs have been used to stabilize wide varieties of unusual molecules.<sup>34</sup>

**1.3.2 Theoretical studies:** Soon after the unprecedented synthesis of decamethyldizincocene compound,  $\text{Cp}^*\text{Zn-ZnCp}^*$  ( $\text{Cp}^* = \text{C}_5\text{Me}_5$ ), containing a Zn-Zn bond by Carmona and co-workers in 2004,<sup>35</sup> theoreticians predicted that the thermally stable low oxidation state Group 2 compounds with metal-metal bonds should be isolable. New era in the Group 2 low oxidation state compounds with metal-metal bonds was shown by Jones and co-workers in 2007, by synthesizing well-defined stable dimeric magnesium(I) compounds.<sup>36</sup>

There are only a few reports on computational studies of low oxidation state Group 2 metal complexes with metal-metal bonds.<sup>21,37</sup> Notably, in 2005 Xie et al.,<sup>38</sup> reported a series of

stable species containing Group 2 elements, CpM–MCp [Cp = C<sub>5</sub>H<sub>5</sub>; M = Be, Mg & Ca] by theoretical methods. Zhang and coworkers have studied the binuclear metallocene using DFT methods,<sup>39</sup> and concluded the existence of single bond between the metal-metal atoms and a predominant ionic bond between metal and the ligand. But, until now there is no report on the stability of NHC supported low oxidation state alkaline earth metal complexes with M–M bonds (M = Be, Mg, Ca, Sr, and Ba), both in theory and in experiment.

#### **1.4 NHC stabilized main group metal complexes: Catalytic applications**

NHC as a ligand got enormous importance when compared to phosphorus analogues towards complexation with metals.<sup>3,40</sup> The straightforward synthetic route, stability and strong binding affinity towards metal that makes them better ligands than phosphorus analogues. The chemistry of NHC with transition<sup>5b</sup> and lanthanide metals in catalysis has been proven impressively versatile. NHC has been realized as a potential supporting ligand for homogeneous catalysis.<sup>41</sup>

In recent years, one of the fast growing areas of research involves the development of main group metal (or element) based catalysts for chemical transformations.<sup>42</sup> Organometallic compounds of main group elements are known to behave as catalysts towards various organic transformations<sup>43</sup> including dimerization of aldehydes,<sup>44</sup> ring opening polymerization of cyclic esters,<sup>45</sup> hydroboration of esters,<sup>46</sup> inter and intra molecular hydroamination reactions,<sup>47</sup> coupling reactions of alkynes with carbodiimides<sup>48</sup> and cross dehydrocoupling reactions of amines with silanes.<sup>49</sup> With regard to Group 2 and 12 metals, especially Mg and Zn complexes<sup>50</sup> have been used as catalysts in a wide range of chemical reactions due to their low toxicity, large abundance and low cost. It has been known that the presence of NHC significantly improves and modulates

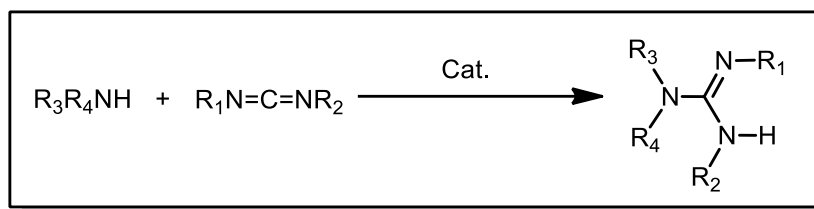
catalytic performance of metal complexes. Despite the fact that a large number of NHC adducts of main group compounds have been reported to bind metals, there are only a few reports in literatures on NHC adducts of magnesium and zinc complexes and their catalytic applications.

**1.4.1 C–N bond formation in guanylation reaction of amines to diimides:** Guanidines, an important class of organic molecules due to their stronger basicity,<sup>51</sup> have been employed as catalysts for various base catalyzed reactions.<sup>52</sup> The guanidine moiety is an essential substructure in many biologically and pharmaceutically important molecules<sup>53</sup> and also in natural products.<sup>54</sup> More importantly, negatively charged guanidates play a vital role in stabilizing metal complexes of various elements across the periodic table.<sup>55</sup> In 2006, Coles in his excellent review pointed out that the guanidine framework constitutes a versatile ligand set for use in coordination chemistry.<sup>56</sup>

Guanidines are organic compounds consisting of a triangular array of nitrogen atoms surrounding a carbon atom. The general formula of guanidine is  $R_1-N=C(NR_2R_3)NR_4R_5$ , in which the carbon atom of the  $N_3C$  moiety is connected to one imino and two amino nitrogen atoms. Generally, the synthesis of guanidines can be achieved by two routes. The first synthetic route i.e. ‘classical guanidine synthesis’, using reagents named as ‘guanylation agents’ is mainly based on stoichiometric reactions, where guanidine unit can be built up by chemical transformation from amidines, sulfonic acids, carbodiimides, cyanamides and isothiureas.<sup>57</sup> Secondly, the synthesis can be achieved by the utilization of organometallic compounds as catalysts. In this regard, a few review articles have appeared in the literature.<sup>58</sup> Although the synthesis of guanidine has been thoroughly examined by a variety of methods, the most convenient method is the direct addition of amines to carbodiimides (Scheme 1.4.1.1). It is documented that carbodiimides react with primary aliphatic amines, in the absence of a catalyst,

## Introduction

to generate the corresponding guanidine under harsh reaction conditions.<sup>59</sup> In contrast, primary aromatic and secondary amines do not react with carbodiimides without catalyst, even under harsh reaction conditions.<sup>60</sup> Metal catalyzed<sup>61</sup> C–N bond formation reaction from the addition of amines to carbodiimides is the primary alternative route to guanidines.<sup>62</sup>



**Scheme 1.4.1.1** Synthesis of substituted guanidine

In 2006, Richeson's group reported the first example of the commercially available lithium amide catalyzed C–N bond formation in guanylation reaction.<sup>63</sup> Hill and coworkers have shown the heavier Group 2 element catalyzed hydroamination of carbodiimides.<sup>47b</sup> Alonso-Moreno *et al.* demonstrated the lithium alkyl and magnesium dialkyls catalyzed reaction of amines with carbodiimides.<sup>60c</sup> Moreover, very recently, Bergman's group described the guanidinato stabilized aluminum(III) alkyl complex catalyzed hydroamination of carbodiimide.<sup>47c</sup> Carrillo-Hermosilla *et al.* described the catalytic synthesis of guanidines<sup>58c</sup>. The catalytic formation of guanidines follows any one of the four types of mechanisms known for addition of amines to carbodiimides.<sup>64</sup>

Although research groups of Jones and Gagliardi & Kempe, have reported the addition of metallated amides to *N,N'*-diaryl substituted carbodiimides, followed by aqueous work-up to afford the tetra-substituted guanidines,<sup>65</sup> this synthetic route is limited to the availability of very few bulky aryl carbodiimides.<sup>66</sup> Thus, it is very clear that *N,N'*-diaryl carbodiimides are important precursors for the preparation of bulky guanidine type ligands, even related bulky

amidines. In solution state guanidine, amidine and formamidine molecules are found to exist as more than one isomeric forms depending on position of the substituents with respect to carbon-nitrogen double (C=N) and single (C-N) bonds (Figure 1.4.1.1).<sup>56</sup>

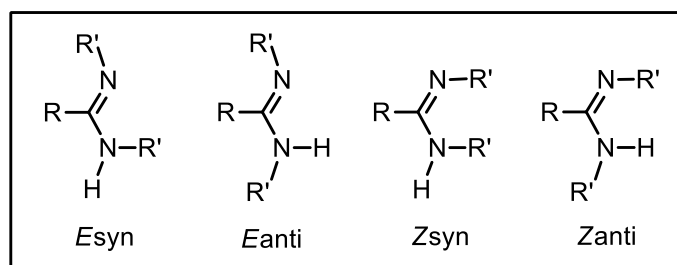
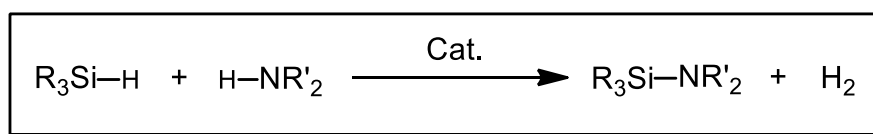


**Figure 1.4.1.1** Conformational isomers

**1.4.2 Cross dehydrogenative coupling of amines with silanes:** Compounds containing Si-N bond have important applications in synthetic chemistry such as bases,<sup>67</sup> silylating agents<sup>68</sup> as well as a ligands for metal centers and polymeric precursors for ceramic materials.<sup>69</sup> Cross dehydrogenative coupling of amines with silanes to give a controlled product is a challenging task as it leads to several products with different Si/N ratio and polysilazane. The reactivity and selectivity of catalyst plays an important role in controlling the product formation. The catalytic dehydrocoupling of amines and hydrosilanes presents a complementary synthetic way for Si-N bond forming compounds (Scheme 1.4.2.1).



**Scheme 1.4.2.1** Cross-dehydrocoupling of organosilanes with amines

In this regard, only a few metal catalysts of transition<sup>70</sup> and main group elements are known in literatures. Recently, Sadow and his group reported magnesium-methyl catalyzed dehydrocoupling of organosilanes with amines.<sup>49a</sup> Later, Cui and coworkers used

## Introduction

[(IMes)Yb{N(SiMe<sub>3</sub>)<sub>2</sub>}<sub>2</sub>], {IMes = 1,3-bis-(2,4,6-trimethylphenyl)imidazole-2-ylidene} as co-catalyst and found that NHC (IMes) plays an important role for the significant improvement of yield and/or modulating the catalytical performance of the rare earth metal bis(amide).<sup>11</sup> In very recent studies, Hill and co-workers in their edge article have shown that Group 2 metal amides are active catalysts for the hetero-dehydrocoupling of silanes with amines.<sup>49b</sup>

### 1.5 NHC adducts of heteroallenes

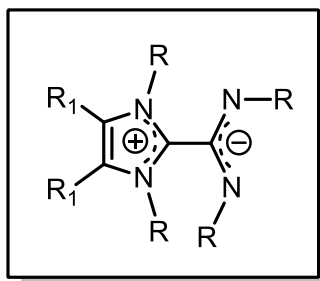
Apart from being excellent ligands for metals in synthesis and catalysis, NHCs have their own place as reagents in organic synthesis. The strong nucleophilicity of NHC allows them to form stable adducts with different organic molecules having electrophilic centers. In the year 2009, Delaude wrote a review on betaine adducts of NHCs, in which NHCs form stable zwitterionic adducts with unsaturated organic molecules such as heteroallenes, ketenes, and allenes.<sup>71</sup>

#### 1.5.1 “NHC-CDI” Adducts or Zwitterions

In 1999, Kuhn and coworkers reported the first example of a structurally characterized “NHC-CDI” adduct, (Scheme 1.5.1.1) prepared by the direct addition of 1,3-diisopropyl-4,5-dimethylimidazol-2-ylidene (<sup>Me</sup>iPr) to the commercially available diisopropylcarbodiimide (DIC).<sup>72</sup> Recently, Johnson and co-workers reported NHC-CDI adducts by [3+2] cyclo-elimination of saturated NHCs upon heating at 110 °C for 31 h in [D<sub>8</sub>] toluene.<sup>73</sup> Further, they have extended their studies to prepare three NHC-CDI adducts by the direct addition of either unsaturated or saturated NHCs with 1,3-di-p-tolyl carbodiimide. Interestingly, Johnson and co-worker’s NHC-CDI adducts are air stable because aryl substituent in the CDI portion of the

## Introduction

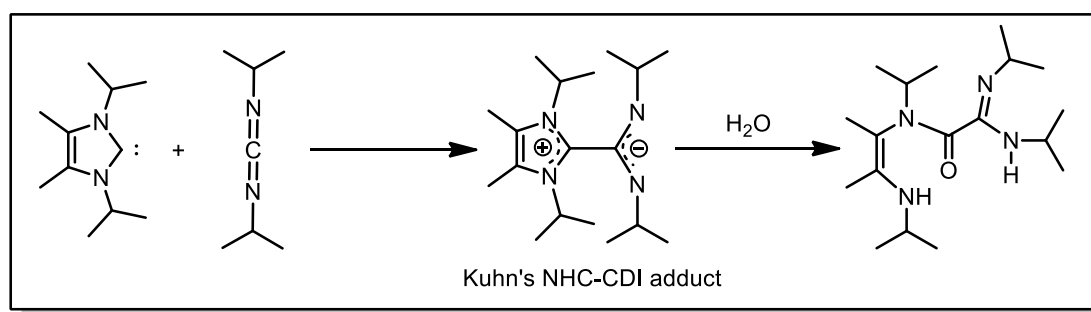
NHC-CDI provides increase in stability likely through delocalization of the amidinate negative charge. The general structure of NHC-CDI adduct is depicted below:



$R_1 = \text{H or Me}$

$R = \text{aliphatic or aromatic group}$

**Figure 1.5.1.1** “NHC-CDI” adducts or zwitterions



**Scheme 1.5.1.1** Synthesis of NHC-CDI adducts

## 1.5.2 Coordination Chemistry of zwitterions (“NHC-CDI” adducts)

NHCs have been used as neutral ligands for the construction of metal complexes across the periodic table. Surprisingly, coordination chemistry of these air stable neutral NHC-CDI adducts or zwitterions is not known with any element other than copper in the periodic table. Very recently, Ca'mpora and co-workers for the first time have shown the co-ordination chemistry of NHC-CDI with copper(I) complexes (Figure 1.5.2.1).<sup>74</sup> And also, “NHC-CDI” adducts have been found as ligands for the preparation of very small (1–1.3 nm) ruthenium nanoparticles (RuNPs).<sup>75</sup>



Ca'mpora and co-workers prepared a series of Cu(I) complexes supported by NHC-CDI adducts that are the very first examples of their kind. The coordination of NHC-CDI adducts with Cu(I)-acetate forms complexes with various binding modes such as terminal, bridging or binuclear paddlewheel structures depending on the steric nature of ligand.

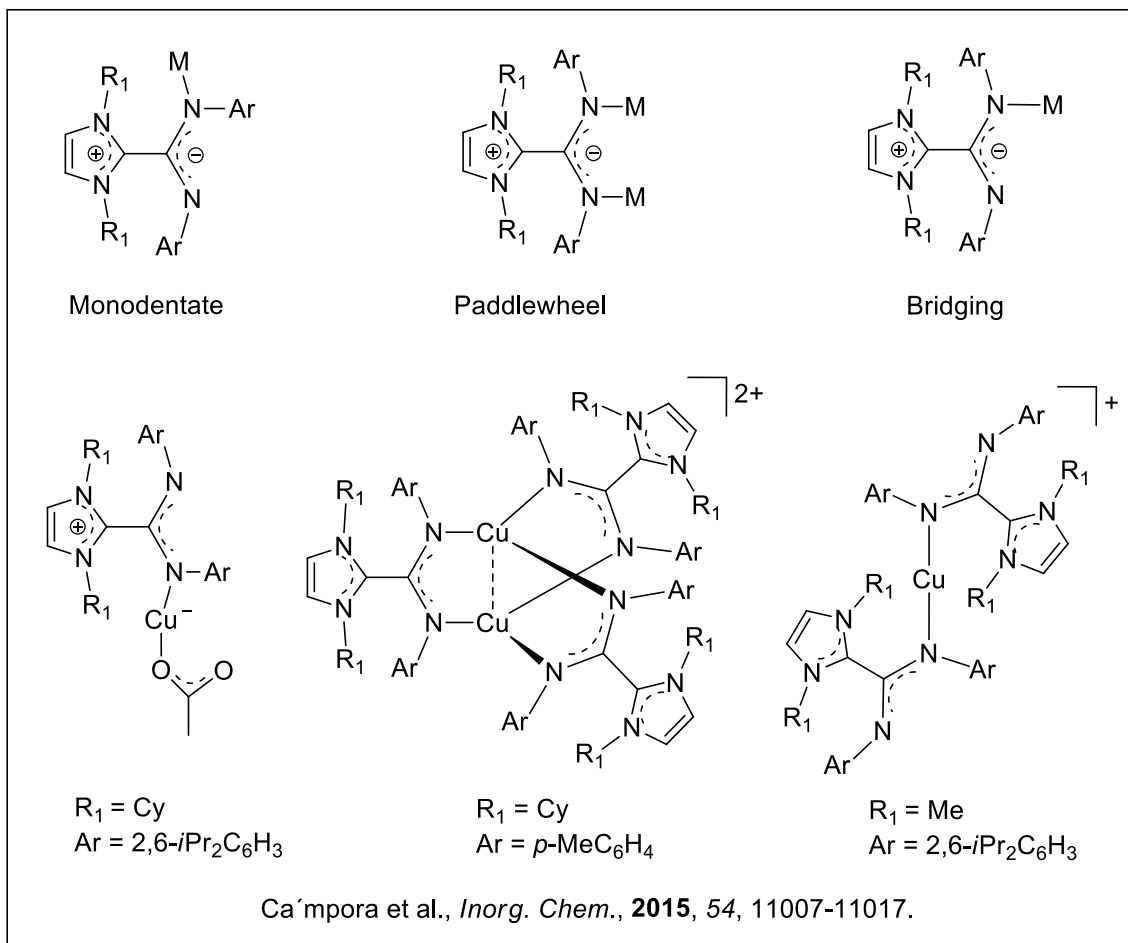


**Figure 1.5.2.1** bonding modes in zwitterions (top) and their metal complexes (bottom)

In contrast to the above,  $N,N'$ -chelated and bidentate zwitterions supported metal complexes are not known in the literature. We presume that such a bonding mode is very important especially for metal catalyzed organic transformations, where  $N,N'$ -chelated ligand

acts as a spectator ligand and also helps in the stabilization of metal complex. The terminal ligand which is attached to *N,N'*-chelated metal center actually participates in the reaction.

### **1.6 Aim, scope and objective of the present work:**

The chemistry of magnesium(I) and zinc(I) is known in literature.<sup>76</sup> The first synthesis of Zn–Zn bonded compound, Cp\*Zn–ZnCp\*, where Zn atom is in +1 oxidation state, is a remarkable achievement.<sup>35,77</sup> After the first preparation of Zn(I) compound, a number of complexes have been prepared with different varieties of monoanionic (e.g. guanidinate, diketiminate) and dianionic (diimines) ligands.<sup>22</sup> In the year 2007, Jones et al. isolated the first room temperature stable Mg(I) compound with Mg–Mg bond stabilized by bulky guanidinate ligand.<sup>36</sup> However, the low valent chemistry of magnesium and zinc metals stabilized by NHCs are not known in the literature.

The chemistry of NHC complexes with magnesium and zinc metal amides/alkyls are already known in literature,<sup>15</sup> which are used as starting precursor to prepare reactive metal hydrides.<sup>16-17</sup> NHC supported zinc hydrides are already described as potential catalysts towards various organic reactions such as methanolysis of silanes,<sup>18a,78</sup> catalytic hydrogenation of imines,<sup>20</sup> hydrosilylation and hydroboration of ketones,<sup>18</sup> etc. From the above reports it has been observed that the chemistry of NHC supported homoleptic or heteroleptic magnesium and zinc amide complexes for organometallic synthesis and catalysis are not yet explored.

The chemistry of NHC-CDI adducts as ligand is an emerging growing area of recent research interest. There are only a few literature reports on chemistry of NHC-CDI adducts. After the first synthesis of Kuhn's "NHC-CDI" adduct from the direct addition of aliphatic NHC

## Introduction

to commercially available aliphatic carbodiimides,<sup>72</sup> Johnson and co-workers reported the saturated and unsaturated NHC-CDI adducts of either saturated or unsaturated NHCs with aryl carbodiimides (1,3-di-p-tolyl CDI).<sup>73</sup> The formation of NHC-CDI adducts are limited due to the lack of availability of the bulky aryl carbodiimides. More importantly, Ca'mpora and co-workers for the first time have shown the coordination chemistry of NHC-CDI adducts with copper(I).<sup>75</sup>

Based on these facts, the objectives of the present work are as follows-

1. To isolate NHC stabilized low oxidation state Mg and Zn complexes with M–M bond.
2. To synthesize NHC supported magnesium and zinc amide complexes, and to explore their catalytic activity towards various organic transformations.
3. To develop new ligand systems by employing NHC and to study their coordination chemistry with main group elements.

## 1.7 References:

- (1) Herrmann, W. A.; Köcher, C. *Angew. Chem. Int. Ed.*, **1997**, *36*, 2162.
- (2) Arduengo, A. J.; Harlow, R. L.; Kline, M. *J. Am. Chem. Soc.*, **1991**, *113*, 361.
- (3) Herrmann, W. A. *Angew. Chem. Int. Ed.*, **2002**, *41*, 1290.
- (4) Viciu, M. S.; Navarro, O.; Germaneau, R. F.; Kelly, R. A.; Sommer, W.; Marion, N.; Stevens, E. D.; Cavallo, L.; Nolan, S. P. *Organometallics*, **2004**, *23*, 1629.
- (5) (a) Garrison, J. C.; Youngs, W. J. *Chem. Rev.* **2005**, *105*, 3978; (b) Nolan, S. P. *Acc. Chem. Res.*, **2011**, *44*, 91; (c) Kantchev, E. A. B.; O'Brien, C. J.; Organ, M. G. *Angew. Chem. Int. Ed.*, **2007**, *46*, 2768; (d) Budagumpi, S.; Haque, R. A.; Salman, A. W. *Coord. Chem. Rev.*, **2012**, *256*, 1787; (e) Velazquez, H. D.; Verpoort, F. *Chem. Soc. Rev.*, **2012**, *41*, 7032; (f) Budagumpi, S.; Haque, R. A.; Endud, S.; Rehman, G. U.; Salman, A. W.

- Eur. J. Inorg. Chem.*, **2013**, 4367; (g) Hock, S. J.; Schaper, L.-A.; Herrmann, W. A.; Kuhn, F. E. *Chem. Soc. Rev.*, **2013**, *42*, 5073.
- (6) Nair, V.; Bindu, S.; Sreekumar, V. *Angew. Chem. Int. Ed.*, **2004**, *43*, 5130.
- (7) (a) Duong, H. A.; Cross, M. J.; Louie, J. *Org. Lett.*, **2004**, *6*, 4679; (b) Flanigan, D. M.; Romanov-Michailidis, F.; White, N. A.; Rovis, T. *Chem. Rev.*, **2015**, *115*, 9307; (c) Csihony, S.; Culkin, D. A.; Sentman, A. C.; Dove, A. P.; Waymouth, R. M.; Hedrick, J. L. *J. Am. Chem. Soc.*, **2005**, *127*, 9079; (d) Kamber, N. E.; Jeong, W.; Waymouth, R. M.; Pratt, R. C.; Lohmeijer, B. G. G.; Hedrick, J. L. *Chem. Rev.*, **2007**, *107*, 5813; (e) Jeong, W.; Hedrick, J. L.; Waymouth, R. M. *J. Am. Chem. Soc.*, **2007**, *129*, 8414; (f) Enders, D.; Niemeier, O.; Henseler, A. *Chem. Rev.*, **2007**, *107*, 5606.
- (8) (a) Nelson, D. J.; Nolan, S. P. *Chem. Soc. Rev.*, **2013**, *42*, 6723; (b) Leuthäuser, S.; Schwarz, D.; Plenio, H. *Chem. -Eur. J.*, **2007**, *13*, 7195; (c) Clavier, H.; Nolan, S. P. *Chem. Commun.*, **2010**, *46*, 841.
- (9) (a) Wang, Y.; Robinson, G. H. *Inorg. Chem.*, **2011**, *50*, 12326; (b) Bourissou, D.; Guerret, O.; Gabbai, F. P.; Bertrand, G. *Chem. Rev.*, **2000**, *100*, 39; (c) Carmalt, C. J.; Cowley, A. H. *Adv. Inorg. Chem.*, **2000**, *50*, 1.
- (10) Díez-González, S.; Marion, N.; Nolan, S. P. *Chem. Rev.*, **2009**, *109*, 3612.
- (11) Xie, W.; Hu, H.; Cui, C. *Angew. Chem. Int. Ed.*, **2012**, *51*, 11141.
- (12) (a) Wang, Y.; Robinson, G. H. *Dalton Trans.*, **2012**, *41*, 337; (b) Ghadwal, R. S.; Azhakar, R.; Roesky, H. W. *Acc. Chem. Res.*, **2013**, *46*, 444; (c) Wang, Y.; Robinson, G. H. *Chem. Commun.*, **2009**, 5201.
- (13) Bantu, B.; Manohar Pawar, G.; Wurst, K.; Decker, U.; Schmidt, A. M.; Buchmeiser, M. R. *Eur. J. Inorg. Chem.*, **2009**, 1970.

- (14) (a) Hill, M. S.; Kociok-Köhn, G.; MacDougall, D. J. *Inorg. Chem.*, **2011**, *50*, 5234; (b) Gilliard, R. J.; Abraham, M. Y.; Wang, Y.; Wei, P.; Xie, Y.; Quillian, B.; Schaefer, H. F.; Schleyer, P. v. R.; Robinson, G. H. *J. Am. Chem. Soc.*, **2012**, *134*, 9953.
- (15) (a) Arduengo, A. J.; Davidson, F.; Krafczyk, R.; Marshall, W. J.; Tamm, M. *Organometallics*, **1998**, *17*, 3375; (b) Arnold, P. L.; Casely, I. J.; Turner, Z. R.; Bellabarba, R.; Tooze, R. B. *Dalton Trans.*, **2009**, 7236; (c) Kennedy, A. R.; Mulvey, R. E.; Robertson, S. D. *Dalton Trans.*, **2010**, *39*, 9091; (d) Kennedy, A. R.; Klett, J.; Mulvey, R. E.; Robertson, S. D. *Eur. J. Inorg. Chem.*, **2011**, 4675; (e) Arnold, P. L.; Edworthy, I. S.; Carmichael, C. D.; Blake, A. J.; Wilson, C. *Dalton Trans.*, **2008**, 3739; (f) Barrett, A. G. M.; Crimmin, M. R.; Hill, M. S.; Kociok-Köhn, G.; MacDougall, D. J.; Mahon, M. F.; Procopiou, P. A. *Organometallics*, **2008**, *27*, 3939.
- (16) Arrowsmith, M.; Hill, M. S.; MacDougall, D. J.; Mahon, M. F. *Angew. Chem. Int. Ed.*, **2009**, *48*, 4013.
- (17) Roberts, A. J.; Clegg, W.; Kennedy, A. R.; Probert, M. R.; Robertson, S. D.; Hevia, E. *Dalton Trans.*, **2015**, *44*, 8169.
- (18) (a) Rit, A.; Spaniol, T. P.; Maron, L.; Okuda, J. *Angew. Chem. Int. Ed.*, **2013**, *52*, 4664; (b) Lummis, P. A.; Momeni, M. R.; Lui, M. W.; McDonald, R.; Ferguson, M. J.; Miskolzie, M.; Brown, A.; Rivard, E. *Angew. Chem. Int. Ed.*, **2014**, *53*, 9347.
- (19) Rit, A.; Spaniol, T. P.; Maron, L.; Okuda, J. *Organometallics*, **2014**, *33*, 2039.
- (20) Jochmann, P.; Stephan, D. W. *Angew. Chem. Int. Ed.*, **2013**, *52*, 9831.
- (21) Krieck, S.; Yu, L.; Reiher, M.; Westerhausen, M. *Eur. J. Inorg. Chem.*, **2010**, 197.
- (22) Li, T.; Schulz, S.; Roesky, P. W. *Chem. Soc. Rev.*, **2012**, *41*, 3759.

- (23) Wang, Y.; Xie, Y.; Wei, P.; King, R. B.; Schaefer, H. F.; von R. Schleyer, P.; Robinson, G. H. *Science*, **2008**, *321*, 1069.
- (24) Ghadwal, R. S.; Roesky, H. W.; Merkel, S.; Henn, J.; Stalke, D. *Angew. Chem. Int. Ed.*, **2009**, *48*, 5683.
- (25) Filippou, A. C.; Chernov, O.; Schnakenburg, G. *Angew. Chem. Int. Ed.*, **2009**, *48*, 5687.
- (26) (a) Al-Rafia, S. M. I.; Malcolm, A. C.; Liew, S. K.; Ferguson, M. J.; Rivard, E. *J. Am. Chem. Soc.*, **2011**, *133*, 777; (b) Thimer, K. C.; Al-Rafia, S. M. I.; Ferguson, M. J.; McDonald, R.; Rivard, E. *Chem. Commun.*, **2009**, 7119.
- (27) (a) Sidiropoulos, A.; Jones, C.; Stasch, A.; Klein, S.; Frenking, G. *Angew. Chem. Int. Ed.*, **2009**, *48*, 9701; (b) Jones, C.; Sidiropoulos, A.; Holzmann, N.; Frenking, G.; Stasch, A. *Chem. Commun.*, **2012**, *48*, 9855.
- (28) Rivard, E. *Dalton Trans.*, **2014**, *43*, 8577.
- (29) Braunschweig, H.; Dewhurst, R. D.; Hammond, K.; Mies, J.; Radacki, K.; Vargas, A. *Science*, **2012**, *336*, 1420.
- (30) Frenking, G.; Holzmann, N. *Science*, **2012**, *336*, 1394.
- (31) Bonyhady, S. J.; Collis, D.; Frenking, G.; Holzmann, N.; Jones, C.; Stasch, A. *Nat Chem*, **2010**, *2*, 865.
- (32) Quillian, B.; Wei, P.; Wannere, C. S.; Schleyer, P. v. R.; Robinson, G. H. *J. Am. Chem. Soc.*, **2009**, *131*, 3168.
- (33) Jones, C. *Chem. Commun.*, **2001**, 2293.
- (34) (a) Masuda, J. D.; Schoeller, W. W.; Donnadiou, B.; Bertrand, G. *J. Am. Chem. Soc.*, **2007**, *129*, 14180; (b) Wang, Y.; Xie, Y.; Wei, P.; King, R. B.; Schaefer, I. I. I. H. F.; Schleyer, P. v. R.; Robinson, G. H. *J. Am. Chem. Soc.*, **2008**, *130*, 14970; (c) Abraham,

- M. Y.; Wang, Y.; Xie, Y.; Wei, P.; Schaefer, H. F.; Schleyer, P. v. R.; Robinson, G. H. *Chem. -Eur. J.*, **2010**, *16*, 432.
- (35) Resa, I.; Carmona, E.; Gutierrez-Puebla, E.; Monge, A. *Science*, **2004**, *305*, 1136.
- (36) Green, S. P.; Jones, C.; Stasch, A. *Science*, **2007**, *318*, 1754.
- (37) (a) Velazquez, A.; Fernández, I.; Frenking, G.; Merino, G. *Organometallics*, **2007**, *26*, 4731; (b) Westerhausen, M.; Gärtner, M.; Fischer, R.; Langer, J.; Yu, L.; Reiher, M. *Chem. -Eur. J.*, **2007**, *13*, 6292.
- (38) Xie, Y.; Schaefer Iii, H. F.; Jemmis, E. D. *Chem. Phys. Lett.*, **2005**, *402*, 414.
- (39) Zhang, X.; Li, S.; Li, Q.-S. *Mol. Phys.*, **2009**, *107*, 855.
- (40) Arnold, P. L.; Pearson, S. *Coord. Chem. Rev.*, **2007**, *251*, 596.
- (41) Herrmann, W. A. *Angew. Chem. Int. Ed.*, **2002**, *41*, 1290.
- (42) Power, P. P. *Nature*, **2010**, *463*, 171.
- (43) Harder, S. *Chem. Rev.*, **2010**, *110*, 3852.
- (44) Barman, M. K.; Baishya, A.; Nembenna, S. *J. Organomet. Chem.*, **2015**, *785*, 52.
- (45) (a) Wu, J.; Yu, T.-L.; Chen, C.-T.; Lin, C.-C. *Coord. Chem. Rev.*, **2006**, *250*, 602; (b) Sarazin, Y.; Carpentier, J.-F. *Chem. Rev.*, **2015**, *115*, 3564.
- (46) (a) Mukherjee, D.; Ellern, A.; Sadow, A. D. *Chem. Sci.*, **2014**, *5*, 959; (b) Hadlington, T. J.; Hermann, M.; Frenking, G.; Jones, C. *J. Am. Chem. Soc.*, **2014**, *136*, 3028.
- (47) (a) Crimmin, M. R.; Casely, I. J.; Hill, M. S. *J. Am. Chem. Soc.*, **2005**, *127*, 2042; (b) Lachs, J. R.; Barrett, A. G. M.; Crimmin, M. R.; Kociok-Köhn, G.; Hill, M. S.; Mahon, M. F.; Procopiou, P. A. *Eur. J. Inorg. Chem.*, **2008**, 4173; (c) Koller, J.; Bergman, R. G. *Organometallics*, **2010**, *29*, 5946; (d) Datta, S.; Roesky, P. W.; Blechert, S. *Organometallics*, **2007**, *26*, 4392.

- (48) (a) Zhang, W.-X.; Nishiura, M.; Hou, Z. *J. Am. Chem. Soc.*, **2005**, *127*, 16788; (b) Barrett, A. G. M.; Crimmin, M. R.; Hill, M. S.; Hitchcock, P. B.; Lomas, S. L.; Mahon, M. F.; Procopiu, P. A.; Suntharalingam, K. *Organometallics*, **2008**, *27*, 6300.
- (49) (a) Dunne, J. F.; Neal, S. R.; Engelkemier, J.; Ellern, A.; Sadow, A. D. *J. Am. Chem. Soc.*, **2011**, *133*, 16782; (b) Hill, M. S.; Liptrot, D. J.; MacDougall, D. J.; Mahon, M. F.; Robinson, T. P. *Chem. Sci.*, **2013**, *4*, 4212.
- (50) (a) Li, D.; Guang, J.; Zhang, W. X.; Wang, Y.; Xi, Z. *Org. Biomol. Chem.*, **2010**, *8*, 1816; (b) Chamberlain, B. M.; Cheng, M.; Moore, D. R.; Ovitt, T. M.; Lobkovsky, E. B.; Coates, G. W. *J. Am. Chem. Soc.*, **2001**, *123*, 3229; (c) Corey, E. J.; Shimoji, K. *Tetrahedron Lett.*, **1983**, *24*, 169.
- (51) (a) Kovačević, B.; Maksić, Z. B. *Org. Lett.*, **2001**, *3*, 1523; (b) Vazdar, K.; Kunetskiy, R.; Saame, J.; Kaupmees, K.; Leito, I.; Jahn, U. *Angew. Chem. Int. Ed.*, **2014**, *53*, 1435.
- (52) (a) Selig, P.; Turočkin, A.; Raven, W. *Synlett*, **2013**, *24*, 2535; (b) Yang, C.; Chen, W.; Yang, W.; Zhu, B.; Yan, L.; Tan, C.-H.; Jiang, Z. *Chem. Asian J.*, **2013**, *8*, 2960.
- (53) (a) Durant, G. J. *Chem. Soc. Rev.*, **1985**, *14*, 375; (b) Heys, L.; Moore, C. G.; Murphy, P. *J. Chem. Soc. Rev.*, **2000**, *29*, 57.
- (54) (a) Berlinck, R. G. S. *Nat. Prod. Rep.*, **1996**, *13*, 377; (b) G. S. Berlinck, R. *Nat. Prod. Rep.*, **1999**, *16*, 339; (c) Berlinck, R. G. S. *Nat. Prod. Rep.*, **2002**, *19*, 617.
- (55) (a) Zhou, Y.; Yap, G. P. A.; Richeson, D. S. *Organometallics*, **1998**, *17*, 4387; (b) Tin, M. K. T.; Yap, G. P. A.; Richeson, D. S. *Inorg. Chem.*, **1999**, *38*, 998; (c) Tin, M. K. T.; Yap, G. P. A.; Richeson, D. S. *Inorg. Chem.*, **1998**, *37*, 6728; (d) Foley, S. R.; Yap, G. P. A.; Richeson, D. S. *Inorg. Chem.*, **2002**, *41*, 4149; (e) Bazinet, P.; Wood, D.; Yap, G. P. A.; Richeson, D. S. *Inorg. Chem.*, **2003**, *42*, 6225; (f) Jones, C. *Coord. Chem. Rev.*, **2010**,



- 254, 1273; (g) Jones, C.; Furness, L.; Nembenna, S.; Rose, R. P.; Aldridge, S.; Stasch, A. *Dalton Trans.*, **2010**, 39, 8788; (h) Heitmann, D.; Jones, C.; Mills, D. P.; Stasch, A. *Dalton Trans.*, **2010**, 39, 1877; (i) Mück, F. M.; Junold, K.; Baus, J. A.; Burschka, C.; Tacke, R. *Eur. J. Inorg. Chem.*, **2013**, 5821; (j) Jones, C.; Schulten, C.; Nembenna, S.; Stasch, A. *J. Chem. Crystallogr.*, **2012**, 42, 866.
- (56) Coles, M. P. *Dalton Trans.*, **2006**, 985.
- (57) (a) Katritzky, A. R.; Rogovoy, B. V. *ARKIVOC*, **2005**, 49; (b) Wu, Y.-Q.; Hamilton, S. K.; Wilkinson, D. E.; Hamilton, G. S. *J. Org. Chem.*, **2002**, 67, 7553.
- (58) (a) Zhang, W.-X.; Hou, Z. *Org. Biomol. Chem.*, **2008**, 6, 1720; (b) Zhang, W.-X.; Xu, L.; Xi, Z. *Chem. Commun.*, **2015**, 51, 254; (c) Alonso-Moreno, C.; Antinolo, A.; Carrillo-Hermosilla, F.; Otero, A. *Chem. Soc. Rev.*, **2014**, 43, 3406.
- (59) Thomas, E. W.; Nishizawa, E. E.; Zimmermann, D. C.; Williams, D. J. *J. Med. Chem.*, **1989**, 32, 228.
- (60) (a) Zhang, W.-X.; Nishiura, M.; Hou, Z. *Synlett*, **2006**, 2006, 1213; (b) Tu, J.; Li, W.; Xue, M.; Zhang, Y.; Shen, Q. *Dalton Trans.*, **2013**, 42, 5890; (c) Alonso-Moreno, C.; Carrillo-Hermosilla, F.; Garcés, A.; Otero, A.; López-Solera, I.; Rodríguez, A. M.; Antiñolo, A. *Organometallics*, **2010**, 29, 2789; (d) Zhang, W.-X.; Li, D.; Wang, Z.; Xi, Z. *Organometallics*, **2009**, 28, 882; (e) Cao, Y.; Du, Z.; Li, W.; Li, J.; Zhang, Y.; Xu, F.; Shen, Q. *Inorg. Chem.*, **2011**, 50, 3729.
- (61) (a) Shen, H.; Xie, Z. *J. Organomet. Chem.*, **2009**, 694, 1652; (b) Baishya, A.; Barman, M. K.; Peddarao, T.; Nembenna, S. *J. Organomet. Chem.*, **2014**, 769, 112.
- (62) (a) Pottabathula, S.; Royo, B. *Tetrahedron Lett.*, **2012**, 53, 5156; (b) Du, Z.; Li, W.; Zhu, X.; Xu, F.; Shen, Q. *J. Org. Chem.*, **2008**, 73, 8966; (c) Li, Q.; Wang, S.; Zhou, S.; Yang,

- G.; Zhu, X.; Liu, Y. *J. Org. Chem.*, **2007**, *72*, 6763; (d) Zhu, X.; Du, Z.; Xu, F.; Shen, Q. *J. Org. Chem.*, **2009**, *74*, 6347; (e) Montilla, F.; Pastor, A.; Galindo, A. n. *J. Organomet. Chem.*, **2004**, *689*, 993; (f) Shen, H.; Chan, H.-S.; Xie, Z. *Organometallics*, **2006**, *25*, 5515; (g) Zhou, S.; Wang, S.; Yang, G.; Li, Q.; Zhang, L.; Yao, Z.; Zhou, Z.; Song, H.-b. *Organometallics*, **2007**, *26*, 3755; (h) Wu, Y.; Wang, S.; Zhang, L.; Yang, G.; Zhu, X.; Liu, C.; Yin, C.; Rong, J. *Inorg. Chim. Acta*, **2009**, *362*, 2814; (i) Romero-Fernandez, J.; Carrillo-Hermosilla, F.; Antinolo, A.; Alonso-Moreno, C.; Rodriguez, A. M.; Lopez-Solera, I.; Otero, A. *Dalton Trans.*, **2010**, *39*, 6419; (j) Shen, H.; Wang, Y.; Xie, Z. *Org. Lett.*, **2011**, *13*, 4562.
- (63) Ong, T.-G.; O'Brien, J. S.; Korobkov, I.; Richeson, D. S. *Organometallics*, **2006**, *25*, 4728.
- (64) (a) Xu, L.; Zhang, W.-X.; Xi, Z. *Organometallics*, **2015**, *34*, 1787; (b) Elorriaga, D.; Carrillo-Hermosilla, F.; Antinolo, A.; Suarez, F. J.; Lopez-Solera, I.; Fernandez-Galan, R.; Villasenor, E. *Dalton Trans.*, **2013**, *42*, 8223.
- (65) (a) Jin, G.; Jones, C.; Junk, P. C.; Lippert, K.-A.; Rose, R. P.; Stasch, A. *New J. Chem.*, **2009**, *33*, 64; (b) Noor, A.; Bauer, T.; Todorova, T. K.; Weber, B.; Gagliardi, L.; Kempe, R. *Chem. -Eur. J.*, **2013**, *19*, 9825.
- (66) Findlater, M.; Hill, N. J.; Cowley, A. H. *Dalton Trans.*, **2008**, 4419.
- (67) (a) Tanabe, Y.; Misaki, T.; Kurihara, M.; Iida, A.; Nishii, Y. *Chem. Commun.*, **2002**, 1628; (b) Iida, A.; Horii, A.; Misaki, T.; Tanabe, Y. *Synthesis*, **2005**, *2005*, 2677.
- (68) (a) Roth, C. A. *Ind. Eng. Chem. Prod. Res. Dev.*, **1972**, *11*, 134; (b) Tanabe, Y.; Murakami, M.; Kitaichi, K.; Yoshida, Y. *Tetrahedron Lett.*, **1994**, *35*, 8409; (c) Yan, K.; Ellern, A.; Sadow, A. D. *J. Am. Chem. Soc.*, **2012**, *134*, 9154.

- (69) Armitage, D. A.; Armitage, D. A.; Corriu, R. J. P.; Kendrick, T. C.; Parbhoo, B.; Tilley, T. D.; White, J. W.; Young, J. C. In *The Silicon–Heteroatom Bond*; Wiley: Chichester, **1991**.
- (70) (a) Blum, Y. D.; Schwartz, K. B.; Laine, R. M. *J. Mater. Sci.*, **1989**, *24*, 1707; (b) Wang, W. D.; Eisenberg, R. *Organometallics*, **1991**, *10*, 2222; (c) Blum, Y.; Laine, R. M. *Organometallics*, **1986**, *5*, 2081; (d) Biran, C.; Blum, Y. D.; Glaser, R.; Tse, D. S.; Youngdahl, K. A.; Laine, R. M. *J. Mol. Catal.*, **1988**, *48*, 183.
- (71) Delaude, L. *Eur. J. Inorg. Chem.*, **2009**, 1681.
- (72) N. Kuhn, M. S., G. Weyers, G. Henkel, *Z. Naturforsch. B.*, **1999**, *54b*, 434.
- (73) Zhukhovitskiy, A. V.; Geng, J.; Johnson, J. A. *Chem. -Eur. J.*, **2015**, *21*, 5685.
- (74) Márquez, A.; Ávila, E.; Urbaneja, C.; Álvarez, E.; Palma, P.; Cámpora, J. *Inorg. Chem.*, **2015**, *54*, 11007.
- (75) Martínez-Prieto, L. M.; Urbaneja, C.; Palma, P.; Campora, J.; Philippot, K.; Chaudret, B. *Chem. Commun.*, **2015**, *51*, 4647.
- (76) (a) Bonyhady, S. J.; Jones, C.; Nembenna, S.; Stasch, A.; Edwards, A. J.; McIntyre, G. J. *Chem. -Eur. J.*, **2010**, *16*, 938; (b) Westerhausen, M. *Angew. Chem. Int. Ed.*, **2008**, *47*, 2185.
- (77) Carmona, E.; Galindo, A. *Angew. Chem. Int. Ed.*, **2008**, *47*, 6526.
- (78) Rit, A.; Spaniol, T. P.; Okuda, J. *Chem. Asian J.*, **2014**, *9*, 612.

## **RESULTS AND DISCUSSION**

Chapter 2

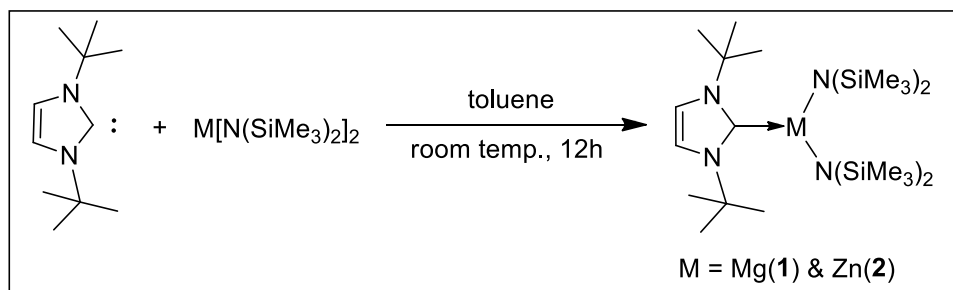
**N-Heterocyclic carbene Supported Magnesium and Zinc Bis(amide)  
Complexes: Catalytic and Catalyst free C–N bond formation  
Reactions**

## Part A: Catalytic C–N bond formation in guanylation reaction by NHC supported magnesium(II) and zinc(II) amide complexes

The catalytic activity of NHC supported magnesium(II) and zinc(II) amide complexes towards the C–N bond formation of amines with carbodiimides were studied. Treatment of the free carbene 1,3-di-*tert*-butylimidazol-2-ylidene (*I'*Bu) with  $M[N(SiMe_3)_2]_2$ ,  $M = Mg$  or  $Zn$  in toluene led to the formation of  $I'Bu:M[N(SiMe_3)_2]_2$ ,  $M = Mg$  (**1**) or  $Zn$  (**2**) compounds, respectively. Both compounds **1** and **2** were characterized by multinuclear ( $^1H$ ,  $^{13}C$  and  $^{29}Si$ ) NMR spectroscopy and single X-ray crystal structure analysis. Solid state structures revealed that both compounds are monomeric in nature and their metal atoms are three coordinated and distorted trigonal planar in geometries. Furthermore, compounds **1** and **2** were tested as catalysts for the guanylation reaction of addition of amine to carbodiimide and turned to be excellent catalysts.

### 2A.1 Reaction of *I'*Bu with $M[N(SiMe_3)_2]_2$ : Synthesis and characterization

The synthesis of *I'*Bu adducts of magnesium and zinc bis(amide),  $I'Bu:M[N(SiMe_3)_2]_2$ ,  $M = Mg$  (**1**) &  $Zn$  (**2**) has been achieved by the treatment of *I'*Bu with corresponding metal bis(amide)  $M[N(SiMe_3)_2]_2$  in toluene, at room temperature stirring for 12 h (Scheme 2A.1.1).



**Scheme 2A.1.1** Synthesis of  $I'Bu:M[N(SiMe_3)_2]_2$ , **1** & **2**

The crude compounds were recrystallized from toluene at  $-25\text{ }^\circ\text{C}$  to give colorless crystals with

moderate yields 68 and 62 % for complexes **1** and **2** respectively. The isolated crystals of **1** and **2** are melting without any decomposition at temperatures 128 & 120 °C, respectively. The compounds **1** and **2** are freely soluble in organic solvents such as tetrahydrofuran, toluene and benzene and sparingly soluble in hexane. Both compounds are sensitive toward air and moisture and require inert atmosphere for their stability. The compounds **1** and **2** were characterized by multinuclear ( $^1\text{H}$ ,  $^{13}\text{C}$  and  $^{29}\text{Si}$ ) NMR spectroscopic methods. Furthermore, the molecular structures of compounds **1** and **2** were confirmed by single crystal X-ray structural analysis.

$^1\text{H}$  NMR spectrum of complex **1** in  $\text{C}_6\text{D}_6$  exhibits three resonances as singlet, two singlet resonances for the NHC ligand at 6.35 and 1.42 ppm and one singlet for amide ligand i.e.  $\text{N}(\text{SiMe}_3)_2$  at 0.38 ppm. Similarly,  $^1\text{H}$  NMR spectrum for complex **2** shows two singlets for the NHC ligand at 6.41 and 1.44 ppm and a broad signal at 0.36 ppm for the amide ligand.  $^{13}\text{C}$   $\{^1\text{H}\}$  NMR signals appear at 178 and 176 ppm corresponding to carbene carbon of compounds **1** and **2**, respectively (in free  $t\text{Bu}$ , carbene carbon resonates at 213 ppm). In  $^{29}\text{Si}$   $\{^1\text{H}\}$  NMR complex **1** exhibits a peak at  $-17.12$  ppm for the silyl group, whereas a peak at  $-5.00$  ppm for compound **2** was observed.

Crystals of **1** and **2** suitable for X-ray structure determination were grown from a toluene solution by slow cooling to  $-25$  °C. Molecular structures along with selected bond lengths and bond angles of **1** & **2** are summarized in Figure 2A.1.1. Compounds **1** and **2** were crystallized in the monoclinic  $P2(1)/n$  and monoclinic  $P2(1)$  space groups, respectively. Both compounds exist as monomers and their metal atoms are bonded to one carbenic carbon atom and two nitrogen atoms of the amido ligands. Thus, both magnesium and zinc atoms are three coordinated with a distorted structure from the trigonal planar by widening the angles between two silylamide groups [ $\text{N4-Mg1-N5}$   $128.42(7)$  and  $\text{N4-Zn1-N3}$   $131.43(18)$  ( $^\circ$ )], in complexes **1** and **2**

respectively. This is due the larger steric demands of the substitution.

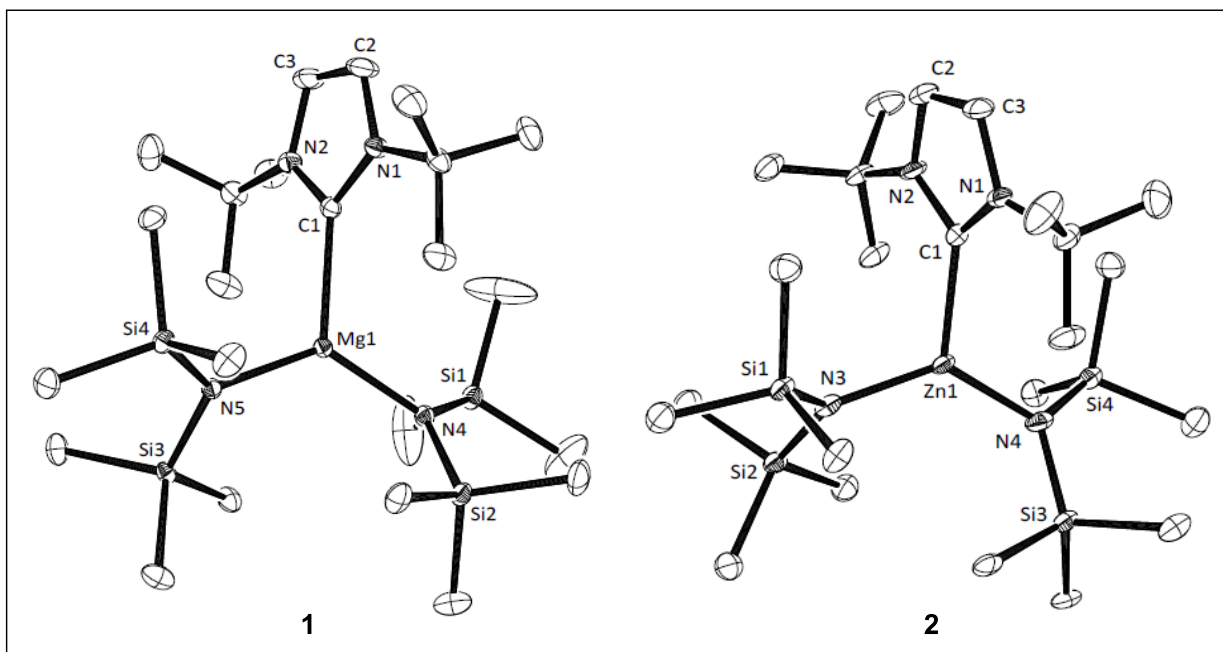


**Figure 2A.1.1** Molecular structures of **1** and **2**. All hydrogen atoms are removed for clarity. Selected bond lengths (Å) and angles (°), for **1**: Mg1–C1 2.241(2), Mg1–N4 2.0142(18), C1–N1 1.3670(25); C1–Mg1–N4 116.97(7), C1–Mg1–N5 114.59(7), N4–Mg1–N5 128.42(7); for **2**: Zn1–C1 2.082(5), Zn1–N3 1.958(5), C1–N1 1.361(6), Zn1–N4 1.956(5); C1–Zn1–N3 110.90(19), C1–Zn1–N4 117.66(19), N3–Zn1–N4 131.43(18).

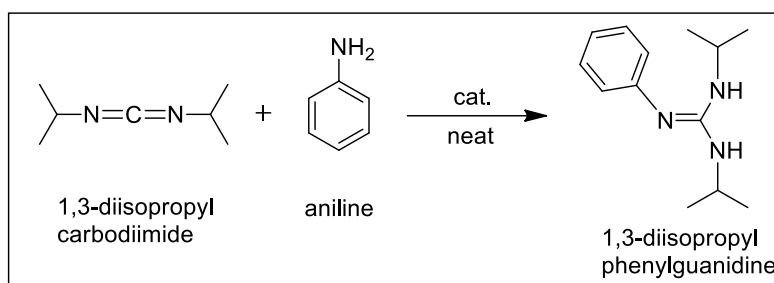
The  $C_{\text{NHC}}\text{--Mg}$  bond length in complex **1** is 2.241(2) Å, which is longer than that of  $C_{\text{NHC}}\text{--Zn}$  bond distance in complex **2** (2.082(5) Å), this is due to the 0.19 Å longer covalent radii of magnesium element (1.41 Å) than that of zinc element (1.22 Å).<sup>1</sup> The bond distance of  $C_{\text{NHC}}\text{--Mg}$  of **1** (2.241(2) Å) is in good agreement with other  $\text{NHC--Mg(II)}$  adducts (2.194–2.279 Å).<sup>2</sup> And also,  $C_{\text{NHC}}\text{--Zn}$  bond distance (2.082(5) Å) in **2** matches well with recently reported Okuda's NHC stabilized zinc dihydride complexes  $\{(\text{IMes}:\text{ZnH}_2)_2$  2.052 (Å) &  $(\text{IPr}:\text{ZnH}_2)_2$  2.054 (Å)}.3



## 2A.2 Catalytic activity: Guanylation reactions of aromatic primary and cyclic secondary amines with carbodiimides

The catalytic activity of NHC supported magnesium(II)  $\text{t}^{\text{Bu}}\text{Mg}[\text{N}(\text{SiMe}_3)_2]_2$  (**1**) and zinc(II)  $\text{t}^{\text{Bu}}\text{Zn}[\text{N}(\text{SiMe}_3)_2]_2$  (**2**) bis(amide) complexes were investigated by performing the reaction of aniline with isopropyl carbodiimide (Table 2A.2.1).

**Table 2A.2.1** Metal catalyzed reaction of aniline with  $N,N'$ -diisopropylcarbodiimide



Entry	Catalyst	Catalyst load (mol %)	Temp.(°C)	Solvent	Time [min]	Yield (%) <sup>a</sup>
1	<b>1</b>	1	25	-----	1	quant.
2	<b>2</b>	1	25	-----	1	quant.
3	$\text{Mg}[\text{N}(\text{SiMe}_3)_3]_2$	1	25	-----	1	quant.
4	$\text{Mg}[\text{N}(\text{SiMe}_3)_3]_2$	0.1	50	thf( $d_8$ )	720	73 <sup>b</sup>
5	$\text{Mg}[\text{N}(\text{SiMe}_3)_3]_2$	0.5	60	-----	120	80
6	<b>1</b>	0.1	50	thf( $d_8$ )	120	88 <sup>b</sup>
7	<b>1</b>	0.5	60	-----	5	94
8	<b>1</b>	1	25	thf	120	quant.
9	<b>1</b>	1	25	toluene	120	quant.
10	<b>2</b>	1	25	toluene	120	quant.
11	<b>2</b>	0.5	60	-----	5	92

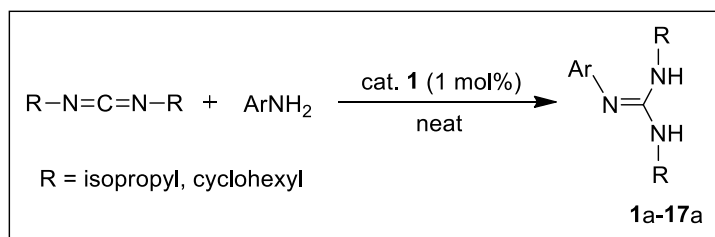
The reaction was performed by treating 1 equiv of aniline with 1 equiv of  $N,N'$ -diisopropylcarbodiimide.

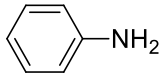
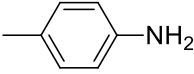
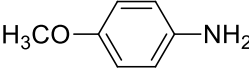
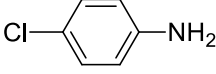
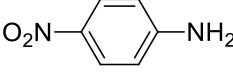
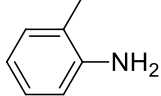
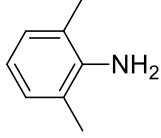
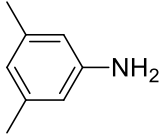
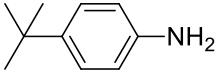
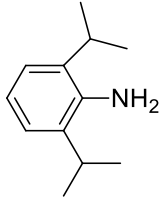
<sup>a</sup> Isolated yield.

<sup>b</sup> NMR yield measured by integration of consumption of starting material relative to the formation of product.

The addition of aniline to isopropyl carbodiimide in the presence of 1 mol % either compound **1** or **2** at room temperature without solvent, immediate formation of the *N,N',N''*-trisubstituted guanidine product was occurred (Table 2A.2.1, Entry 1 and 2). To know the effect of *t*Bu, which is coordinated to the metal bis(amide), alternatively another reaction performed by using  $\text{Mg}[\text{N}(\text{SiMe}_3)_2]_2$  as catalyst (at same reaction conditions) led to no change in the product yield (Table 2A.2.1, Entry 3). Furthermore, compounds  $\text{Mg}[\text{N}(\text{SiMe}_3)_2]_2$  and **1** were tested with less catalyst load of 0.1 % at reaction temperature 50 °C in thf (Table 2A.2.1, Entry 4 and 6) and also 0.5 % catalyst load at reaction temperature 60 °C without any solvent (Table 2A.2.1, Entry 5 and 7). From the above reactions, it is indicated that compound **1** slightly better catalyst than that of  $\text{Mg}[\text{N}(\text{SiMe}_3)_2]_2$ . In addition to this compound **1** catalyzed (1 mol %) guanylation reaction was performed in toluene and thf solvents at room temperature led to the formation of product in quantitative yield (Table 2A.2.1, Entry 8 and 9). The scope of compound *t*Bu: $\text{Mg}[\text{N}(\text{SiMe}_3)_2]_2$  (**1**) catalyzed addition of amines to carbodiimides was examined by taking examples of a wide variety of primary aromatic and cyclic secondary amines. The results are given in Tables 2A.2.2 and 2A.2.3. Herewith, worthy to mention that considering the same catalytic activities of both compounds **1** and **2** in the reaction of aniline with 1,3-diisopropylcarbodiimide (Table 2A.2.1, Entries 9,10 and 7, 11) for further reactions, selection of only compound **1** is justified.

**Table 2A.2.2** Results of reaction of various anilines with *N,N'*-dialkyl carbodiimides catalyzed by *t*Bu: $\text{Mg}[\text{N}(\text{SiMe}_3)_2]_2$  (**1**).



Entry	R	ArNH <sub>2</sub>	Temp (°C)	Time (min)	Product <sup>a</sup>	Yield (%) <sup>b</sup>
1	<i>i</i> -Pr		25	1	<b>1a</b>	94
2	Cy		25	40	<b>2a</b>	99
3	<i>i</i> -Pr		25	1	<b>3a</b>	97
4	Cy		25	60	<b>4a</b>	98
5	<i>i</i> -Pr		25	1	<b>5a</b>	97
6	Cy		25	10	<b>6a</b>	96
7	<i>i</i> -Pr		25	240	<b>7a</b>	97
8	Cy		60	720	<b>8a</b>	66
9	<i>i</i> -Pr		60	1440	<b>9a</b>	No reaction
10	<i>i</i> -Pr		25	60	<b>10a</b>	96
11	Cy		25	20	<b>11a</b>	96
12	<i>i</i> -Pr		25	120	<b>12a</b>	81
13	<i>i</i> -Pr		25	1	<b>13a</b>	94
14	Cy		25	10	<b>14a</b>	95
15	<i>i</i> -Pr		25	10	<b>15a</b>	96
16	Cy		25	5	<b>16a</b>	96
17	<i>i</i> -Pr		100	720	<b>17a</b>	86 <sup>c</sup>

<sup>a</sup> The reaction was performed by treating 1 equiv of aniline with 1 equiv of *N,N'*-diisopropylcarbodiimide.

<sup>b</sup> Isolated yield.

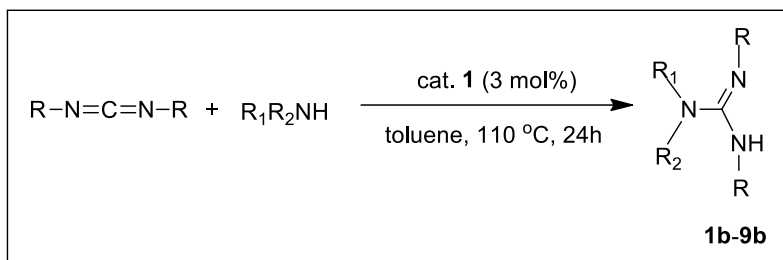
<sup>c</sup> The reaction was done in toluene, at 100 °C, 12 h.

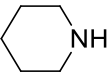
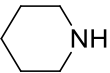
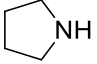
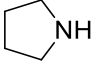
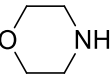
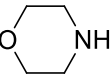
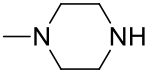
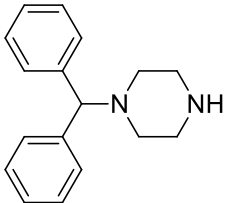
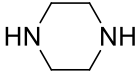
It is notable from Table 2A.2.2 that the catalyst **1** is compatible with various substituents on the phenyl ring such as –OCH<sub>3</sub>, CH<sub>3</sub>, Cl etc., and formation of corresponding *N,N,N'*-trisubstituted

guanidine products (**1a-17a**) in high yields, except **9a**. When the substituents on the phenyl ring are electron donating such as  $-\text{CH}_3$ ,  $-\text{OCH}_3$ , excellent yields were obtained at room temperature (Table 2A.2.2, Entries 3, 4 and 5, 6). In case of electron withdrawing substituent as Cl, on the phenyl ring, good yield (Table 2A.2.2, Entry 8) was obtained at room temperature. No product could be isolated from the reaction of 4- $\text{NO}_2$  aniline with isopropyl carbodiimide at 60 °C for 24 h (Table 2A.2.2, Entry 9) in presence of catalyst **1**. This indicates that the electronic factor has a great influence on the catalytic activity of the reaction.

The steric effect also shows influence on the catalytic reaction. The reaction of 2-methyl aniline with isopropyl carbodiimide produced almost quantitative yield (96 %) (Table 2A.2.2, Entry 10), while the reaction with 2,6-dimethyl aniline gave a good yield 81% over room temperature stirring for 2 h (Table 2A.2.2, Entry 12). Interestingly, if the methyl substituent at both ortho positions of the phenyl ring and more bulky alkyl group such as *tert*-butyl group at the para position of the phenyl ring led to the formation of expected product in quantitative yields (Table 2A.2.2, Entries 13-16). In fact the reaction of more bulky aniline, 2,6-diisopropylaniline with isopropyl carbodiimide requires higher temperature (Table 2A.2.2, Entry 17).

Furthermore, we examined the catalytic activity of compound **1** towards addition of various cyclic secondary amines with carbodiimides (Table 2A.2.3). *N,N,N'*-trisubstituted guanidine products (**1b-9b**) were obtained in good to excellent yields. However, the reaction generally requires a higher temperature 110 °C and longer reaction time 24 h for the completion. From the above results (Tables 2A.2.2 and 2A.2.3), it indicates that catalyst **1** is compatible towards hydroamination of various amines.

**Table 2A.2.3** Results of reaction of various cyclic secondary amines with *N,N'*-dialkyl carbodiimide catalyzed by **1**.

Entry	R	R <sub>1</sub> R <sub>2</sub> NH	Product <sup>a</sup>	Yield (%) <sup>b</sup>
1	<i>i</i> -Pr		<b>1b</b>	96
2	Cy		<b>2b</b>	96
3	<i>i</i> -Pr		<b>3b</b>	92
4	Cy		<b>4b</b>	95
5	<i>i</i> -Pr		<b>5b</b>	93
6	Cy		<b>6b</b>	96
7	<i>i</i> -Pr		<b>7b</b>	86
8	<i>i</i> -Pr		<b>8b</b>	97
9	<i>i</i> -Pr		<b>9b</b>	93

<sup>a</sup> Reaction was performed by treating 1 equiv of cyclic secondary amine with 1 equiv of carbodiimide.

<sup>b</sup> Isolated yield.

Based on the above results, a possible catalytic cycle for the addition of primary aromatic or cyclic secondary amines to carbodiimides is proposed in Figure 2A.2.1. The reaction of primary/secondary amine with NHC metal bis(amide) adduct gave the new bis(amido) intermediate **A** through an elimination of  $\text{NH}(\text{SiMe}_3)_2$ . The postulated intermediate **A** further

reacts with carbodiimide to produce metal guanidinate intermediate **B** through an insertion reaction. Interaction of metal guanidinate species **B** with amine releases the guanidine product along with the regeneration of the catalytically active species. For primary aromatic amines, a 1,3-H shift occurs to give the final stable guanylation product. Efforts were made to isolate and characterize the intermediates **A** and **B**, and turned to be unsuccessful.

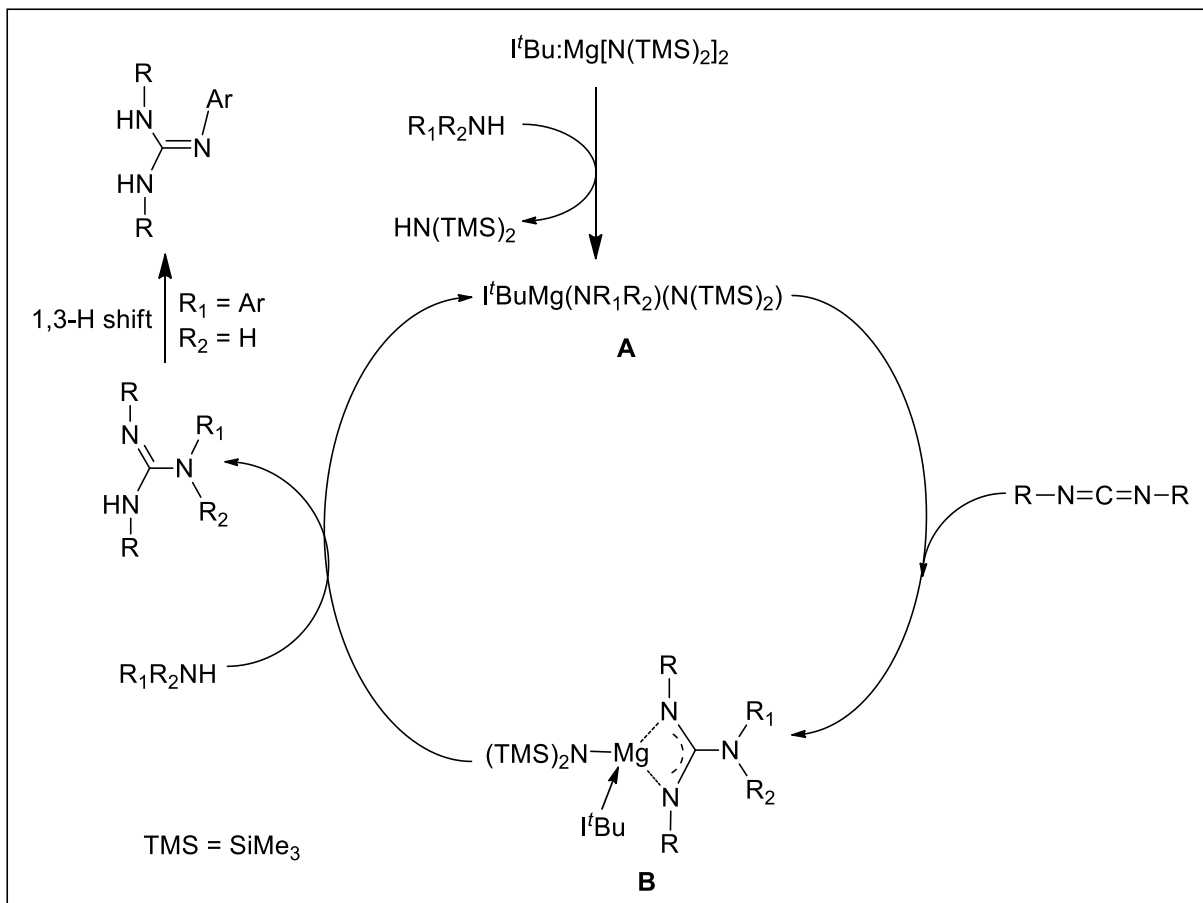


**Figure 2A.2.1** Proposed mechanism for the guanylation reaction catalyzed by the [tBu:Mg{N(SiMe<sub>3</sub>)<sub>2</sub>]<sub>2</sub>] (**1**)

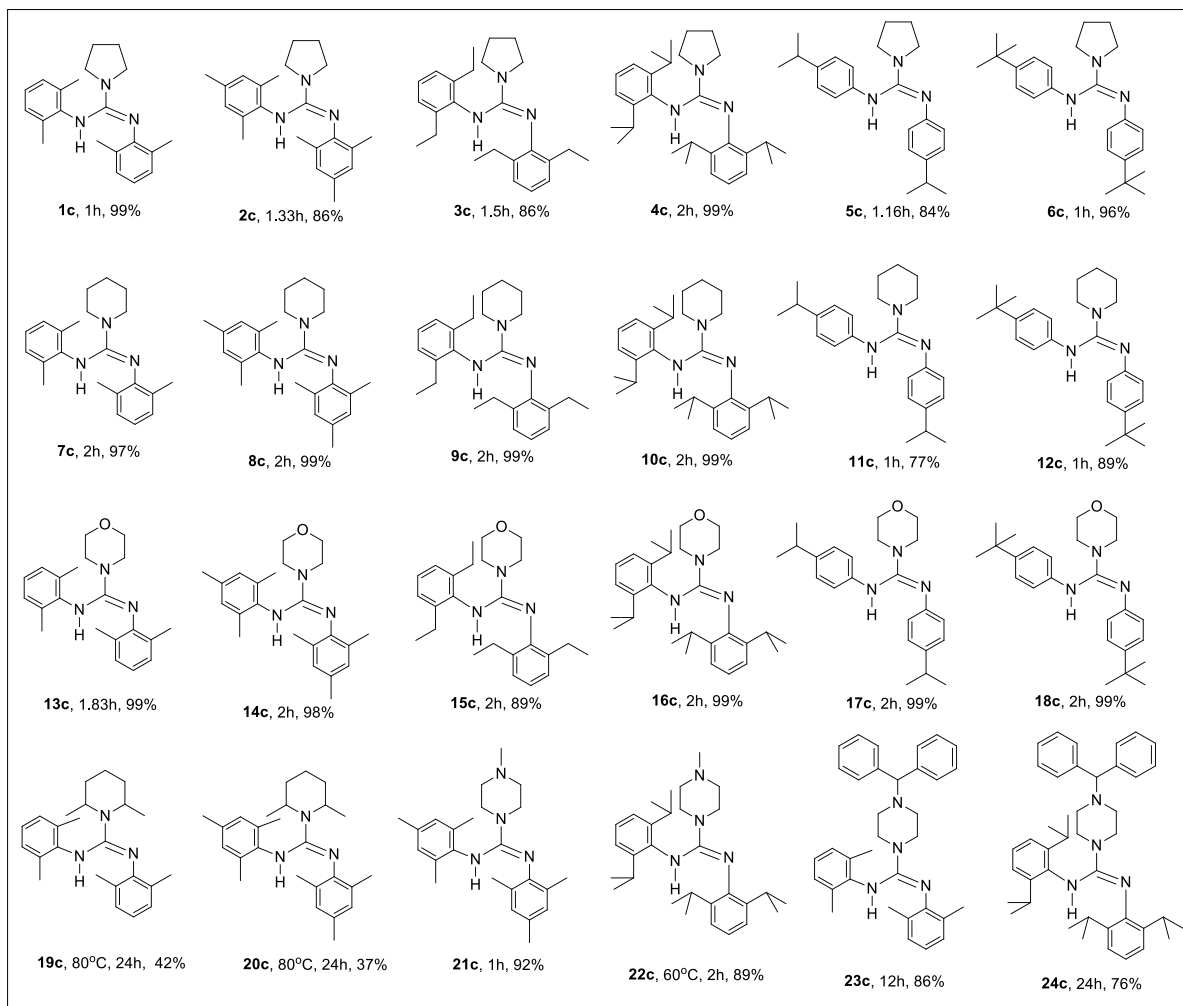
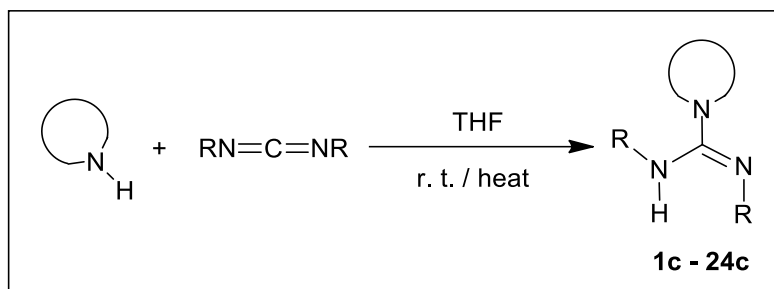
## Part B: Catalyst-free C–N bond formation by the reaction of amines with diimides; bulky guanidines

We have shown an atom economical and catalyst-free addition of cyclic secondary amines to various bulky aryl symmetrical and unsymmetrical carbodiimides to afford *N,N',N'',N''*-tetra substituted guanidines in quantitative yields at ambient reaction conditions. Furthermore, it was established that the addition of diamine to bulky aryl symmetrical carbodiimides (2 equiv.) led to the formation of bulky aryl biguanidines.

### 2B.1 Addition reaction of aromatic carbodiimides to cyclic secondary amines

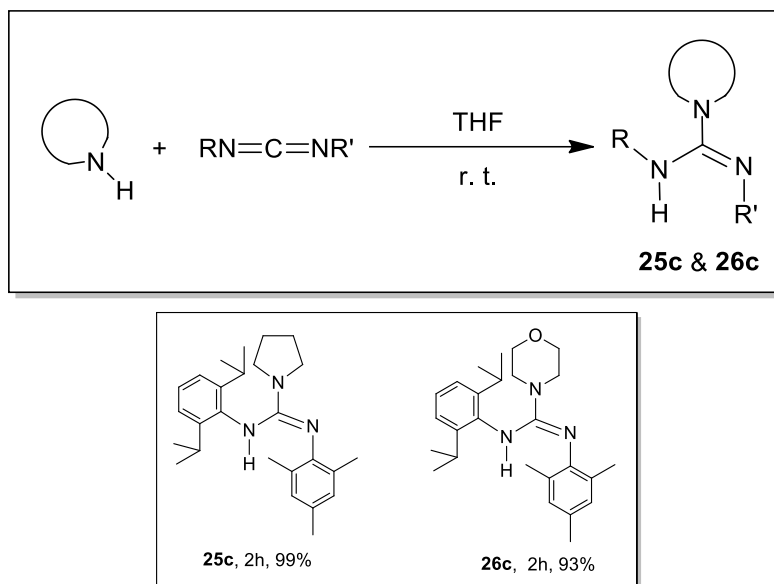
The sp hybridized carbon atom in the N=C=N core of carbodiimides is more electrophilic in *N,N'*-diaryl substituted carbodiimides when compared to aliphatic carbodiimides. Taking advantage of the high electrophilic nature of the carbon atom in the N=C=N moiety in *N,N'*-diaryl substituted carbodiimides,<sup>4</sup> we have treated cyclic secondary amines with various bulky aryl symmetrical and unsymmetrical carbodiimides to obtain tetra-substituted acyclic guanidines.<sup>5</sup>

Our investigations began with the reaction of *N,N'*-diaryl substituted carbodiimide with cyclic secondary amines at room temperature either in a hydrocarbon or ethereal solvent. We were pleased to notice that the cyclic secondary amines react with *N,N'*-diaryl substituted carbodiimides to give tetra-substituted guanidine at an ambient temperature condition (**1c-24c**, Table 2B.1.1) in very good to excellent yields, except for compounds **19c** and **20c**. The poor yield obtained for compounds **19c** (42 %) and **20c** (37 %) even at an elevated temperature was probably because of steric congestion. Thus in both cases, the ortho methyl substituent attached in the secondary amine (2,6-dimethylpiperidine) hinders the addition of the amine N–H bond to the C=N double bond of the carbodiimide.

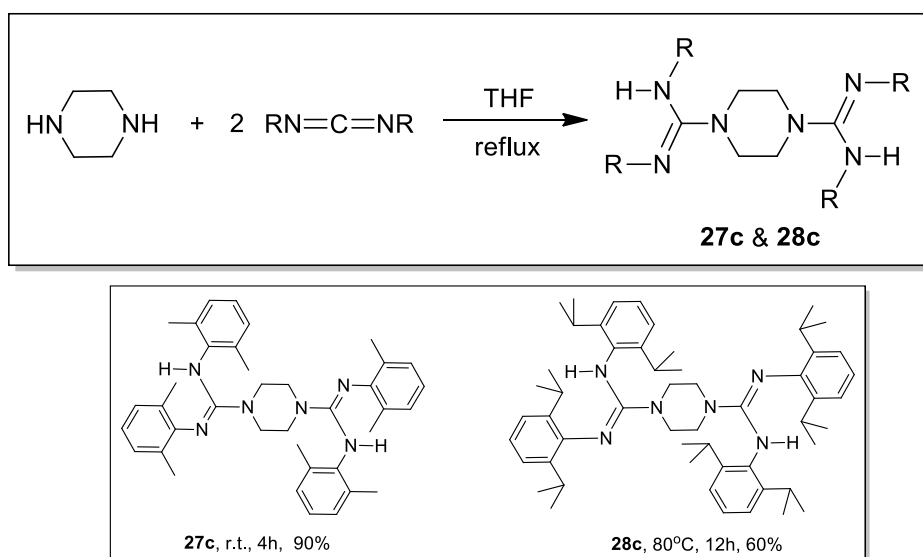
**Table 2B.1.1** Addition of cyclic secondary amines to symmetrical aryl carbodiimides <sup>a, b</sup><sup>a</sup> Unless otherwise mentioned all reactions were performed at room temperature,<sup>b</sup> Isolated yield.

After these results, we were interested in exploring the catalyst free addition of unsymmetrical *N,N*-diaryl substituted carbodiimide with cyclic secondary amines. To our delight those reactions resulted in excellent yields (**25c** & **26c**) (Table 2B.1.2).



**Table 2B.1.2** Addition of cyclic secondary amines to unsymmetrical aryl carbodiimides <sup>a</sup><sup>a</sup> Isolated yield.

Furthermore, the addition of two equivalents of symmetric *N,N*-diaryl substituted carbodiimide to one equivalent of piperazine in THF led to the formation of biguanidines (**27c** & **28c**) in moderate to good yields at room or reflux temperature (Table 2B.1.3).

**Table 2B.1.3** Synthesis of bulky aryl biguanidines <sup>a</sup><sup>a</sup> Isolated yield

**2B.2 Spectroscopic characterization:** All compounds (**1c-28c**) were characterized by  $^1\text{H}$ ,  $^{13}\text{C}$  NMR, IR and mass spectrometry analyses. Furthermore, the products **1c**, **22c** and **27c** have been confirmed by single crystal X-ray structural analysis.

For compounds **1c-24c**, they display simple  $^1\text{H}$  and  $^{13}\text{C}$  NMR spectra and this indicates the presence of only one isomer in the solution. In the  $^1\text{H}$  NMR spectra the singlet *NH* resonance has been observed in the range of 4.94–5.52 ppm for the symmetrical tetra-substituted guanidines (**1c-24c**). In case of the unsymmetrical tetra-substituted guanidines (**25c** & **26c**), the *NH* peak shows two broad singlet in the range of 4.96–5.10 ppm indicating the presence of two isomeric forms of guanidine in solution. In the biguanidines (**27c** & **28c**), both *NH* protons show a singlet peak at 5.03 ppm, which indicates the symmetrical behavior of the molecules and also that there is only one isomeric form i.e.,  $Z_{\text{anti}}$  in both of the guanidine moieties. In the  $^{13}\text{C}$  NMR spectra, all compounds (**1c-28c**) show a significant peak for the  $\text{N}_3\text{C}$  carbon atom in the range of 148.2–152.2 ppm, which is well in agreement with the reported guanidines (148–160 ppm).<sup>6</sup> And also, all compounds were confirmed by IR spectra, where it shows the *NH* and  $\text{C}=\text{N}$  functional group peaks in the range of 3317–3394  $\text{cm}^{-1}$  and 1610–1631  $\text{cm}^{-1}$  respectively. Furthermore, purity of newly synthesized compound was confirmed by HRMS analysis.

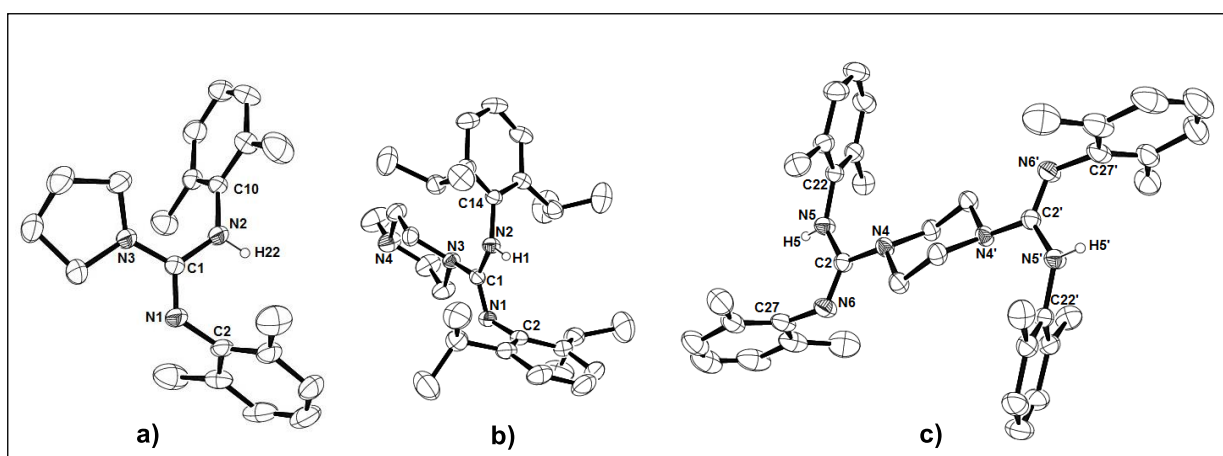


**Figure 2B.2.1** Molecular structures of a) **1c**, b) **22c** and c) **27c**, with 30 % probability density; H-atoms (except N–H bond) are omitted for clarity.

The molecular structures for **1c**, **22c** and **27c** are presented in Figure 2B.2.1 and selected bond lengths and angles are provided in the Table 2B.2.1. Concerning the tetra-substituted guanidines, the rotation and isomerization around the C–N & C=N bond, forms four different tautomeric structures as  $E_{syn}$ ,  $E_{anti}$ ,  $Z_{syn}$  &  $Z_{anti}$  (Figure 1.4.1.1).<sup>6</sup>

Analysis of the carbon-nitrogen bond distances for compounds **1c**, **22c** & **27c** distinguishes the C=N imine from the C–N amine bonds, 1.288(2), 1.281(19) & 1.273(18); 1.365(2), 1.380(19) & 1.396(18) Å respectively, which are very close to the typical C=N and C–N bond distances {(1.28 (C=N) and 1.38 (C–N) Å)}. Solid state structures for both compounds **1c** and **22c** exhibit the  $Z_{anti}$  conformation, where the central carbon atom is surrounded by three nitrogen atoms in a planar arrangement. It is found that the nitrogen atom part of the cyclic secondary amine is perpendicular to the N=C=N core of the carbodiimide moiety. Also the X-ray crystal structure for biguanidine (**27c**) reveals a  $Z_{anti}$ – $Z_{anti}$  conformation (Figure 2B.2.1).

**Table 2B.2.1** Selected bond lengths (Å) and bond angles (°) of compound **1c**, **22c** & **27c**

<b>1c</b>		<b>22c</b>		<b>27c</b>	
N–H	0.800	N–H	0.831	N–H	0.860
N(1)–C(1)	1.288(2)	N(1)–C(1)	1.2810(19)	C(2)–N(4)	1.3966(18)
N(2)–C(1)	1.365(2)	N(2)–C(1)	1.3805(19)	C(2)–N(6)	1.2734(18)
N(3)–C(1)	1.364(2)	N(3)–C(1)	1.3941(19)	C(2)–N(5)	1.3705(18)
N(1)–C(2)	1.397(3)	N(1)–C(2)	1.416(2)	C(22)–N(5)	1.4336(19)
N(2)–C(10)	1.431(2)	N(2)–C(14)	1.4370(19)	C(27)–N(6)	1.417(2)
N(1)–C(1)–N(2)	123.60(17)	N(1)–C(1)–N(2)	125.02(13)	N(6)–C(2)–N(5)	124.92(13)
N(1)–C(1)–N(3)	118.75(17)	N(1)–C(1)–N(3)	119.43(13)	N(6)–C(2)–N(4)	119.84(13)
N(3)–C(1)–N(2)	117.65(16)	N(3)–C(1)–N(2)	115.54(13)	N(5)–C(2)–N(4)	115.23(12)
C(1)–N(2)–C(10)	128.37(17)	C(1)–N(2)–C(14)	126.52(13)	C(2)–N(5)–C(22)	126.62(12)
C(1)–N(1)–C(2)	122.71(17)	C(1)–N(1)–C(2)	121.83(12)	C(2)–N(6)–C(27)	121.23(13)

Furthermore, we explored the possibility of catalyst-free addition of aromatic primary and acyclic secondary amines to *N,N'*-diaryl substituted carbodiimides to obtain tri- and tetra-substituted guanidines, respectively. The reaction between the acyclic secondary amine and *N,N'*-diaryl substituted carbodiimide resulted in a very poor yield at forced reaction conditions. However, the addition of aromatic amine to *N,N'*-diaryl substituted carbodiimide failed to produce the expected tri-substituted guanidine product, even at reflux temperature in either hydrocarbon or ethereal solvents. This is due to the decreased nucleophilicity of the aromatic amines in comparison to cyclic secondary amines.

**Conclusion:** In summary, we have synthesized and characterized *t*Bu supported magnesium (II) and zinc (II) bis(amide) complexes  $t\text{Bu}:\text{M}[\text{N}(\text{SiMe}_3)_2]_2$ ,  $\text{M} = \text{Mg}(\mathbf{1})$  &  $\text{Zn}(\mathbf{2})$ , by simple addition of 1,3-di-*tert*-butylimidazol-2-ylidene (*t*Bu) to the corresponding metal bis(amide). These NHC metal bis(amide) complexes exhibited catalytic activity toward addition of primary aromatic and cyclic secondary amines with aliphatic carbodiimides. Moreover, compound **1** is found to be compatible to a wide range of substrates and solvents.

Further, we have developed a straightforward and an atom economical, catalyst free C–N bond formation in a guanylation reaction by the addition of cyclic secondary amines to various bulky aryl symmetrical and unsymmetrical carbodiimides to afford tetra-substituted guanidines in quantitative yields at ambient reaction conditions.

**Crystal data and structural refinement details:****Table 2S.1** Crystal data and structural refinement summary for complexes **1** and **2**,

	<b>1</b>	<b>2</b>
Empirical formula	C <sub>23</sub> H <sub>56</sub> MgN <sub>4</sub> Si <sub>4</sub>	C <sub>23</sub> H <sub>56</sub> N <sub>4</sub> Si <sub>4</sub> Zn
CCDC	985052	985053
Formula weight	525.39	566.45
Crystal system	Monoclinic	Monoclinic
Space group	<i>P</i> 2(1)/n	<i>P</i> 2(1)
a(Å)	11.949(5)	11.334(5)
b(Å)	23.325(9)	12.060(5)
c(Å)	12.104(5)	11.995(5)
β (°)	95.190(5)	96.655(5)
V (Å <sup>3</sup> )	3360(2)	1628.5(12)
T (K)	100	100
Density (calc.) mg/m <sup>3</sup>	1.039	1.155
Z	4	2
F(000)	1160	616
No. of reflections collected	42181	18736
No. of independent reflections	6243 [R(int) = 0.0367]	6046 [R(int) = 0.1017]
λ (Å)	0.71073	0.71069
Absorption coefficient (mm <sup>-1</sup> )	0.212	0.918
Theta range (deg)	2.51 – 25.50	1.71 – 25.50
Goodness-of-fit on F <sup>2</sup>	1.022	0.859
R [I > 2σ (I)]	R1 = 0.0439, wR2 = 0.1089	R1 = 0.0538, wR2 = 0.1268
Largest diff. peak and hole (e.Å <sup>-3</sup> )	1.329, -0.999	1.268, -0.716

**Table 2S.2** Crystal data and structural refinement summary for compounds **1c**, **22c** & **27c**,

	<b>1c</b>	<b>22c</b>	<b>27c</b>
Empirical formula	C <sub>21</sub> H <sub>27</sub> N <sub>3</sub>	C <sub>30</sub> H <sub>46</sub> N <sub>4</sub>	C <sub>38</sub> H <sub>46</sub> N <sub>6</sub>
CCDC	1400660	1400662	1400661
Formula weight	321.46	462.71	586.81
Temperature, K	296(2)	296(2)	296(2)
Wavelength, Å	0.71073	0.71073	0.71073
Crystal system	Triclinic	Monoclinic	Monoclinic

## Chapter 2: Part B

Space group	<i>P</i> -1	<i>P</i> 2(1)/ <i>c</i>	<i>C</i> 2/ <i>c</i>
Unit cell dimensions (Å) & (°)	a = 8.443(2) b = 10.304(2) c = 12.134(2) $\alpha$ = 69.409(10) $\beta$ = 81.907(10) $\gamma$ = 77.454(10)	a = 9.405(2) b = 17.120(3) c = 18.715(3) $\alpha$ = 90 $\beta$ = 102.705 $\gamma$ = 90	a = 18.007(7) b = 13.927(7) c = 15.535(7) $\alpha$ = 90 $\beta$ = 113.869(4) $\gamma$ = 90
Volume, Å <sup>3</sup>	962.2(8)	2939.6(19)	3563.0(3)
Z	2	4	4
Density (calc.) mg/m <sup>3</sup>	1.110	1.046	1.094
Absorption coefficient, mm <sup>-1</sup>	0.066	0.062	0.065
F(000)	348	1016	1264
Crystal size, mm <sup>3</sup>	0.18 x 0.12 x 0.098	0.12 x 0.097 x 0.089	0.22 x 0.16 x 0.10
Theta range for data collection (°)	2.96 to 25.50	2.22 to 25.50	2.68 to 27.76
Index ranges	-10 ≤ h ≤ 10, -12 ≤ k ≤ 12, -14 ≤ l ≤ 14	-11 ≤ h ≤ 11, -20 ≤ k ≤ 20, -22 ≤ l ≤ 22	-23 ≤ h ≤ 23, -18 ≤ k ≤ 18, -18 ≤ l ≤ 20
Reflections collected	13541	42851	25181
Independent reflections	3582 [R(int) = 0.0280]	5475 [R(int) = 0.0382]	4188 [R(int) = 0.0542]
Completeness to theta = 25.50°	99.8 %	99.9 %	99.7 %
Max. and min. transmission	0.7461 and 0.7010	0.7461 and 0.6946	0.7456 and 0.7002
Data / restraints / parameters	3582 / 0 / 225	5475 / 0 / 320	4188 / 6 / 203
Goodness-of-fit on <i>F</i> <sup>2</sup>	1.041	1.052	1.039
Final R indices [I > 2σ(I)]	R1 = 0.0587, wR2 = 0.1640	R1 = 0.0549, wR2 = 0.1445	R1 = 0.0513, wR2 = 0.1291
R indices (all data)	R1 = 0.0810, wR2 = 0.1838	R1 = 0.0724, wR2 = 0.1691	R1 = 0.0885, wR2 = 0.1504
Largest diff. peak & hole, eÅ <sup>-3</sup>	0.369 and -0.206	0.283 and -0.369	0.156 and -0.179

**References:**

- (1) Cordero, B.; Gomez, V.; Platero-Prats, A. E.; Reves, M.; Echeverria, J.; Cremades, E.; Barragan, F.; Alvarez, S. *Dalton Trans.*, **2008**, 2832.
- (2) (a) Arduengo, A. J.; Davidson, F.; Krafczyk, R.; Marshall, W. J.; Tamm, M. *Organometallics*, **1998**, *17*, 3375; (b) Arrowsmith, M.; Hill, M. S.; MacDougall, D. J.; Mahon, M. F. *Angew. Chem. Int. Ed.*, **2009**, *48*, 4013; (c) Kennedy, A. R.; Klett, J.; Mulvey, R. E.; Robertson, S. D. *Eur. J. Inorg. Chem.*, **2011**, 4675; (d) Kennedy, A. R.; Mulvey, R. E.; Robertson, S. D. *Dalton Trans.*, **2010**, *39*, 9091.
- (3) Rit, A.; Spaniol, T. P.; Maron, L.; Okuda, J. *Angew. Chem. Int. Ed.*, **2013**, *52*, 4664.
- (4) Peddaraao, T.; Baishya, A.; Barman, M. K.; Kumar, A.; Nembenna, S. *New J. Chem.*, **2016**, *40*, 7627-7636.
- (5) Thomas, E. W.; Nishizawa, E. E.; Zimmermann, D. C.; Williams, D. J. *J. Med. Chem.*, **1989**, *32*, 228.
- (6) (a) Coles, M. P. *Dalton Trans.*, **2006**, 985; (b) Jin, G.; Jones, C.; Junk, P. C.; Lippert, K.-A.; Rose, R. P.; Stasch, A. *New J. Chem.*, **2009**, *33*, 64.

Chapter 3

**N-Heterocyclic carbene Adducts of Magnesium(II) and Zinc(II)  
Complexes: Synthesis, Reactivity and Theoretical studies**



**Part A: Structure, bonding and energetics of NHC stabilized low oxidation state Group 2 (Be, Mg, Ca, Sr and Ba) metal complexes; A theoretical study**

A series of N-heterocyclic carbene stabilized low oxidation state group 2 metal halide and hydrides with metal-metal bonds ( $[L(X)M-M(X)L]$ ; L = NHC  $[(CHNH)_2C:]$ , M = Be, Mg, Ca, Sr & Ba, and X = Cl or H) has been studied by computational methods. The main objective of this study is to predict whether it is possible to stabilize neutral ligated low oxidation state alkaline-earth metal complexes with metal-metal bonds. The homolytic metal-metal Bond Dissociation Energy (BDE) calculation, Natural Bond Orbital (NBO) and Energy Decomposition Analyses (EDA) on density functional theory (DFT) optimized  $[L(X)M-M(X)L]$  complexes reveal that they are as stable as their  $\beta$ -diketiminato, guanidinate and  $\alpha$ -diimine counterparts. The optimized structures of the complexes are in trans-linear geometries. The bond order analyses such as Wiberg Bond Indices (WBI) and Fuzzi Bond Order (FBO) confirm the existence of single bond between two metal atoms, and it is covalent in nature.

**3A.1 Structure:** The schematic representation of the  $[L(X)M-M(X)L]$  complex is shown in Figure 3A.1.1 (M = Be, Mg, Ca, Sr, & Ba; X = Cl and H; L = NHC).

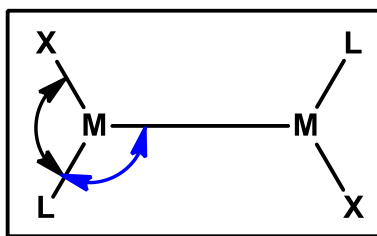


**Figure 3A.1.1** Schematic representation of  $[L(X)M-M(X)L]$  complex, where X = H or Cl, L = NHC, M = Be, Mg, Ca, Sr and Ba. The bond angles are indicated by double headed arrow.

The  $\omega$ -B97XD/def2-TZVP optimized structure of [(Cl)(NHC)Mg–Mg(NHC)(Cl)] and [(H)(NHC)Mg–Mg(NHC)(H)] complexes are shown in Figure 3A.1.2 along with the important structural parameters presented in Tables 3A.1.1 and 3A.1.2, respectively.

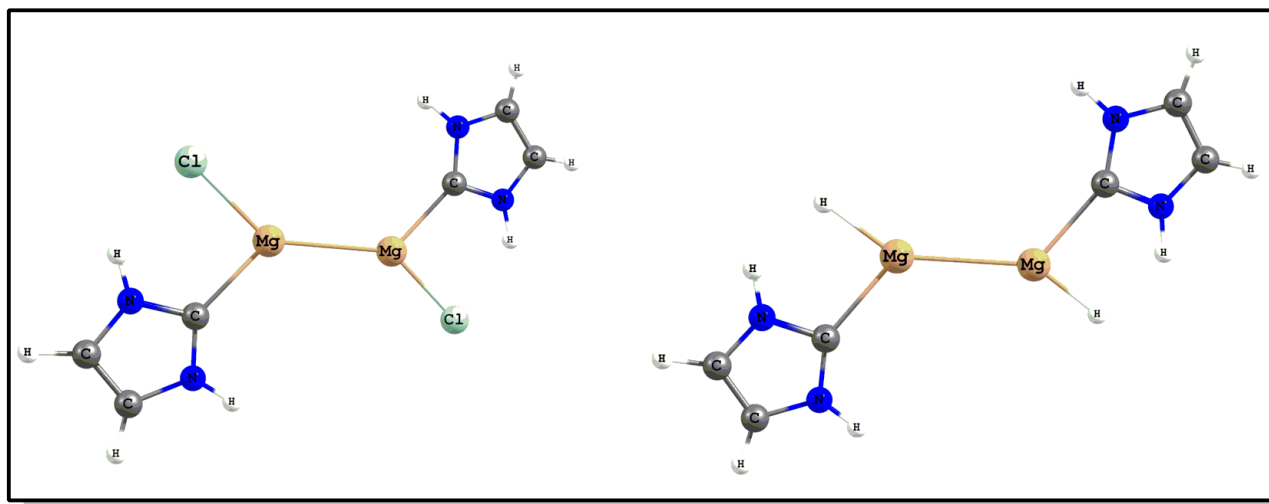


**Figure 3A.1.2**  $\omega$ -B97X-D/def2-TZVP-optimized geometries of [(Cl)(NHC)Mg–Mg(Cl)(NHC)] and [(H)(NHC)Mg–Mg(H)(NHC)]

**Table 3A.1.1** Selected bond lengths (Å), angles (°) and dihedral angles (°) in [(H)(NHC)M–M(H)(NHC)] as obtained from the  $\omega$ -B97X-D/def2-TZVP-optimized structures

Species	X = H, L = NHC					
	M-L	M-X	M-M	L-M-X	L-M-M	L-M-M-L
[(X)(L)Be–Be(L)(X)]	1.812	1.411	2.128	111.9	103.8	180.0
[(X)(L)Mg–Mg(L)(X)]	2.277	2.277	2.937	87.1	125.9	180.0
[(X)(L)Ca–Ca(L)(X)]	2.574	2.133	3.836	78.0	132.0	180.0
[(X)(L)Sr–Sr(L)(X)]	2.754	2.308	4.196	74.3	134.7	180.0
[(X)(L)Ba–Ba(L)(X)]	2.927	2.452	4.542	69.9	124.7	82.3

We have chosen  $\omega$ -B97X-D with def2-TZVP basis set for the geometry optimization and binding energy calculation as it is shown to predict bond dissociation energy (BDEs) of metal complexes within 1kcal/mol of CCSD(T) level BDEs.<sup>1</sup> The choice is further justified by comparing the computed structural parameters of a model compound  $K_2[(NHCH)_2Mg-Mg(NHCH)_2]$  with those of crystallographic data of  $[K(THF)_3]_2[LMg-MgL]$ ; (L= [(2,6-<sup>i</sup>Pr<sub>2</sub>C<sub>6</sub>H<sub>3</sub>)NC(Me)]<sub>2</sub><sup>2-</sup>).<sup>2</sup> The important structural parameters around the metal atoms are provided in Table 3A.1.3.

**Table 3A.1.2** Selected bond lengths (Å), angles (°) and dihedral angles (°) in [(Cl)(NHC)M-M(Cl)(NHC)] as obtained from the  $\omega$ -B97X-D/def2-TZVP optimized structures.

Species	X=Cl, L= NHC					
	M-L	M-X	M-M	L-M-X	L-M-M	L-M-M-L
[(X)(L)Be-Be(L)(X)]	1.792	1.977	2.128	113.3	116.06	180.0
[(X)(L)Mg-Mg(L)(X)]	2.245	2.341	2.881	92.1	133.302	180.0
[(X)(L)Ca-Ca(L)(X)]	2.563	2.580	3.788	84.7	127.054	180.0
[(X)(L)Sr-Sr(L)(X)]	2.754	2.740	4.148	81.1	134.257	168.8
[(X)(L)Ba-Ba(L)(X)]	2.913	2.878	4.507	77.1	113.942	106.6

It can be seen from the tables that  $\omega$ -B97X-D/def2-TZVP is good enough to predict the structure of alkaline earth metal complexes. Except the Ba complexes (see the dihedral angle L-M-M-L in Table 3A.1.1 and 3A.1.2), all other complexes are trans linear structure. Longer bond distances of M-L, M-X and M-M bonds were observed, when going down the group (Be to Ba). The M-M and M-L bond lengths of [(Cl)(NHC)M-M(NHC)(Cl)] are slightly shorter than the corresponding M-M bond length in [(H)(NHC)Mg-Mg(NHC)(H)], suggesting that Cl atoms

strengthen both M–M and M–L bonds. This is further confirmed by NBO analysis and BDEs, *vide infra*. The M–M bond distances can be compared with those of  $\alpha$ -diimine complexes of alkaline earth metals. The NHC stabilized M–M bonds are slight shorter than  $\alpha$ -Diimine complexes.<sup>2-3</sup> The computed Mg–Mg bond distances are within the range 2.845–3.196 Å observed experimentally for binuclear Mg complexes.<sup>4</sup> The structural analysis of the optimized metal complexes provides a direct clue that NHC stabilized Group 2 binuclear metal complexes can be synthesized in the laboratory.

**Table 3A.1.3** Selected bond lengths (Å) and angles (°) in  $K_2[(CHNH)_2Mg-Mg(CHNH)_2]$  and compared with the corresponding crystallographic data<sup>2</sup> [ $K(THF)_3$ ]<sub>2</sub>[LMg–MgL]; (L= [(2,6-*i*-Pr<sub>2</sub>C<sub>6</sub>H<sub>3</sub>)NC(Me)]<sub>2</sub><sup>2-</sup>).

Methods	$K_2[(CHNH)_2Mg-Mg(CHNH)_2]$			
	Mg-Mg	Mg-N	N-Mg-Mg	N-Mg-N
<b>Theoretical</b> ( $\omega$ -B97X-D/def2-TZVP)	2.939	2.045	135.8	81.2
<b>Experimental</b>	2.937	2.047 <sup>a</sup>	138.9 <sup>a</sup>	81.5 <sup>a</sup>

<sup>[a]</sup> Arithmetic mean of the two bond lengths/angles.

**3A.2 Bonding:** The natural bond orbital analysis has been performed to understand the bonding nature of these complexes. The Wiberg bond indices (WBI) and the charge on the metal atom are presented in Table 3A.2.1.

The WBI of M–M bonds are very close to one (0.932–0.975). This indicates the presence of single bond between two metal atoms and it is covalent in nature. The WBI of M–X bond except Be complexes are below 0.5, suggesting these bonds are weaker than M–M bond, can be coordinate bonds rather than covalent bonds.

**Table 3A.2.1** The Wiberg Bond Index (WBI) of metal-metal bond (M–M) and natural charge of metal ( $q_M$ ) in [(X)(L)M–M(L)(X)] complexes.

Species	X = H, L = NHC		X=Cl, L= NHC	
	WBI (M-M)	q (M)	WBI (M-M)	q (M)
[(X)(L)Be–Be(L)(X)]	0.942	0.146	0.942	0.295
[(X)(L)Mg–Mg(L)(X)]	0.933	0.477	0.933	0.581
[(X)(L)Ca–Ca(L)(X)]	0.935	0.606	0.964	0.627
[(X)(L)Sr–Sr(L)(X)]	0.932	0.676	0.963	0.692
[(X)(L)Ba–Ba(L)(X)]	0.940	0.713	0.975	0.739

In addition, Fuzzy bond order (FBO) analysis was done with Multiwfn software.<sup>5</sup> The FBO bond order has been found to be more accurate and appropriate over Mayer bond order and AIM indices. It is also relatively less sensitive to basis functions.<sup>6</sup> The FBO is also consistent with WBI. The donor-acceptor NBO second order interaction ( $\Delta E_{ij}$ )<sup>7</sup> energies have also been estimated. It is noticed that there is non-covalent interaction between N–H group of NHC and X, forming some short of weak hydrogen/dihydrogen bonds. For instance, in [(X)(L)Mg–Mg(L)(X)] complexes, lone pair (LP) of the Cl atom ( $LP_{Cl}$ ) interacts with the sigma anti bonding orbital of N–H bond ( $\sigma^*_{N-H}$ ), similarly the sigma bonding orbital of Mg–H ( $\sigma_{Mg-H}$ ) interacts with the  $\sigma^*_{N-H}$ . The  $\Delta E_{ij}$  values for the above mentioned two interactions are 3.9 and 4.2 kJ/mol, respectively. The striking results obtained from the NBO analysis is the strengthening of the M–M bond by the presence of Cl atoms. This is confirmed by the donor-acceptor interaction energy between Cl and metal atoms. The  $LP_{Cl}$  interacts with the sigma anti bonding orbital of M–C<sub>NHC</sub> ( $\sigma^*_{M-C}$ ) bond and with the empty non-lewis NBOs of the metals atoms ( $LP^*_M$ ). The interaction energy for  $LP_{Cl}$  and  $\sigma^*_{M-C}$  is 17.62 kJ/mol, while that is 88.63 kJ/mol for  $LP_{Cl}$  and  $LP^*_{Mg}$  interaction. The

low oxidation state of the metal in the complexes is verified by the natural population analysis within the NBO frame work. The natural charge so obtained is tabulated in Table 3A.2.1. The natural charge of metals ( $q_M$ ) except Be is within the range of +0.45 to +0.75 au and  $q_H$  and  $q_{Cl}$  values range from -0.43 to -0.75 and -0.58 to -0.82, respectively. The low positive charge on metal atom suggests that they are in low oxidation state (+1).

**3A.3 Energetics:** The dimerization energies or metal-metal bond dissociation energies (BDEs) of the complexes were calculated using the dimerization scheme as  $[(X)(L)M-M(L)(X)] = 2[(X)(L)M]$ . The zero point vibrational energy (ZPVE) contribution is also incorporated in all BDE calculations. The BDE, enthalpy ( $\Delta H$ ) and free energy ( $\Delta G$ ) of bond dissociation are given in Table 3A.3.1.

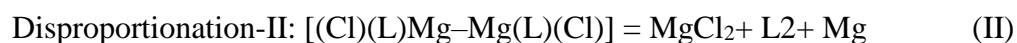
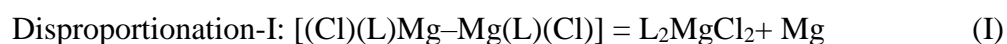
**Table 3A.3.1**  $\omega$ -B97X-D/def2-TZVP calculated bond dissociation energies (BDE in kJ/mol), enthalpy ( $\Delta H$  in kJ/mol) and free energies ( $\Delta G$  in kJ/mol) of the fragmentation of the complex  $[(X)(L)M-M(L)(X)] \rightarrow 2[(X)(L)M]$ .

Species	X = H, L = NHC			X=Cl, L=NHC		
	BDE	$\Delta H$	$\Delta G$	BDE	$\Delta H$	$\Delta G$
$[(X)(L)Be-Be(L)(X)]$	-189.1	-193.8	-138.6	-296.7	-295.6	-247.8
$[(X)(L)Mg-Mg(L)(X)]$	-193.3	-191.7	-149.2	-211.8	-209.5	-166.1
$[(X)(L)Ca-Ca(L)(X)]$	-144.2	-141.0	-108.6	-152.5	-149.0	-113.4
$[(X)(L)Sr-Sr(L)(X)]$	-126.7	-123.8	-84.6	-136.1	-132.1	-98.0
$[(X)(L)Ba-Ba(L)(X)]$	-120.4	-117.7	-75.6	-127.3	-124.0	-83.2

To ensure about the reliability of current level of theory in predicting BDE correctly, the BDE for  $Mg_2Cl_2$  has been calculated and compared with the experimental value obtained from

Mg–Mg stretching vibration and its overtones.<sup>8</sup> The computed value of Mg–Mg bond energy in Mg<sub>2</sub>Cl<sub>2</sub> (–198.8 kJ/mol) is about 2 kJ/mol higher than the experimental value (–197 kJ/mol). This establishes that the current level of theory can be used for the precise prediction of BDEs. The BDE, ΔH and ΔG decreases down the group i.e. from Be–Be to Ba–Ba. This trend was previously reported in other complexes of binuclear alkaline earth metals. The M–M BDE for [(Cl)(NHC)M–M(NHC)(Cl)] are higher compared to that of [(H)(NHC)M–M(NHC)(H)] complexes. This has already been noticed in shorter M–M bond length in [(Cl)(NHC)M–M(NHC)(Cl)] than in [(H)(NHC)M–M(NHC)(H)] complexes. The reason for larger BDE in [(Cl)(NHC)M–M(NHC)(Cl)] is the LP<sub>Cl</sub> and LP\*<sub>M</sub> interactions which is lacking in [(H)(NHC)M–M(NHC)(H)] complexes (vide supra).

The disproportionation of [(Cl)(L)Mg–Mg(L)(Cl)] has also been considered for the comparison with the dimerization. The disproportionation energy (DPE) has been determined by the two schemes (I & II) shown below-



The disproportionation energy, enthalpy and free energy are given in Table 3A.3.2. For the scheme I the DPE is endothermic and for scheme II it is exothermic. However, the exothermic disproportionation energy (~-75 kJ/mol) is almost one-third of the BDE and half of atomization energy (~-148 kJ/mol) of (Mg)<sub>n</sub> cluster. Comparing these values (Scheme I and II) with the dimerization energy, it can be concluded that dimerization is thermodynamically more favorable than the disproportionation.

To understand the nature of the M–M bond and contribution of different energy components such as the electrostatic energy ( $\Delta E_{ES}$ ), the exchange energy ( $\Delta E_{EX}$ ), the repulsion energy ( $\Delta E_{Rep}$ ), the polarization energy ( $\Delta E_{PL}$ ) and the dispersion energy ( $\Delta E_{Disp}$ ) to the total interaction energy ( $\Delta E_{Int}$ ), LMO-EDA calculation was performed at the B97-D/def2-TZVP level. The different energy contributions for [(Cl)(NHC)Mg–Mg(NHC)(Cl)] and [(H)(NHC)Mg–Mg(NHC)(H)] are represented graphically in Figure 3A.3.1.

**Table 3A.3.2** Comparison of the  $\omega$ -B97X-D/def2-TZVP-estimation of bond dissociation energy, enthalpy, free energy with disproportionation energy, enthalpy, free energy (all the energies and enthalpy are in kJ/mol). The atomic energy of Mg atom was taken from reference.<sup>8</sup>

[(Cl)(L)Mg–Mg(L)(Cl)], L=NHC	$\Delta E$ (ZPE)	$\Delta H$	$\Delta G$
Dimerisation, [(Cl)(L)Mg–Mg(L)(Cl)] = 2(Cl)(L)Mg	-211.8	-209.5	-166.1
Disproportionation-I, [(Cl)(L)Mg–Mg(L)(Cl)] = L <sub>2</sub> MgCl <sub>2</sub> + Mg	193.1	198.6	181.3
Disproportionation-II, [(Cl)(L)Mg–Mg(L)(Cl)] = MgCl <sub>2</sub> + L <sub>2</sub> + Mg	-74.6	-68.4	-47.9

It can be seen from the LMO-EDA that the Mg–Mg interaction is not completely electrostatic in nature, although it is the major contributor to the total interaction energy. The contributions from polarization as well as from dispersion are also significant. The polarization and dispersion energy contribution for [(Cl)(NHC)Mg–Mg(NHC)(Cl)] is ~21 kJ/mol more than



that for [(H)(NHC)Mg–Mg(NHC)(H)] which also accounts for the  $\sim 27$  kJ/mol total interaction energy difference between these two complexes.

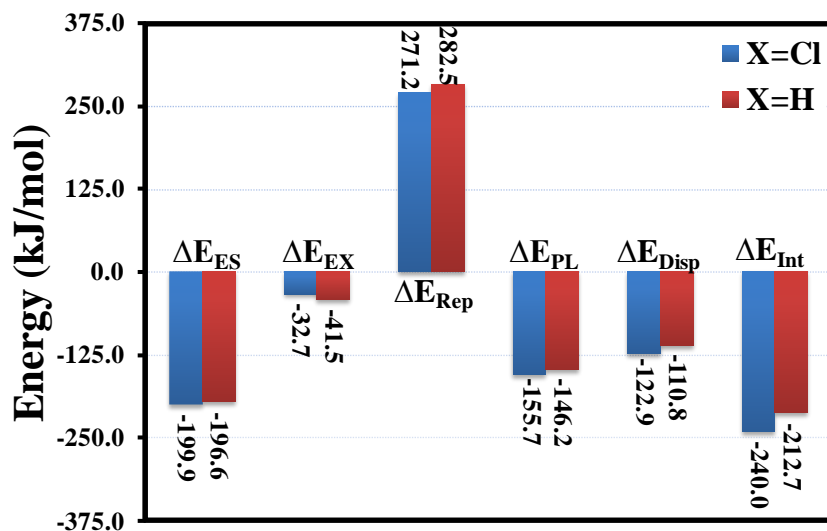


**Figure 3A.3.1** Different energy components as obtained from LMO-EDA calculation at the  $\omega$ -B97X-D/def2-TZVP level of theory for [(Cl)(NHC)Mg–Mg(Cl)(NHC)] and [(H)(NHC)Mg–Mg(H)(NHC)].

Finally a comparative study of NHC stabilized Mg(I)–Mg(I) complexes and CpMg–MgCp and Na<sub>2</sub>[(NHCH)<sub>2</sub>Mg–Mg(NHCH)<sub>2</sub>] is presented. The  $\omega$ -B97X-D/def2-TZVP level of theory was used for the geometry optimization, WBI and BDE calculation of the complexes. These values along with previously reported values are presented in Table 3A.3.3. The BDEs of [(Cl)(NHC)Mg–Mg(NHC)(Cl)] and CpMg–MgCp are  $\sim 210$  kJ/mol while those for [(H)(NHC)Mg–Mg(NHC)(H)] and Na<sub>2</sub>[(NHCH)<sub>2</sub>Mg–Mg(NHCH)<sub>2</sub>] are  $\sim 190$  kJ/mol. The BDEs of CpMg–MgCp and Na<sub>2</sub>[(NHCH)<sub>2</sub>Mg–Mg(NHCH)<sub>2</sub>] at the  $\omega$ -B97X-D/def2-TZVP level are  $\sim 20$  kJ/mol more than those obtained at the BP86/TZ2P<sup>9</sup> and B3LYP/def2TZVPP<sup>10</sup> level of theory, respectively. However, the trend of stabilization of the complexes follows the same order

irrespective of the level of theory. The BDEs of [(Cl)(NHC)Mg–Mg(NHC)(Cl)] and [(H)(NHC)Mg–Mg(NHC)(H)] at B3LYP/def2-TZVP level are -193.5 and -175.7 kJ/mol respectively and those at the BP86/def2-TZVP level are -188.1 and -173.0 kJ/mol, respectively. The WBI of all the complexes are very close to one which infers that NHC stabilized low oxidation state binuclear Mg–Mg complexes are stable and can be synthesized in the laboratory.

**Table 3A.3.3** Comparison of the  $\omega$ -B97X-D/def2-TZVP estimation of bond dissociation energy (BDE in kJ/mol), Wiberg Bond Index and bond length (Å) of Mg–Mg bond with those in the related Mg(I)–Mg(I) systems reported in the literature.

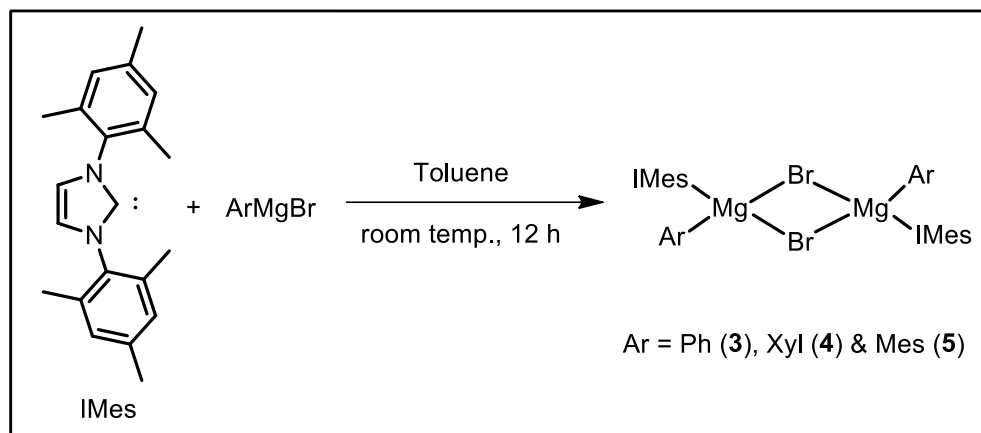
Species	This Work			Previous Work		
	Mg-Mg	BDE	WBI (Mg-Mg)	Mg-Mg	BDE	WBI (Mg-Mg)
(H)(NHC)Mg–Mg(H)(NHC)	2.937	-193.3	0.933			
(Cl)(NHC)Mg–Mg(Cl)(NHC)	2.881	-211.8	0.942			
CpMg–MgCp	2.811	-210.3	0.986	2.790	-186.35	
Na <sub>2</sub> [(CHNH) <sub>2</sub> Mg–Mg(CHNH) <sub>2</sub> ]	2.921	-193.0	0.921	2.887	-167.36	0.886

## Part B: IMes adducts of organo-magnesium(II) complexes: Synthesis, characterization and reactivity studies

The first examples of structurally characterized products of magnesium mediated ( $sp^3$ ) CH bond activation of IMes [IMes = {1,3-bis-(2,4,6-trimethylphenyl)imidazol-2-ylidene}] ligand have been reported. Six membered cyclometalated complexes of organo magnesium(II) [ $\{\text{IMesMg}(\text{IMes}')\text{Ar}\}$ ] {Ar = 2,6-dimethylphenyl (Xyl); **(7)** and 2,4,6-trimethylphenyl (Mes); **(8)**}, have been isolated in presence of neutral, IMes, monoanionic C,C-chelated ( $\text{IMes}'$ ) [ $\text{IMes}' = \{1-(2,4,6\text{-trimethylphenyl})-3-(3,5\text{-dimethylbenzyl})\text{-imidazol-2-ylidene}$  and terminal aryl group as ligand sets. IMes supported aryl magnesium(II) bromide [ $\{\text{IMesMg}(\text{Ar})\text{Br}\}_2$ ] {Ar = Xyl **(4)** and Mes **(5)**} complexes upon reduction with sodium metal led to the formation of compounds **7** and **8**, respectively. The reaction proceeds *via* insertion of *in situ* generated organo Mg(I) radical into CH bond, thereby, magnesium mediated intramolecular  $sp^3(\text{C-H})$  bond activation of one ortho methyl group of IMes occurs.

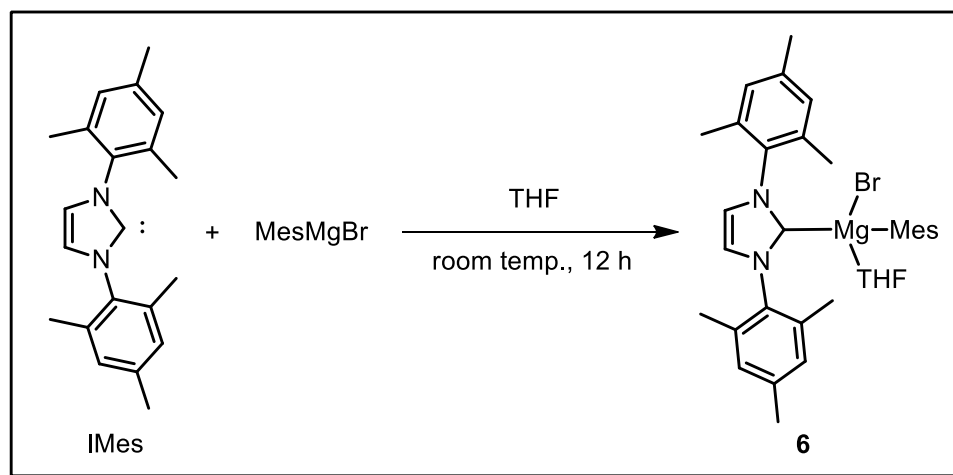
### 3B.1 Reactions of IMes with $\text{ArMgBr}$ (Ar = Ph, Xyl & Mes)

**3B.1.1 Synthesis:** The reaction between unsaturated NHC *i.e.*, IMes and a series of commercially available aryl Grignard reagents with a 1:1 molar ratio in toluene at room temperature, led to the formation of IMes adduct of organo-magnesium(II) halide complexes, [ $\{\text{IMesMg}(\text{Ar})\text{Br}\}_2$ ] {Ar = Ph **(3)**; Xyl **(4)**; Mes **(5)**} in moderate to good yields (Scheme 3B.1.1.1). We noticed the high yield formation of NHC adduct of aryl-magnesium(II) halides when more bulky aryl-magnesium(II) bromide reagents are treated with IMes when compared to less bulky aryl magnesium halide ( $\text{ArMgBr}$ ; Ar = Ph < Xyl < Mes).



**Scheme 3B.1.1.1** Synthesis of  $[\{\text{IMesMg}(\text{Ar})\text{Br}\}_2]$ ; Ar = Ph (3), Xyl (4) & Mes (5).

A similar stoichiometric reaction of IMes with MesMgBr (1M in THF) in tetrahydrofuran (THF) is carried out to afford the THF co-ordinated product **6**,  $[\text{IMesMg}(\text{Mes})\text{Br}(\text{THF})]$  (Scheme 3B.1.1.2). Subsequently, compound **6** can also be obtained from the re-crystallization of dimeric compound of IMes supported organo-magnesium(II) bromide **5**,  $[\{\text{IMesMg}(\text{Mes})\text{Br}\}_2]$  in THF.



**Scheme 3B.1.1.2** Synthesis of  $[\text{IMesMg}(\text{Mes})\text{Br}(\text{THF})]$  (**6**).

**3B.1.2 Spectroscopic characterization:** All these compounds, **3-6** are characterized by both NMR and single crystal X-ray structure analyses. The  $^1\text{H}$  NMR studies for compounds **3-5** in benzene- $d_6$  at room temperature exhibits a singlet resonances at 5.88, 5.90 & 5.88 ppm corresponding to imidazole backbone  $\{\text{NC}(\text{H})\}$  proton (6.47 ppm for IMes), respectively. The

appearances of singlet resonance for backbone CH of the imidazole ring for compounds **3-5** indicate the symmetric nature of the molecules. In contrast, compound **6** displays two sets of resonances at 5.93 and 6.11 ppm in the  $^1\text{H}$  NMR spectrum, each corresponding to one of the imidazole backbone {NC(H)} proton, indicates the asymmetric behavior of the molecule in solution. The characteristic peak for carbene carbon in  $^{13}\text{C}\{^1\text{H}\}$  NMR spectra resonances at 182.6, 182.9 and 183.0 ppm, which are 36.7, 36.5 and 36.0 ppm value shifted to un-coordinated IMes (219.4 ppm) for compound **3**, **4** and **5**, respectively. The  $^{13}\text{C}\{^1\text{H}\}$  NMR spectrum of compound **6** exhibit two peaks at 183.06 and 186.31 ppm for carbene carbon, are in consistent with the resonances of NHC-metal complexes and confirms the presence of two isomeric forms in solution state, (Figure 3B.1.2.1) and is probably due to mesityl group exchange.<sup>11</sup>

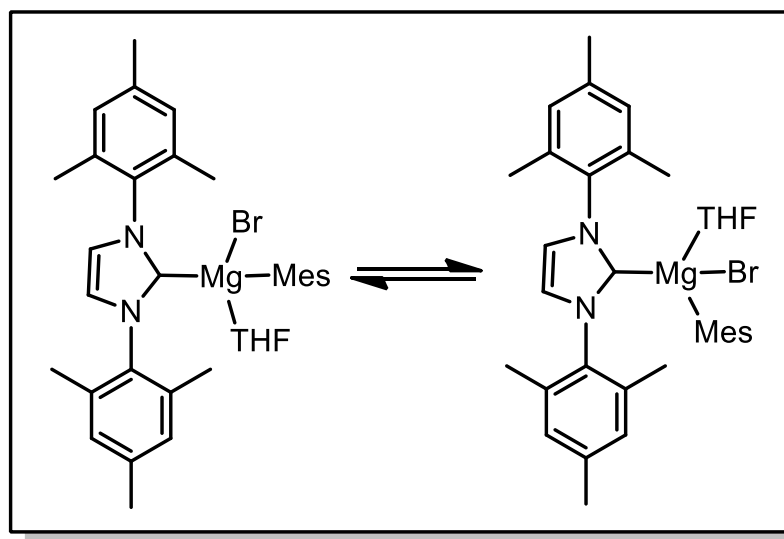


**Figure 3B.1.2.1** Isomeric forms of [IMesMg(Mes)Br(THF)].

Elemental analysis has been performed for compounds **3-6** to confirm the composition of the molecules and are found in good agreements to the calculated value (despite several attempts, accurate elemental analysis could not be obtained for compounds **4**, **5** and **6**).

**3B.1.3 Crystallographic characterization:** Colorless compounds of **3-5** are crystallized from a saturated benzene solution (65 °C to room temp.; slow cooling) and elucidated by single crystal X-ray structure analyses.

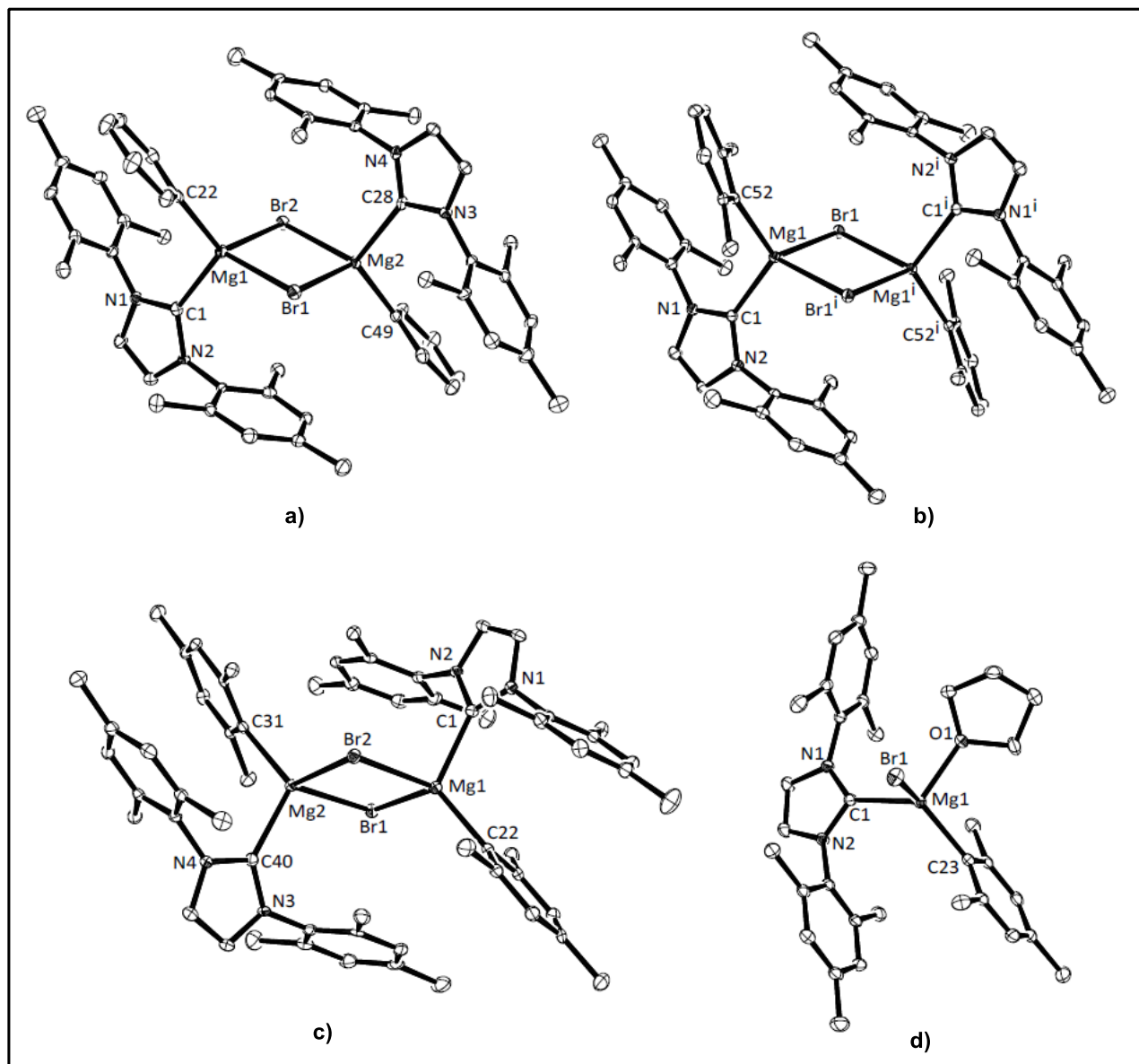


**Figure 3B.1.3.1** Molecular structures of a)  $[\{\text{IMesMg}(\text{Ph})\text{Br}\}_2]$  (**3**), b)  $[\{\text{IMesMg}(\text{Xyl})\text{Br}\}_2]$  (**4**), c)  $[\{\text{IMesMg}(\text{Mes})\text{Br}\}_2]$  (**5**) and d)  $[\text{IMesMg}(\text{Mes})\text{Br}(\text{THF})]$  (**6**) (ORTEP view, 35% probability ellipsoid), with selected atom labels. Hydrogen atoms are omitted for clarity.

The solid state structures of IMes supported organo-magnesium(II) bromide adducts **3-5** are shown in Figure 3B.1.3.1 with selected bond parameters in Table 3B.1.3.1. Compound **3** crystallizes in triclinic  $P\bar{1}$  space group and molecular structure reveals the dimeric form of the molecules, in which the bromine atoms are in bridging position to the magnesium centers. The magnesium atoms in compound **3** is tetra co-ordinated with NHC-metal-aryl bond angles around magnesium center is C1-Mg1-C22 115.1(4) and close to 120 ( $^{\circ}$ ), displays the distorted structure of compound **3** from the tetrahedral geometry. The magnesium atom in compound **3** is surrounded by anionic ligands, a halide and an aryl group and a neutral IMes ligand. The carbene-metal ( $C_{\text{IMes}}\text{-Mg}$ ) bond distance in complex **3**, C1-Mg1 2.229(9) ( $\text{\AA}$ ) is good in agreement with known value of  $C_{\text{NHC}}\text{-Mg}$  bond distances (2.194-2.279  $\text{\AA}$ ).<sup>12</sup> The metal-aryl carbon bond distances in complex **3**, Mg1-C22 2.132(10) ( $\text{\AA}$ ) is slightly shorter than the known value of magnesium-carbon bond distances (2.20  $\text{\AA}$ ).

The molecular structures of  $[\{\text{IMesMg}(\text{Xyl})\text{Br}\}_2]$  (**4**) and  $[\{\text{IMesMg}(\text{Xyl})\text{Br}\}_2]$  (**5**) are consistent with compound **3**, whereas the compound **6**,  $[\text{IMesMg}(\text{Mes})\text{Br}(\text{THF})]$  displays the monomeric form of the molecule, in which the magnesium atom is in distorted tetrahedral geometry with +2 oxidation state. Compounds **4**, **5** & **6** crystallize in monoclinic  $P2_1/c$ , monoclinic  $P2_1/c$  and triclinic  $P\bar{1}$  space groups, respectively.

The carbene-metal ( $C_{\text{IMes}}\text{-Mg}$ ) bond distances in complexes (**4-6**), **4**: 2.225(2); **5**: 2.233(4) & **6**: 2.232(2) ( $\text{\AA}$ ) are similar with  $C_{\text{IMes}}\text{-Mg}$  bond distance of compound **3** (C1-Mg1 2.229(9) ( $\text{\AA}$ )). The metal-aryl carbon ( $\text{Mg-C}_{\text{Ar}}$ ) bond distance for compounds **4**, **5** and **6** are 2.1574(19), 2.149(4) and 2.166(2) ( $\text{\AA}$ ) respectively, are close to the metal-aryl carbon bond distance Mg1-C22 2.132(10) of compound **3**. The bridging Mg-Br bond distance in compounds **3**: 2.579(3); **4**: 2.592(12) & **5**: 2.561(12) ( $\text{\AA}$ ), are slightly longer than that of terminal Mg-Br

bond distance in compound **6**: 2.509(11) Å. The IMes-metal-aryl bond angle around magnesium center i.e. C<sub>IMes</sub>-Mg-C<sub>Ar</sub> are 118.61(7), 117.00(14) & 115.22(8) (°), respectively for compounds **4**, **5** & **6**, are in agreement with the distorted tetrahedral geometry.

**Table 3B.1.3.1** Selected bond lengths (Å) and angles (°) for compounds **3-6**

<b>3</b>		<b>4</b>	
C1-Mg1	2.229(9)	C1-Mg1	2.225(2)
Mg1-Br1	2.579(3)	Mg1-Br1	2.5928(12)
Mg1-C22	2.132(10)	Mg1-C52	2.1574(19)
C1-Mg1-C22	115.1(4)	C1-Mg1-C52	118.61(7)
C1-Mg1-Br2	101.4(3)	C1-Mg1-Br1	104.07(5)
C22-Mg1-Br2	120.4(3)	C52-Mg1-Br1	117.61(6)
C1-Mg1-Br1	111.8(3)	C1-Mg1-Br1 <sup>i</sup>	110.68(5)
C22-Mg1-Br1	112.9(3)	C52-Mg1-Br1 <sup>i</sup>	112.77(5)
<b>5</b>		<b>6</b>	
C1-Mg1	2.233(4)	C1-Mg1	2.232(2)
Mg1-Br1	2.5611(12)	Mg1-Br1	2.5096(11)
Mg1-C22	2.149(4)	Mg1-C23	2.166(2)
C1-Mg1-C22	117.00(14)	Mg1-O1	2.0741(18)
C1-Mg1-Br2	100.93(9)	C1-Mg1-C23	115.22(8)
C22-Mg1-Br2	117.27(10)	C23-Mg1-Br1	125.93(7)
C1-Mg1-Br1	108.11(10)	C1-Mg1-Br1	103.72(7)
C22-Mg1-Br1	117.27(10)	C1-Mg1-O1	111.12(7)

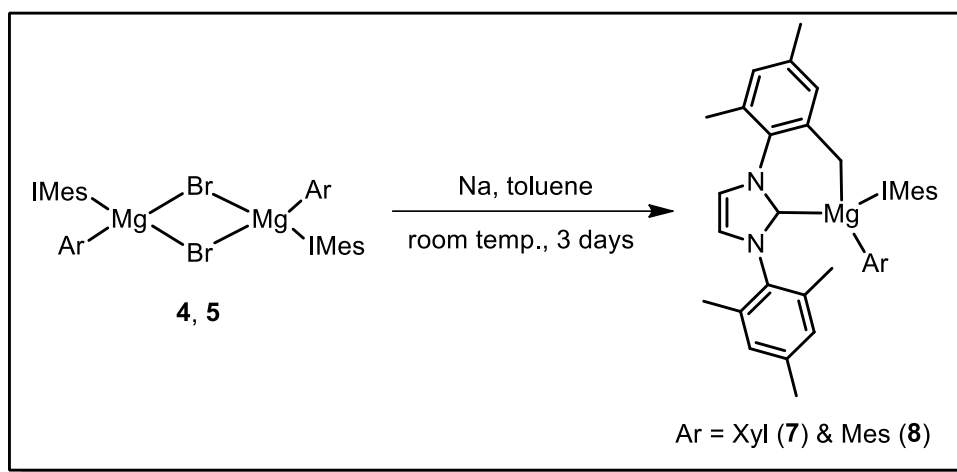


### 3B.2 Reduction of IMes supported aryl magnesium bromide complexes: Intramolecular (sp<sup>3</sup>)C–H bond activation

Six membered cyclometalated compounds of organo-magnesium(II), [IMesMgAr(IMes')] Ar = Xyl (**7**) and Mes (**8**) have been isolated and structurally characterized for the first time in presence of ligand IMes and (IMes') {1-(2,4,6-trimethylphenyl)-3-(3,5-dimethylbenzyl)-imidazol-2-ylidene}. We presumed that the reaction proceeds *via* insertion of *in situ* generated aryl Mg(I) radical into (sp<sup>3</sup>) CH bond, thereby, magnesium mediated intramolecular sp<sup>3</sup>(C–H) bond activation of one ortho-methyl group of IMes occurs.

**3B.2.1 Synthesis of [IMesMgAr(IMes')]:** Complexes with higher oxidation state ligated metal halides are known to be ideal precursors to obtain low oxidation state metal–metal bonded compounds. In view of this, our investigation began with the reduction of NHC supported magnesium(II) halides by metal (sodium or potassium) as classical reducing agent in toluene at room temperature to obtain low oxidation state organo-magnesium(I) complex with Mg–Mg bond and were found to be unsuccessful in our hands. Then our attention turned to choose NHC supported organo-magnesium(II) halide complexes as precursors, where one of the halide groups is replaced with sterically bulky aromatic group. Initial attempt to isolate NHC supported organo-magnesium (I) species from the reduction of compound (**3**), [{IMesMg(Ph)Br}<sub>2</sub>] in presence of excess sodium metal in toluene was failed, in which we observed a free IMes ligand. In contrast to the reduction of compound **3**, sterically more bulky precursors of IMes supported organo-magnesium (II) halide compounds **4** & **5**, [{IMesMg(Ar)Br}<sub>2</sub>; Ar = Xyl (**4**) and Mes (**5**)] with excess sodium in toluene for 3 days stirring at room temperature, yields cyclometalated compounds of magnesium **7** and **8** with isolated yield of 22 & 32 %, respectively (Scheme 3B.2.1.1). The compounds **7** and **8** represent the first examples of structurally characterized

cyclometalated compounds of magnesium, where the metal atom magnesium mediated the activation of (sp<sup>3</sup>)C–H bond of ortho-methyl proton of mesityl (IMes) group. In lieu of widely known (sp<sup>3</sup>)C–H bond activation by transition metals such as Co, Rh & Ir etc., among main group elements only boron is known to be insert into benzylic (sp<sup>3</sup>)C–H bond of IMes. To the best of our knowledge there have been no reports on Group 2 metal mediated (sp<sup>3</sup>)C–H bond activation of IMes ligand or any p-block elements, except with boron.



**Scheme 3B.2.1.1** Synthesis of [IMesMgAr(IMes')]; Ar = Xyl (7) and Mes (8).

Similarly, the formation of magnesium metallacyclic compound (8), [IMesMg(Mes)(IMes')] was observed from the reaction of THF co-ordinated IMes supported organo-magnesium(II) halide (6), [IMesMg(Mes)Br(THF)] with sodium metal reduction in toluene. A simultaneous attempt for the reduction of IMes supported organo-magnesium(II) halide complexes 3-6 in stoichiometric ratio with Mg(I) species, LMg–MgL; a 2c–2e reductant, where L = CH{CMe-(2,4,6-Me<sub>3</sub>C<sub>6</sub>H<sub>2</sub>N)<sub>2</sub>}<sub>2</sub> in deuterated benzene has been carried out, which turned to be unsuccessful to isolate the pure compounds, in place of it yields intractable mixture of products. Further, the steric nature of the NHC ligand has been tuned by changing the N-substitution at

1,3-positions of the imidazole ring. The 2,4,6-trimethylphenyl moiety of the IMes NHC was substituted with sterically more bulky groups such as 2,6-diisopropylphenyl in IPr (1,3-bis-(2,6-diisopropylphenyl)imidazole-2-ylidene) and *tert*-butyl in I<sup>t</sup>Bu (1,3-di-*tert*-butylimidazole-2-ylidene) ligand, respectively. Isolation of NHC adducts of IPr and I<sup>t</sup>Bu stabilized aryl magnesium (II) bromide, ArMgBr; Ar = Ph, Xyl & Mes were unsuccessful as it leads to the intractable mixture of compounds.

**3B.2.2 Spectroscopic analysis of [IMesMgAr(IMes')]:** Colorless Compounds of **7** and **8** are characterized by NMR {<sup>1</sup>H and <sup>13</sup>C} and elemental analysis, and further confirmation of molecular structures is done by single crystal X-ray structural analyses. The colorless compounds of IMes supported cyclometalated magnesium, **7** and **8** are highly soluble in non-polar solvents such as benzene, toluene and partially soluble in n-hexane. Compounds **7** and **8** are thermally stable, highly air & moisture sensitive and can be stored in inert atmosphere without further decomposition.

The formation of (sp<sup>3</sup>)C–H activated compounds of magnesium **7** and **8** are characterized by NMR studies. The <sup>1</sup>H and <sup>13</sup>C{<sup>1</sup>H} NMR resonances for compounds **7** and **8** are consistent with their molecular composition. <sup>1</sup>H NMR spectrum of compound **7** in benzene-d<sub>6</sub> displays resonances at 5.93 (d, 1H) & 6.42 (br, 1H) for (IMes') and 5.99 (s, 2H) for IMes ligand, corresponding to the backbone protons {NC(H)} of imidazole ring. The benzylic CH<sub>2</sub> attached to magnesium atom displays two doublet resonances in aliphatic region 1.70 (1H) and 1.81 (1H), indicates the two protons are in chemically different environment. In <sup>13</sup>C{<sup>1</sup>H} NMR, the characteristic resonances for carbene carbon exhibits at 191.2 & 192.4 ppm for ligand IMes and (IMes') co-ordinated to magnesium, which are correspondingly increasing and decreasing magnetic field value in compare to free IMes (219.4 ppm) and IMes supported organo-

magnesium(II) halide adduct **4** (182.9 ppm). Similarly,  $^1\text{H}$  NMR spectrum for compound **8** exhibits three resonances for imidazole backbone CH at 5.94 (d, 1H), 6.42 (d, 1H) and 5.99 (s, 2H) ppm for (*IMes*' ) and IMes ligands, respectively and two doublets at 1.68 (1H) and 1.78 (1H) ppm corresponding to benzylic  $\text{CH}_2$  protons.  $^{13}\text{C}\{^1\text{H}\}$  NMR for compound **8** appears at 191.2 and 192.5 ppm values corresponding to carbene carbon. The  $^{13}\text{C}\{^1\text{H}\}$  resonance at 31.9 ppm for both compounds **7** and **8** corresponds to the benzylic  $\text{CH}_2$  of mesityl group attached to magnesium center and the presence of methylene group is noticed from DEPT 135 spectrum of compound **8** at 31.9 ppm as negative resonance.

**3B.2.3 X-ray diffraction studies of [IMesMgAr(*IMes*' )]:** The colorless single crystals of **7** & **8** suitable for X-ray structural analysis were obtained from saturated hexane solution at room temperature. Compounds **7** & **8** crystallize in the monoclinic crystal system with  $C2/c$  and  $P2_1/c$  space groups, respectively. Molecular structures for compounds **7** & **8** are shown in figure 3B.2.3.1 (See Table 3B.2.3.1 for selected bond parameters). Compound **7** is surrounded by a neutral IMes and a bi-dentate mono anionic (*IMes*' ) ligand, and an aryl group. The bond angles ( $^\circ$ ) around the metal center for compound **7** are, C43-Mg1-C33 123.12(12); & C25-Mg1-C21 119.41(12) deviates from the ideal bond angle ( $109^\circ$ ) for tetrahedral geometry. It displays the distorted structure from tetrahedral geometry and makes +2 oxidation state of magnesium metal in compound **7**. The (*IMes*' ) ligand co-ordinates to magnesium atom in a bi-dentate fashion and forms a six membered heterocyclic compound of magnesium  $\text{C}_4\text{Mg}_1\text{N}_1$ , with  $\text{C}_{\text{IMes}}-\text{magnesium}$  and magnesium-C(benzylic) bond distances C21-Mg1 2.288(3) and Mg1-C43 2.255(3) (Å), respectively. Here, the magnesium atom activates the ( $\text{sp}^3$ )C-H bond of ortho-methyl mesityl moiety of the IMes ligand and produces metallacyclic product of magnesium with the formation of magnesium-carbon(benzylic) bond. Further, the solid state structure of compound **8** confirms

the consistent formation of cyclometalated magnesium compound {C1–Mg1 2.262(4); Mg1–C10 2.222(4) (Å)}, with intra-molecular ( $sp^3$ )C–H bond activation of ortho-methyl mesityl group. The Mg–C(benzylic) bond distance for compound **8**; Mg1–C10 2.222(4) (Å) is close to Mg1–C43 2.255(3) (Å) for compound **7** and both are well in agreement with the magnesium-carbon(aliphatic) bond distances.<sup>12b,c</sup> The  $C_{IMes}$ –magnesium bond distances (Å): C25–Mg1 2.271(3) & C31–Mg1 2.264(4), and magnesium-carbon(aryl) bond distances (Å): Mg1–C33 2.203(3) & Mg1–C22 2.179(4) of compounds **7** and **8** are matches well with known values of ( $C_{NHC}$ –Mg)<sup>13</sup> and {Mg–C(aryl)}<sup>11</sup> bond distances (Å), respectively.

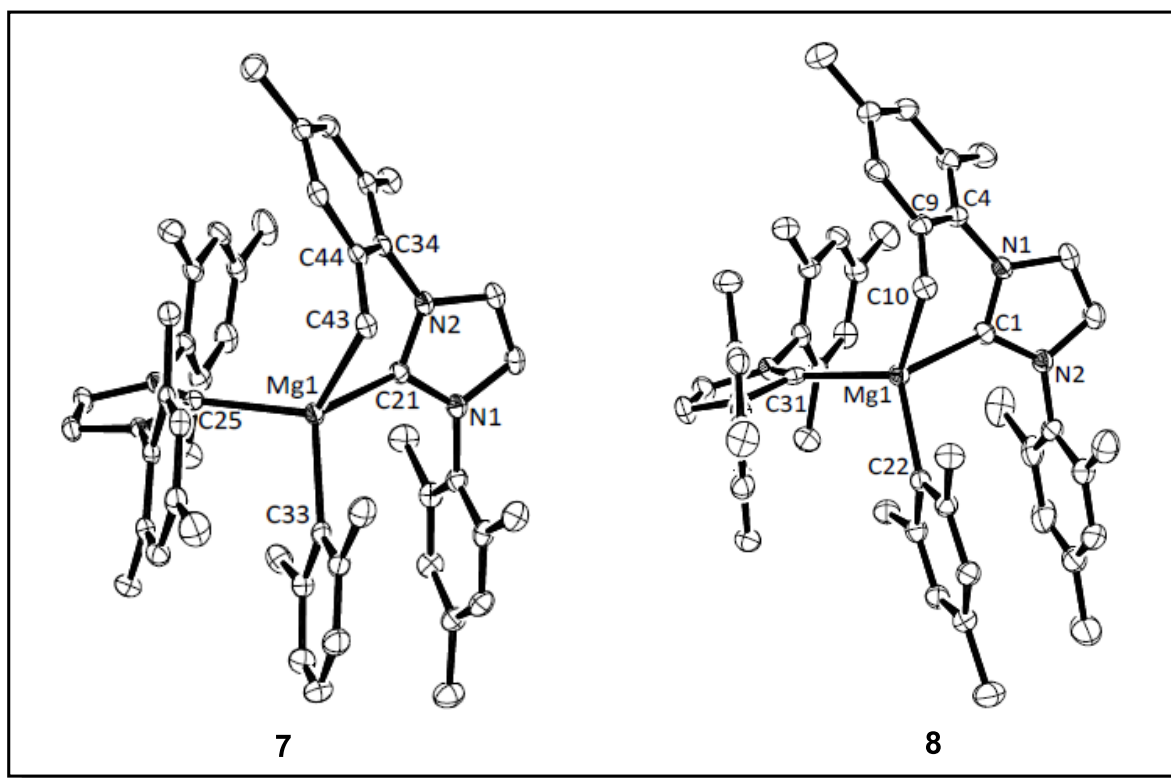


**Figure 3B.2.3.1** Molecular structure of [IMesMg(Xyl)(*IMes*')] (**7**) and [IMesMg(Mes)(*IMes*')] (**8**) (ORTEP view, 35% probability ellipsoid) with selected atom labels. Hydrogen atoms are omitted for clarity.

**Table 3B.2.3.1** Selected bond distances (Å) and angles (°) for compounds **7** & **8**,

<b>7</b>		<b>8</b>	
C21–Mg1	2.288(3)	C1–Mg1	2.262(4)
C43–C44	1.457(4)	C1–C10	1.450(5)
Mg1–C43	2.255(3)	Mg1–C10	2.222(4)
Mg1–C25	2.271(3)	Mg1–C31	2.264(4)
Mg1–C33	2.203(3)	Mg1–C22	2.179(4)
C35–C38	1.505(4)	C5–C11	1.503(5)
C25–Mg1–C21	119.41(11)	C1–Mg1–C31	119.41(14)
C43–Mg1–C33	123.12(12)	C22–Mg1–C10	122.73(14)
C33–Mg1–C21	114.55(12)	C22–Mg1–C1	109.41(14)
C25–Mg1–C43	116.60(12)	C31–Mg1–C10	116.68(14)

The formation of six membered cyclometalated compound of magnesium is proposed to proceed *via* radical mechanism (Figure 3B.2.3.2). Where, the radical intermediate, [IMesMg•(Ar)] (**A**) generated from the IMes supported organo-magnesium(II) bromide adduct in presence of excess sodium metal, undergoes intramolecular ( $sp^3$ )C–H bond activation with the ortho-methyl proton of mesityl group (IMes), instead of sterically unfavourable metal-metal bonded organo-magnesium(I) compound. The intermediate **A** undertakes intramolecular H transfer from the ortho-methyl proton of mesityl (IMes) group to the magnesium radical, generates carbon radical and results the simultaneous formation of Mg–C(benzylic) bond of six membered metallacycle and eliminates insoluble solid of polymeric magnesium hydride as a side product.

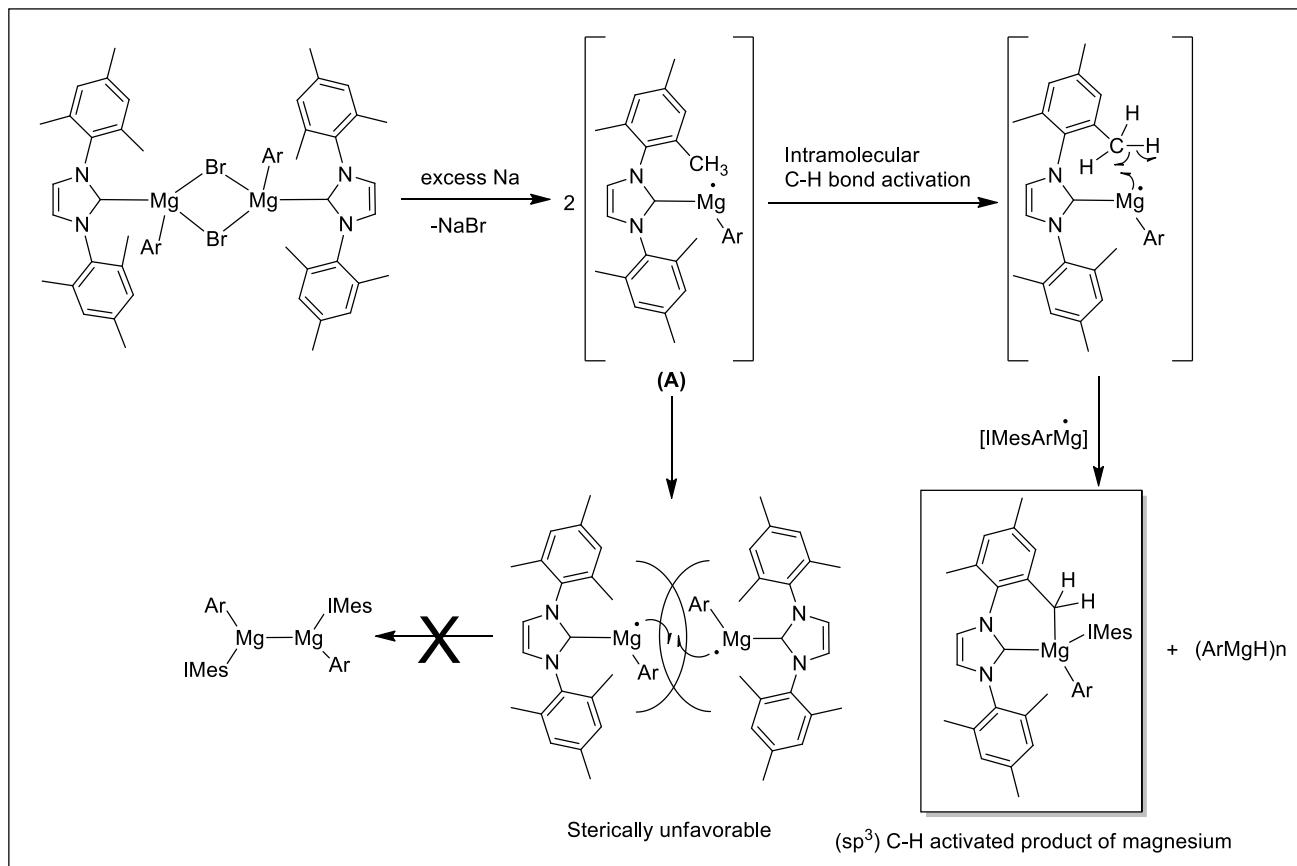
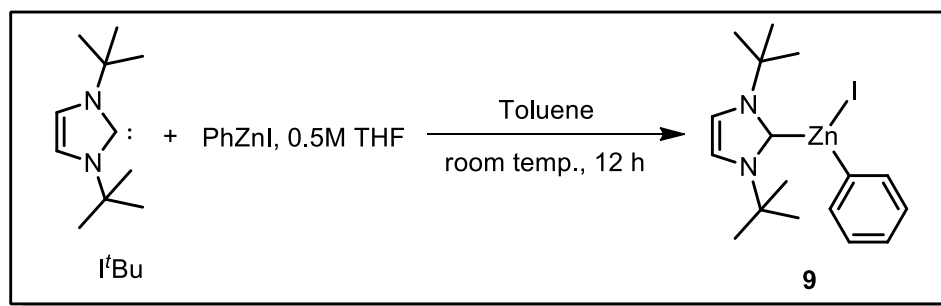


**Figure 3B.2.3.2** Proposed mechanism for intramolecular ( $sp^3$ )C–H bond activation of magnesium.

### Part C. Reactions of NHCs with PhZnI: NHC supported organo-zinc(II) complexes

Here, we report the synthesis of NHC supported organo-zinc(II) halide complexes,  $t^i\text{BuZn(Ph)I}$  (**9**) and  $\text{IPrZn(Ph)I}$  (**10**) by the reaction between  $\text{PhZnI}$  with  $t^i\text{Bu}$  and  $\text{IPr}$  NHC, respectively. Unprecedented synthesis of compound  $\text{IPr(ZnI}_2\text{)}\text{aIPr}$ , zinc(II) halides supported by NHC & aNHC has been isolated and characterized from the reaction of  $\text{IPr}$  with  $\text{PhZnI}$  for the first time. The formation of **11** presumably proceeds *via* intramolecular H-transfer from imidazole backbone C–H to carbene carbon of  $\text{IPr}$  and generates abnormal  $\text{IPr}$ .

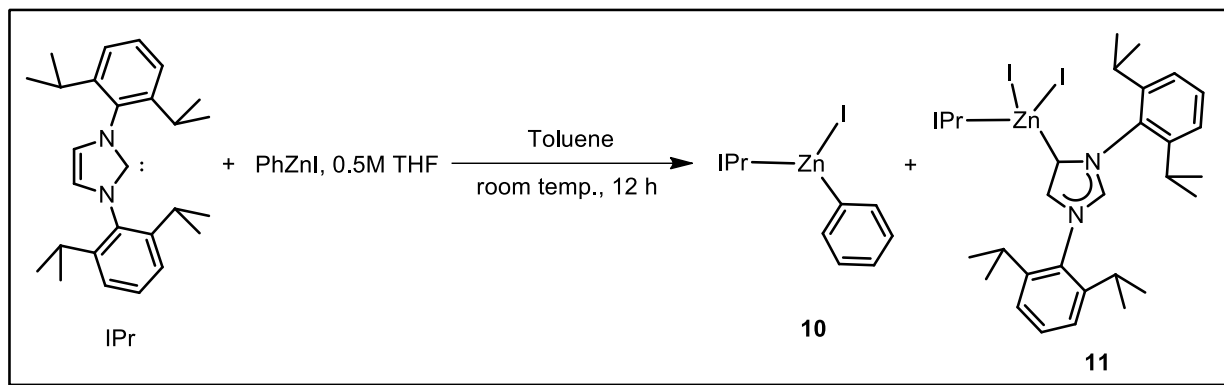
**3C.1 Synthetic aspects:** The reactions of phenylzinc iodide with NHCs *i.e.*  $t^i\text{Bu}$ ,  $\text{IPr}$  &  $\text{IMes}$  are carried out.  $t^i\text{Bu}$  reacts with phenylzinc iodide (0.5 M THF) at room temperature stirring for 12 h led to the formation of NHC adduct of  $\text{PhZnI}$ ,  $t^i\text{BuZn(Ph)I}$  (**9**) (Scheme 3C.1.1) while the reaction between  $\text{IMes}$  and  $\text{PhZnI}$  was allowed to the formation of intractable mixture of products.



**Scheme 3C.1.1** Synthesis of  $t^i\text{BuZn(Ph)I}$  (**9**).

In a similar reaction of  $\text{IPr}$  with  $\text{PhZnI}$  (0.5 M THF) in toluene produces NHC adduct of  $\text{PhZnI}$ ,  $\text{IPrZn(Ph)I}$  (**10**). During the course of reaction between  $\text{IPr}$  and  $\text{PhZnI}$  along with the NHC adducts of phenylzinc iodide *i.e.* compound **10**, colorless crystals of zinc dihalide supported by normal and abnormal binding mode of NHC,  $\text{IPr(ZnI}_2\text{)}\text{aIPr}$  (**11**) is isolated as an additional product (Scheme 3C.1.2).





**Scheme 3C.1.2** Reaction of IPr with PhZnI; Synthesis of **10** and **11**,

Both compounds **9** & **10**, NHC adduct of aryl-zinc(II) iodide are highly soluble in tetrahydrofuran and partially soluble in nonpolar solvents such as benzene and toluene. On the other hand, compound **11** i.e. NHC and aNHC supported of zinc(II) iodide is partially soluble in THF and sparingly soluble in benzene and toluene.

Further, reactivity of NHC supported organozinc(II) halide compounds **9** & **10** has been explored. Reduction of compounds **9** & **10** with sodium or potassium in toluene at room temperature was unsuccessful, which results in free NHCs instead of low valent organozinc compounds. Furthermore, the reactions with metal bis(amide),  $\text{KN}(\text{SiMe}_3)_2$  in toluene failed to produce pure compounds of NHC supported organozinc(II) amide.

**3C.2 Spectroscopic characterization:** The formation of compound **9** is confirmed by  $^1\text{H}$  &  $^{13}\text{C}$  NMR analysis. The backbone imidazole  $\text{CH}$  protons of compound **9** shifts up-field to 6.33 ppm in compared to free  $t\text{Bu}$  (6.78 ppm). The singlet resonance at 1.24 ppm corresponds to *tert*-butyl,  $\text{C}(\text{CH}_3)_3$  protons of compound **9** and is different from the singlet resonance of (1.51 ppm)  $t\text{Bu}$ . The resonances at 7.33 (m, 1H), 7.46 (m, 2H) & 8.15 (m, 2H) agrees to the phenyl protons for compound **9**.  $^{13}\text{C}\{^1\text{H}\}$  NMR signal appearing at 170.5 ppm corresponds to the co-ordinated carbene carbon of compound **9** (in free  $t\text{Bu}$ , carbene carbon resonates at 213.1 ppm).

Similarly, compound **10** has been characterized by  $^1\text{H}$  &  $^{13}\text{C}$  NMR spectra and shows resonance for respective composition. The spectroscopic resonances for compound **10** have been shifted when compared to the uncoordinated NHC (IPr). For example, the *CH* proton of the imidazole moiety resonates as a singlet at high magnetic field shift (6.44 ppm) in compound **10**; than that of free IPr (6.62 ppm). Further, the peaks for *i*-Pr *CH* and  $\text{CH}_3$  in compound **10** resonate at 2.78 as septet and 1.32 & 0.97 ppm as two doublets, respectively {2.96 (sept); 1.29 (d) & 1.19 (d) ppm: for free IPr}. Furthermore, in  $^{13}\text{C}\{^1\text{H}\}$  NMR spectra the missing of the carbene carbon peak for free ligand at 220.6 ppm confirms the co-ordination of the IPr through carbene carbon to the metal center.

**3C.3 Crystallographic characterization:** The formation of compound **11** was spectroscopically considered from  $^1\text{H}$  NMR analysis. To obtain analytically pure compound of **11** was unsuccessful, as it was crystallized as a side product with compound **10**, from the reaction mixture of IPr and PhZnI. Further, compound **11** has been confirmed by single crystal X-ray analysis whereas colorless hairy crystals obtained for compound **10** was not good enough for single crystal X-ray data analysis.

Molecular structure of compound **9** is shown in Figure 3C.3.1 with selected bond parameters in caption. Compound **9** crystallizes in monoclinic space group *P21/c* with the crystal data and structure refinement summary in table 3S.3. The asymmetric unit of compound **9** contains two *t*BuZn(Ph)I molecules, in which three coordinated zinc atom adopts a distorted trigonal planar geometry, where the ligand *t*Bu and phenyl group are widened by an angle of 136.8(2) ( $^\circ$ ) [C1–Zn1–C4 136.8(2) ( $^\circ$ )] with the centered Zn metal. The C1–Zn1–I1 & C4–Zn1–I1 bond angles for compound **9** are 108.72(16) & 114.45(17) ( $^\circ$ ), respectively. The  $\text{C}_{\text{NHC}}\text{–Zn1}$  bond distance in compound **9** [2.006(6) ( $\text{\AA}$ )] is in agreement with  $\text{C}_{\text{NHC}}\text{–Zn}$  bond distance

[2.082(5) (Å)] for known compound,  $t\text{Bu}:\text{Zn}\{\text{N}(\text{SiMe}_3)_2\}_2$ . The Zn1–I1 & Zn1–C4 bond lengths of **9** are 2.640(10) & 1.981(6) (Å) respectively.

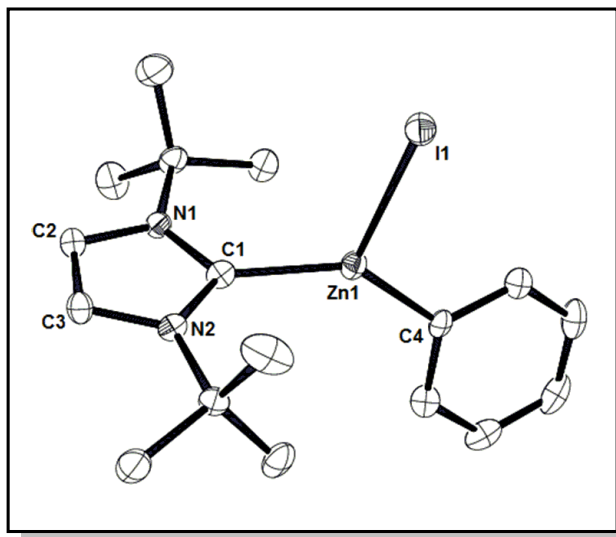


**Figure 3C.3.1** Molecular structure of  $t\text{BuZn}(\text{Ph})\text{I}$  (**9**); (ORTEP view, 35% probability ellipsoid), with selected atom levels. Hydrogen atoms are omitted for clarity. Selected bond lengths (Å) and bond angles (°): Zn1–C1 2.006(6), Zn1–I1 2.6403(10), Zn1–C4 1.981(6), C1–Zn1–C4 136.8(2), C1–Zn1–I1 108.72(16), C4–Zn1–I1 114.45(17).

Suitable single crystal for compound **11** is obtained from saturated solution of toluene at room temperature kept for several days. Compound **11** crystallizes in monoclinic crystal system with space group  $P21/c$  (Table 3S.3). The molecular structure for **11** is shown in Figure 3C.3.2 with the selected bond parameters. The solid state structure for compound **11** reveals that the aIPr is co-ordinated to the zinc atom through the carbene carbon C4 along with the normal C2 carbene carbon of IPr. In compound **11** the zinc atom is surrounded by two carbene ligands and two iodine atoms, results a distorted tetrahedral geometry of zinc with +2 oxidation states. The C25–Zn1 and C30–Zn1 bond distances 2.078(4) & 2.037(4) (Å) are nearly same and are

matching with  $C_{NHC}-Zn$  bond distances for reported compound. The Zn1–I1 & Zn1–I2 bond lengths for compound **11** are 2.5987(8) & 2.7074(8) (Å) respectively, while the I1–Zn1–I2 bond angle is 108.25(19) (°).

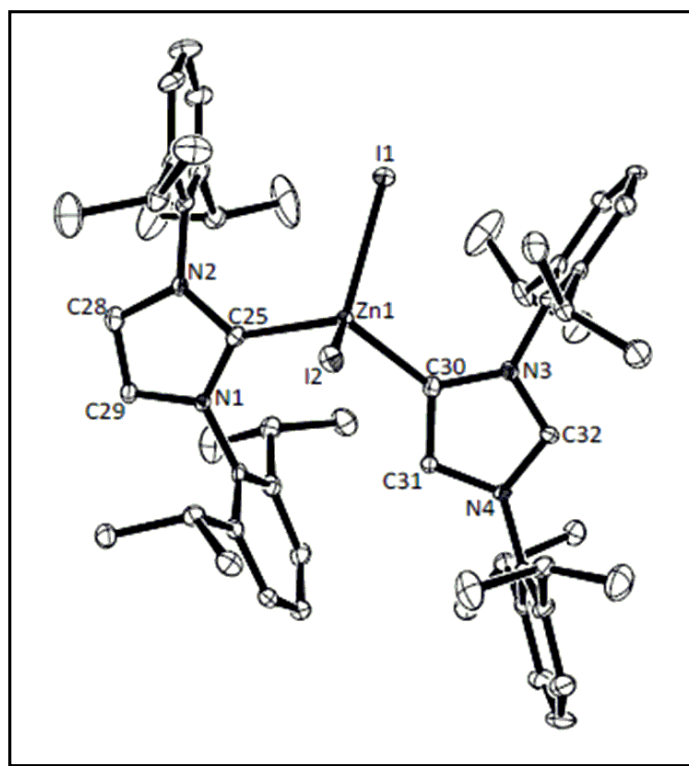


**Figure 3C.3.2** Molecular structure of IPr(ZnI<sub>2</sub>)aIPr (**11**); (ORTEP view, 35% probability ellipsoid), with selected atom levels. Hydrogen atoms are omitted for clarity. Selected bond lengths(Å) and bond angles(°); Zn1–I1 2.5987(8), Zn1–I2 2.7074(8), Zn1–C25 2.078(4), Zn1–C30 2.037(4); C25–Zn1–C30 120.90(15), I1–Zn1–I2 108.255(19), C25–Zn1–I1 111.46(11), C25–Zn1–I2 103.16(10), C30–Zn1–I1 110.70(11), C30–Zn1–I2 100.82(10).

**Conclusion:** In summary, DFT studies revealed that low oxidation state Group 2 metals with metal-metal bond (Be, Mg, Ca, Sr, and Ba) are strongly stabilized by the neutral N-heterocyclic carbene ligand. All metal-metal bonded low oxidation state compounds are trans linear in

geometry. The WBIs of M–M bonds are close to one, indicating the existence of single bond between two metal atoms. The high stability (in terms of BDE) of [(Cl)(NHC)Mg–Mg(NHC)(Cl)] emphasize the possibility of synthesizing such complexes in the laboratory.

In our laboratory, a series of well-defined IMes supported aryl magnesium bromide (Grignard reagent) complexes (**3-6**) have been synthesized and structurally characterized. Further, compounds **4** and **5** were reduced with excess sodium metal in toluene do not yield as low oxidation state organo-magnesium(I) compounds with Mg–Mg bond, as expected, but lead to formation of cyclometalated products [{IMes(IMes')MgAr}] (Ar = 2,6-dimethylphenyl) (**7**) and [{IMes(IMes')MgAr}] (Ar = 2,4,6-trimethylphenyl) (**8**), instead. In both cases, we presume that *in situ* generated IMes supported aryl-magnesium(I) radical do not dimerize to yield magnesium(I) complex with Mg-Mg bond, due to steric hindrance, instead, magnesium mediated intramolecular (sp<sup>3</sup>)C–H bond activation occurs. Additionally, intermolecular H radical transfer from one ortho methyl group of IMes to the other aryl-magnesium radical moiety occurs to yield aryl magnesium hydride as a side product.

Similarly, NHC adducts of organo-zinc(II) halide complexes *t*BuZn(Ph)I and IPrZn(Ph)I are synthesized and characterized. Further, Normal and abnormal NHC supported zinc(II) iodide complex, IPr(ZnI<sub>2</sub>)aIPr have been isolated and their structures confirmed from X-ray analysis.

**Crystallographic data and structure refinement details:****Table 3S.1:** Crystal data and structure refinement details for compounds **3-6**,

	<b>3</b>	<b>4</b>	<b>5</b>	<b>6</b>
Empirical formula	C <sub>54</sub> H <sub>58</sub> Br <sub>2</sub> Mg <sub>2</sub> N <sub>4</sub>	C <sub>35</sub> H <sub>39</sub> BrMgN <sub>2</sub>	C <sub>66</sub> H <sub>76</sub> N <sub>4</sub> Mg <sub>2</sub> Br <sub>2</sub>	C <sub>34</sub> H <sub>43</sub> BrMgN <sub>2</sub> O
Formula weight	971.48	591.90	1133.74	599.92
Crystal system	Triclinic	Monoclinic	Monoclinic	Triclinic
Space group	<i>P</i> $\bar{1}$	<i>P</i> 2(1)/ <i>c</i>	<i>P</i> 2 <sub>1</sub> / <i>c</i>	<i>P</i> $\bar{1}$
<i>a</i> /Å	12.0473(6)	11.573(2)	11.1351(10)	9.133(3)
<i>b</i> /Å	14.0634(7)	12.240(2)	18.813(2)	13.643(5)
<i>c</i> /Å	24.8538(12)	22.344(4)	28.805(3)	13.953(5)
$\alpha$ /°	78.657(2)	90.000	90.000	76.882(2)
$\beta$ /°	76.564(3)	100.655(10)	94.379(5)	73.611(2)
$\gamma$ /°	68.739(2)	90.000	90.000	80.863(2)
Volume/Å <sup>3</sup>	3787.4(3)	3110.5(9)	6016.5(11)	1616.0(12)
Z	3	4	4	2
$\rho_{\text{calc}}$ /cm <sup>3</sup>	1.278	1.264	1.252	1.233
$\mu$ /mm <sup>-1</sup>	1.669	1.367	1.410	1.319
F(000)	1512	1240	2376.0	632
Crystal size /mm <sup>3</sup>	0.21x0.17x0.11	0.074x0.051x0.037	0.22x0.17x0.12	0.087x0.060x0.047
2 $\theta$ range for data collection/°	4.10 to 25.03	3.45 to 25.50	4.26 to 51	2.39 to 25.50
Index ranges	-14<= <i>h</i> <=14, -16<= <i>k</i> <=16, -29<= <i>l</i> <=29.	-12<= <i>h</i> <=14, -14<= <i>k</i> <=14, -27<= <i>l</i> <=27.	-13 ≤ <i>h</i> ≤ 13, -22 ≤ <i>k</i> ≤ 22, -34 ≤ <i>l</i> ≤ 34.	-11<= <i>h</i> <=11, -15<= <i>k</i> <=16, -16<= <i>l</i> <=16.
Reflections collected	48284	40419	74126	20478
Independent reflections	13287	5754	11205	5998
R(int)	0.0484	0.0455	0.1293	0.0406
Data/restraints/parameters	13287 / 1128 / 856	5754 / 0 / 360	11205/0/685	5998 / 0 / 362
Goodness-of-fit on F <sup>2</sup>	0.964	0.823	1.013	0.889
R1, wR2 [ <i>I</i> ≥ 2 $\sigma$ ( <i>I</i> )]	0.0288, 0.0763	0.0256, 0.0903	0.0445, 0.0833	0.0348, 0.1050

R1, wR2 [all data]	0.0985, 0.1016	0.0322, 0.0987	0.0877, 0.0983	0.0438, 0.1143
Largest diff. peak/hole/eÅ <sup>-3</sup>	0.520,-0.252	0.295,-0.256	0.40,-0.36	0.739, -0.361

**Table 3S.2:** Crystal data and structure refinement details for compounds **7** & **8**,

	<b>7</b>	<b>8</b>
Empirical formula	C <sub>50</sub> H <sub>56</sub> MgN <sub>4</sub>	C <sub>51</sub> H <sub>59</sub> MgN <sub>4</sub>
Formula weight	737.30	752.33
Crystal system	Monoclinic	Monoclinic
Space group	<i>C2/c</i>	<i>P2<sub>1</sub>/c</i>
Unit cell dimensions(Å) & (°)	a = 38.1300(10) α = 90.000, b = 10.0208(3) β = 102.723(3), c = 23.0416(7) γ = 90.000.	a = 18.260(14) α = 90.000, b = 11.167(8) β = 105.474(5), c = 22.513(18) γ = 90.000.
Volume/Å <sup>3</sup>	8587.9(4)	4424(6)
Z	8	4
ρ <sub>calc</sub> /cm <sup>3</sup>	1.141	1.129
μ/mm <sup>-1</sup>	0.079	0.078
F(000)	3168.0	1620.0
Crystal size /mm <sup>3</sup>	0.17×0.11×0.06	0.047×0.033×0.026
2θ range for data collection/°	2.18 to 51	5.3 to 51
Index ranges	-46 ≤ h ≤ 44, -12 ≤ k ≤ 12, -27 ≤ l ≤ 27	-22 ≤ h ≤ 21, -13 ≤ k ≤ 12, -25 ≤ l ≤ 27
Reflections collected	51827	25025
Independent reflections	7984	8197
R(int)	0.0827	0.1155
Data/restraints/parameters	7984/0/496	8197/0/519
Goodness-of-fit on F <sup>2</sup>	1.011	0.949
R1, wR2 [I ≥ 2σ (I)]	0.0668, 0.1847	0.0635, 0.1495
R1, wR2 [all data]	0.1012, 0.2162	0.1616, 0.2056
Largest diff. peak/hole/eÅ <sup>-3</sup>	0.62, -0.65	0.31, -0.63

**Table 3S.3:** Crystal data and structure refinement details for compounds **9** & **11**,

	<b>9</b>	<b>11</b>
Empirical formula	C <sub>41</sub> H <sub>58</sub> I <sub>2</sub> N <sub>4</sub> Zn <sub>2</sub>	C <sub>54</sub> H <sub>72</sub> N <sub>4</sub> ZnI <sub>2</sub>
Formula weight	991.45	1096.32
Crystal system	Monoclinic	Monoclinic
Space group	P2(1)/c	P2 <sub>1</sub> /c
Unit cell dimensions(Å) & (°)	a = 15.846(5) α = 90.000, b = 21.135(5) β = 111.742(2), c = 13.906(3) γ = 90.000.	a = 16.081(5) α = 90.000(5), b = 17.326(5) β = 104.524(5), c = 20.570(5) γ = 90.000(5).
Volume(Å <sup>3</sup> )	4326(2)	5548(3)
Z	4	4
Density(Mg/m <sup>3</sup> ) (calculated)	1.522	1.313
Absorption coefficient(mm <sup>-1</sup> )	2.567	1.591
F(000)	1992	2240.0
Crystal size(mm <sup>3</sup> )	0.27 × 0.21 × 0.12	0.21 × 0.16 × 0.11
Theta range for data collection(°)	2.37 to 25.50	4.718 to 56.788
Index ranges	-19 ≤ h ≤ 16, -25 ≤ k ≤ 25, -16 ≤ l ≤ 15.	-21 ≤ h ≤ 21, -22 ≤ k ≤ 23, -21 ≤ l ≤ 27.
Reflections collected	28743	43303
Independent reflections	8037 [R(int) = 0.0638]	13582 [Rint = 0.0812]
Completeness to theta = 25.50°	99.9 %	97.5 %
Max. and min. transmission	0.7457 & 0.5493	0.746 & 0.506
Data / restraints / parameters	8037 / 15 / 443	13582 / 0 / 566
Goodness-of-fit on F <sup>2</sup>	1.032	0.952
Final R indices [I>2sigma(I)]	R <sub>1</sub> = 0.0468, wR <sub>2</sub> = 0.1056	R <sub>1</sub> = 0.0490, wR <sub>2</sub> = 0.0961
R indices (all data)	R <sub>1</sub> = 0.0773, wR <sub>2</sub> = 0.1220	R <sub>1</sub> = 0.0917, wR <sub>2</sub> = 0.1084
Largest diff. peak and hole(e.Å <sup>-3</sup> )	2.080 & -1.336	1.44 & -1.56



**References:**

- (1) Chen, M.; Craciun, R.; Hoffman, N.; Dixon, D. A. *Inorg. Chem.*, **2012**, *51*, 13195.
- (2) Liu, Y.; Li, S.; Yang, X.-J.; Yang, P.; Wu, B. *J. Am. Chem. Soc.*, **2009**, *131*, 4210.
- (3) Li, S.; Yang, X.-J.; Liu, Y.; Zhao, Y.; Li, Q.-S.; Xie, Y.; Schaefer, H. F.; Wu, B. *Organometallics*, **2011**, *30*, 3113.
- (4) (a) Green, S. P.; Jones, C.; Stasch, A. *Angew. Chem. Int. Ed.*, **2008**, *47*, 9079; (b) Green, S. P.; Jones, C.; Stasch, A. *Science*, **2007**, *318*, 1754; (c) Stasch, A.; Jones, C. *Dalton Trans.*, **2011**, *40*, 5659.
- (5) Lu, T.; Chen F. *J. Comp. Chem.* **2012**, *33*, 580.
- (6) Matito, E.; Poater, J.; Solà, M.; Duran, M.; Salvador, P. *J. Phys. Chem. A*, **2005**, *109*, 9904.
- (7) Reed, A. E.; Curtiss, L. A.; Weinhold, F. *Chem. Rev.*, **1988**, *88*, 899.
- (8) Köppe, R.; Henke, P.; Schnöckel, H. *Angew. Chem. Int. Ed.*, **2008**, *47*, 8740.
- (9) Kan, Y.-H. *J. Mol. Struct. THEOCHEM*, **2009**, *894*, 88.
- (10) Li, S.; Yang, X. -J.; Liu, Y.; Zhao, Y.; Li, Q. -S. *Organometallics*, **2011**, *30*, 3113.
- (11) Stucky, G. D.; Rundle, R. E. *J. Am. Chem. Soc.*, **1963**, *85*, 1002.
- (12) (a) Arduengo, A. J.; Davidson, F.; Krafczyk, R.; Marshall, W. J.; Tamm, M. *Organometallics*, **1998**, *17*, 3375; (b) Kennedy, A. R.; Klett, J.; Mulvey, R. E.; Robertson, S. D. *Eur. J. Inorg. Chem.*, **2011**, 4675; (c) Kennedy, A. R.; Mulvey, R. E.; Robertson, S. D. *Dalton Trans.*, **2010**, *39*, 9091.
- (13) (a) Arrowsmith, M.; Hill, M. S.; MacDougall, D. J.; Mahon, M. F. *Angew. Chem. Int. Ed.*, **2009**, *48*, 4013; (b) Baishya, A.; Barman, M. K.; Peddarao, T.; Nembenna, S. *J. Organomet. Chem.*, **2014**, *769*, 112.

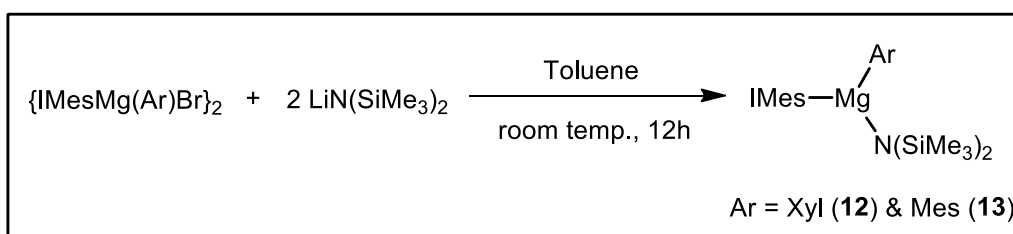
Chapter 4:

**IMes Supported Organo-magnesium(II) Amide Complexes as Pre-catalysts for Cross Dehydro-coupling of Silanes with Amines**

**Abstract:** Two new examples of IMes supported organo-magnesium(II) amide complexes, [IMesMg(Ar){N(SiMe<sub>3</sub>)<sub>2</sub>}] {Ar = 2,6-dimethylphenyl (Xyl) (**12**), and 2,4,6-trimethylphenyl (Mes) (**13**)} are synthesized and structurally characterized. The reactions of {IMesMg(Ar)Br}<sub>2</sub> with non-nucleophilic bases such as LiN(SiMe<sub>3</sub>)<sub>2</sub> undergoes salt elimination reaction to yield [IMesMg(Ar){N(SiMe<sub>3</sub>)<sub>2</sub>}]. Both complexes are tested as pre-catalysts for cross dehydrogenative coupling reactions of amines including primary aliphatic & aromatic amines, cyclic & acyclic secondary amines with silanes (both 1° & 2° hydrosilanes). The compound **13** is found to be superior catalyst than those of compounds **12** and Mg{N(SiMe<sub>3</sub>)<sub>2</sub>}<sub>2</sub> for the isolation of aminosilane products in good to excellent yields.

#### 4.1 Synthesis of IMes supported organo-magnesium(II) amide complexes:

The synthesis of [IMesMg(Ar){N(SiMe<sub>3</sub>)<sub>2</sub>}], Ar = Xyl (**12**) & Mes (**13**) was achieved through salt elimination reaction of {IMesMg(Ar)Br}<sub>2</sub> with 2 equivalents of lithium bis(trimethylsilyl)-amide, LiN(SiMe<sub>3</sub>)<sub>2</sub> in toluene at room temperature stirring for 12 h (Scheme 4.1.1).



**Scheme 4.1.1** Synthesis of [IMesMg(Ar){N(SiMe<sub>3</sub>)<sub>2</sub>}]; Ar = Xyl (**12**) & Mes (**13**)

The formations of products were monitored by <sup>1</sup>H NMR analysis of 1 mL reaction mixture aliquot. The reaction mixture was filtered through Celite frit to exclude the salt formed (LiBr) in the reaction and concentrated in high vacuum to get analytically pure colorless compounds of **12** & **13**. Compounds **12** & **13** were isolated as highly air and moisture sensitive colorless solids and are highly soluble in nonpolar solvents such as benzene and toluene, and partially soluble in *n*-

hexane. These compounds (**12** & **13**) are stable both in solid and solution state at room temperature under an inert atmosphere of dinitrogen. The colorless compounds of **12** and **13** are melted without decomposition at 138 and 160 °C, respectively.

**4.2 Spectroscopic characterization:** Both compounds **12** & **13** are characterized by  $^1\text{H}$ ,  $^{13}\text{C}$  and  $^{29}\text{Si}$  NMR spectroscopy and further confirmed by single crystal X-ray structural analysis.

The  $^1\text{H}$  NMR spectra of compounds **12** & **13** show singlet peaks for backbone imidazole *CH* in 6.0 & 6.03 ppm, respectively (IMes imidazole *CH* resonance at 6.47 ppm). The 18 protons corresponding to amide group  $\text{N}[\text{Si}(\text{CH}_3)_2]_2$ , exhibits broad singlet at 0.16 & 0.14 ppm for compounds **12** and **13** respectively, which are in up-field chemical shift corresponding to both metal bis(amide) and NHC co-ordinated magnesium bis(amide);  $[\text{Mg}\{\text{N}(\text{SiMe}_3)_2\}_2 \cdot 2\text{THF}]$  (0.45 & 0.37 ppm),  $t\text{Bu}:\text{Mg}\{\text{N}(\text{SiMe}_3)_2\}_2$  (0.36 ppm)]. In  $^{13}\text{C}\{^1\text{H}\}$  NMR spectra, the characteristic peak for carbene carbon atom resonates at 184.3 & 184.0 ppm for compound **12** and **13** respectively, are significantly up-field shift from free carbene carbon (IMes: 219.4 ppm), which is expected for NHC co-ordinated metal complexes. In  $^{29}\text{Si}\{^1\text{H}\}$  NMR complex **12** & **13** exhibits singlet resonance at -9.28 & -9.26 ppm, respectively for the silyl group, which are good in agreement with the four coordinated Si compounds.<sup>1</sup>

**4.3 Crystallographic characterization:** Colorless crystals suitable for X-ray structural analysis of compounds **12** and **13** were grown from a saturated toluene solution by slow cooling to -25 °C. The molecular structures for compounds **12** and **13** reveal the monomeric behavior of the molecules in the solid state. The central magnesium atom is enclosed with an IMes ligand, an aryl group and an amide moiety, forms tri co-ordinated magnesium complexes. The single

crystal X-ray structures for compounds **12** & **13**, with selected bond parameters are shown in Figure 4.3.1.

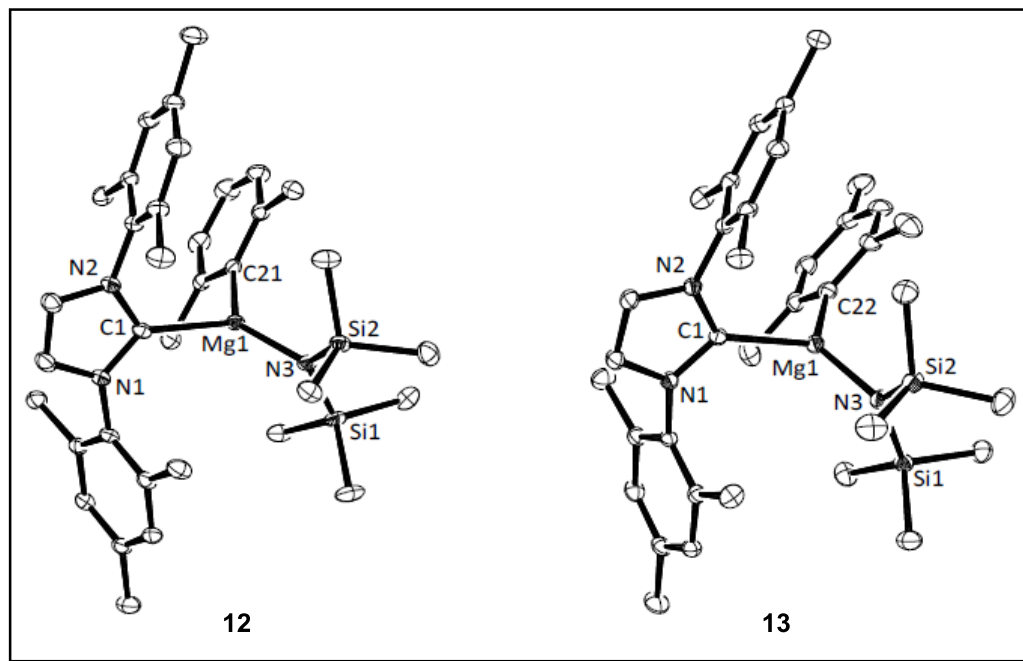


**Figure 4.3.1** Molecular structures of  $[\text{IMesMg}(\text{Ar})\{\text{N}(\text{SiMe}_3)_2\}]$ ; Ar = Xyl (**12**) and Mes (**13**) (ORTEP view, 35% probability ellipsoid, with selected atom labels). All Hydrogen atoms are omitted for clarity. Selected bond distances ( $\text{\AA}$ ) and angles ( $^\circ$ ); for compound **12**: C1–Mg1 2.241(19), Mg1–C21 2.153(18), Mg1–N3 2.009(15); C1–Mg1–C21 111.52(7), N3–Mg1–C21 130.19(7), N3–Mg1–C1 118.21(7), and for compound **13**: Mg1–C1 2.2398(15), Mg1–C22 2.1552(16), Mg1–N3 1.993(14); C1–Mg1–C22 115.92(6), N3–Mg1–C22 127.67(6), N3–Mg1–C1 116.41(6).

The bond angle around magnesium center *i.e.*, C1–Mg1–C21 111.52(7) ( $^\circ$ ) and C1–Mg1–C22 115.92(6) ( $^\circ$ ), for compounds **12** and **13** respectively, are near to  $120^\circ$  and makes the magnesium atom distorted in structure from the regular three co-ordinate trigonal planar geometry. The amide-magnesium-aryl bond angle in compound **12** [N3–Mg1–C21 130.19(7) ( $^\circ$ )]

is wider by an angle of 2.5 ( $^{\circ}$ ), in comparison to compound **13** [N3-Mg1-C22 127.67(6) ( $^{\circ}$ )]. The magnesium-carbene carbon (Mg–C1) bond lengths for compounds **12** & **13** are 2.239(15) & 2.240(2) (Å), which are in the range of known value of Mg–C<sub>NHC</sub> bond distances (2.194-2.279 Å).<sup>1</sup> The magnesium-aryl carbon bond lengths for compounds **12**; Mg1–C21 2.1538(18) (Å) and **13**; Mg1–C22 2.1552(16) (Å), are close to magnesium-carbon(aryl) bond distances of our previously synthesized compounds [ $\{IMesMg(Ar)Br\}_2$ ; Ar = Ph, Xyl & Mes (2.132-2.149 Å)].<sup>2</sup>

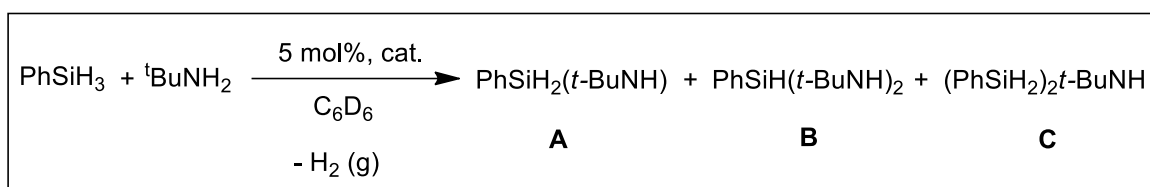
#### 4.4 Catalytic application of organo-magnesium(II) amide complexes

A handful examples of metal catalyzed dehydrocoupling reactions of silanes with amines are known in the literature.<sup>3</sup> To the best of our knowledge, main group metal catalyzed dehydrocoupling of silanes with amines are concerned there have been only two reports available in the literature. Sadow and his group first reported ligated magnesium methyl complex  $To^M MgMe$  [ $To^M$  = tris(4,4-dimethyl-2-oxazolinyl)phenylborate] as catalyst for dehydrocoupling of Si-H to N-H bonds, and thereafter, Hill and co-workers demonstrated tetrahydrofuran (THF) co-ordinated homoleptic alkaline earth hexamethyldisilazide compounds,  $[M\{N(SiMe_3)_2\}_2]_2 \cdot 2THF$  (M = Mg, Ca & Sr) as active pre-catalysts for cross-dehydrocoupling of silanes with amines.<sup>4</sup>

In this regard, we have examined the catalytic Si–N bond formation reactions of silanes with amines with newly synthesized organo-magnesium(II) amide complexes, **12** and **13**. The reactions were carried out in the presence of 5 mol% loading of either complex **12** or **13**, in benzene at room temperature. A large varieties of amines such as primary aliphatic, aromatic, cyclic and acyclic secondary amines to both 1 $^{\circ}$  and 2 $^{\circ}$  silanes have been tested. In all cases (Table 4.2.2, entries 1-18), good to excellent yields for the aminosilane products were isolated.

The dehydro-coupling reactions of one equivalent of *t*-BuNH<sub>2</sub> to PhSiH<sub>3</sub> have been screened with catalysts **12**, **13** and Mg{N(SiMe<sub>3</sub>)<sub>2</sub>}<sub>2</sub> (Table 4.4.1) at room temperature stirring for 1 min in benzene-d<sub>6</sub>. Catalyst **13** produces the mono(amino)silane product **A**, in higher reaction yield *i.e.* 70 % in comparison to **12** and Mg{N(SiMe<sub>3</sub>)<sub>2</sub>}<sub>2</sub>, 56 % and 39 % respectively. Furthermore, the reaction mixtures were heated at 60 °C for 12 h, while the catalyst **13** yielded the bis(amino)silane product (**B**) as major compound over mono-aminated one (**A**) (26:34), whereas the catalyst **12** produced mixture of mono and di-aminated, and disilylated products in the ratios of 17:19:29 (**A** : **B** : **C**). On the contrary, Mg{N(SiMe<sub>3</sub>)<sub>2</sub>}<sub>2</sub> gives the mono-aminated compound (**A**) over di-aminated product (**B**) as major compound (36 : 16) (Table 4.4.1).

**Table 4.4.1** Metal catalyzed dehydro-coupling of *t*-BuNH<sub>2</sub> with PhSiH<sub>3</sub>



Catalyst <sup>a</sup>	Temp (°C)	Time (min)	Products	Conversions
<b>12</b>	25	1	A	56
	60	60	A : B : C	24 : 24 : 3
	60	720	A : B : C	17: 19 : 29
<b>13</b>	25	1	A	70
	60	60	A : B	38 : 27
	60	720	A : B	26 : 34
Mg{N(SiMe <sub>3</sub> ) <sub>2</sub> } <sub>2</sub>	25	1	A	39
	60	60	A : B	49 : 7
	60	720	A : B	36 : 16

<sup>[a]</sup> Reaction conditions: amine (0.13 mmol, 1 equiv), silanes (0.13 mmol, 1 equiv), catalyst (5 mol %) and C<sub>6</sub>D<sub>6</sub> (0.5 ml).

Conversions were obtained on the basis of consumption of PhSiH<sub>3</sub> from integration of signals in the <sup>1</sup>H NMR spectra.

For further dehydro-coupling of silanes with amines, choice of catalyst **13** has been justified (Table 4.4.2). It is understood from table 4.4.2 that the steric nature around the substrates both in amines and silanes plays an important role on the control over the selective formation of aminosilane products. As of entry 2, 11 and 16, increasing the steric substitution of silanes, from PhSiH<sub>3</sub> to more bulky Ph<sub>2</sub>SiH<sub>3</sub> and PhMeSiH<sub>3</sub>, monosilyl-aminated compound i.e. product **A**, is preferred over the disilylamination (product **B**). As well, the reactions of sterically less bulky substrates, i.e. aliphatic secondary amine (HNEt<sub>2</sub>) with 1° silane (PhSiH<sub>3</sub>) favors the formation of bis(amino)silane product **B**, {PhSiH(NEt<sub>2</sub>)<sub>2</sub>} (entry 3, Table 4.4.2). Further, it is noted that the increased steric crowd in amines and silanes subjects to the formation of monosilyl-aminated product (**A**) over (**B**) (entry 4-7, 12-14 & 17-18, Table 4.4.2).

**Table 4.4.2** Compound **13** catalyzed dehydrogenative coupling reactions of amines with silanes.<sup>a</sup>

Entry	Silanes	Amines (equiv)	Temp.(°C)/ time(h)	Products	Conversion (isolated)
1	PhSiH <sub>3</sub>	<i>i</i> -PrNH <sub>2</sub> (2.1)	rt(12)	PhSiH(HN <i>i</i> -Pr) <sub>2</sub>	99(76)
2		<i>t</i> -BuNH <sub>2</sub> (2.1)	rt(20)	PhSiH(HN <i>t</i> -Bu) <sub>2</sub>	99(78)
3		HNEt <sub>2</sub> (2.1)	rt(20)	PhSiH(NEt <sub>2</sub> ) <sub>2</sub>	99(91)
4		C <sub>5</sub> H <sub>10</sub> NH (2.1)	rt(20)	PhSiH(NC <sub>5</sub> H <sub>10</sub> )	99(90)
5		HN <i>i</i> -Pr <sub>2</sub> (1.1)	70(12)	PhSiH <sub>2</sub> (N <i>i</i> -Pr <sub>2</sub> )	99(77)
6		C <sub>7</sub> H <sub>14</sub> NH (1.1)	80(10)	PhSiH <sub>2</sub> (NC <sub>7</sub> H <sub>14</sub> )	99(81)
7		HNPh <sub>2</sub> (1.0)	100(36)	PhSiH <sub>2</sub> (NPh <sub>2</sub> )	99(63)
8		PhNH <sub>2</sub> (2.2)	rt(15)	PhSiH(HNPh) <sub>2</sub> + PhSiH <sub>2</sub> (HNPh) + (PhSiH <sub>2</sub> ) <sub>2</sub> NPh	99(82:8:9) <sup>b</sup>
9		DippNH <sub>2</sub> (2.2)	70(17)	PhSiH(HNDipp) <sub>2</sub> + PhSiH <sub>2</sub> (HNDipp) + (PhSiH <sub>2</sub> ) <sub>2</sub> NDipp	99(97:2:1) <sup>b</sup>



10	Ph <sub>2</sub> SiH <sub>2</sub>	<i>i</i> -PrNH <sub>2</sub> (1.1)	rt(20)	Ph <sub>2</sub> SiH(HN <i>i</i> -Pr)	99(92)
11		<i>t</i> -BuNH <sub>2</sub> (1.1)	rt(20)	Ph <sub>2</sub> SiH(HN <i>t</i> -Bu)	99(96)
12		HNEt <sub>2</sub> (1.1)	rt(20)	Ph <sub>2</sub> SiH(NEt <sub>2</sub> )	99(94)
13		C <sub>5</sub> H <sub>10</sub> NH (1.1)	60(24)	Ph <sub>2</sub> SiH(NC <sub>5</sub> H <sub>10</sub> )	92(87)
14		C <sub>7</sub> H <sub>14</sub> NH (1.1)	100(72)	Ph <sub>2</sub> SiH(NC <sub>7</sub> H <sub>14</sub> )	89 <sup>b</sup>
15	PhMeSiH <sub>2</sub>	<i>i</i> -PrNH <sub>2</sub> (2.1)	rt(20)	PhMeSi(HN <i>i</i> -Pr) + PhMeSi(HN <i>i</i> -Pr) <sub>2</sub>	85(42)
16		<i>t</i> -BuNH <sub>2</sub> (2.1)	60(20)	PhMeSiH(HN <i>t</i> -Bu)	99(88)
17		HNEt <sub>2</sub> (1.1)	rt(24)	PhMeSiH(NEt <sub>2</sub> )	99(84)
18		C <sub>5</sub> H <sub>10</sub> NH (1.1)	60(24)	PhMeSiH(NC <sub>5</sub> H <sub>10</sub> )	90(82)

<sup>[a]</sup> Reaction conditions: amine, silanes (1 equiv) catalyst (5 mol %), Benzene (5 mL), 20 h rt. Conversions were obtained on the basis of consumption of silanes from integration of signals in the <sup>1</sup>H NMR spectra. <sup>[b]</sup> NMR scale reaction; yield on the basis of <sup>1</sup>H NMR analysis.

However, the reactions of bulky acyclic secondary amines, HN<sup>*i*</sup>Pr<sub>2</sub> & HNPh<sub>2</sub> with 2° silanes, Ph<sub>2</sub>SiH<sub>2</sub> & PhMeSiH<sub>2</sub> ends up with no reaction in presence of catalyst **13**, even at higher reaction temperature up to 100 °C and period (48 h). On the otherhand, the reactions of 1° silane (PhSiH<sub>3</sub>) with aliphatic and aromatic primary amines afforded the bis(amino)silanes (product **B**, entries 1-2, 8-9), secondary silanes, Ph<sub>2</sub>SiH<sub>2</sub> and PhMeSiH<sub>2</sub> yielded mono(amino)silanes (product **A**, entries 10-11 & 16). In case of entry 15, even though <sup>1</sup>H NMR of 1 mL reaction aliquot shows the formation of mono(amino)silane product PhMeSiH(HN*i*-Pr) (85 % NMR conversion), while isolation (distillation, 80 °C, 5 x 10<sup>-1</sup> mbar) it ends up with bis(amino)silane product, PhMeSi(HN*i*-Pr)<sub>2</sub> in 42 % yield. In entry 8, 9 & 14 yields were obtained based on the consumption of silanes from integration of signals in the <sup>1</sup>H NMR spectra, where the attempts to isolate pure products were unsuccessful.

A plausible mechanistic pathway for cross dehydro-coupling of silanes with amines catalyzed by compound **13** is shown in Figure 4.4.1. It has been proposed to proceed *via* formation of Mg-H intermediate (**D**) supported by IMes, which undergoes Mg-N/Si-H metathesis reaction with amines to yield the amido intermediate, (**E**) with evolution of H<sub>2</sub> (g). Intermediate (**E**) further reacts with one more equivalent of silanes to release the aminosilane products along with the regeneration of the hydride intermediate (**D**). Efforts were made to isolate and characterize the intermediates, which turned to be unsuccessful.

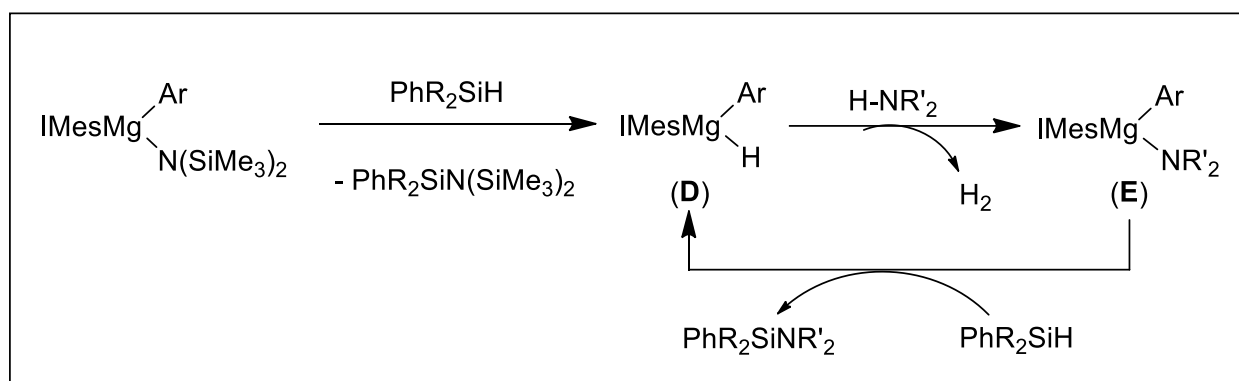


**Figure 4.4.1** Proposed mechanism for  $[\text{IMesMg}(\text{Ar})\{\text{N}(\text{SiMe}_3)_2\}]$  catalyzed dehydro-coupling of silanes with amines

**Conclusion:** In summary, we have reported the synthesis and characterization of IMes supported heteroleptic organo-magnesium(II) amide complexes  $[\text{IMesMg}(\text{Xyl})\{\text{N}(\text{SiMe}_3)_2\}]$  (**12**) and  $[\text{IMesMg}(\text{Mes})\{\text{N}(\text{SiMe}_3)_2\}]$  (**13**), which are achieved by salt metathesis reactions of  $\{\text{IMesMg}(\text{Ar})\text{Br}\}_2$  with lithium bis(trimethylsilyl)amide. Both compounds **12** and **13** have been presented as active pre-catalysts for cross dehydro-coupling of silanes with amines. The catalytical activity of compound **13** remained superior to compounds **12** and magnesium bis(amide).

## Crystallographic data and structure refinement details:

Table 4S.1: Crystal data and structure refinement summary for compounds **12** & **13**

	<b>12</b>	<b>13</b>
Empirical formula	C <sub>42</sub> H <sub>51</sub> MgN <sub>3</sub> Si <sub>2</sub>	C <sub>36</sub> H <sub>53</sub> N <sub>3</sub> MgSi <sub>2</sub>
Formula weight	678.34	608.30
Crystal system	Triclinic	Triclinic
Space group	<i>P</i> $\bar{1}$	<i>P</i> $\bar{1}$
a/Å	9.4770(4)	9.1877(3)
b/Å	12.9087(6)	11.2375(3)
c/Å	18.2858(8)	18.5799(5)
$\alpha$ /°	72.347(3)	85.9850(10)
$\beta$ /°	76.154(3)	77.6490(10)
$\gamma$ /°	89.454(3)	1830.86(9)
Volume/Å <sup>3</sup>	2064.92(16)	1830.86(9)
Z	2	2
$\rho_{\text{calc}}/\text{cm}^3$	1.091	1.103
$\mu/\text{mm}^{-1}$	0.132	0.141
F(000)	728.0	660.0
Crystal size /mm <sup>3</sup>	0.16 × 0.14 × 0.1	0.19 × 0.14 × 0.1
2 $\theta$ range for data collection/°	7.738 to 60.226	4.49 to 61.14
Index ranges	--13 ≤ h ≤ 12, -18 ≤ k ≤ 17, -25 ≤ l ≤ 25.	-12 ≤ h ≤ 13, -15 ≤ k ≤ 16, -24 ≤ l ≤ 26.
Reflections collected	31500	29800
Independent reflections	11837 [R <sub>int</sub> = 0.0442, R <sub>sigma</sub> = 0.0567]	10999 [R <sub>int</sub> = 0.0416, R <sub>sigma</sub> = 0.0518]
Data/restraints/parameters	11837 / 48 / 498	10999 / 0 / 394
Goodness-of-fit on F <sup>2</sup>	1.028	1.040
R <sub>1</sub> , wR <sub>2</sub> [I ≥ 2 $\sigma$ (I)]	R <sub>1</sub> = 0.0552, wR <sub>2</sub> = 0.1409	R <sub>1</sub> = 0.0505, wR <sub>2</sub> = 0.1344
R <sub>1</sub> , wR <sub>2</sub> [all data]	R <sub>1</sub> = 0.0891, wR <sub>2</sub> = 0.1638	R <sub>1</sub> = 0.0736, wR <sub>2</sub> = 0.1521
Largest diff. peak/hole/eÅ <sup>-3</sup>	0.65/-0.46	0.73/-0.38

**References:**

- (1) Baishya, A.; Barman, M. K.; Peddaraao, T.; Nembenna, S. *J. Organomet. Chem.*, **2014**, 769, 112-118.
- (2) Baishya, A.; Barman, M. K.; Biswal, H. S.; Nembenna, S. (*manuscript under preparation*).
- (3) (a) Reichl, J. A.; Berry, D. H. *Adv. Organomet. Chem.* **1998**, 43, 197. (b) Wang, W. D.; Eisenberg, R. *Organometallics*, **1991**, 10, 2222. (c) Matarasso-Tchiroukhine, E.; *J. Chem. Soc., Chem. Commun.* **1990**, 681. (d) Liu, H. Q.; Harrod, J. F. *Can. J. Chem.* **1992**, 70, 107. (e) Wang, J. X.; Dash, A. K.; Berthet, J. C.; Ephritikhine, M.; Eisen, M. S. *J. Organomet. Chem.* **2000**, 610, 49. (f) Hill, M. S.; Liptrot, D. J.; MacDougall, D. J.; Mahon, M. F.; Robinson, T. P. *Chem. Sci.*, **2013**, 4, 4212. (g) Xie, W.; Hu, H.; Cui, C. *Angew. Chem. Int. Ed.*, **2012**, 51, 11141.
- (4) (a) Dunne, J. F.; Neal, S. R.; Engelkemier, J.; Ellern, A.; Sadow, A. D. *J. Am. Chem. Soc.*, **2011**, 133, 16782-16785. (b) Hill, M. S.; Liptrot, D. J.; MacDougall, D. J.; Mahon, M. F.; Robinson, T. P. *Chem. Sci.*, **2013**, 4, 4212-4222.

Chapter 5:

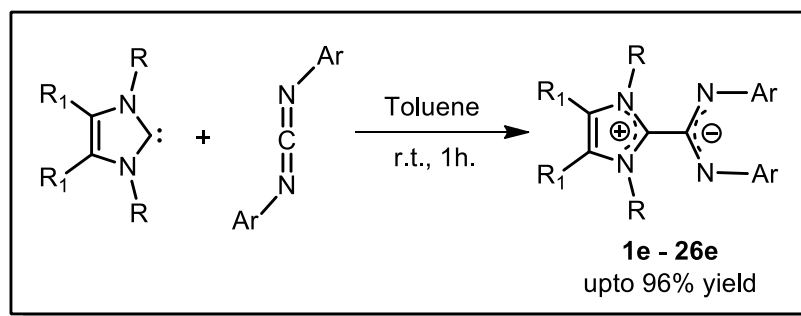
**Reactions of N-Heterocyclic carbenes with Aromatic Carbodiimides: Air Stable Zwitterions (NHC-CDI Adducts) and their Co-ordination Chemistry**

### Part A: Air stable “NHC-CDI” adducts; Zwitterionic type bulky amidinates

Herein, we have reported the synthesis of N-heterocyclic carbene-carbodiimide (“NHC-CDI”) adducts *i.e.*, zwitterionic type amidinates from the reaction between *N,N'*-diaryl substituted symmetrical or unsymmetrical carbodiimide and N-heterocyclic carbene at room temperature. In contrast to normal amidinates, which are air and moisture sensitive, and generally prepared by the treatment of amidines with bases under air and moisture free conditions, these new zwitterionic type bulky amidinate compounds are neutral and air stable. All new compounds were characterized by NMR and HRMS analyses. Further, the structures of representative compounds were confirmed by single crystal X-ray structures.

#### 5A.1 Synthesis and characterization of air stable bulky amidinates

Direct addition of unsaturated N-heterocyclic carbene to a symmetrical *N,N'*-diaryl carbodiimide in toluene at room temperature, immediate formation of precipitate was noticed. Progress of the reaction was monitored by thin layer chromatography. Finally the solvent was removed and the residue washed with *n*-hexane affording the air stable bulky amidinate (Scheme 5A.1.1).

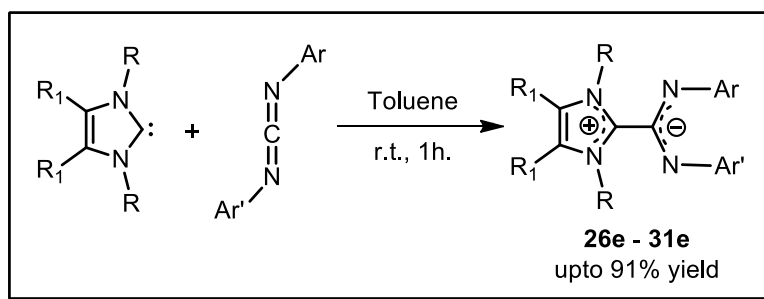


#### Scheme 5A.1.1 Direct addition of NHC to symmetrical *N,N'*-diaryl carbodiimides

Further, we have prepared a wide range of bulky amidinates (Figure 5A.1.1). For this study, we chose unsaturated N-heterocyclic carbenes such as 1,3-dimethyl-4,5-dimethylimidazol-2-ylidene

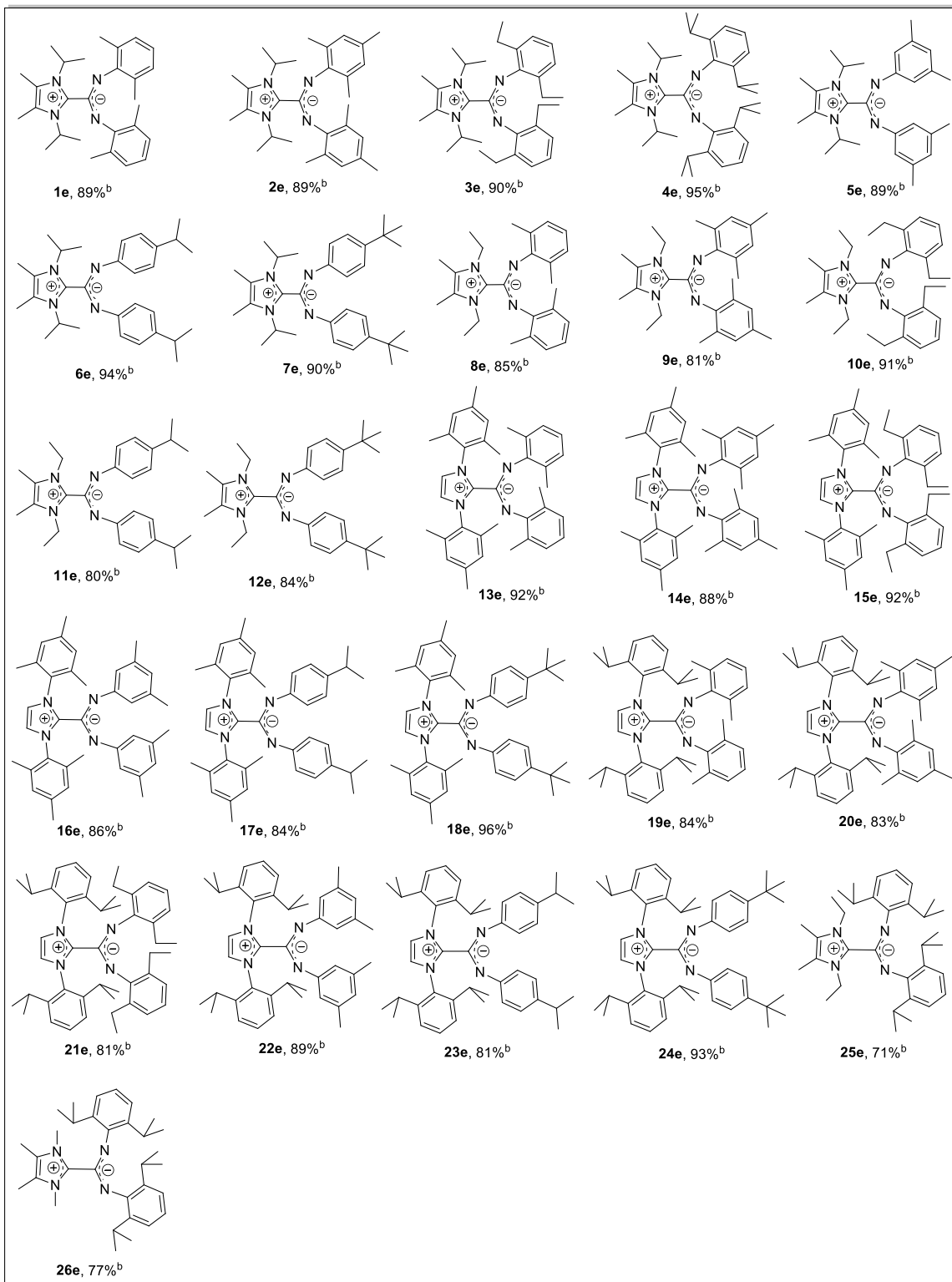
(<sup>Me</sup>IME),<sup>1</sup> 1,3-diisopropyl-4,5-dimethylimidazol-2-ylidene (<sup>Me</sup>IPr),<sup>1</sup> 1,3-diethyl-4,5-dimethylimidazol-2-ylidene (<sup>Me</sup>IEt),<sup>1</sup> 1,3-bis-(2,4,6-trimethylphenyl)imidazole-2-ylidene (IMes)<sup>2</sup> and 1,3-bis-(2,6-diisopropylphenyl)imidazole-2-ylidene (IPr)<sup>2</sup> and also symmetrical and unsymmetrical *N,N'*-diaryl CDIs to construct air stable amidinates.

To the best of our knowledge there have been no reports on the unsymmetrical NHC–CDI adducts in the literature. Therefore, considering the importance of such bulky amidinate systems in preparing metal complexes and nanoparticles,<sup>3</sup> our attention turned to prepare few more examples of bulky amidinates by direct addition of NHCs to unsymmetrical *N,N'*-diaryl CDIs (R–N=C=N–R') (Scheme 5A.1.2 and Figure 5A.1.2).



**Scheme 5A.1.2** Direct addition of NHC to unsymmetrical *N,N'*-diaryl carbodiimides.

Bulky *N,N'*-diaryl carbodiimides are important precursors for the preparation of bulky amidines, guanidines etc.<sup>4</sup> Alkyl carbodiimides such as dicyclohexylcarbodiimide (DCC), diisopropylcarbodiimide (DIC) and di-tert-butylcarbodiimide (DTC) are commercially available. In contrast, availability of *N,N'*-diaryl carbodiimides are very limited. However, in 2007, Cowley and co-workers have reported two examples of symmetrical *N,N'*-diaryl carbodiimides i.e., 1,3-di-(2,6-diisopropylphenyl) CDI and 1,3-di-(2,4,6-trimethylphenyl) CDI.<sup>5</sup> These CDIs can be prepared by the desulphurization of corresponding thioureas upon treatment with toxic mercuric oxide and anhydrous magnesium sulfate at harsh reaction conditions.

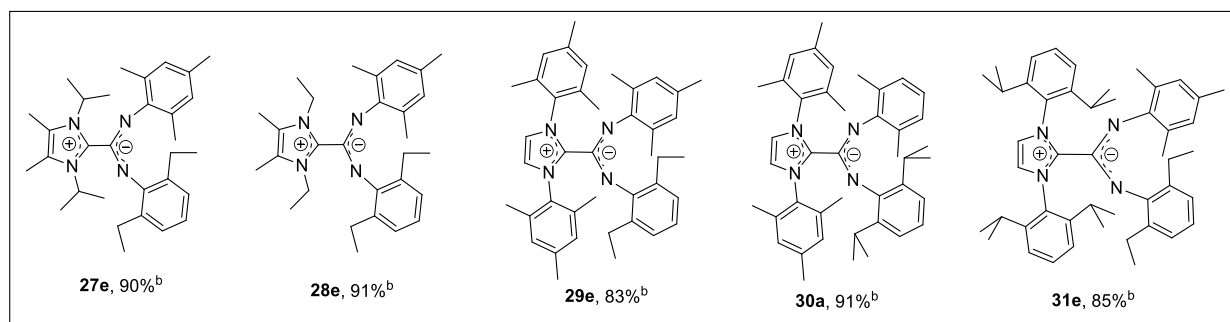


<sup>b</sup> Isolated yield

**Figure 5A.1.1** NHC-CDI adducts or zwitterion type bulky amidinates (**1e-26e**)



Recently, our group found a method for metal free access of various symmetrical and unsymmetrical *N,N'*-diaryl CDIs by the dehydrosulfurisation of thioureas upon treatment with base and thiophilic agent at mild reaction conditions.<sup>6</sup>



<sup>b</sup> Isolated yield

**Figure 5A.1.2** NHC-CDI (unsymmetrical) zwitterion type bulky amidinates (**27e-31e**)

From the literature, it is well known that amidinates can be obtained by the deprotonation of amidines in the presence of bases such as *n*-butyl lithium, phenyl lithium and  $\text{KN}(\text{SiMe}_3)_2$  etc. (Figure 5A.1.3).

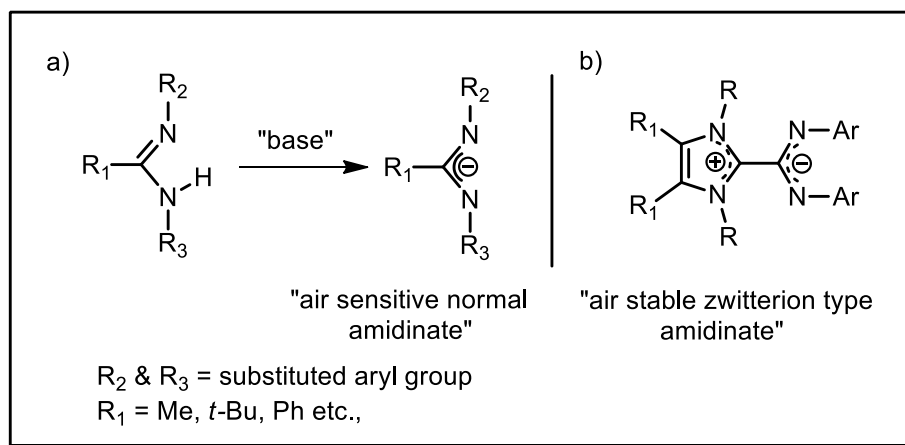


**Figure 5A.1.3** a) Normal amidinates vs b) Zwitterion type amidinates

By using these amidinates a variety of metal complexes can be synthesized. Bulky amidinates are very important precursors for the isolation of unusual low valent and/or low oxidation state

metal complexes. The most prevalent methods for the synthesis of amidinate metal complexes include: a) insertion of carbodiimides into an existing metal-carbon bond b) deprotonation of the neutral ligand with/using metal-alkyl or amide reagent and c) salt metathesis between a metal-halide and the lithiated ligand (usually generated by method a or b).

All novel, air stable zwitterion type amidinates were characterized by  $^1\text{H}$ ,  $^{13}\text{C}\{^1\text{H}\}$  NMR, mass spectrometry analysis. Further, compounds **1e**, **8e**, **12e**, **13e**, **16e**, **25e**, **26e** & **29e** have been confirmed with single crystal X-ray structural analysis.

Compounds **1e-31e** show expected number of signals in the  $^1\text{H}$  NMR spectra and consistent with their composition. More importantly, NHC upon reaction with CDI led to the formation of NHC-CDI adduct, this can be easily confirmed by the  $^{13}\text{C}\{^1\text{H}\}$  NMR spectrum. The  $^{13}\text{C}\{^1\text{H}\}$  NMR spectra for (**1e-31e**), the carbenic carbon of “NHC-CDI” adducts *i.e.*,  $\text{N}_2\text{C}^+$  of NCN resonance is in the region 140–152 ppm; is in good agreement with other reported NHC-CDI adducts.<sup>3b, 3c</sup> In contrast, carbene carbon peak (NCN) for unsaturated NHCs resonates in the range of 205–220 ppm (see Table 5A.1.1).

**Table 5A.1.1** Comparisons of carbene carbon peak (NCN) of free NHCs with “NHC-CDI” adducts in  $^{13}\text{C}\{^1\text{H}\}$  NMR

NCN of NHCs (ppm)		NCN of $(\text{N}_2\text{C})^+$ in NHC-CDI adducts (ppm) <sup>c,d</sup>	
1,3-diisopropyl-4,5-dimethylimidazol-2-ylidene ( <sup>Me</sup> IPr)	205.8 <sup>a</sup> , Ref <sup>1</sup>	<b>1e</b>	148.2
		<b>2e</b>	145.1
		<b>3e</b>	148.2
		<b>4e</b>	148.3
		<b>5e</b>	147.7

		<b>6e</b>	141.8
		<b>7e</b>	149.4
1,3-diethyl-4,5-dimethylimidazol-2-ylidene ( <sup>Me</sup> IEt)	211.1 <sup>a</sup> , Ref <sup>1</sup>	<b>8e</b>	147.4
		<b>9e</b>	145.2
		<b>10e</b>	146.9
		<b>11e</b>	140.2
		<b>12e</b>	148.2
1,3-bis-(2,4,6-trimethylphenyl)imidazole-2-ylidene (IMes)	219.4 <sup>b</sup> , Ref <sup>2</sup>	<b>13e</b>	149.2
		<b>14e</b>	149.4
		<b>15e</b>	149.3
		<b>16e</b>	152.2
		<b>17e</b>	150.1
		<b>18e</b>	149.6
1,3-bis-(2,6-diisopropylphenyl)imidazole-2-ylidene (IPr)	220.6 <sup>c</sup> , Ref <sup>2</sup>	<b>19e</b>	149.9
		<b>20e</b>	150.0
		<b>21e</b>	150.0
		<b>22e</b>	152.3
		<b>23e</b>	150.9
		<b>24e</b>	150.9
<sup>Me</sup> IEt	211.1 <sup>a</sup> , Ref <sup>1</sup>	<b>25e</b>	148.8
1,3-dimethyl-4,5-dimethylimidazol-2-ylidene ( <sup>Me</sup> IME)	212.7 <sup>a</sup> , Ref <sup>1</sup>	<b>26e</b>	141.0
<sup>Me</sup> IPr	205.8 <sup>a</sup> , Ref <sup>1</sup>	<b>27e</b>	140.7
<sup>Me</sup> IEt	211.1 <sup>a</sup> , Ref <sup>1</sup>	<b>28e</b>	146.4
IMes	219.4 <sup>b</sup> , Ref <sup>1</sup>	<b>29e</b>	148.4
		<b>30e</b>	149.4
IPr	220.6 <sup>c</sup> , Ref <sup>2</sup>	<b>31e</b>	150.0

<sup>a</sup> C<sub>6</sub>D<sub>6</sub>; <sup>b</sup> THF-d<sub>8</sub>; <sup>c</sup> CDCl<sub>3</sub>; <sup>d</sup> [Our work]

The molecular structures of compounds **1e**, **8e**, **12e**, **13e**, **16e**, **25e**, **26e** & **29e** are shown in Figure 5A.1.4 with selected bond lengths and bond angles in Table 5A.1.2.

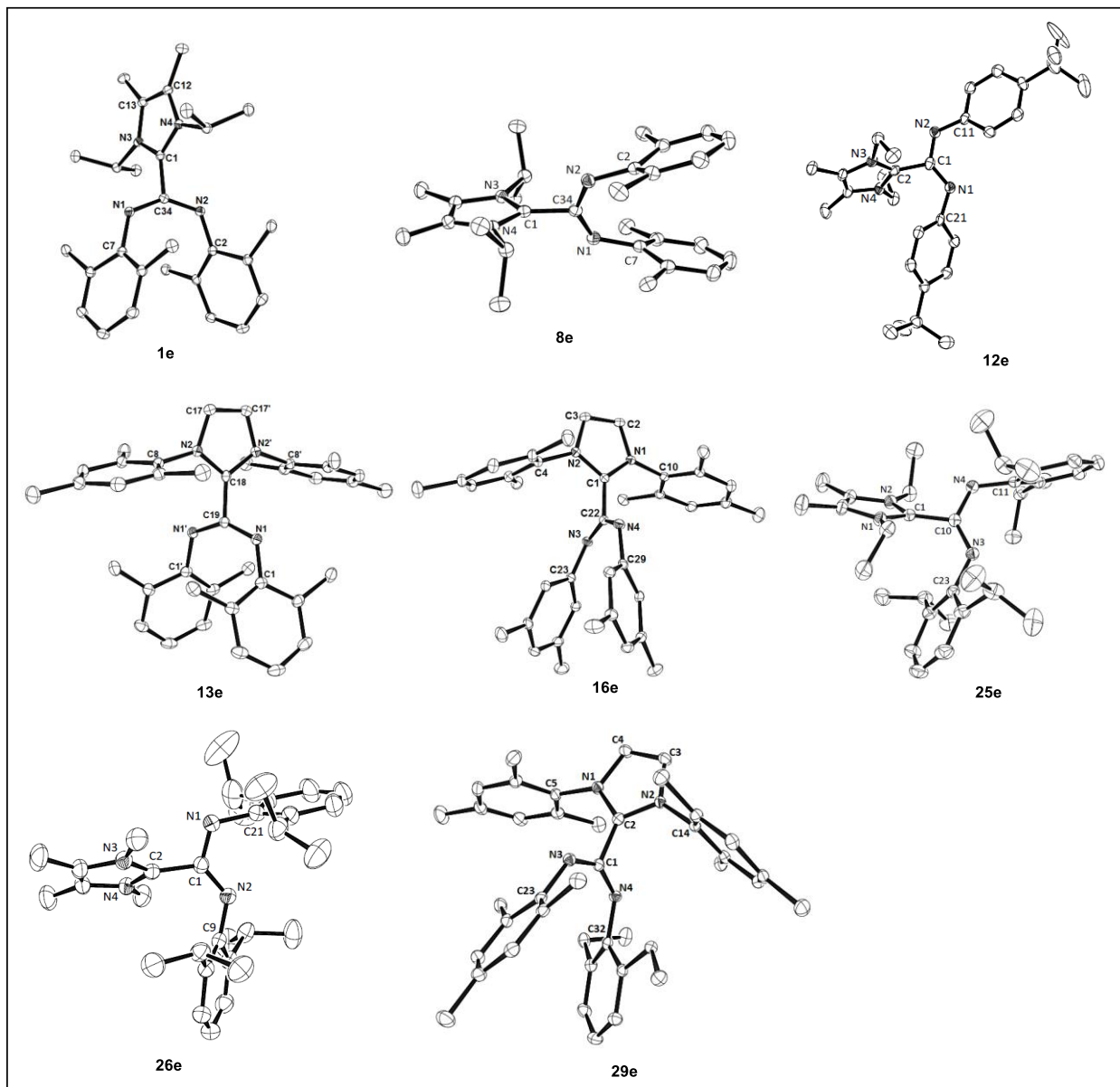


**Figure 5A.1.4** Molecular structures of **1e**, **8e**, **12e**, **13e**, **16e**, **25e**, **26e** & **29e**; with selected atom labels. All hydrogen atoms are removed for clarity

Compounds **1e**, **8e**, **12e**, **13e**, **16e**, **25e**, **26e** & **29e** crystallize in  $P\bar{1}$ ,  $C2/c$ ,  $P2_1/c$ ,  $Pbca$ ,  $C2/c$ ,  $P2_1/n$ ,  $P2_1/c$  &  $P2_1/n$  space groups, respectively. Crystal data and structure refinement details for compounds **1e**, **8e**, **12e**, **13e**, **16e**, **25e**, **26e** & **29e** can be found in Table 5S.1.

**Table 5A.1.2** Selected bond lengths (Å) and angles (°) for compounds **1e**, **8e**, **12e**, **13e**, **16e**, **25e**, **26e** & **29e**

<b>1e</b>		<b>8e</b>		<b>12e</b>	
C1–C34	1.509(2)	C1–C2	1.498(16)	C1–C2	1.506(6)
N1–C34	1.319(2)	C1–N1	1.323(8)	C1–N1	1.319(5)
N2–C34	1.320(2)	C1–N1 <sup>i</sup>	1.323(8)	C1–N2	1.331(5)
N1–C34–N2	139.94(17)	N1–C1–N1 <sup>i</sup>	139.50(12)	N1–C1–N2	130.30(4)
N3–C1–N4	108.26(15)	N2–C2–N2 <sup>i</sup>	107.75(11)	N3–C2–N4	107.2(4)
<b>13e</b>		<b>16e</b>		<b>25e</b>	
C18–C19	1.504(3)	C1–C22	1.502(15)	C1–C10	1.514(16)
N1–C19	1.316(14)	C22–N3	1.321(14)	C10–N3	1.320(15)
C19–N1 <sup>i</sup>	1.316(14)	C22–N4	1.323(14)	C10–N4	1.316(15)
N1 <sup>i</sup> –C19–N1	139.90(19)	N3–C22–N4	138.97(10)	N3–C10–N4	127.24(11)
N2 <sup>i</sup> –C18–N2	106.73(17)	N2–C1–N1	107.29(9)	N2–C1–N1	106.81(10)
<b>26e</b>		<b>29e</b>			
C1–C2	1.507(2)	C1–C2	1.501(3)		
C1–N1	1.311(2)	C1–N3	1.315(3)		
C1–N2	1.314(2)	C1–N4	1.316(3)		
N1–C1–N2	126.45(16)	N3–C1–N4	140.7(2)		
N3–C2–N4	106.81(15)	N1–C2–N2	106.90(19)		

Solid state structures for the compounds **1e**, **8e**, **13e**, **16e** & **29e** reveal that they exhibit structural similarities: The central NHC-CDI, C–C bond lengths 1.509(2), 1.498(16), 1.504(3), 1.502(15) & 1.501(3) Å for **1e**, **8e**, **13e**, **16e** & **29e**, respectively are comparable with the Kuhn's adduct (1.516 Å)<sup>1</sup> and more close to the Johnson's adduct (1.498–1.502 Å).<sup>3c</sup> N–C=N Core of

$\text{N}_2\text{C}^-$  moiety having both C–N and C=N bond distances are identical ( $\Delta_{\text{CN}} = 0$ ;  $\Delta_{\text{CN}} = d(\text{C–N}) - d(\text{C=N})$ ) this indicates the complete delocalization of the double bond. The dihedral angle between the  $\text{N}_2\text{C}^+$  and  $\text{N}_2\text{C}^-$  moieties (measured in Newman projection) in compounds **1e**, **8e**, **13e**, **16e** & **29e** found to be 66.41, 63.45, 61.06, 87.79, & 79.71 ( $^\circ$ ), respectively. These findings are in line with the reported Johnson's NHC–CDI adducts (63.32–85.15 ( $^\circ$ )). NCN bond angles in compounds **1e**, **8e**, **13e**, **16e** & **29e** for  $\text{N}_2\text{C}^+$  and  $\text{N}_2\text{C}^-$  moieties are 139.94(17), 108.26(15); 139.50(12), 107.75(11); 139.90(19), 106.73(17); 138.97(10), 107.29(9) and 140.70(2), 106.90(19) ( $^\circ$ ), respectively. These parameters are well in agreement with Johnson's NHC–CDI adducts; amidinate N–C=N bond angles are 139–140.02 ( $^\circ$ ) and the (slight wider) NHC N–C=N bond angles are 110–111.26 ( $^\circ$ ).<sup>3c</sup> Curiously, the crystal structures of compounds **12e**, **25e** & **26e** reveal that the  $\text{N}_2\text{C}^-$  moieties of amidinate N–C=N angles are somewhat acute (130.30(4), 127.24(11) & 126.45(16) ( $^\circ$ )) when compared to other five structures are in agreement with recently reported Cámpora's NHC–CDI adducts (126.5–131.1 ( $^\circ$ )).<sup>3b</sup>

## Part B: “NHC-CDI” adduct or zwitterionic type neutral amidinate supported Mg(II) and Zn(II) complexes

Five new examples of structurally characterized magnesium and zinc complexes of the form  $L^{4-t\text{-BuPh}}\text{-Mg}\{\text{N}(\text{SiMe}_3)_2\}_2$  (**14**); [ $L^{4-t\text{-BuPh}} = 1,3\text{-diethyl-4,5-dimethylimidazolium-2-}\{N,N'\text{-bis(4-}t\text{-butylphenyl)amidinate}\}$ ],  $L^{4-i\text{PrPh}}\text{-Mg}\{\text{N}(\text{SiMe}_3)_2\}_2$  (**15**);  $L^{4-i\text{PrPh}} = 1,3\text{-diethyl-4,5-dimethylimidazolium-2-}\{N,N'\text{-bis(4-isopropylphenyl)amidinate}\}$ ,  $L^{4-t\text{-BuPh}}\text{-Zn}\{\text{N}(\text{SiMe}_3)_2\}_2$  (**16**),  $L^{4-i\text{PrPh}}\text{-Zn}\{\text{N}(\text{SiMe}_3)_2\}_2$  (**17**) and  $L^{4-i\text{PrPh}}\text{-Zn}(\text{Et})_2$  (**18**), bearing zwitterionic type neutral amidinate or N-heterocyclic carbene-carbodiimide (“NHC-CDI”) adducts and monoanionic amido or alkyl ligands are reported. Compounds **14-18** were synthesized from the direct treatment of air stable “NHC-CDI” adducts with corresponding metal bis(bis-trimethylsilylamide) or dialkyl reagents. Solid state structures of compounds **14-18** reveal that the neutral zwitterionic ligand bonded to metal in a  $N,N'$ -chelated fashion with amido or alkyl ligands occupied the terminal positions that results a four co-ordinated distorted tetrahedral geometry around the metal center. In contrast, sterically bulky zwitterions such as  $L^{\text{Dipp}}$  [ $L^{\text{Dipp}} = 1,3\text{-diethyl-4,5-dimethylimidazolium-2-}\{N,N'\text{-bis(2,6-diisopropylphenyl)amidinate}\}$ ] upon treatment with lithium bis-trimethylsilylamide  $\text{LiN}(\text{SiMe}_3)_2$ , instead of chelated zwitterionic adduct  $L^{\text{Dipp}}\text{-LiN}(\text{SiMe}_3)_2$ , affords the dimeric compound of  $^{\text{Me}}\text{IEt}\text{-}\{\text{LiN}(\text{SiMe}_3)_2\}_2$  (**19**), in which one molecule of NHC ( $^{\text{Me}}\text{IEt} = 1,3\text{-diethyl-4,5-dimethylimidazol-2-ylidene}$ ) coordinates to one of the two lithium centers. Similarly, the reaction between  $L^{\text{Dipp}}$  and  $\text{Mg}\{\text{N}(\text{SiMe}_3)_2\}_2$ , instead of zwitterionic adduct of metal bis-(bis-trimethylsilylamide), formation of NHC adduct of metal bis(bis-trimethylsilylamide),  $^{\text{Me}}\text{IEt}\text{-Mg}\{\text{N}(\text{SiMe}_3)_2\}_2$  (**20**) was occurred. Alternatively, both compounds **19** and **20** were synthesized by the direct addition of one equivalent of NHC *i.e.*  $^{\text{Me}}\text{IEt}$  to  $\text{LiN}(\text{SiMe}_3)_2$  (2.0 equiv) and  $\text{Mg}\{\text{N}(\text{SiMe}_3)_2\}_2$  (1.0 equiv), in benzene- $d_6$  respectively.

### 5B.1 Coordination of zwitterions (“NHC-CDI”adducts) to magnesium and zinc elements:

The ligands used for complexation reaction are shown in Figure 5B.1.1.  $L^{4-t-BuPh} = [1,3\text{-diethyl-4,5-dimethylimidazolium-2-}\{N,N'\text{-bis(4-}t\text{-butylphenyl)amidinate}\}]$ ,  $L^{4-iPrPh} = [1,3\text{-diethyl-4,5-dimethylimidazolium-2-}\{N,N'\text{-bis(4-isopropylpropylphenyl)amidinate}\}]$ ,  $L^{Xyl} = [1,3\text{-diethyl-4,5-dimethylimidazolium-2-}\{N,N'\text{-bis(2,6-dimethylphenyl)amidinate}\}]$  &  $L^{Dipp} = [1,3\text{-diethyl-4,5-dimethylimidazolium-2-}\{N,N'\text{-bis(2,6-diisopropylphenyl)amidinate}\}]$ .

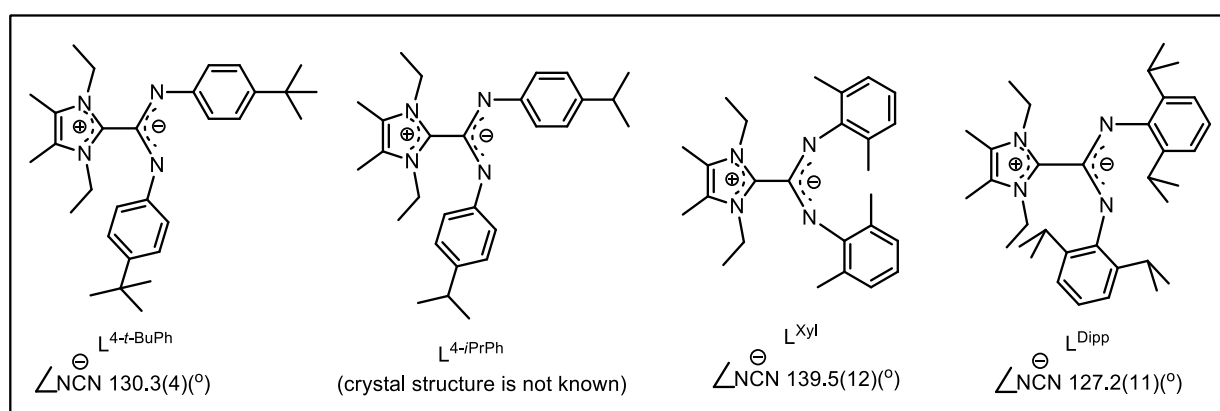
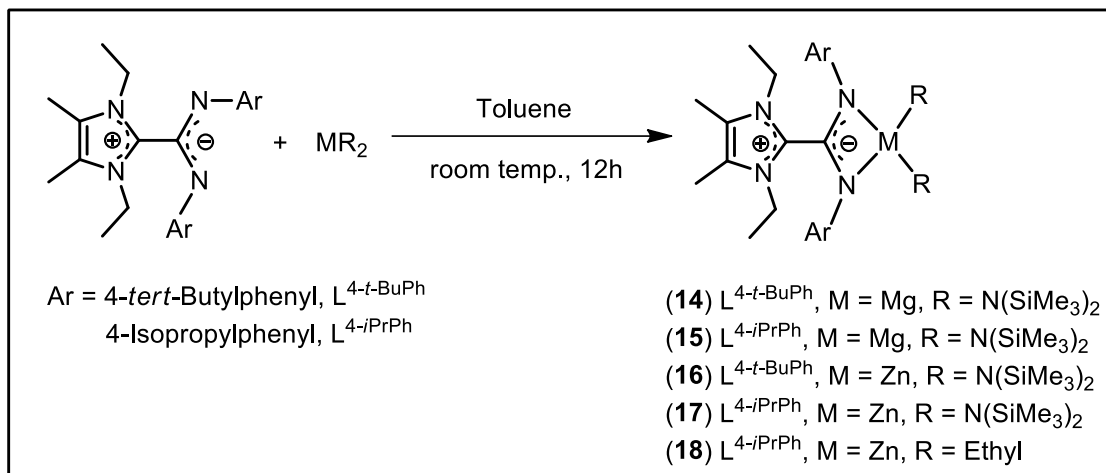


**Figure 5B.1.1** Zwitterionic amidinates with NCN bond angles.

Coordination chemistry of zwitterions began with direct addition of “NHC-CDI” adducts with metal bis(amide). Stoichiometric reaction of  $L^{4-t-BuPh}$  &  $L^{4-iPrPh}$  with  $Mg\{N(SiMe_3)_2\}_2$ , in toluene or benzene at room temperature results in the formation of NHC-CDI adduct of metal bis(amide),  $L^{4-t-BuPh}\text{-}Mg\{N(SiMe_3)_2\}_2$  (**14**) &  $L^{4-iPrPh}\text{-}Mg\{N(SiMe_3)_2\}_2$  (**15**), respectively in quantitative yield (Scheme 5B.1.1). Similar reaction of  $L^{4-t-BuPh}$  &  $L^{4-iPrPh}$  with zinc bis(amide)  $Zn\{N(SiMe_3)_2\}_2$  yields metal amido product of zwitterions, i.e.  $L^{4-t-BuPh}\text{-}Zn\{N(SiMe_3)_2\}_2$  (**16**) &  $L^{4-iPrPh}\text{-}Zn\{N(SiMe_3)_2\}_2$  (**17**), respectively. A similar reaction of  $L^{4-iPrPh}$  with zinc dialkyl,  $ZnEt_2$  has been carried out to obtain the alkylated product of zwitterions, i.e.  $L^{4-iPrPh}\text{-}ZnEt_2$  (**18**).



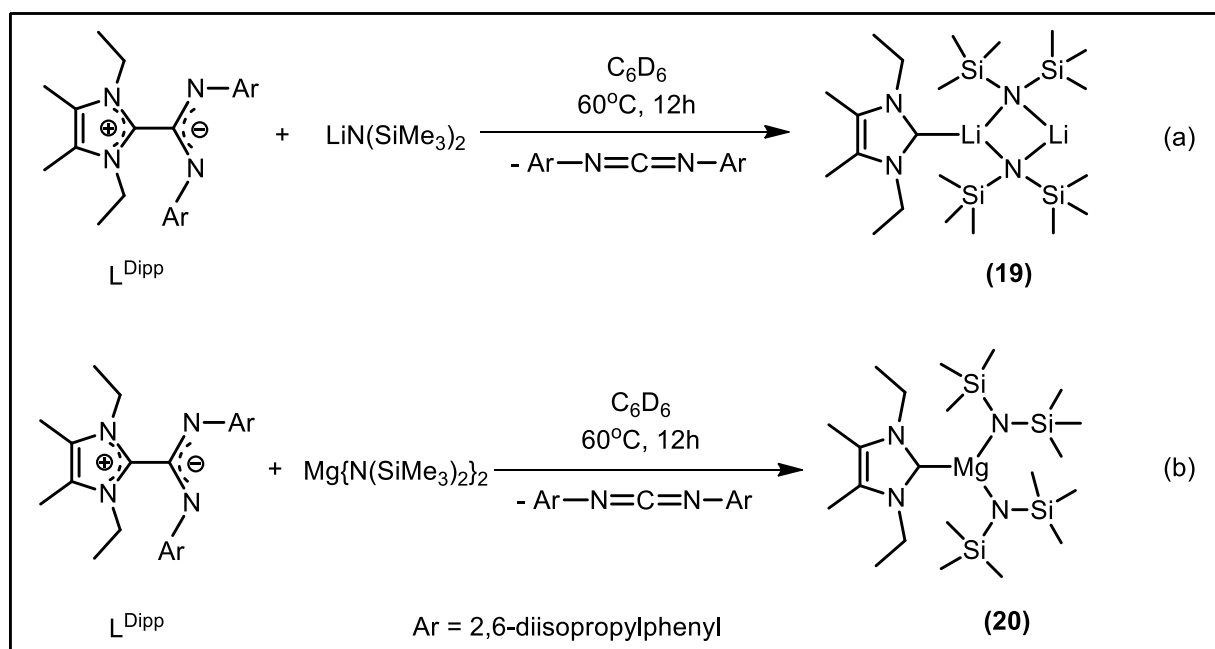


**Scheme 5B.1.1** Synthesis of zwitterionic complexes of metal bis(amide) & dialkyl

Further, we decided to extend the coordination chemistry of zwitterions with Group 1 metal amido reagents. In view of this, reaction of either L<sup>4-*t*-BuPh</sup> or L<sup>4-*i*PrPh</sup> zwitterion with MN(SiMe<sub>3</sub>)<sub>2</sub> (M = Li, Na and K) was carried out to obtain zwitterion supported Group 1 metal amides. Unfortunately, we could not isolate the desired products, although <sup>1</sup>H NMR of reaction mixture in each case indicated the formation of interaction of metal ion to ligand along with some unknown impurities. Therefore, our attention turned to choose less and more bulky zwitterions such as L<sup>Xyl</sup> and L<sup>Dipp</sup>, respectively, when compared to L<sup>4-*t*-BuPh</sup> or L<sup>4-*i*PrPh</sup> zwitterions. Accordingly, we explored the coordination chemistry of these zwitterions with Group 1 and Group 2 metal amido reagents. Reactions of L<sup>Xyl</sup> ligand with Group 1 and Group 2 metal amido reagents were failed, leaving the starting precursors intact even at forced reaction condition.

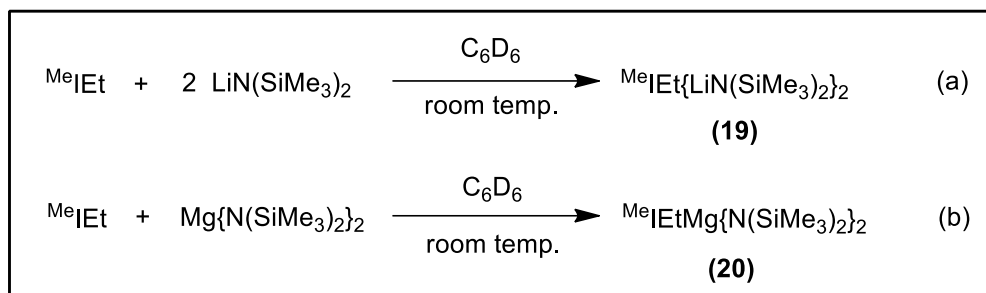
Next, a direct reaction between L<sup>Dipp</sup> with LiN(SiMe<sub>3</sub>)<sub>2</sub> in benzene-d<sub>6</sub> at room temperature was performed to obtain LiN(SiMe<sub>3</sub>)<sub>2</sub> complex bearing a zwitterion ligand. The <sup>1</sup>H NMR spectrum reveals that there is no product formation in the above reaction and both precursors were intact. However, the reaction mixture was heated to 60 °C and cooled to room

temperature, which allows the formation of single crystals within 1 day. X-ray crystal structure reveals the formation of dimeric  $\text{LiN}(\text{SiMe}_3)_2$  bearing one free NHC ligand,  $^{\text{Me}}\text{IEt}\{\text{LiN}(\text{SiMe}_3)_2\}_2$  (**19**) in which bulky dipp-N=C=N-dipp (dipp = 2,6-*i*-Pr<sub>2</sub>-C<sub>6</sub>H<sub>3</sub>) CDI is dropped out from the product. Similarly, no reaction was observed when  $\text{L}^{\text{Dipp}}$  mixed with  $\text{Mg}\{\text{N}(\text{SiMe}_3)_2\}_2$  in benzene-*d*<sub>6</sub> at room temperature. However, the same reaction mixture heated to 60 °C for 12 hours that leads to the formation of  $^{\text{Me}}\text{IEt-Mg}\{\text{N}(\text{SiMe}_3)_2\}_2$  (**20**), instead of zwitterionic complex of metal bis(amide), which is confirmed by X-ray single crystal structure (Scheme 5B.1.2).



**Scheme 5B.1.2:** Synthesis of a)  $^{\text{Me}}\text{IEt}\{\text{LiN}(\text{SiMe}_3)_2\}_2$  (**19**) & b)  $^{\text{Me}}\text{IEtMg}\{-\{\text{N}(\text{SiMe}_3)_2\}_2$  (**20**)

Alternatively, both compounds **19** and **20** can be easily accessed from the direct treatment of free NHC *i.e.*  $^{\text{Me}}\text{IEt}$  with corresponding metal bis (amide)s in required equivalents in benzene-*d*<sub>6</sub> at ambient reaction condition (Scheme 5B.1.3).



**Scheme 5B.1.3:** Direct synthesis of a)  $\text{MeIEt}\{\text{LiN}(\text{SiMe}_3)_2\}_2$  (**19**), b)  $\text{MeIEtMg}\{\text{N}(\text{SiMe}_3)_2\}_2$  (**20**)

The ambiguity of the above results can be answered from the conformational studies of these ligands. The solid state structures for ligands  $\text{L}^{4-t\text{-BuPh}}$ ,  $\text{L}^{\text{Xyl}}$  and  $\text{L}^{\text{Dipp}}$  are already presented in the previous part i.e. part A of the chapter 5 (Figure 5A.1.4) along with selected bond parameters (Table 5A.1.2). The structural conformation along with the amidinate NCN bond angles for ligands  $\text{L}^{4-t\text{-BuPh}}$ ,  $\text{L}^{\text{Dipp}}$  and  $\text{L}^{\text{Xyl}}$  are shown in figure 5B.1.1. The solid state structures for the ligands reveals that there is a difference in conformation between  $\text{L}^{4-t\text{-BuPh}}$ ,  $\text{L}^{\text{Dipp}}$  and  $\text{L}^{\text{Xyl}}$  results from the substituents attached with the nitrogen atoms of amidinate ( $\text{N}_2\text{C}^-$ ) moiety. In case of  $\text{L}^{4-t\text{-BuPh}}$ , the C–N bonds of the amidinate moiety adopt cisoid-transoid configuration with regards to imidazolyl and aryl groups, whereas,  $\text{L}^{\text{Xyl}}$  exhibits transoid-transoid configuration (Figure 5B.1.1). The solid state conformation of  $\text{L}^{4-t\text{-BuPh}}$  ligand is almost matches  $\text{L}^{\text{Dipp}}$  with the amidinate NCN bond angle of 130.3(4) ( $^\circ$ ) and 127.2(11) ( $^\circ$ ) respectively, are within the range of reported values of Ca'mpora's zwitterions [126.5–130.12 ( $^\circ$ ); ICy-CDI<sup>Dipp</sup> 126.5(2) ( $^\circ$ ), IMe-CDI<sup>Dipp</sup> 127.5(4) ( $^\circ$ ), ICy-CDI<sup>Tol</sup> 130.12(12) ( $^\circ$ )]. On the other hand, the NCN bond angle of amidine moiety in  $\text{L}^{\text{Xyl}}$  is found 139.5(12) ( $^\circ$ ), which is wider by an angle of 9.2 and 12.3 ( $^\circ$ ) in comparison with  $\text{L}^{4-t\text{-BuPh}}$  and  $\text{L}^{\text{Dipp}}$  zwitterions, respectively.

It is the conformation and NCN<sup>-</sup> wide bond angle in  $\text{L}^{\text{Xyl}}$  which restricts the interaction with the metal ions of metal amido and alkyls. Further, reaction between  $\text{L}^{\text{Dipp}}$  and either Group 1

or 2 metal bis(amide) failed to produce *N,N'*-chelated metal bis(amide) adducts of zwitterions, instead leads to NHC adducts of metal bis(amides) **19** and **20**. Having the same conformation and nearly similar NCN bond angles of the amidine moiety for L<sup>Dipp</sup> and L<sup>4-*t*-BuPh</sup>, surprisingly, no coordination of L<sup>Dipp</sup> zwitterion with metal bis(amide) was observed. This is due to the presence of sterically encumbered dipp group to the N-substituents of amidinate moiety in L<sup>Dipp</sup>, prevents the formation of chelated metal complexes or any other interaction with metal bis(amide).

**5B.2 Characterization of zwitterionic metal complexes:** The metal complexes **14-20** were characterized by multinuclear NMR {<sup>1</sup>H, <sup>13</sup>C, <sup>29</sup>Si (for **14**, **15**, **16**, **17**, **19** and **20**) and <sup>7</sup>Li (only for **19**)} and single crystal X-ray structural analysis. Compounds **14-18** are thermally stable and melting without decomposition at the range of 182-184, 185-188, 139-142, 145-148 and 153-155 °C, respectively. They are found to be soluble in benzene, toluene and tetrahydrofuran, but sparingly soluble in *n*-hexane. Compounds **14-20** show expected number of signals in the <sup>1</sup>H and <sup>13</sup>C NMR spectra and are in consistent with their composition. The <sup>1</sup>H NMR spectra of compounds **14-17** exhibit a singlet resonance at 0.61, 0.61, 0.62 & 0.63 ppm values, respectively, corresponds to 36 protons of amide group i.e. M{N(SiMe<sub>3</sub>)<sub>2</sub>}<sub>2</sub>. These values are found to be deshielded in comparison to both magnesium and zinc bis(amide) and NHC ligated metal bis(amide) compounds [0.45 & 0.37 ppm; Mg{N(SiMe<sub>3</sub>)<sub>2</sub>}<sub>2</sub>·2THF, 0.20 ppm; Zn{N(SiMe<sub>3</sub>)<sub>2</sub>}<sub>2</sub>, and 0.38 ppm; <sup>t</sup>Bu:Mg{N(SiMe<sub>3</sub>)<sub>2</sub>}<sub>2</sub> and 0.36 ppm; <sup>t</sup>Bu:Zn{N(SiMe<sub>3</sub>)<sub>2</sub>}<sub>2</sub> in C<sub>6</sub>D<sub>6</sub>]. Further, <sup>29</sup>Si{<sup>1</sup>H} NMR corresponding to silyl group of ligated metal amide for compounds **14-17** exhibit resonance at -9.74, -12.17, -6.13 & -8.63 ppm, respectively, these values are within the expected values of four coordinated silicon atom (-17.12 ppm in <sup>t</sup>Bu:Mg{N(SiMe<sub>3</sub>)<sub>2</sub>}<sub>2</sub> and -5.00 ppm in <sup>t</sup>Bu:Zn{N(SiMe<sub>3</sub>)<sub>2</sub>}<sub>2</sub>). For compound **18**, <sup>1</sup>H NMR spectrum displays a triplet

resonance at 1.73 (6H) and a quartet at 0.47 (4H) ppm, corresponding to the  $CH_3$  &  $CH_2$  protons of ethyl groups attached with zinc atom.

$^1H$  NMR spectra of compounds **19** and **20** exhibit a singlet resonance for amide ligand,  $M\{N(SiMe_3)_2\}_2$  at 0.34 & 0.36 ppm, respectively. The amido group resonance of compound **20** (0.36 ppm) is well in agreement with the NHC supported magnesium bis(amide),  $tBu:Mg\{N(SiMe_3)_2\}_2$  (0.38 ppm). The  $^{13}C$  NMR spectra for compounds **19** and **20** show characteristic peaks for metal co-ordinated carbene carbon at 194.2 and 177.9 ppm, respectively (free  $^{Me}IEt$  resonates at 211.9 ppm). The carbene carbon peak for compound **20** (177.9 ppm) is well agreement with the known value of NHC co-ordinate metal bis(amide), 177.7 ppm in  $tBuMg\{N(SiMe_3)_2\}_2$ .  $^{29}Si$  NMR for compounds **19** and **20** resonates at  $-11.24$  &  $-8.19$  ppm, respectively, which are good in agreement with four coordinate silicon atom. Further, in case of compound **19**,  $^7Li$  NMR confirms the presence of Li atom by displaying a singlet resonance at 1.64 ppm.

**5B.3 X-Ray crystallographic studies of zwitterionic complexes:** The molecular structures of compounds **18-20** were determined by single crystal X-ray diffraction analysis with bond parameters showing in Table 5B.3.1. For crystal data and structure refinement see Table 5S.2. The solid state structures for compounds **14-18** (Figure 5B.3.1) exhibits a similarity in structural motif, where zwitterionic type ligands either  $L^{4-t-BuPh}$  or  $L^{4-iPrPh}$  coordinates to the metal center in a  $N,N'$ -chelated, bidentate fashion. In each case, the five membered NHC heterocycle  $C_3N_2$  ring is connected through a C-C single bond with four membered amidinate metal heterocycle,  $N_2CM$  ( $M = Mg$  or  $Zn$ ). The molecular structure of complex **14** is shown in Figure 5B.3.1a. Compound **14** crystallizes in the orthorhombic system with  $P2_12_12_1$  space group. The magnesium atom in **14** is tetra co-ordinated, where the metal is bonded to two nitrogen atoms of the neutral

bidentate ligand and two terminal amido ligands. Thus the magnesium atom in compound **14** is in +2 oxidation states with a distorted tetrahedral geometry.

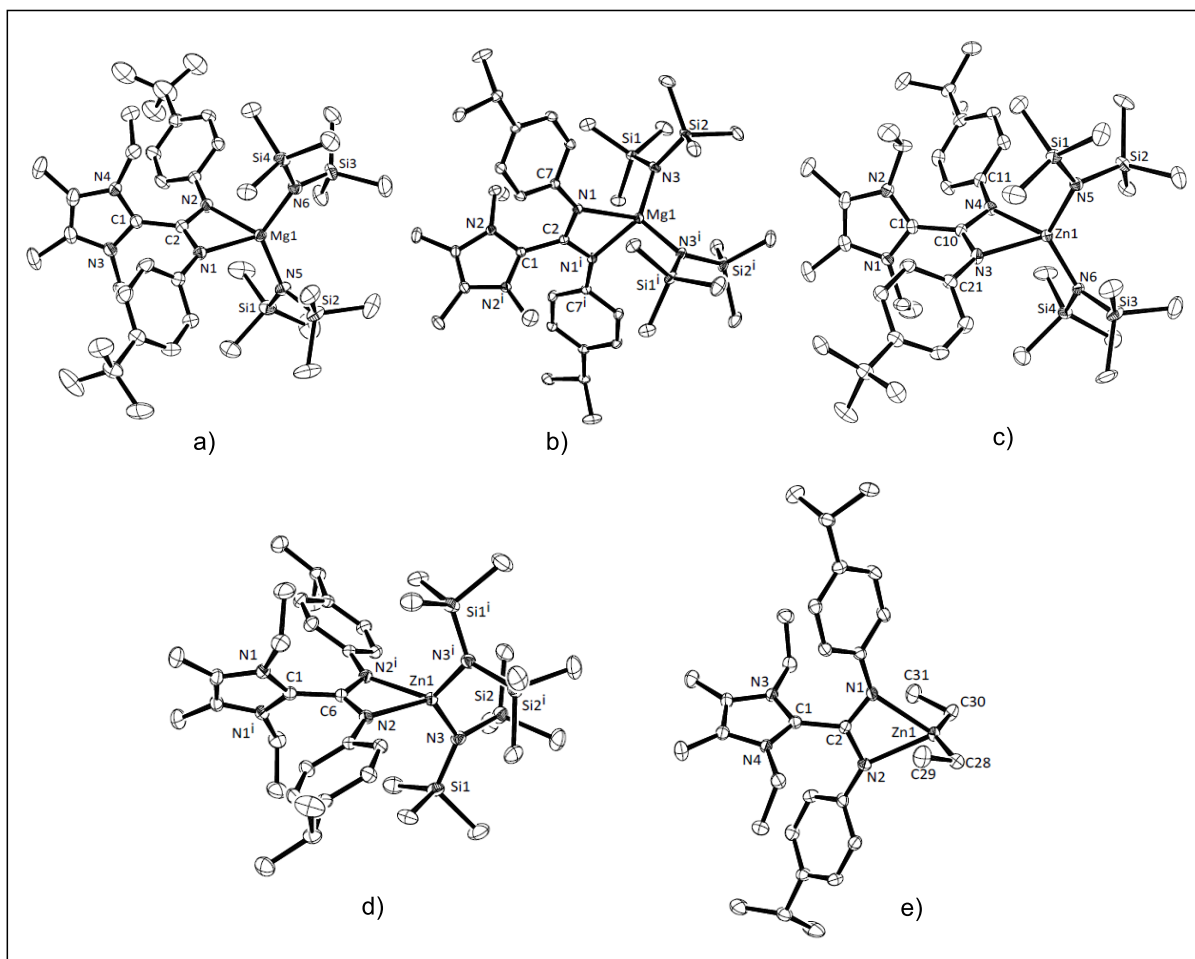


**Figure 5B.3.1** Molecular structures of a)  $L^{4-t-BuPh}-Mg\{N(SiMe_3)_2\}_2$  (**14**), b)  $L^{4-i-PrPh}-Mg\{N(SiMe_3)_2\}_2$  (**15**), c)  $L^{4-t-BuPh}-Zn\{N(SiMe_3)_2\}_2$  (**16**), d)  $L^{4-i-PrPh}-Zn\{N(SiMe_3)_2\}_2$  (**17**) & e)  $L^{4-i-PrPh}-ZnEt_2$  (**18**), (ORTEP view, 35% probability ellipsoid) with selected atom labels. All hydrogen atoms are removed for the clarity.

To study the coordination behavior of complex **14**, the bond parameters are compared with the respective ligand *i.e.*  $L^{4-t-BuPh}$ . The central NHC–CDI C–C bond and amidinate C–N bond lengths for **14** are C1–C2 1.490(5) & C2–N1 1.329(5) (Å) are close to the free ligand bond

lengths C1–C2 1.507(2), C1–N1 1.311(2) (Å). The NCN bond angle of the amidinate moiety in **14** is N1–C2–N2 115.2(3) (°), which contracts by 11.25 (°) on chelation to the metal center, free ligand ( $L^{4-t-BuPh}$ ) NCN bond angle is N1–C1–N2 126.45(16) (°). The solid structure of **14** reveals that the both C–N bonds are in cisoid configuration with regard to imidazolyl and aryl groups in contrast to  $L^{4-t-BuPh}$ , where one C–N bond is cisoid and other is in transoid configuration.

**Table 5B.3.1** Selected bond distances (Å) and angles (°) for compounds **14–18**,

<b>14</b>	<b>15</b>	<b>16</b>
C1–C2 1.490(5)	C1–C2 1.490(2)	C1–C10 1.493(9)
C2–N1 1.329(5)	C2–N1 1.328(11)	C10–N3 1.316(9)
C1–N4 1.338(6)	C1–N2 1.338(12)	C1–N1 1.330(9)
N1–C2–N2 115.2(3)	N1–C2–N1 <sup>i</sup> 114.57(12)	N4–C10–N3 116.0(6)
N3–C1–N4 108.8(3)	N2–C1–N2 <sup>i</sup> 107.94(12)	N2–C1–N1 108.4(6)
<b>17</b>	<b>18</b>	
C1–C6 1.489(4)	C1–C2 1.502(5)	
C6–N2 1.320(2)	C2–N1 1.322(5)	
C1–N1 1.338(2)	C1–N4 1.343(5)	
N2–C6–N2 <sup>i</sup> 114.7(2)	N1–C2–N2 116.2(3)	
N1–C1–N1 <sup>i</sup> 107.8(2)	N3–C1–N4 108.0(3)	
	Zn1–C28 1.997(4)	
	Zn1–C30 2.002(4)	

Similarly, compounds **15**, **16**, **17** and **18** are crystalized in monoclinic  $C2/c$ , triclinic  $P\bar{1}$ , monoclinic  $C2/c$  and triclinic  $P\bar{1}$  space groups, respectively. The C–N bond configuration around the amidinate moiety is in cisoid configuration for compounds **15**, **16**, **17** and **18** with the NCN bond angle of the amidinate core are N1–C2–N1<sup>i</sup> 114.57(12), N4–C10–N3 116.0(6), N2–C6–N2<sup>i</sup> 114.7(2) and N1–C2–N2 116.2(3) (°) close to the compound **14**. The central C–C (NHC–CDI)

and C–N (amidine core) bond lengths for **15**, **16**, **17** and **18** are C1–C2 1.490(2), 1.328(11); C1–C10 1.493(9), C10–N3 1.316(9); C1–C6 1.489(4); C6–N2 1.320(2) (Å) and C1–C2 1.502(5); C2–N1 1.322(5) (Å), respectively and are in consistent with compound **14**. The Zn–C<sub>Et</sub> bond distance for compound **18** i.e. Zn1–C28 1.997(4) & Zn1–C30 2.002(4) (Å) are matches with the zinc-carbon bond distance of IPr–ZnEt<sub>2</sub>.<sup>7</sup>

Compounds **19** and **20** were crystallized in the monoclinic  $P2_1/c$  and triclinic  $P\bar{1}$  space groups, respectively. The solid state structures for **19** and **20**, with selected bond parameters (Figure 5B.3.2), display the three coordinate metal centers with nearly trigonal planar arrangements with carbene-metal-amide bond angles, wider in case of compound **19** (C1–Li1–N4 131.66(15) (°)) and is acute for compound **20** (C1–Mg1–N4 111.89(8) (°)). The molecular structure reveals the monomeric form of compound **20** with the NHC bonded to magnesium bis(amide). Whereas compound **19** exists as dimeric structure of lithium bis(amide) where one of the two lithium center is coordinated with NHC ligand. It is worthy to mention that despite the significant research interest in coordination chemistry of NHC ligands, only a handful of structurally characterized lithium complexes bearing NHC ligands have been reported.<sup>8</sup> The Mg–C<sub>NHC</sub> bond length in **20** is 2.204(2) Å is in good agreement with our previously reported Mg–C<sub>NHC</sub> [2.241(Å) of compound I<sup>t</sup>BuMg{N(SiMe<sub>3</sub>)<sub>2</sub>}<sub>2</sub>] bond distance and other NHC–Mg-adducts (2.194–2.279) (Å). As well for compound **19**, the Li–C<sub>NHC</sub> bond distance is 2.189(4) (Å), in good agreement with known lithium-carbene bond distances [2.089–2.322 (Å)].



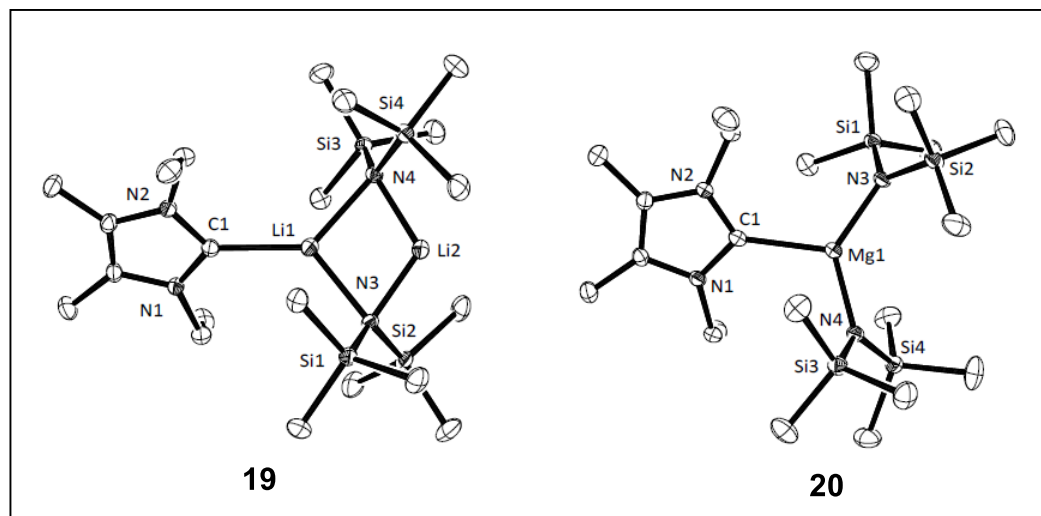


**Figure 5B.3.2** Molecular structures of a)  $^{\text{Me}}\text{IEt}\{\text{LiN}(\text{SiMe}_3)_2\}_2$  (**19**), b)  $^{\text{Me}}\text{IEt}-\text{Mg}\{\text{N}(\text{SiMe}_3)_2\}_2$  (**20**), (ORTEP view, 35% probability ellipsoid) with selected atom labels. All hydrogen atoms are removed for the clarity. Selected bond lengths (Å) and angles ( $^\circ$ ): for **19**: C1–Li1 2.189(4), C1–N1 1.356(2), C1–N2 1.362(2), Li1–N3 2.120(3), C1–Li1–N4 131.66(15), N1–C1–N2 102.5(15), N3–Li1–N4 99.8(14); for **20**: C1–Mg1 2.204(2), C1–N1 1.355(2), C1–N2 1.362(3), Mg1–N3 1.993(18), C1–Mg1–N4 111.89(8), N1–C1–N2 103.5(17), N3–Mg1–N4 131.5(8).

**Conclusion:** In conclusion, we have prepared 31 examples of well characterized new air stable “NHC-CDI” adducts i. e., bulky amidinates from the direct addition of *N,N'*-diaryl substituted symmetrical and unsymmetrical carbodiimides to unsaturated N-heterocyclic carbenes at ambient reaction conditions. From the X-ray structural investigation of few adducts, we assume that acute NCN bond angle at the amidinate moiety favors for interaction with a metal in the traditional coordination of amidinate ligand, this statement was supported by Ca'mpora and co-worker's work on copper (I) complexes bearing NHC-CDI ligand systems.<sup>3b</sup>

Further, in part B section we have established the co-ordination chemistry of zwitterions or “NHC-CDI” adducts with magnesium and zinc elements. Here, we have synthesized magnesium and zinc bis-amide and di-alkyl complexes bearing neutral amidinate type zwitterions or “NHC-CDI” adducts, where it co-ordinates to the metal center in a *N,N'*-chelated fashion. This was achieved by the direct treatment of metal reagent  $MR_2$  ( $M = Mg$  or  $Zn$ ;  $R = N(SiMe_3)_2$  or  $Et$ ) with air stable and neutral “NHC-CDI” adduct in toluene. Our work clearly shows air stable zwitterions are alternative to neutral N-heterocyclic carbenes, phosphines or other neutral ligand systems. Moreover, unlike air and moisture sensitive, monoanionic amidinates, these are air & moisture stable and neutral type. More importantly, C–N bond configuration of “NHC-CDI” adducts, steric nature of substituents, NCN bond angle of the amidinate core and choice of metal ion and substituents attached to metal center play a key role in isolating metal complexes bearing the *N,N'*-chelated zwitterions or “NHC-CDI” adducts.

## Crystal data and structural refinement details:

**Table 5S.1:** Crystallographic data and structure refinement summary of compounds **1e**, **8e**, **12e**, & **13e**

	<b>1a</b>	<b>8e</b>	<b>12e</b>	<b>13a</b>
Chemical formula	C <sub>28</sub> H <sub>38</sub> N <sub>4</sub> , C <sub>6</sub> H <sub>6</sub>	C <sub>26</sub> H <sub>34</sub> N <sub>4</sub>	C <sub>30</sub> H <sub>46</sub> N <sub>4</sub> O <sub>2</sub>	C <sub>38</sub> H <sub>42</sub> N <sub>4</sub>
Formula weight	508.73	402.57	494.71	554.76
Crystal system	triclinic	monoclinic	monoclinic	monoclinic
Space group	$P\bar{1}$	$C2/c$	$P21/c$	$C2/c$
$T$ [K]	100	100	100	100
$a$ [Å]	10.1699(9)	14.6483(4)	14.4467(16)	21.769(4)
$b$ [Å]	12.0562(11)	12.5461(4)	12.2095(15)	10.408(2)
$c$ [Å]	13.5328(11)	13.3415(4)	16.688(2)	15.133(3)
$\alpha$ [°]	101.227(4)	90	90	90
$\beta$ [°]	104.394(5)	111.948(2)	94.141(7)	110.34(3)
$\gamma$ [°]	107.501(4)	90	90	90
$V$ [Å <sup>3</sup> ]	1466.1(2)	2274.18(12)	2935.9(6)	3215.1(11)
$Z$	2	4	4	4
$D$ (calcd.), [gcm <sup>-3</sup> ]	1.152	1.176	1.119	1.146
$\mu$ (Mo- $K\alpha$ ) [mm <sup>-1</sup> ]	0.068	0.070	0.070	0.067
$F(000)$	552	872.0	1080.0	1192
$\theta$ range [°]	2.80 to 25.50	4.42 to 61.06	2.826 to 50.73	2.43 to 25.49
Reflections collected	19051	18652	15564	21089
Independent reflections	5446 [R(int) = 0.0484]	3479 [Rint = 0.0472]	5349 [Rint = 0.1258]	2999 [R(int) = 0.0551]
Data / restraints / parameters	5446 / 0 / 342	3479/0/141	5349/0/341	2999 / 0 / 197
Completeness to theta = 25.49°	99.8 %	99.8 %	99.3 %	99.9 %
Max. and min. transmission	0.7457 & 0.6637	0.746 & 0.692	0.745 & 0.505	0.7456 & 0.6735
Final R indices	R1 = 0.058,	R1 = 0.043,	R1 = 0.070,	R1 = 0.042, wR2

[I>2sigma(I)]	wR2 = 0.150	wR2 = 0.119	wR2 = 0.162	= 0.104
GOF on F <sup>2</sup>	0.995	1.056	0.930	1.033
Largest diff. peak and hole, [eÅ <sup>-3</sup> ]	0.70 / -0.664	0.36 / -0.25	0.38/-0.32	0.233/-0.182

**Table 5S.2:** Crystallographic data and structure refinement summary of compounds **16e**, **25e**, **26e** & **29e**

	<b>16a</b>	<b>25a</b>	<b>26a</b>	<b>29a</b>
Chemical formula	C <sub>38</sub> H <sub>42</sub> N <sub>4</sub>	C <sub>34</sub> H <sub>50</sub> N <sub>4</sub>	C <sub>32</sub> H <sub>48</sub> N <sub>4</sub>	C <sub>41</sub> H <sub>48</sub> N <sub>4</sub>
Formula weight	554.76	514.78	488.74	596.83
Crystal system	monoclinic	monoclinic	monoclinic	orthorhombic
Space group	<i>P</i> 2 <sub>1</sub> / <i>n</i>	<i>P</i> 2 <sub>1</sub> / <i>n</i>	<i>P</i> 2 <sub>1</sub> / <i>c</i>	<i>Pbca</i>
<i>T</i> [K]	100	296.15	296.15	100
<i>a</i> [Å]	14.7510(3)	9.9549(4)	19.2041(5)	14.5283(8)
<i>b</i> [Å]	14.7625(3)	18.9440(9)	9.9910(2)	15.5494(8)
<i>c</i> [Å]	16.2288(4)	16.4110(7)	16.9489(4)	30.1269(17)
$\alpha$ [°]	90	90	90	90
$\beta$ [°]	112.376(10)	101.702(2)	113.432(2)	90
$\gamma$ [°]	90	90	90	90
<i>V</i> [Å <sup>3</sup> ]	3267.92(12)	3030.6(2)	2983.77(13)	6805.9(6)
<i>Z</i>	8	4	4	8
<i>D</i> (calcd.), [gcm <sup>-3</sup> ]	1.128	1.128	1.088	1.165
$\mu$ (Mo- <i>K</i> $\alpha$ ) [mm <sup>-1</sup> ]	0.066	0.066	0.064	0.068
<i>F</i> (000)	1192	1128	1072	2576.0
$\theta$ range [°]	1.94 to 30.53	3.324 to 56.708	4.812 to 51.492	4.694 to 50.992
Reflections collected	54428	46488	32303	40504
Independent reflections	9959 [R(int) = 0.0573]	7524 [R(int) = 0.0595]	5682 [R(int) = 0.0486]	6330 [R(int) = 0.1121]
Data / restraints / parameters	9959 / 0 / 389	7524 / 0 / 356	5682 / 0 / 337	6330/0/418
Completeness to theta	99.7 %	99.3 %	99.5 %	99.9%

= 25.49°				
Max. and min. transmission	0.7461 & 0.6834	0.746 & 0.652	0.745 & 0.700	0.746 & 0.647
Final R indices [I>2sigma(I)]	R1 = 0.050, wR2 = 0.128	R1 = 0.049 wR2 = 0.129	R1 = 0.052 wR2 = 0.133	R1 = 0.052, wR2 = 0.114
GOF on F <sup>2</sup>	1.035	1.053	1.033	1.021
Largest diff. peak and hole, [eÅ <sup>-3</sup> ]	0.355/-0.271	0.69 / -0.34	0.24 /-0.21	0.24 / -0.26

**Table 5S.3:** Crystallographic data and structure refinement summary of compounds **14-18**,

	<b>14</b>	<b>15</b>	<b>16</b>	<b>17</b>	<b>18</b>
Empirical formula	C <sub>42</sub> H <sub>78</sub> MgN <sub>6</sub> Si <sub>4</sub> (C <sub>6</sub> H <sub>6</sub> )	C <sub>40</sub> H <sub>74</sub> MgN <sub>6</sub> Si <sub>4</sub>	C <sub>42</sub> H <sub>78</sub> N <sub>6</sub> Si <sub>4</sub> Zn	C <sub>40</sub> H <sub>74</sub> N <sub>6</sub> Si <sub>4</sub> Zn	C <sub>32</sub> H <sub>48</sub> N <sub>4</sub> Zn
Formula weight	881.88	775.72	844.83	816.78	554.11
Crystal system	orthorhombic	monoclinic	triclinic	monoclinic	triclinic
Space group	<i>P2<sub>1</sub>2<sub>1</sub>2<sub>1</sub></i>	<i>C2/c</i>	<i>P<math>\bar{1}</math></i>	<i>C2/c</i>	<i>P<math>\bar{1}</math></i>
a (Å)	11.6197(6)	13.6576(4)	12.2741(11)	13.7426(19)	11.604(2)
b (Å)	17.5580(10)	19.3486(4)	12.5738(12)	19.2902(19)	12.155(2)
c (Å)	28.0501(15)	18.8731(4)	18.1124(16)	18.823(3)	14.005(3)
α (°)	90	90	96.992(4)	90	93.418(5)
β (°)	90	108.3360(10)	103.950(4)	108.465(9)	112.815(5)
γ (°)	90	90	108.498(4)	90	117.529(5)
Volume (Å <sup>3</sup> )	5722.7(5)	4734.1(2)	2512.3(4)	4733.0(11)	1544.2(5)
T (K)	100	100	100	100	100
Z	4	4	2	4	2
ρ <sub>calc</sub> g/cm <sup>3</sup>	1.024	1.088	1.117	1.146	1.192
F(000)	1928.0	1696.0	916.0	1768.0	596.0
Reflections collected	69156	38590	28075	39876	15827
Independent reflections	11630 [Rint = 0.0482]	7222 [Rint = 0.0322]	8973 [Rint = 0.0604]	7242 [Rint = 0.0950]	5786 [Rint = 0.0638]
μ/mm <sup>-1</sup>	0.149	0.171	0.617	0.653	0.821
GOF on F <sup>2</sup>	1.015	1.046	1.045	1.037	1.046

R1 [ $I \geq 2\sigma(I)$ ]	R1 = 0.0573, wR2 = 0.1467	R1 = 0.0363, wR2 = 0.0926	R1 = 0.1071, wR2 = 0.3064	R1 = 0.0515, wR2 = 0.1304	R1 = 0.0610, wR2 = 0.1443
Largest diff. peak/ hole/ $e\text{\AA}^{-3}$	1.13/-0.86	0.41/-0.24	1/-0.83	1.20/-1.03	1.13/-0.53

**Table 5S.4:** Crystallographic data and structure refinement summary of compounds **19** & **20**,

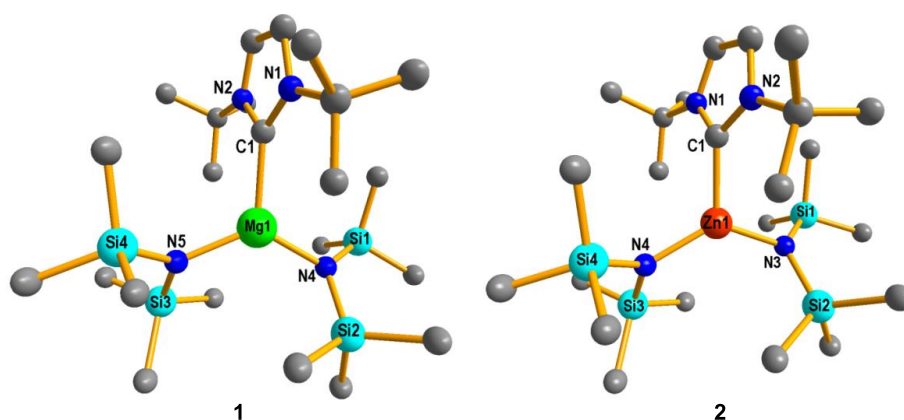
	<b>19</b>	<b>20</b>
Empirical formula	$C_{21}H_{50}Li_2N_4Si_4$	$C_{21}H_{52}MgN_4Si_4$
Formula weight	484.89	497.33
Crystal system	monoclinic	triclinic
Space group	$P2_1/c$	$P\bar{1}$
a ( $\text{\AA}$ )	15.0867(8)	11.2467(15)
b ( $\text{\AA}$ )	12.5389(7)	11.5651(17)
c ( $\text{\AA}$ )	17.5687(11)	14.428(2)
$\alpha$ ( $^\circ$ )	90	68.473(9)
$\beta$ ( $^\circ$ )	108.844(3)	72.788(9)
$\gamma$ ( $^\circ$ )	90	66.865(8)
Volume ( $\text{\AA}^3$ )	3145.3(3)	1579.9(4)
T (K)	100	100
Z	4	2
$\rho_{\text{calc}}$ $\text{g/cm}^3$	1.024	1.045
F(000)	1064.0	548.0
Reflections collected	21289	25072
Independent reflections	7692 [Rint = 0.0369]	7835 [Rint = 0.0720]
$\mu/\text{mm}^{-1}$	0.203	0.222
GOF on $F^2$	1.026	1.017
R1 [ $I \geq 2\sigma(I)$ ]	R1 = 0.0462, wR2 = 0.1284	R1 = 0.0497, wR2 = 0.1098
Largest diff. peak/ hole/ $e\text{\AA}^{-3}$	0.60/-0.56	0.32/-0.27

**References:**

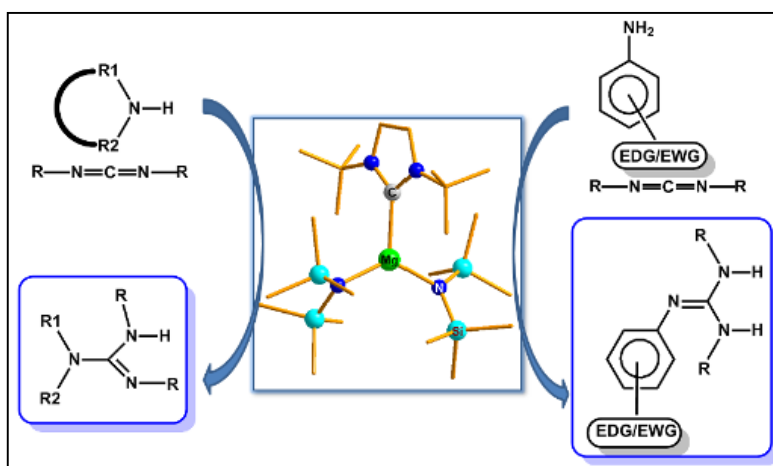
- (1) Kuhn, N.; Kratz, T. *Synthesis*, **1993**, *6*, 561-562.
- (2) Bantreil, X.; Nolan, S. P. *Nat. Protocols*, **2011**, *6*, 69-77.
- (3) (a) Martinez-Prieto, L. M.; Urbaneja, C.; Palma, P.; Campora, J.; Philippot, K.; Chaudret, B. *Chem. Commun.*, **2015**, *51*, 4647-4650; (b) Márquez, A.; Ávila, E.; Urbaneja, C.; Álvarez, E.; Palma, P.; Cámpora, J. *Inorg. Chem.*, **2015**, *54*, 11007-11017; (c) Zhukhovitskiy, A. V.; Geng, J.; Johnson, J. A. *Chem. -Eur. J.*, **2015**, *21*, 5685-5688.
- (4) (a) Jin, G.; Jones, C.; Junk, P. C.; Lippert, K.-A.; Rose, R. P.; Stasch, A. *New J. Chem.*, **2009**, *33*, 64-75; (b) Baishya, A.; Peddarao, T.; Barman, M. K.; Nembenna, S. *New J. Chem.*, **2015**, *39*, 7503-7510.
- (5) Findlater, M.; Hill, N. J.; Cowley, A. H. *Dalton Trans.*, **2008**, *33*, 4419-4423.
- (6) Peddarao, T.; Baishya, A.; Barman, M. K.; Kumar, A.; Nembenna, S. *New J. Chem.*, **2016**, *40*, 7627.
- (7) (a) Arduengo, A. J.; Dias, H. V. R.; Davidson, F.; Harlow, R. L. *J. Organomet. Chem.*, **1993**, *462*, 13-18; (b) Jensen, T. R.; Breyfogle, L. E.; Hillmyer, M. A.; Tolman, W. B. *Chem. Commun.*, **2004**, *21*, 2504-2505.
- (8) (a) Mungur, S. A.; Liddle, S. T.; Wilson, C.; Sarsfield, M. J.; Arnold, P. L. *Chem. Commun.*, **2004**, *23*, 2738-2739; (b) Asay, M. J.; Fisher, S. P.; Lee, S. E.; Tham, F. S.; Borchardt, D.; Lavallo, V. *Chem. Commun.*, **2015**, *51*, 5359-5362.

**6. Summary and Future Directions:** The thesis work has been summarized in the following points-

i) In recent years, NHC supported main group metal complexes have found significant applications in synthesis and catalytic transformation of organic reactions. In view of this, we have synthesized and structurally characterized non-functionalized monodentate NHC supported magnesium(II) and zinc(II) amide complexes  $t^t\text{Bu}:M[\text{N}(\text{SiMe}_3)_2]_2$ ,  $M = \text{Mg}$  (**1**) &  $\text{Zn}$  (**2**).



The catalytic activity of complexes **1** & **2** in guanylation reaction; toward C–N bond formation reaction by addition of primary aromatic and cyclic secondary amines with carbodiimides has been explored.

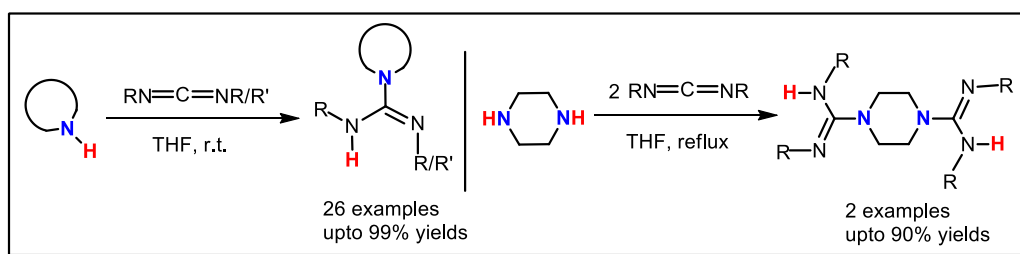




## Summary and Future directions

Further studies aimed at the catalytic addition of terminal alkyne and phosphine to carbodiimide, and also NHC supported magnesium bis(amide) compound catalysed ring opening polymerization of cyclic ester are underway.

ii) In addition to main group metal catalysed C–N bond forming reaction, we have established a catalyst free synthetic way to tetra-substituted symmetric and un-symmetric guanidine, from the reaction of cyclic secondary amine with library of bulky aryl symmetrical and unsymmetrical carbodiimide. These sterically and/or electronically stabilizing bulky acyclic guanidine may serve as important precursors to synthesize unusual metal complexes, particularly, low valent and/or low oxidation state main group, transition and lanthanide metal complexes.



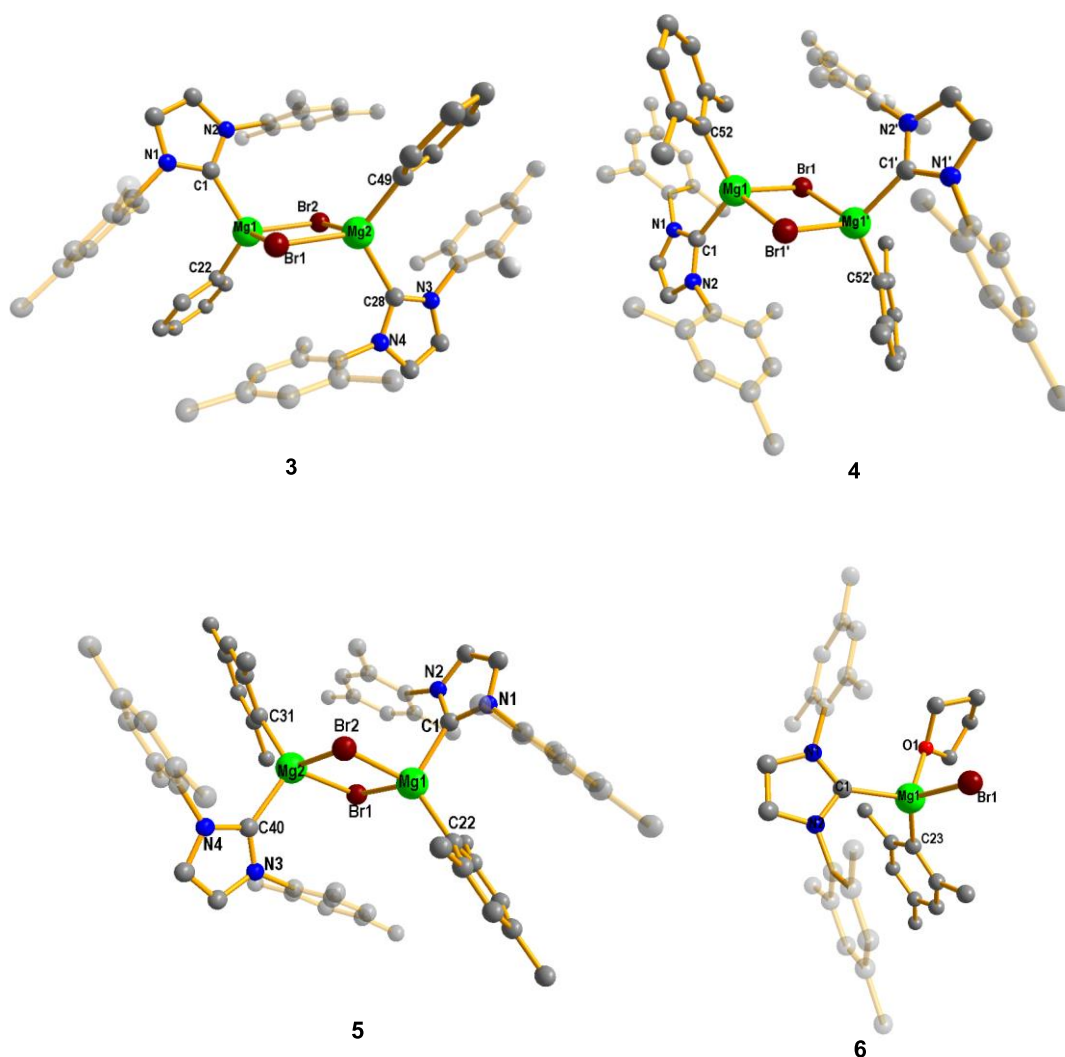
Furthermore, the direct addition of diamine to symmetrical aryl carbodiimides (2 equiv.) led to the formation of biguanidines, which are ideal precursors for constructing dinuclear metal complexes.

iii) A series of NHC stabilized low oxidation state group 2 metal halide and hydride complexes with metal-metal bonds,  $[L(X)M-M(X)L]$ ;  $\{L = \text{NHC} [(\text{CHNH})_2\text{C}:], (M = \text{Be, Mg, Ca, Sr \& Ba, and } X = \text{Cl or H})\}$  has been studied by computational methods. The homolytic M–M Bond Dissociation Energy (BDE) calculation, Natural Bond Orbital (NBO) and Energy Decomposition Analyses (EDA) on density functional theory (DFT) are carried out, which shed light on the

### Summary and Future directions

room temperature stable isolation of NHC stabilized low oxidation state group 2 metal complexes with metal-metal bond, which are not yet reported experimentally.

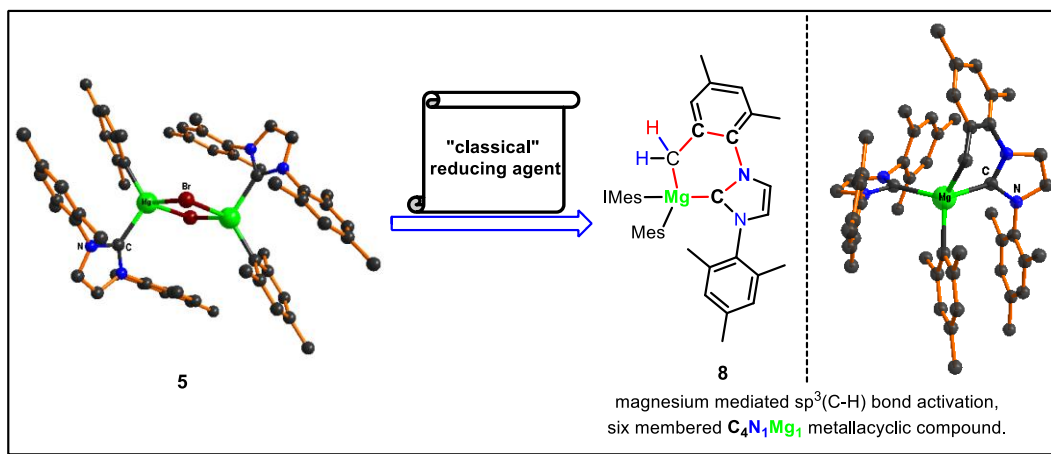
iv) Aiming for the synthesis of low oxidation state organo-magnesium(I) compounds, with Mg–Mg bond supported by neutral NHC ligand in the laboratory, a series of IMes supported organo-magnesium(II) bromide complexes  $[\{\text{IMesMg}(\text{Ar})\text{Br}\}_2]$  were synthesized and structurally characterized.



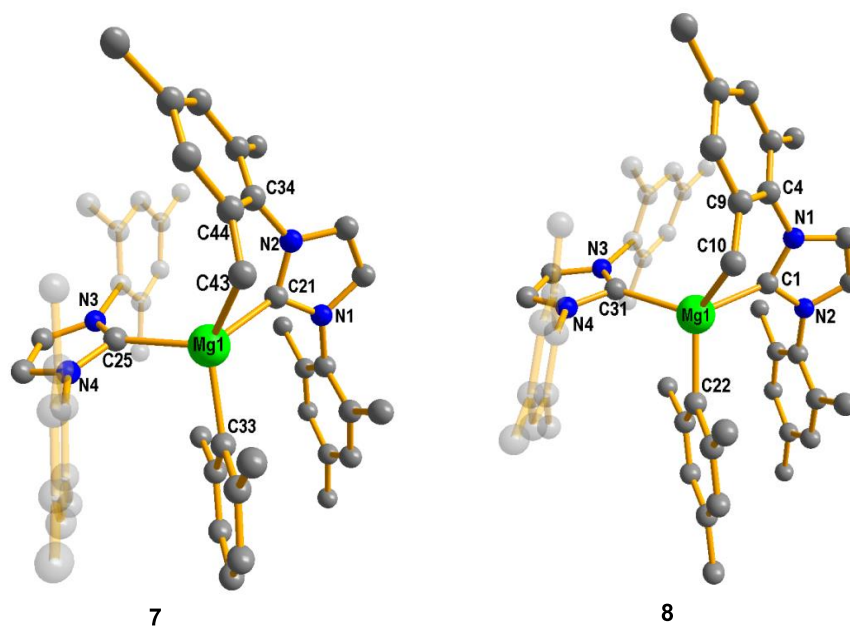
Solid state structures of IMes supported organo-magnesium(II) bromide complexes are found in both dimeric and monomeric form based on the solvents used for crystallization.

Summary and Future directions

v) Further, IMes adducts of organo-magnesium(II) bromide complexes were reduced using classical reducing agent such as sodium (excess), in toluene led to the unprecedented synthesis of cyclometalated compounds of magnesium, [IMesMgAr(IMes')].



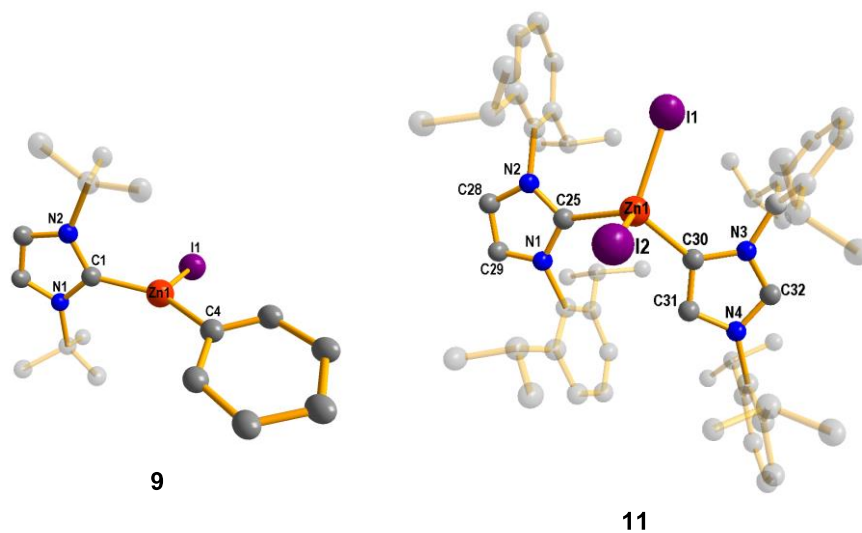
The formation of cyclometalated compound of Mg(II) was proposed to proceed *via* generation of magnesium radical intermediate, which activates the ( $sp^3$ )C-H bond of the ortho-methyl mesityl group of IMes to form the metallacyclic compound of magnesium.



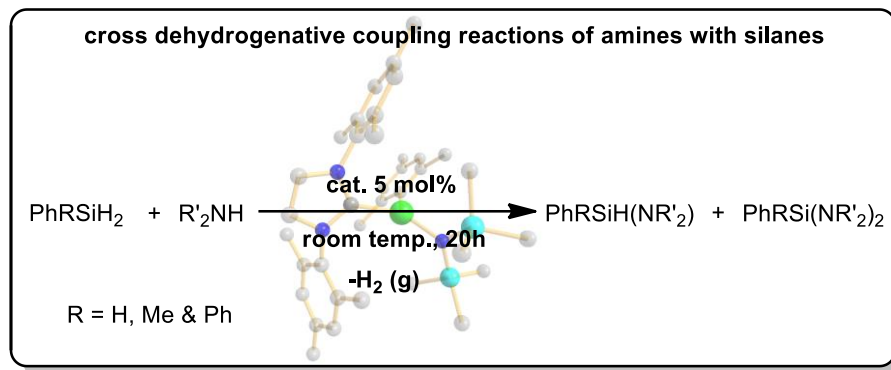
### Summary and Future directions

vi) Similarly, NHC adducts of organo-zinc(II) halide complexes  $t\text{BuZn(Ph)I}$  (**9**) &  $\text{IPrZn(Ph)I}$  (**10**) were synthesized and characterized, by the direct addition of NHCs to the phenyl zinc iodide in toluene. Furthermore, Normal and abnormal NHC supported zinc(II) iodide complex,  $\text{IPr(ZnI}_2\text{)}\text{aIPr}$  (**11**) has been isolated from the stoichiometric reactions of IPr with  $\text{PhZnI}$ , along with the formation of normal IPr- $\text{PhZnI}$  adduct.

These NHC supported organo-metal(II) halide complexes might be used as promising precursors for the synthesis of varieties of reactive unusual molecules such as metal hydrides, metal amides, diatomic molecules and low valent and oxidation state molecules, which are further known to be used as catalysts for activation of small molecules.

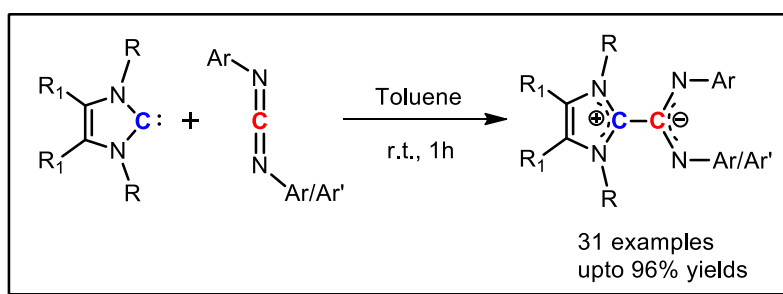


vii) Extending the reactivity studies of IMes supported organo-magnesium(II) bromide complexes, heteroleptic compounds of magnesium amide  $[\text{IMesMg(Ar)}\{\text{N}(\text{SiMe}_3)_2\}]$  **12** and **13** have been prepared by salt metathesis reactions of  $[\{\text{IMesMg(Ar)Br}\}_2]$  with lithium bis(amide). Both compounds have been presented as active pre-catalysts, and furthermore compound **13** has displayed excellent catalytic activity towards cross dehydrogenative coupling reactions of amines and silanes.



These NHC stabilized heteroleptic amide complexes might be used as an excellent catalyst for different organic transformation reactions, namely cyclotrimerization reactions of aryl isocyanates, dimerization of aldehydes and hydroamination reactions etc.

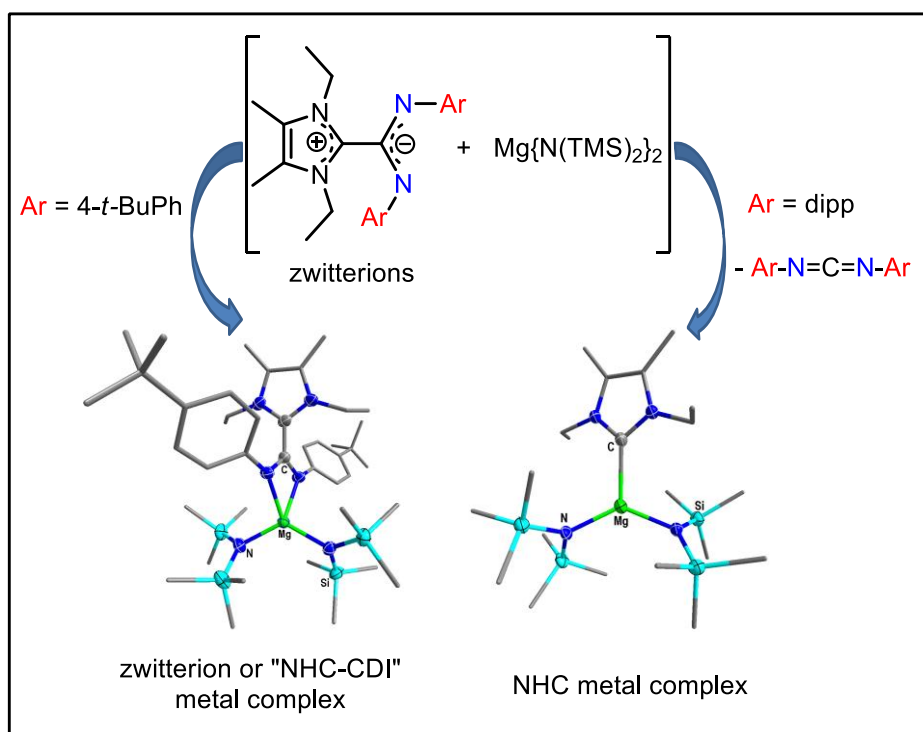
vii) Exploring the chemistry of NHCs as a reagent to the synthesis of new ligand systems for the stabilization of reactive main group molecules, we have prepared a library of well characterized new air stable “NHC-CDI” adducts i.e., bulky amidinates from the direct addition of *N,N'*-diaryl substituted symmetrical and unsymmetrical carbodiimides to unsaturated NHCs at ambient reaction conditions.



These new air stable neutral “NHC-CDI” adducts could be an alternative precursor to other neutral ligand systems to construct metal complexes across the period table in low valent and/or low oxidation state, and such studies are underway in our laboratory.

### Summary and Future directions

viii) Further, we have successfully demonstrated magnesium and zinc complexes bearing neutral amidinate type zwitterions or “NHC-CDI” adducts in a *N,N'*-chelated fashion and monoanionic amido or alkyl as terminal ligands. In contrast, sterically bulky zwitterions led to the formation of NHC-metal complexes, instead of chelated zwitterionic adduct of main group metal elements.



Undoubtedly, this study will have broad impact to produce new and very exciting results in the coordination chemistry of zwitterions and their uses. We are currently investigating the coordination chemistry of “NHC-CDI” adducts with other elements of the periodic table and their applications.

## 7. Experimental Section:

*General remarks:* All manipulations were carried out using standard Schlenk line and glovebox techniques under an inert atmosphere of dinitrogen. All glassware were dried at 120 °C in an oven for at least 10h and assembled hot and cooled in vacuo prior to use. Toluene, benzene, diethyl ether, hexane (collected from Mbraun Solvent Purification System) and tetrahydrofuran, & pentane (Na/benzophenone ketyl, dried and distilled under nitrogen) were stored in Na wire and degassed prior to use. Dichloromethane, acetonitrile & pyridine were dried over calcium dihydride and distilled under nitrogen and stored over dried molecular sieves (4 Å).

*Physical measurements:* NMR spectra were recorded on Bruker AV 400 MHz spectrometer for  $^1\text{H}$  NMR ( $^{13}\text{C}$  NMR; 101 MHz,  $^{29}\text{Si}$  NMR; 80 MHz &  $^7\text{Li}\{^1\text{H}\}$ ; 156 Hz). Deuterated NMR solvents  $\text{CDCl}_3$ ,  $\text{C}_6\text{D}_6$ , THF- $d_8$  &  $\text{CD}_2\text{Cl}_2$  were used as the solvent for NMR spectra measurement. The chemical shift values ( $\delta$ ) were reported in parts per million (ppm) relative to the residual signals of the solvents ( $\delta$  7.26, 7.16, 3.58 & 5.32 for  $^1\text{H}$ ;  $\delta$  77.16, 128.06, 67.21 & 53.84 for  $^{13}\text{C}$ ; for  $\text{CDCl}_3$ ,  $\text{C}_6\text{D}_6$ , THF- $d_8$  &  $\text{CD}_2\text{Cl}_2$ , respectively). External standards ( $\text{SiMe}_4$  for  $^{29}\text{Si}$ ;  $\text{LiCl}$  for  $^7\text{Li}$  nucleus) are used for multinuclear NMR spectra measurement and chemical shifts are reported in ppm.  $\text{C}_6\text{D}_6$  & THF- $d_8$  were purchased from Leonid chemicals and dried over sodium followed by distillation under *vacuo* and degassed by freeze-pump-thaw cycles.  $\text{CDCl}_3$  &  $\text{CD}_2\text{Cl}_2$  were purchased from Leonid chemicals and dried over  $\text{CaH}_2$  before distillation under nitrogen and storage over molecular sieves. High Resolution Mass Spectra (HRMS) were recorded on a Bruker micrOTOF-Q II Spectrometer. Elemental analyses were performed in a Vario Micro Cube Elementar CHNS/O analyzer. IR spectra were recorded on a Perkin-Elmer FT-IR spectrometer. Melting points were obtained in sealed capillaries on an electro thermal apparatus and are uncorrected.

## Experimental Section

*X-ray crystal structure determination:* Suitable single crystals of metal complexes were mounted on a glass fiber under the flow of continuous liquid nitrogen maintaining temperature 100 K. Temperature was controlled using an Oxford Cryo-stream 700 instrument. The X-ray data were collected on a Bruker 4-circle Kappa SMART D8 goniometer equipped with an APEX CCD detector and with an INCOATEC micro source (Mo K $\alpha$  radiation,  $\lambda = 0.71073 \text{ \AA}$ ). Intensities were integrated with SAINT<sup>1</sup> and corrected for absorption with SADABS.<sup>2</sup> Structures were solved by direct methods (SHELXS-97) and refined by full-matrix least squares on  $F^2$  (SHELXL-97).<sup>3</sup> Hydrogen atoms were fixed at calculated positions and their positions were refined by a riding model. All non-hydrogen atoms were refined with anisotropic displacement parameters. The crystal data for all compounds along with the final residuals and other pertaining details are tabulated in respective chapters.

*Starting materials:* Sodium/potassium metal, NaH, Potassium *t*-butoxide, <sup>n</sup>BuLi (1.6 M in hexane), Grignard reagents such as PhMgBr (1M THF), XylMgBr (1M THF), MesMgBr (1M THF), PhZnI (0.5M THF) and ZnEt<sub>2</sub> (1M hexane), ZnI<sub>2</sub>, metal bis(amides) such as LiN(SiMe<sub>3</sub>)<sub>2</sub>, KN(SiMe<sub>3</sub>)<sub>2</sub>, Zn[N(Si(Me)<sub>3</sub>)<sub>2</sub>]<sub>2</sub>, were purchased from Aldrich chemicals and used as such. All amines were pre-dried or distilled prior to use. Silanes (Aldrich), *N,N'*-diisopropylcarbodiimide (Across), *N,N'*-dicyclohexylcarbodiimide (Spectrochem), were purchased from respective vendors and used without further purification.

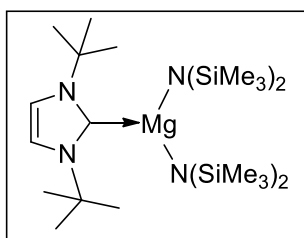
NHC precursors such as 1,3-dimethyl-4,5-dimethylimidazol-2-ylidene (<sup>Me</sup>IME),<sup>4</sup> 1,3-diisopropyl-4,5-dimethylimidazol-2-ylidene (<sup>Me</sup>IiPr),<sup>4</sup> 1,3-diethyl-4,5-dimethylimidazol-2-ylidene (<sup>Me</sup>IEt),<sup>4</sup> 1,3-di-*tert*-butylimidazol-2-ylidene (<sup>t</sup>Bu),<sup>5</sup> 1,3-bis-(2,4,6-trimethylphenyl)imidazole-2-ylidene (IMes)<sup>6</sup> & 1,3-bis-(2,6-diisopropylphenyl)-imidazole-2-ylidene (IPr)<sup>6</sup> and Mg[N(SiMe<sub>3</sub>)<sub>2</sub>]<sub>2</sub><sup>7</sup> were prepared by following reported procedures.



**Theoretical Methods:** The DFT calculations were performed using Gaussian-03/09 and GAMESS ab initio quantum chemistry packages. The dispersion corrected hybrid DFT functional,  $\omega$ -B97X-D<sup>8</sup> as well as B3LYP<sup>9</sup> and BP86<sup>10</sup> functional were used for geometry optimization and frequency calculation. The def2-TZVP<sup>11</sup> basis set was used for Be, Mg, and Ca. For Sr and Ba, the def2-TZVP basis set with the effective core potential was employed. The NBO calculations were done using Gaussian NBO Version 3.1 as implemented in Gaussian-09. The localized molecular orbital energy decomposition analysis (LMO-EDA) analyses were carried out using the Gamess software.

### **6A Synthesis of metal complexes 1-20:**

**Synthesis of  $t\text{Bu:Mg}\{\text{N}(\text{SiMe}_3)_2\}_2$  (1):** 1,3-di-*tert*-butylimidazol-2-ylidene ( $t\text{Bu}$ ) (1.27 g and

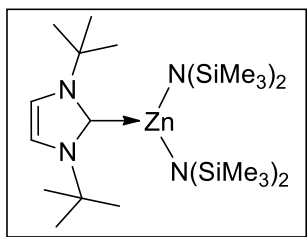


7.07 mmol) and  $\text{Mg}\{\text{N}(\text{SiMe}_3)_2\}_2$  (2.44 g and 7.07 mmol) were dissolved in toluene and stirred at room temperature for 12 h. Upon concentration and cooling to  $-25\text{ }^\circ\text{C}$  afforded compound **1** as colorless crystals. Yield: 2.516 g (68%); M.p.  $128\text{ }^\circ\text{C}$ .  $^1\text{H}$  NMR (400

MHz,  $\text{C}_6\text{D}_6$ ,  $25\text{ }^\circ\text{C}$ ):  $\delta = 6.35$  (s, 2H, NCH), 1.42 (s, 18H,  $\text{C}(\text{CH}_3)_3$ ), 0.38 (s, 36H,  $\text{N}\{\text{Si}(\text{CH}_3)_3\}_2$ ) ppm;  $^{13}\text{C}$   $\{^1\text{H}\}$  NMR (100 MHz,  $\text{C}_6\text{D}_6$ ,  $25\text{ }^\circ\text{C}$ ):  $\delta = 177.7$  (carbene C), 119.1 (NCH), 57.5 ( $\text{C}(\text{CH}_3)_3$ ), 31.0 ( $\text{CH}_3$ ), 6.9 ( $\text{SiCH}_3$ ) ppm;  $^{29}\text{Si}\{^1\text{H}\}$  NMR (80 MHz,  $\text{C}_6\text{D}_6$ ,  $25\text{ }^\circ\text{C}$ ):  $\delta = -17.12$   $\text{N}(\text{SiMe}_3)_2$  ppm.

**Synthesis of  $t\text{Bu:Zn}\{\text{N}(\text{SiMe}_3)_2\}_2$  (2):** This compound was synthesized following the same procedure as described above for compound **1**, with starting materials 1,3-di-*tert*-butylimidazol-2-ylidene (0.190 g and 1.1 mmol) and  $\text{Zn}\{\text{N}(\text{SiMe}_3)_2\}_2$  (0.427 g and 1.1 mmol). Colorless crystalline solid of compound **2** was obtained from toluene. Yield: 0.367 g (62%); M.p.  $120\text{ }^\circ\text{C}$ .

## Experimental Section

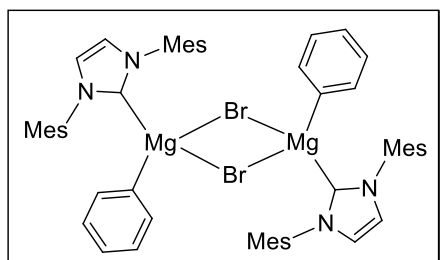


$^1\text{H}$  NMR (400 MHz,  $\text{C}_6\text{D}_6$ , 25  $^\circ\text{C}$ ):  $\delta$  = 6.41 (s, 2H, NCH), 1.44 (s, 18H,  $\text{CH}_3$ ), 0.36 (br, 36H,  $\text{N}(\text{SiCH}_3)_3$ ) ppm;  $^{13}\text{C}$   $\{^1\text{H}\}$  NMR (100 MHz,  $\text{C}_6\text{D}_6$ , 25  $^\circ\text{C}$ ):  $\delta$  = 175.7 (carbene C), 119.2 (NCH), 58.6 ( $\text{C}(\text{CH}_3)_3$ ), 31.4 ( $\text{CH}_3$ ), 6.9 ( $\text{SiCH}_3$ ) ppm;  $^{29}\text{Si}\{^1\text{H}\}$  NMR (80 MHz,

$\text{C}_6\text{D}_6$ , 25  $^\circ\text{C}$ ):  $\delta$  = -5.00  $\text{N}(\text{SiMe}_3)_2$  ppm.

**6A.1 General Procedure (A) for synthesis of IMes adducts of aryl-magnesium (II) bromide complexes (3-5):** To the clear colorless solution of IMes in toluene (20 mL), solution of aryl-magnesium bromide in 1 M THF was added drop wise and the reaction mixtures were stirred for 12 h. The progress of the reaction was monitored from the  $^1\text{H}$  NMR analysis of the 1 mL aliquot of the reaction mixture. The light yellow suspension obtained was removed under reduced pressure to get crude solid product. Colorless crystals suitable for analytical studies were grown from saturated hot benzene solution at room temperature.

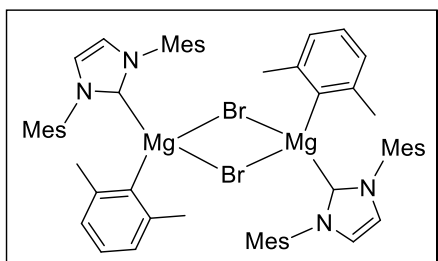
**Synthesis of  $\{\text{IMesMg}(\text{Ph})\text{Br}\}_2$  (3):** Compound **3** was synthesized following the procedure **A** as



described above with starting materials IMes (0.5 g, 1.64 mmol) and  $\text{PhMgBr}$  (1 M THF) (1.72 mL, 1.72 mmol). Off white solid; yield: 0.430 g (54 %); M.p. 159-162  $^\circ\text{C}$ .  $^1\text{H}$  NMR ( $\text{C}_6\text{D}_6$ , 298 K, 400MHz):  $\delta$  = 7.58 (m, 4H, *o*- $\text{C}_6\text{H}_5$ ),

7.36 (m, 6H, *m,p*- $\text{C}_6\text{H}_5$ ), 6.61 (s, 8H, *m*- $\text{C}_6\text{H}_2$ ), 5.88 (s, 4H, NCH), 2.16 (s, 12H, *p*- $\text{CH}_3$ ), 1.82 (s, 24H, *o*- $\text{CH}_3$ ) ppm;  $^{13}\text{C}$  NMR  $\{^1\text{H}\}$ ( $\text{C}_6\text{D}_6$ , 298 K, 100MHz):  $\delta$  = 182.6 (carbene C), 167.9{Mg-C(Ph)}, 140.6, 138.9, 135.2, 129.7, 128.5, 125.5, 124.4 (ArC), 122.2 (NCH), 21.1(*p*- $\text{CH}_3$ ), 17.7 (*o*- $\text{CH}_3$ ) ppm. Elem. Anal. Calc. for  $\text{C}_{54}\text{H}_{58}\text{Br}_2\text{Mg}_2\text{N}_4$ : C 66.76, H 6.02, N 5.77; found: C 66.19, H 6.04, N 5.75.

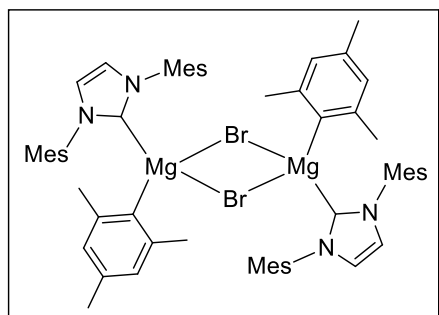
**Synthesis of {IMesMg(Xyl)Br}<sub>2</sub> (4):** Compound **4** was synthesized following the procedure A,



with starting materials IMes (0.5 g, 1.64 mmol) and XylMgBr (1 M THF) (1.72 mL, 1.72 mmol). Off white solid; yield: 0.560 g (66 %); M.p. 181-183 °C. <sup>1</sup>H NMR(C<sub>6</sub>D<sub>6</sub>, 298 K, 400MHz): δ = 7.33 (t, 2H, *J* = 8 Hz, *p*-C<sub>6</sub>H<sub>2</sub>), 7.12 (d, 4H, *J* = 8 Hz, *m*-C<sub>6</sub>H<sub>2</sub>), 6.50 (s, 8H, *m*-C<sub>6</sub>H<sub>2</sub>), 5.90 (s, 4H, NCH), 2.36 (s, 12H, *p*-CH<sub>3</sub>), 2.16 (s, 12H, *o*-CH<sub>3</sub>), 1.90 (s, *o*-24H, CH<sub>3</sub>) ppm; <sup>13</sup>C{<sup>1</sup>H} NMR (C<sub>6</sub>D<sub>6</sub>, 298 K, 100MHz):

δ = 182.9 (carbene C), 167.9{Mg-C(Xyl)}, 147.5, 139.0, 135.4, 135.3, 129.6, 128.5, 125.3, 123.4 (ArC), 122.4 (NCH), 28.7 (*o*-CH<sub>3</sub>), 21.0 (*p*-CH<sub>3</sub>), 17.6 (*o*-CH<sub>3</sub>) ppm. Despite several attempts, accurate elemental analysis could not be obtained for compound **4**.

**Synthesis of {IMesMg(Mes)Br}<sub>2</sub> (5):** Compound **5** was synthesized following the procedure A,



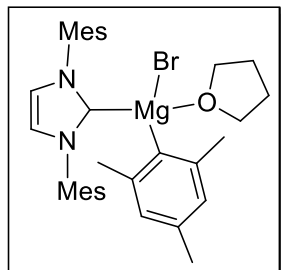
with starting materials IMes (0.5 g, 1.64 mmol) and MesMgBr (1 M in THF) (1.72 mL, 1.72 mmol). Off White solid; yield: (0.61 g, 71 %); M.p. 240 °C (decompose). <sup>1</sup>H NMR (C<sub>6</sub>D<sub>6</sub>, 298 K, 400 MHz): δ = 6.97 (s, 4H, ArH), 6.51 (s, 8H, ArH), 5.88 (s, 4H, NCH), 2.50 (s, 6H, *p*-CH<sub>3</sub>), 2.36

(s, 12H, *p*-CH<sub>3</sub>), 2.17 (s, 12H, *o*-CH<sub>3</sub>), 1.91 (s, 24H, *o*-CH<sub>3</sub>) ppm; <sup>13</sup>C{<sup>1</sup>H} NMR (C<sub>6</sub>D<sub>6</sub>, 298 K, 100 MHz): δ = 183.0 (carbene C), 163.6 {Mg-C(Mes)}, 147.7, 138.9, 135.4, 135.3, 133.3, 128.5, 127.3, 124.5 (ArC), 122.4 (NCH), 28.6 (*o*-CH<sub>3</sub>), 21.9, 21.1 (*p*-CH<sub>3</sub>), 17.7 (*o*-CH<sub>3</sub>) ppm. Despite several attempts, accurate elemental analysis could not be obtained for compound **5**.

**6A.2 Synthesis of THF co-ordinated IMes adducts of aryl-magnesium (II) bromide complex, [IMesMg(Mes)Br(THF)] (6):** To the clear colorless solution of IMes (0.5 g, 1.64

## Experimental Section

mmol) in tetrahydrofuran (20 mL) at room temperature, solution of 2-mesitylmagnesium bromide MesMgBr (1 M THF) (1.72 mL, 1.72 mmol) was added drop wise and the reaction



mixture was stirred for 12 h. The consumption of ligand IMes was observed from the  $^1\text{H}$  NMR analysis of the 1 mL crude reaction mixture.

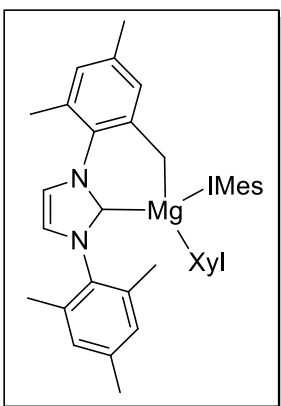
The reaction mixture was concentrated under high vacuum and kept for crystallization. Colorless crystals suitable for single crystal X-ray

diffraction studies were grown from saturated toluene solution in  $-25$

$^{\circ}\text{C}$ . Yield: 0.70 g (71.4%); M.p.  $155-159$   $^{\circ}\text{C}$ .  $^1\text{H}$  NMR( $\text{C}_6\text{D}_6$ , 298 K, 400MHz):  $\delta = 6.94(\text{s}, 1\text{H}, \text{ArH})$ ,  $6.84(\text{s}, 1\text{H}, \text{ArH})$ ,  $6.64(\text{s}, 2\text{H}, \text{ArH})$ ,  $6.49(\text{s}, 2\text{H}, \text{ArH})$ ,  $6.11(\text{s}, 1\text{H}, \text{NCH})$ ,  $5.93(\text{s}, 1\text{H}, \text{NCH})$ ,  $3.40(\text{s}, \text{br. } 4\text{H}, \text{OCH}_2\text{CH}_2)$ ,  $2.40-2.47(\text{m}, 6\text{H}, p\text{-CH}_3)$ ,  $2.33(\text{s}, 3\text{H}, p\text{-CH}_3)$ ,  $2.11-2.16(\text{m}, 12\text{H}, o\text{-CH}_3)$ ,  $1.89(\text{s}, 6\text{H}, o\text{-CH}_3)$ ,  $1.28(\text{s}, \text{br. } 4\text{H}, \text{OCH}_2\text{CH}_2)$  ppm;  $^{13}\text{C}$  NMR  $\{^1\text{H}\}(\text{C}_6\text{D}_6$ , 298 K, 100MHz):  $\delta = 183.0$ ,  $186.3(\text{carbene } \text{C})$ ,  $163.6$ ,  $163.8\{\text{Mg}-\text{C}(\text{Mes})\}$ ,  $147.7$ ,  $147.3$ ,  $139.1$ ,  $138.9$ ,  $135.9$ ,  $135.7$ ,  $135.4$ ,  $135.3$ ,  $133.2$ ,  $133.0$ ,  $129.6$ ,  $129.3$ ,  $124.5$ ,  $124.5(\text{ArC})$ ,  $122.4$ ,  $122.4(\text{NCH})$ ,  $68.3(\text{OCH}_2\text{CH}_2)$ ,  $28.5$ ,  $28.6(o\text{-CH}_3)$ ,  $25.3(\text{OCH}_2)$ ,  $21.7$ ,  $21.9(p\text{-CH}_3)$ ,  $20.9$ ,  $21.1(p\text{-CH}_3)$ ,  $18.1$ ,  $17.7(o\text{-CH}_3)$  ppm. Despite several attempts, accurate elemental analysis could not be obtained for compound **6**.

**6A.3 General Procedure (B) for synthesis of aryl-magnesium (II) complexes (7-8):** Solution of IMes adduct of organo-magnesium (II) bromide complexes (**4** or **5**) in toluene (30 mL) was stirred vigorously over sodium mirror for 3 days at room temperature. The resultant suspension was filtered and concentrated under reduced pressure, and subsequent cooling of the toluene solution to  $-25$   $^{\circ}\text{C}$  afforded analytically pure colorless compounds of **7** or **8**.

**Synthesis of [IMesMg(Xyl)(IMes')] (7):** Compound **7** was synthesized following the procedure **B** as described above with starting materials {IMesMg(Xyl)Br}<sub>2</sub> (1.0 g, 0.9746 mmol) and sodium mirror (0.55 g, 23.913 mmol). Colorless solid; yield: 0.158 g (22%); M.p. 157-159 °C.

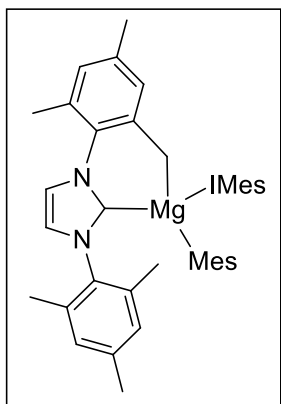


<sup>1</sup>H NMR (400 MHz, C<sub>6</sub>D<sub>6</sub>): δ = 7.19–7.17 (m, 1H, ArH), 7.08 (br, 1H, ArH), 6.96 (d, 1H, ArH), 6.81 (br, 1H, ArH), 6.75 (br, 2H, ArH), 6.63 (s, 1H, ArH), 6.61 (s, 1H, ArH), 6.49 (s, 1H, ArH), 6.45 (br, 1H, ArH), 6.42 (d, 1H, NCH), 6.37 (s, 1H, ArH), 5.99 (s, 2H, NCH), 5.93 (d, *J* = 4 Hz, 1H, NCH), 2.35 (s, 3H, *p*-CH<sub>3</sub>), 2.16 (br, 12H, *o*-CH<sub>3</sub>), 2.05, 1.95 (two s, 9H, *p*-CH<sub>3</sub>), 1.80 (d, *J* = 4.0 Hz, 1H, Mg-CH<sub>2</sub>), 1.70 (d, *J* = 4.0 Hz, 1H, Mg-CH<sub>2</sub>), 1.60 (s, 3H, *o*-CH<sub>3</sub>), 1.51 (s, 6H, *o*-CH<sub>3</sub>), 1.44 (s, 6H, *o*-CH<sub>3</sub>) ppm;

<sup>13</sup>C{<sup>1</sup>H} NMR (101 MHz, C<sub>6</sub>D<sub>6</sub>): δ = 192.4, 191.2 (carbene C), 173.4{Mg-C(Xyl)}, 154.5, 148.4, 147.2, 137.8, 137.3, 136.9, 136.4, 135.4, 134.5, 130.5, 130.3, 129.5, 129.4, 128.7, 124.0, 123.9, 123.2, 122.8 (Ar C), 122.0, 119.3, 118.4 (NCH), 31.9 (CH<sub>2</sub>Mg), 28.5, 28.0 (*o*-CH<sub>3</sub>), 21.7, 21.0 (*p*-CH<sub>3</sub>), 19.9 (*p*-CH<sub>3</sub>), 18.08 (*o*-CH<sub>3</sub>), 17.2, 17.2 (*o*-CH<sub>3</sub>), 16.8 (*o*-CH<sub>3</sub>) ppm. Elem. Anal. Calc. for C<sub>50</sub>H<sub>56</sub>Mg<sub>1</sub>N<sub>4</sub>: C, 81.45; H, 7.66; N, 7.60. Found: C, 80.70; H, 7.57; N, 7.47.

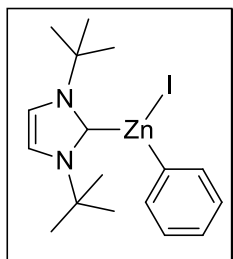
**Synthesis of [IMesMg(Mes)(IMes')] (8):** Compound **8** was synthesized following the procedure **B**, with starting materials {IMesMg(Mes)Br}<sub>2</sub> (2.0 g, 1.89 mmol) and sodium mirror (1.07 g, 46.52 mmol). Colorless solid; yield: 0.460g (32 %); M.p. 161-165 °C. <sup>1</sup>H NMR (400 MHz, C<sub>6</sub>D<sub>6</sub>): δ = 7.06 (s, 1H, ArH), 6.91(br, 1H, ArH), 6.78 (s, 1H, ArH), 6.75 (s, 2H, ArH), 6.67–6.56 (br, 2H, ArH), 6.44 (s, br, 1H, ArH), 6.42 (d, 2H, NCH, ArH), 6.36 (s, 1H, ArH), 5.99 (s, 2H, NCH), 5.94 (d, 1H, NCH), 2.47 (s, 3H, *p*-CH<sub>3</sub>), 2.34 (s, 3H, *p*-CH<sub>3</sub>), 2.27–2.15 (br, 12H, *o*-CH<sub>3</sub>), 2.11–2.15 (m, 3H, CH<sub>3</sub>), 1.95, 2.02 (two s, 9H, *p*-CH<sub>3</sub>), 1.78 (d, *J* = 4.0 Hz, 1H, Mg-CH<sub>2</sub>), 1.68 (d, *J* = 4.0 Hz, 1H, Mg-CH<sub>2</sub>), 1.60 (s, 3H, *o*-CH<sub>3</sub>), 1.51 (s, 6H, *o*-CH<sub>3</sub>), 1.43 (s, 6H, *o*-CH<sub>3</sub>)

## Experimental Section



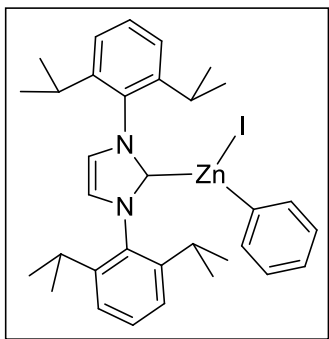
ppm;  $^{13}\text{C}\{^1\text{H}\}$  NMR (101 MHz,  $\text{C}_6\text{D}_6$ ):  $\delta$  = 191.2, 192.5 (carbene C), 168.7 {Mg–C(Mes)}, 154.5, 148.4, 147.3, 137.7, 137.3, 136.9, 136.3, 134.4, 131.7, 130.4, 130.3, 129.5, 128.6, 127.6, 123.9, 123.2, 123.1 (ArC), 121.8, 119.3, 118.3 (NCH), 31.9 ( $\text{CH}_2\text{Mg}$ ), 28.4, 27.8 (*o*- $\text{CH}_3$ ), 21.9, 21.7 (*p*- $\text{CH}_3$ ), 21.0 (*o*- $\text{CH}_3$ ), 21.0 19.9 (*p*- $\text{CH}_3$ ), 17.3, 17.2 (*o*- $\text{CH}_3$ ), 16.8 (*o*- $\text{CH}_3$ ) ppm; DEPT 135 NMR (101 MHz,  $\text{C}_6\text{D}_6$ ):  $\delta$  = 130.3, 129.4, 128.6, 127.6, 127.3, 124.4, 123.9, 123.1, 123.1, 121.9, 119.3, 118.3, (positive) 31.9 (negative), 28.4, 28.3, 27.8, 21.9, 21.7, 21.7, 21.0, 21.0, 19.9, 17.3, 17.2, 16.8 (positive), ppm. Elem. Anal. Calc. for  $\text{C}_{51}\text{H}_{58}\text{Mg}_1\text{N}_4$ : C, 81.53; H, 7.78; N, 7.46. Found: C, 81.32; H, 7.77; N, 6.91.

**Synthesis of [*t*BuZn(Ph)I] (9):** To the clear colorless solution of *t*Bu (0.517g, 2.8722 mmol) in



toluene (20 mL) at room temperature, solution of PhZnI (0.5 M in THF) (5.74 mL, 5.7444 mmol) was added drop wise and the reaction mixtures were stirred for overnight. The solution becomes white suspension. The progress of the reaction was monitored from the  $^1\text{H}$  NMR analysis of the 1 mL aliquot of the reaction mixture. Solvent was removed under reduced pressure to get the off white solid. Colorless crystalline materials were obtained from the saturated solution of benzene at room temperature. Colorless solid; yield: 0.416 g (32 %).  $^1\text{H}$  NMR ( $\text{C}_6\text{D}_6$ , 298 K, 400 MHz):  $\delta$  = 8.16–8.14 (m, 2H, ArH), 7.48–7.44 (m, 2H, ArH), 7.34–7.32 (m, 1H, ArH), 6.33 (s, 2H, NCH), 1.24 (s, 18H,  $\text{C}(\text{CH}_3)_3$ ) ppm;  $^{13}\text{C}\{^1\text{H}\}$  NMR ( $\text{C}_6\text{D}_6$ , 298 K, 100 MHz):  $\delta$  = 172.5 (carbene C), 154.7, 139.6, 128.5, 127.4 (ArC), 118.8 (NCH), 58.5 ( $\text{C}(\text{CH}_3)_3$ ), 30.5 ( $\text{C}(\text{CH}_3)_3$ ).

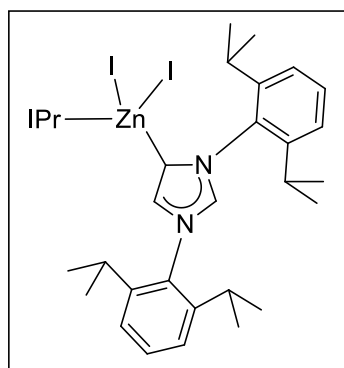
**Synthesis of [IPrZn(Ph)I] (10):** An analogous reaction to that used for the synthesis of **9** was



carried out with IPr (0.5g, 1.2886 mmol) and PhZnI (0.5 M in THF) (2.65ml, 2.6546 mmol) in toluene. Colorless hairy compounds were isolated from the saturated solution of toluene at room temperature and characterized by  $^1\text{H}$  &  $^{13}\text{C}$  NMR spectroscopy. Yield: 0.197 g (23 %); M.p. 218 °C (decomposition).  $^1\text{H}$  NMR ( $\text{C}_6\text{D}_6$ , 298 K, 400

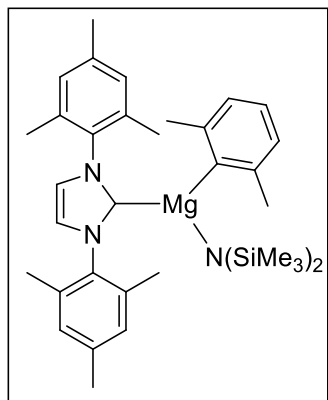
MHz):  $\delta$  = 7.31–7.29 (m, 2H, ArH), 7.22–7.19 (m, 3H, ArH), 7.16–7.12 (m, 2H, ArH), 7.06 (d, 4H, ArH), 6.44 (s, 2H, NCH), 2.78 (sept,  $J$  = 4.0, 8.0 Hz, 4H,  $\text{CH}(\text{CH}_3)_2$ ), 1.32 (d,  $J$  = 8.0 Hz, 12H,  $\text{CH}(\text{CH}_3)_2$ ), 0.98 (d,  $J$  = 8.0 Hz, 12H,  $\text{CH}(\text{CH}_3)_2$ ) ppm;  $^{13}\text{C}\{^1\text{H}\}$  NMR ( $\text{C}_6\text{D}_6$ , 298 K, 100 MHz):  $\delta$  = 145.5, 138.7, 134.3, 131.2, 126.8, 124.9 (ArC), 124.3 (NCH), 29.0 ( $\text{CH}(\text{CH}_3)_2$ ), 25.4 ( $\text{CH}(\text{CH}_3)_2$ ), 23.7 ( $\text{CH}(\text{CH}_3)_2$ ); carbene carbon was not observed.

**Synthesis of [IPr(ZnI<sub>2</sub>)aIPr] (11):** Isolated as a colorless block of crystals from the previous



reaction; IPr ( 0.50 g, 1.288 mmol) with PhZnI in 0.5 M in THF (2.65 ml, 2.6546 mmol). The colorless blocks of crystals were obtained from the crude reaction mixture at room temperature from around 30 days. Yield: 0.105 g (15 %); M.p. 285 °C (decomposition).  $^1\text{H}$  NMR ( $\text{C}_6\text{D}_6$ , 298 K, 400 MHz): 7.13–7.11 (m, 6H, ArH), 7.09–7.07 (m, 6H, ArH), 6.86 (br, 2H, ArH), 6.50 (s, 2H, NCH), 3.23 (m, 4H,  $\text{CH}(\text{CH}_3)_2$ ), 2.83 (m, 2H,  $\text{CH}(\text{CH}_3)_2$ ), 2.38 (m, 2H,  $\text{CH}(\text{CH}_3)_2$ ), 1.63 (d,  $J$  = 4.0 Hz, 6H,  $\text{CH}(\text{CH}_3)_2$ ), 1.55 (d,  $J$  = 4.0 Hz, 12H,  $\text{CH}(\text{CH}_3)_2$ ), 1.23 (d,  $J$  = 4.0 Hz, 9H,  $\text{CH}(\text{CH}_3)_2$ ), 1.06 (d,  $J$  = 4.0 Hz, 12H,  $\text{CH}(\text{CH}_3)_2$ ), 0.94 (d,  $J$  = 4.0 Hz, 12H,  $\text{CH}(\text{CH}_3)_2$ ), 0.88 (d,  $J$  = 4.0 Hz, 9H,  $\text{CH}(\text{CH}_3)_2$ ) ppm.

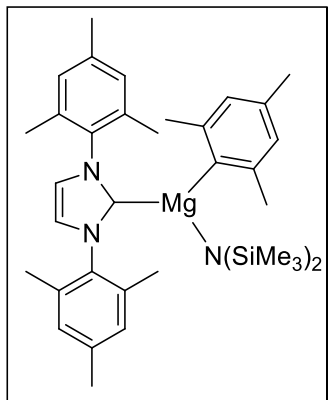
**Synthesis of [IMesMg(Xyl)N(SiMe<sub>3</sub>)<sub>2</sub>] (12):** {IMesMg(Xyl)Br}<sub>2</sub> (1.53g, 1.49mmol) and



Li[N(SiMe<sub>3</sub>)<sub>2</sub>] (0.527g, 3.15mmol) were mixed together and added toluene. The reaction mixture was stirred at room temperature for overnight. The colorless solution formed was filtered using celite through filter frit and concentrated. Colorless crystalline compounds for analytical studies were obtained from the saturated toluene solution by cooling to -25 °C. Yield: 0.49g (55.4 %); M.p. 138-142

°C. <sup>1</sup>H NMR(C<sub>6</sub>D<sub>6</sub>, 298 K, 400MHz): δ = 7.14–7.18(m, 1H, ArH), 6.97 (d, 2H, *J* = 8.0 Hz, ArH), 6.70 (s, 4H, ArH), 6.03 (s, 2H, NCH), 2.29 (s, 6H, *o*-CH<sub>3</sub>), 2.11 (s, 6H, *p*-CH<sub>3</sub>), 1.92 (s, 12H, *o*-CH<sub>3</sub>), 0.14 (s, 18H, NSi(CH<sub>3</sub>)<sub>2</sub>) ppm; <sup>13</sup>C NMR(C<sub>6</sub>D<sub>6</sub>, 298 K, 100MHz): δ = 184.03 (carbene C), 168.67{Mg-C(Xyl)}, 146.05, 139.74, 135.38, 135.03, 129.79, 125.71, 123.58 (ArC), 122.87 (NCH), 29.46 (*o*-CH<sub>3</sub>), 20.95 (*p*-CH<sub>3</sub>), 18.21(*o*-CH<sub>3</sub>), 6.02 (NSi(CH<sub>3</sub>)<sub>2</sub>) ppm; <sup>29</sup>Si NMR(C<sub>6</sub>D<sub>6</sub>, 298 K, 79 MHz): δ = -9.26 ppm.

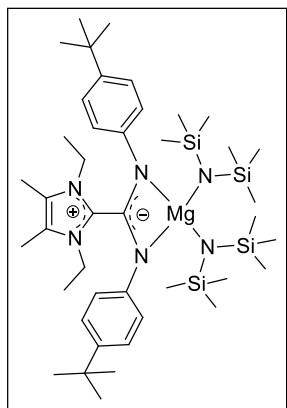
**Synthesis of IMesMg(Mes)N(SiMe<sub>3</sub>)<sub>2</sub> (13):** An analogous reaction to that used for the synthesis



of **12** was carried out using {IMesMg(Mes)Br}<sub>2</sub> (1.50g, 1.42mmol) and Li[N(SiMe<sub>3</sub>)<sub>2</sub>] (0.475g, 2.84mmol). Colorless solid; yield: 1.045g (61 %); M.p. 160-162 °C. <sup>1</sup>H NMR (C<sub>6</sub>D<sub>6</sub>, 298 K, 400 MHz): δ = 6.86 (s, 2H, ArH), 6.70 (s, 4H, ArH), 6.0 (s, 2H, NCH), 2.37 (s, 6H, *p*-CH<sub>3</sub>), 2.32 (s, 6H, *o*-CH<sub>3</sub>), 2.10 (s, 6H, *p*-CH<sub>3</sub>), 1.94 (s, 12H, *o*-CH<sub>3</sub>), 0.16 (s, 18H, NSi(CH<sub>3</sub>)<sub>2</sub>) ppm; <sup>13</sup>C NMR(C<sub>6</sub>D<sub>6</sub>, 298 K, 100 MHz): δ = 184.31(carbene C), 164.17 {Mg-C(Mes)}, 146.14, 139.73, 135.36, 135.04, 133.90, 129.76, 124.74 (ArC), 122.76 (NCH), 29.35 (*o*-CH<sub>3</sub>), 21.70, 20.92 (*p*-CH<sub>3</sub>), 18.26 (*o*-CH<sub>3</sub>), 5.99 (NSi(CH<sub>3</sub>)<sub>2</sub>) ppm; <sup>29</sup>Si NMR(C<sub>6</sub>D<sub>6</sub>, 298 K, 79 MHz): δ = -9.28 ppm.



**Synthesis of  $L^{4-t-BuPh}-Mg\{N(TMS)_2\}_2$  (**14**):**  $L^{4-t-BuPh}$  (0.2 g, 0.436 mmol) and  $Mg\{N(SiMe_3)_2\}_2$

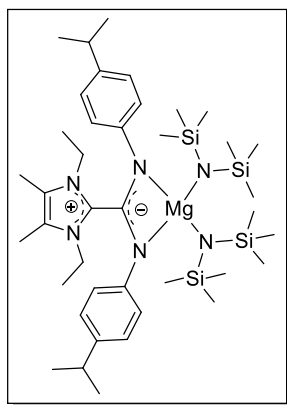


(0.157 g, 0.458 mmol) were mixed together and added toluene (20 mL).

The reaction mixture was stirred at room temperature for 12h. The light yellow suspension of the reaction mixture was removed under reduced pressure and washed with *n*-hexane (2x10 mL). The solid obtained was dried under high vacuum and re-dissolved in minimum amount of hot benzene (60 °C) and solution was slowly cooled to room temperature to

get light yellow color single crystal of the product. Yield: 0.25 g (71.4%); M.p. 182-184 °C.  $^1H$  NMR (400 MHz,  $C_6D_6$ , 25 °C):  $\delta$  = 7.24 (d,  $J$  = 8.0 Hz, 4H, ArH), 6.83 (d,  $J$  = 8.0 Hz, 4H, ArH), 3.46 (q,  $J$  = 8.0 Hz, 4H,  $CH_2CH_3$ ), 1.21 (s, 6H,  $NCCH_3$ ), 1.15 (s, 18H,  $C(CH_3)_3$ ), 0.61 (s, 36H,  $NSi(CH_3)_3$ ), 0.58 (br, 6H,  $CH_2CH_3$ ) ppm;  $^{13}C\{^1H\}$  NMR (101 MHz,  $C_6D_6$ , 25 °C):  $\delta$  = 148.7 (carbene C), 145.9 ( $N_2C$ ), 144.3, 139.8, 126.6, 125.9 (ArC), 122.7 ( $NCCH_3$ ), 42.1 ( $CH_2CH_3$ ), 34.3 ( $C(CH_3)_3$ ), 31.5 ( $C(CH_3)_3$ ), 13.2 ( $CH_2CH_3$ ), 7.9 ( $NCCH_3$ ), 7.0 ( $Si(CH_3)_3$ ) ppm;  $^{29}Si\{^1H\}$  NMR (80 MHz,  $C_6D_6$ , 25 °C):  $\delta$  = -9.74  $N(SiMe_3)_2$ . ESI-MS:  $m/z$  459.34 [ $(M^+ - Mg\{N(TMS)_2\}_2; C_{30}H_{42}N_4 + H)^+$ ].

**Synthesis of  $L^{4-iPrPh}-Mg\{N(TMS)_2\}_2$  (**15**):** An analogous reaction to that used for the synthesis



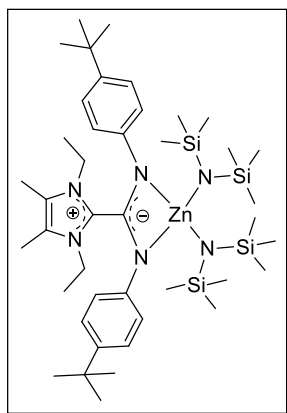
of **14** was carried out with  $L^{4-iPrPh}$  (0.43 g, 1.0 mmol) and  $Mg\{N(SiMe_3)_2\}_2$  (0.345 g, 1.002 mmol). Light yellow solid; yield: 0.530 g (68.4%); M.p. 184-185 °C.  $^1H$  NMR (400 MHz,  $C_6D_6$ , 25 °C):  $\delta$  = 7.02 (d,  $J$  = 8.0 Hz, 4H, ArH), 6.79 (d,  $J$  = 8.0 Hz, 4H, ArH), 3.41 (m, 4H,  $CH_2CH_3$ ), 2.65 (m, 2H,  $CH(CH_3)_2$ ), 1.18 (s, 6H,  $NCCH_3$ ), 1.08 (d,  $J$  = 4.0 Hz, 12H,  $CH(CH_3)_2$ ), 0.61 (br, 36H,  $NSi(CH_3)_3$ ), 0.57 (m,

6H,  $CH_2CH_3$ ) ppm;  $^1H$  NMR (400 MHz,  $thf-d_8$ , 25 °C):  $\delta$  = 6.96 (m, 4H, ArH), 6.60 (m, 4H,

## Experimental Section

ArH), 3.93 (m, 4H, CH<sub>2</sub>CH<sub>3</sub>), 2.78 (m, 2H, CH(CH<sub>3</sub>)<sub>2</sub>), 2.26 (s, 6H, NCCH<sub>3</sub>), 1.16 (br, 12H, CH(CH<sub>3</sub>)<sub>2</sub>), 0.91 (m, 6H, CH<sub>2</sub>CH<sub>3</sub>), 0.04 (s, br, 36H, NSi(CH<sub>3</sub>)<sub>3</sub>) ppm; <sup>13</sup>C{<sup>1</sup>H} NMR (100 MHz, thf-d<sub>8</sub>, 25 °C): δ = 149.7 (carbene C), 145.0, 143.5, 139.6, 128.2, 127.0 (ArH), 123.3 (NCCH<sub>3</sub>), 42.5 (CH<sub>2</sub>CH<sub>3</sub>), 34.1 (CH(CH<sub>3</sub>)<sub>2</sub>), 24.2 (CH(CH<sub>3</sub>)<sub>2</sub>), 13.3 (CH<sub>2</sub>CH<sub>3</sub>), 8.3 (NCCH<sub>3</sub>), 6.5 (SiCH<sub>3</sub>) ppm; <sup>29</sup>Si{<sup>1</sup>H} NMR (80 MHz, C<sub>6</sub>D<sub>6</sub>, 25 °C): δ = -12.17 N(SiMe<sub>3</sub>)<sub>2</sub> ppm. ESI-MS: *m/z* 431.31 [(M<sup>+</sup>-Mg{N(TMS)<sub>2</sub>})<sub>2</sub>; (C<sub>28</sub>H<sub>38</sub>N<sub>4</sub> + H)<sup>+</sup>].

**Synthesis of L<sup>4-*t*-BuPh</sup>-Zn{N(TMS)<sub>2</sub>}}<sub>2</sub> (16):** An analogous reaction to that used for the synthesis



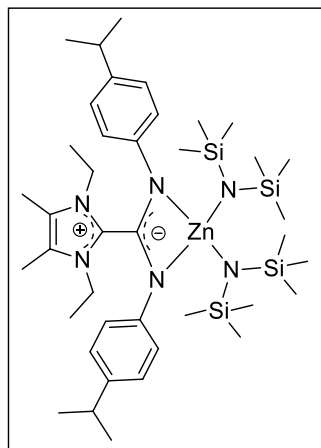
of **14** was carried out with L<sup>4-*t*-BuPh</sup> (0.017 g, 0.0371 mmol) and Zn[N(SiMe<sub>3</sub>)<sub>2</sub>]<sub>2</sub> (0.015 g, 0.0388 mmol). Light yellow solid; yield: 0.022 g (70%); M.p. 140-142 °C. <sup>1</sup>H NMR (400 MHz, C<sub>6</sub>D<sub>6</sub>, 25 °C): δ = 7.22 (d, *J* = 12.0 Hz, 4H, ArH), 6.81 (d, *J* = 8.0 Hz, 4H, ArH), 3.53 (q, *J* = 8.0 Hz, 4H, CH<sub>2</sub>CH<sub>3</sub>), 1.17 (s, 18H, C(CH<sub>3</sub>)<sub>3</sub>), 1.14 (s, 6H, NCCH<sub>3</sub>), 0.62 (s, 36H, NSi(CH<sub>3</sub>)<sub>3</sub>), 0.60 (m, 6H, CH<sub>2</sub>CH<sub>3</sub>) ppm;

<sup>13</sup>C{<sup>1</sup>H} NMR (100 MHz, C<sub>6</sub>D<sub>6</sub>, 25 °C): δ = 145.2 (carbene C), 145.2, 144.8, 141.0, 126.3, 125.9 (ArH), 122.5 (NCCH<sub>3</sub>), 42.0 (CH<sub>2</sub>CH<sub>3</sub>), 34.3 (C(CH<sub>3</sub>)<sub>3</sub>), 31.5 (C(CH<sub>3</sub>)<sub>3</sub>), 13.3 (CH<sub>2</sub>CH<sub>3</sub>), 7.9 (NCCH<sub>3</sub>), 6.9 (SiCH<sub>3</sub>) ppm; <sup>29</sup>Si{<sup>1</sup>H} NMR (80 MHz, C<sub>6</sub>D<sub>6</sub>, 25 °C): δ = -6.13 N(SiMe<sub>3</sub>)<sub>2</sub> ppm. ESI-MS: *m/z* 459.34 [(M<sup>+</sup>-Zn{N(TMS)<sub>2</sub>})<sub>2</sub>; C<sub>30</sub>H<sub>42</sub>N<sub>4</sub> + H)<sup>+</sup>].

**Synthesis of L<sup>4-*i*PrPh</sup>-Zn{N(TMS)<sub>2</sub>}}<sub>2</sub> (17):** An analogous reaction to that used for the synthesis

of **14** was carried out with L<sup>4-*i*PrPh</sup> (0.175 g, 0.406 mmol) and Zn{N(SiMe<sub>3</sub>)<sub>2</sub>}}<sub>2</sub> (0.157 g, 0.407 mmol). Yield: 0.216 g (65%); M.p. 145-148 °C. <sup>1</sup>H NMR (400 MHz, C<sub>6</sub>D<sub>6</sub>, 25 °C): δ = 7.0 (d, *J* = 8.0 Hz, 4H, ArH), 6.79 (d, *J* = 8.0 Hz, 4H, ArH), 3.48 (m, 4H, CH<sub>2</sub>CH<sub>3</sub>), 2.65 (m, 2H, CH(CH<sub>3</sub>)<sub>2</sub>), 1.08 (br, 18H; NCCH<sub>3</sub> (6H) and CH(CH<sub>3</sub>)<sub>2</sub> (12H)), 0.63 (s, 36H, NSi(CH<sub>3</sub>)<sub>3</sub>), 0.56 (t, br, 6H, CH<sub>2</sub>CH<sub>3</sub>) ppm; <sup>1</sup>H NMR (400 MHz, thf-d<sub>8</sub>, 25 °C): δ = 6.94 (d, *J* = 8.0 Hz, 4H, ArH),

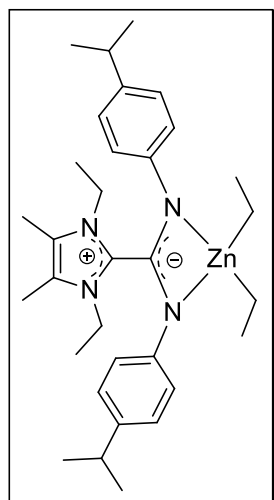
## Experimental Section



6.58 (d,  $J = 8.0$  Hz, 4H, ArH), 3.97 (q,  $J = 4.0, 8.0$  Hz, 4H,  $\text{CH}_2\text{CH}_3$ ), 2.76 (sept,  $J = 4.0, 8.0$  Hz, 2H,  $\text{CH}(\text{CH}_3)_2$ ), 2.24 (s, 6H,  $\text{NCCH}_3$ ), 1.16 (d,  $J = 4.0$  Hz, 12H,  $\text{CH}(\text{CH}_3)_2$ ), 0.91 (t,  $J = 8.0$  Hz, 6H,  $\text{CH}_2\text{CH}_3$ ), 0.06 (s, 36H,  $\text{NSi}(\text{CH}_3)_3$ ) ppm;  $^{13}\text{C}\{^1\text{H}\}$  NMR (101 MHz,  $\text{THF-d}_8$ , 25 °C):  $\delta = 145.9$  (carbene C), 145.7 ( $\text{N}_2\text{C}^-$ ), 142.8, 140.5, 127.9, 126.9, (ArC), 123.1 ( $\text{NCCH}_3$ ), 42.4 ( $\text{CH}_2\text{CH}_3$ ), 34.1 ( $\text{CH}(\text{CH}_3)_2$ ), 24.2 ( $\text{CH}(\text{CH}_3)_2$ ), 13.3 ( $\text{CH}_2\text{CH}_3$ ), 8.3 ( $\text{NCCH}_3$ ), 6.4

( $\text{Si}(\text{CH}_3)_3$ ) ppm;  $^{29}\text{Si}\{^1\text{H}\}$  NMR (80 MHz,  $\text{THF-d}_8$ , 25 °C):  $\delta = -8.63$   $\text{N}(\text{SiMe}_3)_2$  ppm. ESI-MS:  $m/z$  431.31 [ $(\text{M}^+ - \text{Zn}\{\text{N}(\text{TMS})_2\}_2; (\text{C}_{28}\text{H}_{38}\text{N}_4 + \text{H})^+$ ]. Elem. Anal. Cal. for  $\text{C}_{40}\text{H}_{74}\text{ZnN}_6\text{Si}_4$ : C, 58.82; H, 9.13; N, 10.29. Found: C, 58.77; H, 9.16; N, 10.23.

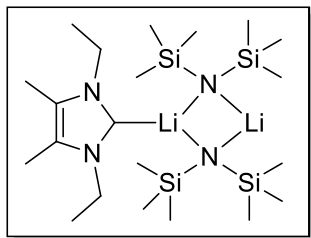
**Synthesis of  $\text{L}^{4\text{-iPrPh}}\text{-ZnEt}_2$  (18):** An analogous reaction to that used for the synthesis of **14** was



carried out with  $\text{L}^{4\text{-iPrPh}}$  (0.250 g, 0.5813 mmol) and  $\text{ZnEt}_2$  (0.61 mL, 0.610 mmol). Yield: 0.170 g (53%); M.p. 153-155 °C.  $^1\text{H}$  NMR (400 MHz,  $\text{C}_6\text{D}_6$ , 25 °C):  $\delta = 7.26\text{--}6.96$  (m, 8H, ArH), 3.70 (br, 4H,  $\text{CH}_2\text{CH}_3$ ), 2.77 (m, 2H,  $\text{CH}(\text{CH}_3)_2$ ), 1.73 (t,  $J = 8.0$  Hz, 6H,  $\text{CH}_2\text{CH}_3$ ), 1.20 (d,  $J = 8.0$  Hz, 12H,  $\text{CH}(\text{CH}_3)_2$ ), 1.10 (s, 6H,  $\text{NCCH}_3$ ), 0.96 (t, br, 6H,  $\text{CH}_2\text{CH}_3$ ), 0.47 (q,  $J = 8.0$  Hz, 4H,  $\text{CH}_2\text{CH}_3$ ) ppm;  $^{13}\text{C}\{^1\text{H}\}$  NMR (101 MHz,  $\text{C}_6\text{D}_6$ , 25 °C):  $\delta = 149.8$  (carbene C), 145.9 ( $\text{N}_2\text{C}^-$ ), 145.5, 141.3, 127.1, 123.5, (ArC), 122.7 ( $\text{NCCH}_3$ ), 41.5 ( $\text{CH}_2\text{CH}_3$ ), 33.9

( $\text{CH}(\text{CH}_3)_2$ ), 24.5 ( $\text{CH}(\text{CH}_3)_2$ ), 14.4 ( $\text{Zn}(\text{CH}_2\text{CH}_3)_2$ ), 14.2 ( $\text{CH}_2\text{CH}_3$ ), 7.4 ( $\text{NCCH}_3$ ), 4.6 ( $\text{Zn}(\text{CH}_2\text{CH}_3)_2$ ) ppm. ESI-MS:  $m/z$  431.31 [ $(\text{M}^+ - \text{ZnEt}_2; (\text{C}_{28}\text{H}_{38}\text{N}_4 + \text{H})^+$ ]. Elem. Anal. Cal. for  $\text{C}_{32}\text{H}_{48}\text{N}_4\text{Zn}$ : C, 69.36; H, 8.73; N, 10.11. Found: C, 69.29; H, 8.70; N, 10.25.

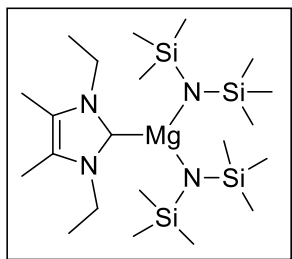
**Synthesis of  $^{\text{Me}}\text{IEt}\{\text{LiN}(\text{TMS})_2\}_2$  (**19**):**



*Method A:*  $\text{L}^{\text{Dipp}}$  (0.01 g, 0.0194 mmol) and  $\text{Li}\{\text{N}(\text{SiMe}_3)_2\}$  (0.004 g, 0.0239 mmol) were mixed together and heated the reaction mixture at 60 °C for overnight and allowed to cool to room temperature results the light yellow color crystals of **19**.

*Method B:* 1,3-Diethyl-4,5-dimethylimidazol-2-ylidene ( $^{\text{Me}}\text{IEt}$ ) (0.02 g, 0.1315 mmol) and  $\text{Li}\{\text{N}(\text{SiMe}_3)_2\}$  (0.044 g, 0.2697 mmol) were dissolved in 1:2 ratio in benzene- $\text{d}_6$  (0.6 mL) to yield the crystalline compound **4**. Yield: 0.042 g (69%); M.p. 73–78 °C.  $^1\text{H}$  NMR (400 MHz,  $\text{C}_6\text{D}_6$ , 25 °C):  $\delta$  = 3.93 (q,  $J$  = 8.0 Hz, 4H,  $\text{CH}_2\text{CH}_3$ ), 1.51 (s, 6H,  $\text{NCCH}_3$ ), 1.11 (t,  $J$  = 4.0, 8.0 Hz, 6H,  $\text{CH}_2\text{CH}_3$ ), 0.31 (s, 36H,  $\text{NSi}(\text{CH}_3)_3$ ) ppm;  $^{13}\text{C}\{^1\text{H}\}$  NMR (101 MHz,  $\text{C}_6\text{D}_6$ , 25 °C):  $\delta$  = 194.2 (carbene C), 123.4 ( $\text{NCCH}_3$ ), 43.6 ( $\text{CH}_2\text{CH}_3$ ), 17.3 ( $\text{CH}_2\text{CH}_3$ ), 8.5 ( $\text{NCCH}_3$ ), 6.0 ( $\text{Si}(\text{CH}_3)_3$ ) ppm;  $^7\text{Li}\{^1\text{H}\}$  NMR (156 MHz,  $\text{C}_6\text{D}_6$ , 25 °C):  $\delta$  = 1.64 ppm;  $^{29}\text{Si}\{^1\text{H}\}$  NMR (80 MHz,  $\text{C}_6\text{D}_6$ , 25 °C):  $\delta$  = -11.24  $\text{N}(\text{SiMe}_3)_2$  ppm. ESI-MS:  $m/z$  153.13 [ $(\text{M}^+ - \{\text{LiN}(\text{TMS})_2\}_2; (\text{C}_9\text{H}_{16}\text{N}_2 + \text{H})^+$ ].

**Synthesis of  $^{\text{Me}}\text{IEt-Mg}\{\text{N}(\text{TMS})_2\}_2$  (**20**):**



*Method A:*  $\text{L}^{\text{Dipp}}$  (0.01 g, 0.0194 mmol) and  $\text{Mg}\{\text{N}(\text{SiMe}_3)_2\}_2$  (0.004 g, 0.0239 mmol) were mixed together and heated the reaction mixture at 60 °C for overnight and allowed to cool to room temperature results the light yellow color crystals of **20**.

*Method B:* An analogous reaction to that used for the synthesis of **19** was carried out with  $^{\text{Me}}\text{IEt}$  (0.02 g, 0.1315 mmol) and  $\text{Mg}\{\text{N}(\text{SiMe}_3)_2\}_2$  (0.045 g, 0.1308 mmol). Yield: 0.042 g (64.6%).  $^1\text{H}$  NMR (400 MHz,  $\text{C}_6\text{D}_6$ , 25 °C):  $\delta$  = 4.09 (q,  $J$  = 8.0 Hz, 4H,  $\text{CH}_2\text{CH}_3$ ), 1.38 (s, 6H,  $\text{NCCH}_3$ ), 1.05 (t,  $J$  = 8.0 Hz, 6H,  $\text{CH}_2\text{CH}_3$ ), 0.36 (s, 36H,  $\text{NSi}(\text{CH}_3)_3$ ) ppm;  $^{13}\text{C}\{^1\text{H}\}$  NMR (101 MHz,

## Experimental Section

C<sub>6</sub>D<sub>6</sub>, 25 °C):  $\delta$  = 177.9 (carbene C), 124.8 (NCH), 42.9 (CH<sub>2</sub>CH<sub>3</sub>), 16.8 (CH<sub>2</sub>CH<sub>3</sub>), 8.1 (NCCH<sub>3</sub>), 6.3 (Si(CH<sub>3</sub>)<sub>3</sub> ppm; <sup>29</sup>Si{<sup>1</sup>H} NMR (80 MHz, C<sub>6</sub>D<sub>6</sub>, 25 °C):  $\delta$  = -8.19 N(SiMe<sub>3</sub>)<sub>2</sub> ppm. ESI-MS:  $m/z$  153.13 [(M<sup>+</sup>-Mg{N(TMS)<sub>2</sub>}<sub>2</sub>; (C<sub>9</sub>H<sub>16</sub>N<sub>2</sub> + H)<sup>+</sup>]. Elem. Anal. Cal. for C<sub>21</sub>H<sub>52</sub>MgN<sub>4</sub>Si<sub>4</sub>: C, 50.72; H, 10.54; N, 11.27. Found: C, 50.66; H, 10.56; N, 11.17.

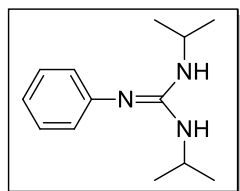
### 6B Experimental section for organic compounds:

#### **6B.1 General procedure for the direct synthesis of guanidines from the reaction of primary aromatic amines with carbodiimides catalyzed by *t*Bu:Mg[N(SiMe<sub>3</sub>)<sub>2</sub>]<sub>2</sub>:**

A 30 mL Schlenk tube under inert atmosphere (N<sub>2</sub>-glovebox) was charged with the catalyst *t*Bu:Mg[N(SiMe<sub>3</sub>)<sub>2</sub>]<sub>2</sub> (0.01 equiv), aromatic amine (1 equiv). To the above mixture carbodiimide (1 equiv) was added. The resulting mixture was stirred at room temperature or heated at 60 °C for a fixed interval. The reaction mixture was then hydrolyzed with water (1 mL) and extracted with dichloromethane (3 x 10 mL). The extracts were combined and dried over anhydrous Na<sub>2</sub>SO<sub>4</sub>. The solvent was removed to get crude compound. The pure product could be obtained by washing the crude product with hexane or diethyl ether.

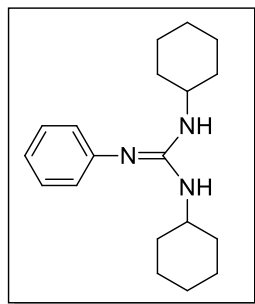
##### **6B.1.1 Spectroscopic data for the products 1a-17a:**

**1,3-diisopropyl-2-phenylguanidine (1a):** Known compound,<sup>12</sup> white solid. <sup>1</sup>H NMR (400 MHz,



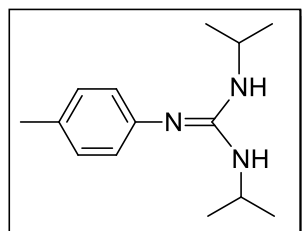
CDCl<sub>3</sub>):  $\delta$  = 7.23 (d,  $J$  = 8.1 Hz, 2H), 6.93 (d,  $J$  = 7.4 Hz, 1H), 6.87–6.83 (m, 2H) (aromatic CH), 3.76 (m,  $J$  = 12.4, 6.1 Hz, 2H, CHPr<sup>*i*</sup><sub>2</sub>), 3.57 (s, NH), 1.15 (d,  $J$  = 6.4 Hz, 12H, CH<sub>3</sub>) ppm; <sup>13</sup>C NMR (101 MHz, CDCl<sub>3</sub>):  $\delta$  = 150.38 (CN<sub>3</sub>), 150.25, 129.32, 123.62, 121.42 (aromatic C), 43.32 (CHPr<sup>*i*</sup><sub>2</sub>), 23.44 (CH<sub>3</sub>) ppm.

**1,3-dicyclohexyl-2-phenylguanidine (2a):** Known compound,<sup>12</sup> white solid. <sup>1</sup>H NMR (400



MHz, CDCl<sub>3</sub>):  $\delta$  = 7.24–7.29 (m, 2H), 6.94 (t,  $J$  = 7.3 Hz, 1H), 6.88 (d,  $J$  = 7.5 Hz, 1H) (aromatic CH), 3.77 (br, NH), 3.43 (br, 2H, CHPr<sup>i</sup><sub>2</sub>), 2.02–1.04 (m, 20H, CH<sub>2</sub>) ppm; <sup>13</sup>C NMR (101 MHz, CDCl<sub>3</sub>):  $\delta$  = 150.31(CN<sub>3</sub>), 150.13, 129.34, 123.72, 121.55 (aromatic C), 50.39 (NCH), 33.90, 25.78, 25.01(CH<sub>2</sub>) ppm.

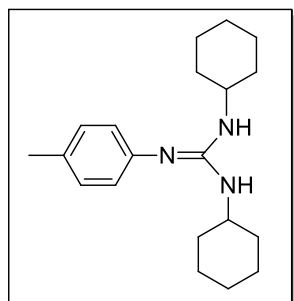
**1,3-diisopropyl-2-(p-tolyl)guanidine (3a):** Known compound,<sup>13</sup> white solid. <sup>1</sup>H NMR (400



MHz, CDCl<sub>3</sub>):  $\delta$  = 7.05 (d,  $J$  = 8.0 Hz, 2H), 6.77 (d,  $J$  = 8.1 Hz, 2H) (aromatic CH), 3.94 (br, NH), 3.76 (m, 2H, CHPr<sup>i</sup><sub>2</sub>), 2.28 (s, 3H, CH<sub>3</sub>), 1.15 (d,  $J$  = 6.4 Hz, 12H, CH<sub>3</sub>) ppm; <sup>13</sup>C NMR (101 MHz, CDCl<sub>3</sub>):  $\delta$  = 150.71 (CN<sub>3</sub>), 146.76, 130.90, 129.97, 123.35 (aromatic

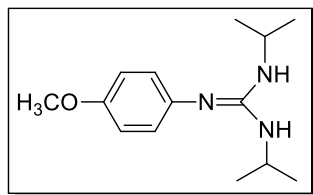
C), 43.43 (CHPr<sup>i</sup><sub>2</sub>), 23.40 (CH<sub>3</sub>), 20.87 (ArCH<sub>3</sub>) ppm.

**1,3-dicyclohexyl-2(p-tolyl)guanidine (4a):** Known compound,<sup>13</sup> white solid. <sup>1</sup>H NMR (400



MHz, CDCl<sub>3</sub>):  $\delta$  = 7.04 (d,  $J$  = 8.0 Hz, 2H), 6.75 (d,  $J$  = 8.1 Hz, 2H) (aromatic CH), 3.77 (br, NH), 3.39 (br, 2H, CHPr<sup>i</sup><sub>2</sub>), 2.27 (s, 3H, ArCH<sub>3</sub>), 1.98-1.07 (m, 20H, CH<sub>2</sub>) ppm; <sup>13</sup>C NMR (101 MHz, CDCl<sub>3</sub>):  $\delta$  150.56 (CN<sub>3</sub>), 147.10, 130.85, 129.97, 123.50 (aromatic C), 50.42 (NCH), 33.91, 25.79, 25.04, 20.90 (CH<sub>2</sub>) ppm.

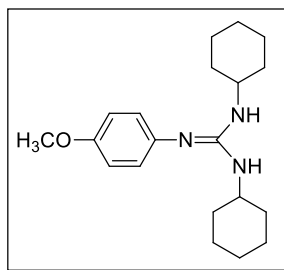
**1,3-diisopropyl-2-(4-methoxyphenyl)guanidine (5a):** Known compound,<sup>12</sup> white solid. <sup>1</sup>H



NMR (400 MHz, CDCl<sub>3</sub>):  $\delta$  = 6.85–6.67 (m, 4H, aromatic CH), 3.75 (br, 5H, OCH<sub>3</sub>, CHPr<sup>i</sup><sub>2</sub>), 1.13 (d,  $J$  = 6.4 Hz, 12H, CH<sub>3</sub>). <sup>13</sup>C NMR (101 MHz, CDCl<sub>3</sub>):  $\delta$  = 154.62 (aromatic C), 150.72 (CN<sub>3</sub>), 143.42,

124.30, 114.70 (aromatic C), 55.52 (OCH<sub>3</sub>), 43.26 (CHPr<sup>i</sup><sub>2</sub>), 23.46 (CH<sub>3</sub>).

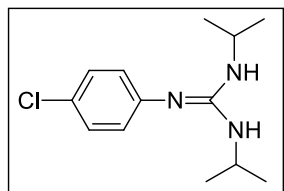
**1,3-dicyclohexyl-2(4-methoxyphenyl)guanidine (6a)** : Known compound,<sup>14</sup> white solid. <sup>1</sup>H



NMR (400 MHz, CDCl<sub>3</sub>):  $\delta$  = 6.82–6.73 (m, 4H, aromatic CH), 3.75 (s, 3H, CH<sub>3</sub>), 3.39 (br, NH), 1.98–1.01 (m, 20H, CH<sub>2</sub>) ppm; <sup>13</sup>C NMR (101 MHz, CDCl<sub>3</sub>)  $\delta$  = 154.62 (aromatic C), 150.61 (CN<sub>3</sub>), 143.55, 124.40, 114.70 (aromatic C), 55.54 (OCH<sub>3</sub>), 50.22 (NCH), 33.94, 25.81, 25.02

(CH<sub>2</sub>) ppm.

**2-(4-Chlorophenyl)-1,3-diisopropylguanidine (7a)**: Known compound,<sup>15</sup> white solid. <sup>1</sup>H NMR

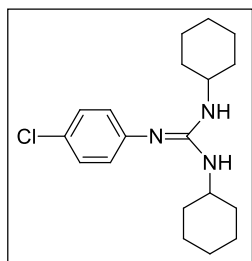


(400 MHz, CDCl<sub>3</sub>):  $\delta$  = 7.23–7.19 (m, 2H, aromatic CH), 6.86 (d, *J* = 8.6 Hz, 2H, aromatic CH), 4.39 (br, 2H, NH), 3.78 (m, 2H, CHPr<sup>i</sup><sub>2</sub>), 1.17 (d, *J* = 6.4 Hz, 12H, CH<sub>3</sub>) ppm; <sup>13</sup>C NMR (101 MHz, CDCl<sub>3</sub>):  $\delta$  =

150.84 (CN<sub>3</sub>), 147.87, 129.41, 126.89, 124.85, 120.87 (aromatic C), 43.66 (CHPr<sup>i</sup><sub>2</sub>), 23.40 (CH<sub>3</sub>)

ppm.

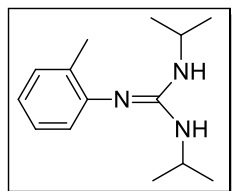
**2-(4-Chlorophenyl)-1,3-dicyclohexylguanidine (8a)**: Known compound,<sup>13</sup> white solid. <sup>1</sup>H



NMR (400 MHz, CDCl<sub>3</sub>):  $\delta$  = 7.17 (d, *J* = 8.3 Hz, 2H), 6.76 (d, *J* = 8.4 Hz, 2H) (aromatic CH), 3.62 (br, 2H, NCH), 3.38 (br, 2H, NH), 2.03–1.00 (m, 20H, CH<sub>2</sub>) ppm; <sup>13</sup>C NMR (101 MHz, CDCl<sub>3</sub>):  $\delta$  150.25 (CN<sub>3</sub>), 149.19, 129.28, 126.31, 124.99 (aromatic C), 50.22 (NCH), 33.85, 25.73,

24.97 (CH<sub>2</sub>) ppm.

**1,3-diisopropyl-2-(o-tolyl)guanidine (10a)**: Known compound,<sup>13</sup> white solid. <sup>1</sup>H NMR (400

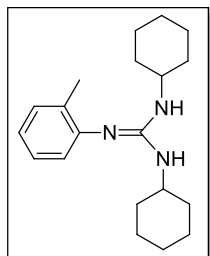


MHz, CDCl<sub>3</sub>):  $\delta$  = 7.14 (d, *J* = 7.4 Hz, 1H), 7.08 (t, *J* = 7.5 Hz, 1H), 6.87 (td, *J* = 7.4, 1.0 Hz, 1H), 6.76 (d, *J* = 7.7 Hz, 1H) (aromatic CH), 3.76 (s, 2H, CHPr<sup>i</sup><sub>2</sub>), 3.43 (s, NH), 2.14 (s, 3H, ArCH<sub>3</sub>), 1.16 (d, *J* = 6.4 Hz, 12H,

## Experimental Section

$\text{CH}_3$ ) ppm;  $^{13}\text{C}$  NMR (100 MHz,  $\text{CDCl}_3$ ):  $\delta$  148.98 ( $\text{CN}_3$ ), 148.50, 131.61, 130.47, 126.70, 123.20, 121.74 (aromatic C), 43.24 ( $\text{CHPr}^i_2$ ), 23.52 ( $\text{CH}_3$ ), 18.15 ( $\text{ArCH}_3$ ) ppm.

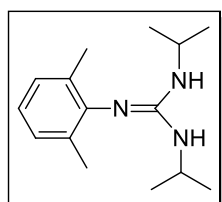
**1,3-dicyclohexyl-2(o-tolyl)guanidine (11a):** Known compound,<sup>13</sup> white solid.  $^1\text{H}$  NMR (400



MHz,  $\text{CDCl}_3$ ):  $\delta$  = 7.13 (d,  $J$  = 7.4 Hz, 1H), 7.07 (t,  $J$  = 7.4 Hz, 1H), 6.85 (t,  $J$  = 7.3 Hz, 1H), 6.76 (d,  $J$  = 7.7 Hz, 1H) (aromatic CH), 3.46 (br, 4H, NH, NCH), 2.13 (s, 3H,  $\text{ArCH}_3$ ), 2.05–1.01 (m, 20H,  $\text{CH}_2$ ) ppm;  $^{13}\text{C}$  NMR (101

MHz,  $\text{CDCl}_3$ ):  $\delta$  148.88 ( $\text{CN}_3$ ), 148.56, 131.74, 130.50, 126.71, 123.32, 121.78 (aromatic C), 50.27 (NCH), 34.05, 25.82, 25.07 ( $\text{CH}_2$ ), 18.21 ( $\text{CH}_3$ ) ppm.

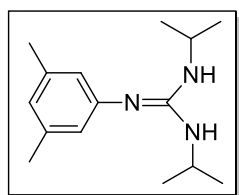
**2-(2,6-dimethylphenyl)1,3-diisopropylguanidine (12a):** Known compound,<sup>15</sup> white solid.  $^1\text{H}$



NMR (400 MHz,  $\text{CDCl}_3$ ):  $\delta$  = 6.99 (d,  $J$  = 7.4 Hz, 2H), 6.82 (t,  $J$  = 7.4 Hz, 1H) (aromatic CH), 3.69 (br, 4H, NH,  $\text{CHPr}^i_2$ ), 2.12 (s, 6H,  $\text{ArCH}_3$ ), 1.16 (s, 12H,  $\text{CH}_3$ ) ppm;  $^{13}\text{C}$  NMR (101 MHz,  $\text{CDCl}_3$ ):  $\delta$  148.15 ( $\text{CN}_3$ ), 145.76,

131.37, 128.03, 122.06 (aromatic C), 43.35 ( $\text{CHPr}^i_2$ ), 23.67 ( $\text{CH}_3$ ), 18.31 ( $\text{ArCH}_3$ ) ppm.

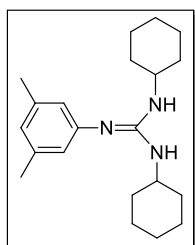
**2-(3,5-dimethylphenyl)1,3-diisopropylguanidine (13a):** White solid.  $^1\text{H}$  NMR (400 MHz,



$\text{CDCl}_3$ ):  $\delta$  = 6.57 (s, 1H), 6.48 (s, 2H) (aromatic CH), 3.76 (m, 2H,  $\text{CHPr}^i_2$ ), 3.59 (br, NH), 2.24 (s, 6H,  $\text{ArCH}_3$ ), 1.16 (d,  $J$  = 6.4 Hz, 12H,  $\text{CH}_3$ ) ppm;  $^{13}\text{C}$  NMR (101 MHz,  $\text{CDCl}_3$ ):  $\delta$  = 150.14 ( $\text{CN}_3$ ), 138.67, 123.12, 121.18

(aromatic C), 43.27( $\text{CHPr}^i_2$ ), 23.43( $\text{CH}_3$ ), 21.37 ( $\text{ArCH}_3$ ) ppm.

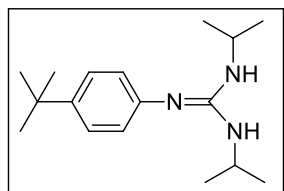
**2-(3,5-dimethylphenyl)1,3-dicyclohexylguanidine (14a):** White solid.  $^1\text{H}$  NMR (400 MHz,



$\text{CDCl}_3$ ):  $\delta$  = 6.56 (s, 1H), 6.48 (s, 2H) (aromatic CH), 3.40 (br, 2H, NCH), 2.04–1.02 (m, 20H,  $\text{CH}_2$ ) ppm;  $^{13}\text{C}$  NMR (101 MHz,  $\text{CDCl}_3$ ):  $\delta$  = 150.27 ( $\text{CN}_3$ ), 150.03, 138.69, 123.12, 121.30 (aromatic C), 50.27 (NCH), 33.94, 25.82, 25.06 ( $\text{CH}_2$ ), 21.41 ( $\text{ArCH}_3$ ) ppm.

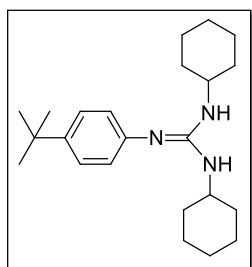


**2-(4(*tert*-butyl)phenyl)1,3-diisopropylguanidine (15a):** Known compound,<sup>16</sup> white solid. <sup>1</sup>H



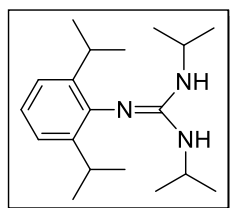
NMR (400 MHz, CDCl<sub>3</sub>): δ = 7.24 (d, *J* = 8.5 Hz, 2H), 6.77 (d, *J* = 8.5 Hz, 2H) (aromatic *CH*). 3.76 (m, 2H, *CHPr*<sup>i</sup><sub>2</sub>), 3.60 (br, *NH*), 1.29 (s, 9H, *tbutCH*<sub>3</sub>), 1.16 (d, *J* = 6.4 Hz, 12H, *CH*<sub>3</sub>) ppm; <sup>13</sup>C NMR (101 MHz, CDCl<sub>3</sub>): δ 150.26 (CN<sub>3</sub>), 147.42, 143.94, 126.15, 122.88 (aromatic *C*), 43.35, (*CHPr*<sup>i</sup><sub>2</sub>), 34.22 (*C(CH*<sub>3</sub>)<sub>2</sub>), 31.66 (*C(CH*<sub>3</sub>)<sub>2</sub>), 23.50 (*CH*<sub>3</sub>) ppm.

**2-(4(*tert*-butyl)phenyl)1,3-dicyclohexylguanidine (16a):** Known compound, white solid. <sup>1</sup>H



NMR (400 MHz, CDCl<sub>3</sub>): δ = 3.21 (s, 1H), 2.87 (s, 1H), 1.37 (s, 1H), 0.99–0.88 (m, 1H). δ 7.23 (d, *J* = 8.5 Hz, 2H), 6.77 (d, *J* = 8.5 Hz, 2H) (aromatic *H*), 3.40 (br, 2H, *NCH*), 2.07–0.99 (m, 20H, *CH*<sub>2</sub>), 1.28 (s, 9H, *CH*<sub>3</sub>) ppm; <sup>13</sup>C NMR (100 MHz, CDCl<sub>3</sub>): δ = 150.16 (CN<sub>3</sub>), 147.48, 143.91, 126.13, 122.93 (aromatic *C*), 50.36 (*NCH*), 34.20 (*C(CH*<sub>3</sub>)<sub>3</sub>), 33.95 (*CH*<sub>2</sub>), 31.65 (*C(CH*<sub>3</sub>)<sub>3</sub>), 25.83, 25.10 (*CH*<sub>2</sub>) ppm.

**2-(2,6-diisopropylphenyl)1,3-diisopropylguanidine (17a):** Known compound,<sup>13</sup> white solid.



<sup>1</sup>H NMR (400 MHz, CDCl<sub>3</sub>): δ = 7.10 (d, *J* = 7.3 Hz, 2H), 6.99 (d, *J* = 7.2 Hz, 1H) (aromatic *CH*), 4.26 (br, *NH*), 3.35 (br, 2H, *NCH*), 3.15 (m, 2H, *CH*), 1.26 (m, 24H, *CH*<sub>3</sub>) ppm; <sup>13</sup>C NMR (101 MHz, CDCl<sub>3</sub>): δ = 147.27 (CN<sub>3</sub>), 144.07, 141.02, 122.78, 121.95, (aromatic *C*), 42.60 (*NCH*), 27.66 (*CH*), 23.50, 23.46 (*CH*<sub>3</sub>) ppm.

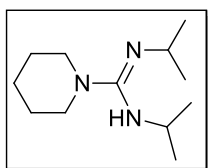
**6B.1.2 General procedure for the direct synthesis of guanidines from cyclic secondary amines with carbodiimides catalyzed by *t*Bu:Mg[N(SiMe<sub>3</sub>)<sub>2</sub>]<sub>2</sub>:** A 30 mL Schlenk tube under inert atmosphere (N<sub>2</sub> glove box) was charged with the catalyst *t*Bu:Mg[N(SiMe<sub>3</sub>)<sub>2</sub>]<sub>2</sub> (0.01 equiv), secondary amine (1.0 equiv), and toluene (5 mL). To this mixture carbodiimide (1.0 equiv) was

## Experimental Section

added. The flask was then closed to prevent evaporation of amines with low boiling points, and the resulting mixture was heated to 110 °C for the desired time. The solvent was removed under reduced pressure; the residue was extracted with hexane (3 × 15 mL) and filtered to give a clear solution. After removing the hexane under reduced pressure, the final products were obtained.

### 6B.1.3 Spectroscopic data for the products 1b-9b:

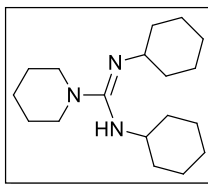
***N,N'*-diisopropylpiperidine-1-carboximidamide (1b):** Known compound,<sup>17</sup> colorless liquid.



<sup>1</sup>H NMR (400 MHz, CDCl<sub>3</sub>): δ = 3.21 (br, 2H, NH), 2.87 (s, 4H, CH<sub>2</sub>), 1.37 (s, 6H, CH<sub>2</sub>), 0.93 (m, 12H, CH<sub>3</sub>) ppm; <sup>13</sup>C NMR (101 MHz, CDCl<sub>3</sub>): δ = 155.92 (CN<sub>3</sub>), 48.84 (CH<sub>2</sub>), 46.29 (CHPr<sup>i</sup><sub>2</sub>), 25.87, 24.85 (CH<sub>2</sub>), 23.96 (CH<sub>3</sub>)

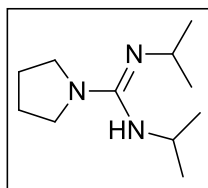
ppm.

***N,N'*-dicyclohexylpiperidine-1-carboximidamide (2b):** Known compound,<sup>17</sup> white solid. <sup>1</sup>H



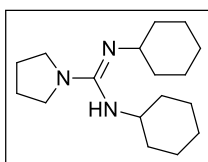
NMR (400 MHz, CDCl<sub>3</sub>): δ = 2.83 (s, 4H, CH<sub>2</sub>), 2.68 (br, NH), 1.75–0.79 (m, 26H, CH<sub>2</sub>) ppm; <sup>13</sup>C NMR (101 MHz, CDCl<sub>3</sub>): δ = 155.36 (CN<sub>3</sub>), 55.21, 52.99 (NCH), 48.66 (CH<sub>2</sub>), 34.52, 25.80, 25.45, 25.09, 24.83 (CH<sub>2</sub>) ppm.

***N,N'*-diisopropylpyrrolidine-1-carboximidamide (3b):** Known compound,<sup>17</sup> colorless liquid.



<sup>1</sup>H NMR (400 MHz, CDCl<sub>3</sub>): δ = 3.34–3.17 (m, 2H, CHPr<sup>i</sup><sub>2</sub>), 3.12 (m, 4H, CH<sub>2</sub>), 1.73–1.59 (m, 4H, CH<sub>2</sub>), 0.97 (d, *J* = 6.4 Hz, 12H, CH<sub>3</sub>) ppm; <sup>13</sup>C

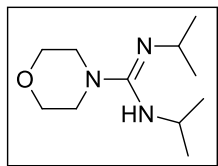
NMR (101 MHz, CDCl<sub>3</sub>): δ = 153.26 (CN<sub>3</sub>), 47.65 (CH<sub>2</sub>), 46.37(CHPr<sup>i</sup><sub>2</sub>), 24.96 (CH<sub>2</sub>), 24.45 (CH<sub>3</sub>) ppm.



***N,N'*-dicyclohexylpyrrolidine-1-carboximidamide (4b):** Known compound,<sup>17</sup> white solid. <sup>1</sup>H NMR (400 MHz, CDCl<sub>3</sub>): δ = 3.09 (m, 4H, CH<sub>2</sub>), 2.80 (m, 2H, NCH), 1.65–0.99 (m, 24H, CH<sub>2</sub>) ppm; <sup>13</sup>C NMR (101

MHz, CDCl<sub>3</sub>): δ = 153.01(CN<sub>3</sub>), 54.57 (NCH), 47.58, 34.97, 25.53, 25.26, 24.90 (CH<sub>2</sub>) ppm.

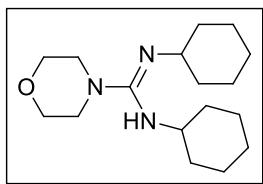
***N,N'*-diisopropylmorpholine-1-carboximidamide (5b)**: Known compound,<sup>17</sup> white solid. <sup>1</sup>H



NMR (400 MHz, CDCl<sub>3</sub>): δ = 3.62 (m, 4H, CH<sub>2</sub>), 3.30 (m, 2H, CHPr<sup>i</sup><sub>2</sub>), 3.02 (m, 4H, CH<sub>2</sub>), 1.04 (s, 12H, CH<sub>3</sub>) ppm; <sup>13</sup>C NMR (101 MHz, CDCl<sub>3</sub>): δ = 155.14 (CN<sub>3</sub>), 67.08, 48.70 (CH<sub>2</sub>), 47.12, 46.33 (CHPr<sup>i</sup><sub>2</sub>), 24.86, 23.77 (CH<sub>3</sub>)

ppm.

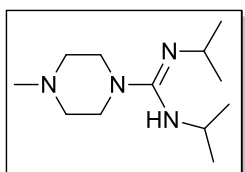
***N,N'*-dicyclohexylmorpholine-1-carboximidamide (6b)**: Known compound,<sup>17</sup> white solid. <sup>1</sup>H



NMR (400 MHz, CDCl<sub>3</sub>): δ = 3.66 (m, 4H, CH<sub>2</sub>), 3.06 (m, 4H, CH<sub>2</sub>), 2.94 (d, *J* = 27.5 Hz, 2H, NCH), 1.96–0.99 (m, 20H, CH<sub>2</sub>) ppm; <sup>13</sup>C NMR (101 MHz, CDCl<sub>3</sub>): δ = 155.07 (CN<sub>3</sub>), 67.21 (CH<sub>2</sub>), 56.44 (NCH),

53.68, 48.79, 35.26, 34.60, 25.52 (CH<sub>2</sub>) ppm.

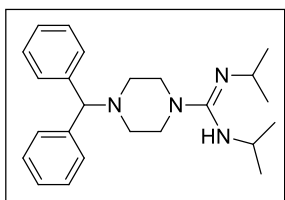
***N,N'*-diisopropyl-4-methylpiperazine-1-carboximidamide (7b)**: Known compound,<sup>18</sup>



colorless liquid. <sup>1</sup>H NMR (400 MHz, CDCl<sub>3</sub>): δ = 3.18 (br, 2H, CHPr<sup>i</sup><sub>2</sub>), 2.93 (s, 4H, CH<sub>2</sub>), 2.21 (s, 4H, CH<sub>2</sub>), 2.10 (m, 3H, NCH<sub>3</sub>), 0.90 (s, 12H, CH<sub>3</sub>) pp; <sup>13</sup>C NMR (CDCl<sub>3</sub>): δ = 154.75 (CN<sub>3</sub>), 55.11 (CH<sub>2</sub>), 47.48, 46.02

(CHPr<sup>i</sup><sub>2</sub>), 24.85, 23.52 (CH<sub>3</sub>) ppm.

**4-benzhydryl-*N,N'*-diisopropylpiperazine-1-carboximidamide (8b)**: White solid. <sup>1</sup>H NMR



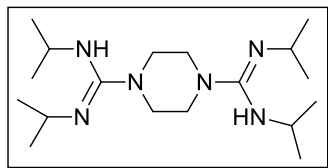
(400 MHz, CDCl<sub>3</sub>): δ = 7.46 (d, *J* = 7.5 Hz, 4H, 7.34–7.23 (m, 4H), 7.19 (d, *J* = 7.4 Hz, 2H) (aromatic CH), 4.30 (s, 1H, CH), 3.45–3.34 (m, 2H, CHPr<sup>i</sup><sub>2</sub>), 3.17 (s, 4H, CH<sub>2</sub>), 2.45 (s, 4H, CH<sub>2</sub>), 1.12 (dd, *J* = 18.1,

6.1 Hz, 12H, CH<sub>3</sub>) ppm; <sup>13</sup>C NMR (CDCl<sub>3</sub>): δ = 155.07 (CN<sub>3</sub>), 142.68, 128.30, 127.83, 126.73, 76.02 (CHAr<sub>2</sub>), 51.90 (CH<sub>2</sub>), 48.06 (CH<sub>2</sub>), 46.94, 45.96 (CHPr<sup>i</sup><sub>2</sub>), 24.87 23.59, (CH<sub>3</sub>) ppm.

***N1,N'1,N4,N'4*-tetraisopropylpiperazine-1,4-bis(carboximidamide) (9b)**: Known

compound,<sup>16</sup> white solid. <sup>1</sup>H NMR (400 MHz, CDCl<sub>3</sub>): δ = 3.35 (br, CHPr<sup>i</sup><sub>2</sub>, NH), 3.03 (s, 8H,

## Experimental Section



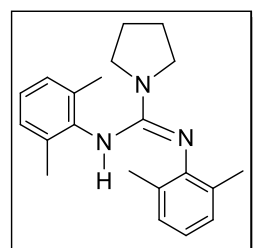
$\text{CH}_2$ ), 1.05 (d,  $J = 6.2$  Hz, 24H,  $\text{CH}_3$ ) ppm;  $^{13}\text{C}$  NMR (101 MHz,  $\text{CDCl}_3$ ):  $\delta = 155.69$  ( $\text{CN}_3$ ), 48.38 ( $\text{CH}_2$ ), 47.11, 46.21 ( $\text{CHPr}^i_2$ ), 24.91, 23.75 ( $\text{CH}_3$ ) ppm.

### 6B.2 General procedure for catalyst free synthesis of guanidines from the reaction of cyclic secondary amines with aromatic carbodiimides:

A 50 mL round bottom flask was charged with secondary amines (1.02 mmol) and aromatic carbodiimides (1 mmol, for biguanidine 2 mmol), and tetrahydrofuran (5 mL) was added to that. The reaction mixture was stirred at room temperature (few cases reflux temperature) for the required time and the progress of the reaction was monitored by TLC. After completion of the reaction, it was extracted with dichloromethane, then the dichloromethane was removed by vacuum and the compound was dried to get the crude compound. The crude residue was recrystallized from diethyl ether or hexane to give an analytically pure compound.

#### 6B.2.1 Spectroscopic data for the products 1c-28c:

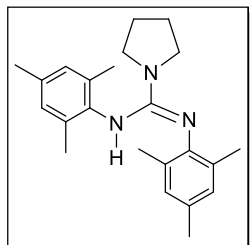
(*Z*)-*N,N'*-bis(2,6-dimethylphenyl)pyrrolidine-1-carboximidamide, (1c): Yield: 99%; M.p.



119–120 °C.  $^1\text{H}$  NMR (400 MHz, 298K,  $\text{CD}_2\text{Cl}_2$ ):  $\delta = 1.71$ -1.74 (m, 4H,  $\text{CH}_2\text{CH}_2$ ), 2.23 (s, 12H, *o*- $\text{CH}_3$ ), 3.03-3.07 (m, 4H,  $\text{NCH}_2$ ), 5.06 (br, 1H,  $\text{NH}$ ), 6.87-7.0 (m, 6H,  $\text{ArH}$ ) ppm;  $^{13}\text{C}\{^1\text{H}\}$  NMR (100 MHz, 298K,  $\text{CDCl}_3$ ):  $\delta = 18.87$  ( $\text{CH}_3$ ), 25.53 ( $\text{CH}_2\text{CH}_2$ ), 47.67 ( $\text{NCH}_2$ ), 122.0, 125.6,

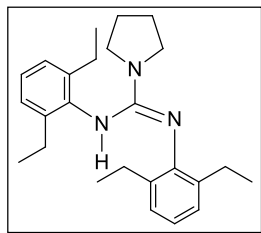
128.3, 130.8, 134.8, 137.8, 147.0 (ArC), 148.4 ( $\text{N}_3\text{C}$ ) ppm. IR (KBr)  $\nu(\text{cm}^{-1})$ : 3364s (N-H), 2942m, 1620m, 1587m, 1407m, 1345m, 1258m, 1215m, 1074m, 776m, 759m, 706m. ESI-MS:  $m/z$  322.5 ( $\text{MH}^+$ ).

**(Z)-N,N'-bis(2,4,6-trimethylphenyl)pyrrolidine-1-carboximidamide (2c):** Yield: 86%; M.p.



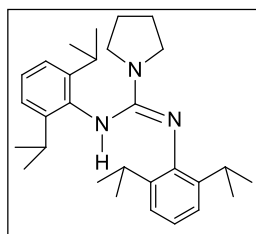
133–134 °C.  $^1\text{H}$  NMR (400 MHz, 298K,  $\text{CD}_2\text{Cl}_2$ ):  $\delta$  = 1.70-1.73 (m, 4H,  $\text{CH}_2\text{CH}_2$ ), 2.18 (s, 12H, *o*- $\text{CH}_3$ ), 2.21 (s, 6H, *p*- $\text{CH}_3$ ), 3.02-3.05 (m, 4H,  $\text{NCH}_2$ ), 5.06 (br, 1H, *NH*), 6.81 (br, 4H, *ArH*) ppm;  $^{13}\text{C}\{^1\text{H}\}$  NMR (100 MHz, 298K,  $\text{CDCl}_3$ ):  $\delta$  = 18.4, 18.9 (*o*- $\text{CH}_3$ ), 20.8 (*p*- $\text{CH}_3$ ), 25.5 ( $\text{CH}_2\text{CH}_2$ ), 47.6 ( $\text{NCH}_2$ ), 128.9, 130.5, 130.8, 134.7, 135.1, 144.4 (*ArC*), 148.9 ( $\text{N}_3\text{C}$ ) ppm. IR (KBr)  $\nu$  ( $\text{cm}^{-1}$ ): 3341s (*N-H*), 2977m, 2919m, 2855s, 1621m, 1596s, 1477m, 1404m, 1393m, 1344m, 1258m, 1226s, 1185s, 1075m, 858m, 759m, 706m. ESI-MS:  $m/z$  350.5 ( $\text{MH}^+$ ).

**(Z)-N,N'-bis(2,6-diethylphenyl)pyrrolidine-1-carboximidamide (3c):** Yield: 86%; M.p. 98–



100 °C.  $^1\text{H}$  NMR (400 MHz, 298K,  $\text{CD}_2\text{Cl}_2$ ):  $\delta$  = 1.17 (br, 12H,  $\text{CH}_2\text{CH}_3$ ), 1.68-1.72 (m, 4H,  $\text{CH}_2\text{CH}_2$ ), 2.60 (br, 8H,  $\text{CH}_2\text{CH}_3$ ), 3.03-3.06 (m, 4H,  $\text{CH}_2\text{CH}_2$ ), 5.05 (1H, *NH*), 6.99-7.05 (m, 6H, *ArH*) ppm;  $^{13}\text{C}\{^1\text{H}\}$  NMR (100 MHz, 298K,  $\text{CD}_2\text{Cl}_2$ ):  $\delta$  = 14.3 ( $\text{CH}_2\text{CH}_3$ ), 24.9 ( $\text{CH}_2\text{CH}_3$ ), 25.8 ( $\text{NCH}_2\text{CH}_2$ ), 48.0 ( $\text{NCH}_2\text{CH}_2$ ), 122.2, 124.4, 126.2, 136.9, 139.9, 141.0 (*ArC*), 148.3 ( $\text{N}_3\text{C}$ ) ppm. IR (KBr)  $\nu$  ( $\text{cm}^{-1}$ ): 3381s (*N-H*), 2964s, 2931s, 2871s, 1610s, 1583s, 1450m, 1422m, 1346s, 1261m, 1215m, 1079m, 808s, 766m, 706m. ESI-MS:  $m/z$  378.3 ( $\text{MH}^+$ ).

**(Z)-N,N'-bis(2,6-diisopropylphenyl)pyrrolidine-1-carboximidamide (4c):** Yield: 99%; M.p.

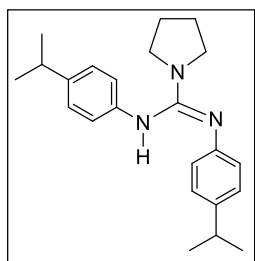


136–137 °C.  $^1\text{H}$  NMR (400 MHz, 298K,  $\text{CD}_2\text{Cl}_2$ ):  $\delta$  = 1.03-1.27 (m, br, 24H,  $\text{CH}(\text{CH}_3)_2$ ), 1.67-1.70 (m, 4H,  $\text{CH}_2\text{CH}_2$ ), 3.0-3.03 (m, 4H,  $\text{NCH}_2\text{CH}_2$ ), 3.21-3.32 (sept,  $J$  = 8.0 Hz, 4H,  $\text{CH}(\text{CH}_3)_2$ ), 5.03 (s, 1H, *NH*), 6.96-7.10 (m, 6H, *ArH*) ppm;  $^{13}\text{C}\{^1\text{H}\}$  NMR (100 MHz, 298K,  $\text{CD}_2\text{Cl}_2$ ):  $\delta$  = 22.7, 24.4, 25.3, ( $\text{CH}(\text{CH}_3)_2$ ), 25.7 ( $\text{NCH}_2\text{CH}_2$ ), 28.7 ( $\text{CH}(\text{CH}_3)_2$ ), 48.3 ( $\text{NCH}_2\text{CH}_2$ ), 122.4,

## Experimental Section

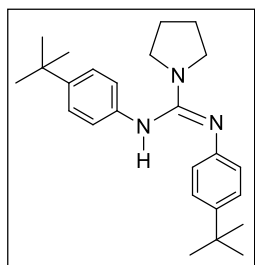
123.2, 123.7, 127.4, 135.1, 141.0, 145.3, 146.5 (ArC), 148.6 (N<sub>3</sub>C) ppm. IR (KBr)  $\nu(\text{cm}^{-1})$ : 3386s (N-H), 2960m, 2869m, 1615m, 1584m, 1463m, 1412m, 1323m, 1257m, 1177m, 1111m, 859m, 762m, 713m. ESI-MS:  $m/z$  434.7 (MH<sup>+</sup>).

**(Z)-N,N'-bis(4-isopropylphenyl)pyrrolidine-1-carboximidamide, 5c.** Yield: 84%; oily. <sup>1</sup>H



NMR (400 MHz, 298K, CD<sub>2</sub>Cl<sub>2</sub>):  $\delta$  = 1.19-1.21(d,  $J$  = 8.0 Hz, 12H, CH(CH<sub>3</sub>)<sub>2</sub>), 1.82-1.85 (m, 4H, CH<sub>2</sub>CH<sub>2</sub>), 2.79-2.84 (sept,  $J$  = 8.0 Hz, 2H, CH(CH<sub>3</sub>)<sub>2</sub>), 3.30-3.33 (m, 4H, NCH<sub>2</sub>CH<sub>2</sub>), 6.78-6.80 (d,  $J$  = 8.0 Hz, 4H, ArH), 7.07-7.09 (d,  $J$  = 8.0 Hz, 4H, ArH) ppm; <sup>13</sup>C{<sup>1</sup>H} NMR (100 MHz, 298K, CD<sub>2</sub>Cl<sub>2</sub>):  $\delta$  = 24.3 (CH(CH<sub>3</sub>)<sub>2</sub>), 25.7 (CH(CH<sub>3</sub>)<sub>2</sub>), 33.8 (NCH<sub>2</sub>CH<sub>2</sub>), 47.8 (NCH<sub>2</sub>CH<sub>2</sub>), 121.1, 127.4, 142.7 (ArC), 149.7 (N<sub>3</sub>C) ppm. IR (KBr)  $\nu(\text{cm}^{-1})$ : 3373s (N-H), 2959m, 2869m, 1618m, 1597m, 1508m, 1397m, 1242m, 1053m, 829m. ESI-MS:  $m/z$  350.2 (MH<sup>+</sup>).

**(Z)-N,N'-bis(4-tert-butylphenyl)pyrrolidine-1-carboximidamide (6c):** Yield: 95%; oily. <sup>1</sup>H

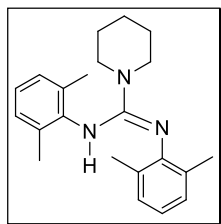


NMR (400 MHz, 298K, CDCl<sub>3</sub>):  $\delta$  = 1.27 (s, 18H, C(CH<sub>3</sub>)<sub>3</sub>), 1.84 (br, 4H, CH<sub>2</sub>CH<sub>2</sub>), 3.35 (br, 4H, NCH<sub>2</sub>CH<sub>2</sub>), 6.86-6.88 (d,  $J$  = 8.0 Hz, 4H, ArH), 7.22-7.24 (d,  $J$  = 8.0 Hz, 4H, ArH) ppm; <sup>13</sup>C{<sup>1</sup>H} NMR (100 MHz, 298K, CDCl<sub>3</sub>):  $\delta$  = 25.3 (NCH<sub>2</sub>CH<sub>2</sub>), 31.5 (C(CH<sub>3</sub>)<sub>3</sub>), 34.2 (C(CH<sub>3</sub>)<sub>3</sub>), 47.8 (NCH<sub>2</sub>CH<sub>2</sub>), 120.9, 126.1, 142.7, 145.1 (ArC), 150.2 (N<sub>3</sub>C) ppm. IR (KBr)  $\nu(\text{cm}^{-1})$ : 3375s (N-H), 2962m, 2869m, 1619m, 1595m, 1515m, 1393m, 1260m, 1190m, 1112m, 1014m, 825m, 559m. ESI-MS:  $m/z$  378.3 (MH<sup>+</sup>).

**(Z)-N,N'-bis(2,6-dimethylphenyl)piperidine-1-carboximidamide (7c):** Yield: 97%; M.p. 137–

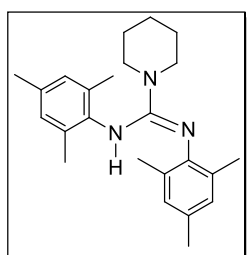
139 °C. <sup>1</sup>H NMR (400 MHz, 298K, CD<sub>2</sub>Cl<sub>2</sub>):  $\delta$  = 1.31-1.36 (m, 4H, CH<sub>2</sub>CH<sub>2</sub>), 1.43-1.49 (m, 2H, CH<sub>2</sub>CH<sub>2</sub>), 2.2 (s, 12H, o-CH<sub>3</sub>), 3.01-3.04 (m, 4H, NCH<sub>2</sub>), 5.0 (s, 1H, NH), 6.82-7.02 (m, 6H,

## Experimental Section



ArH) ppm;  $^{13}\text{C}\{^1\text{H}\}$  NMR (100 MHz, 298K,  $\text{CD}_2\text{Cl}_2$ ):  $\delta = 18.5, 19.2$  (*o*- $\text{CH}_3$ ), 25.2 ( $\text{CH}_2\text{CH}_2$ ), 26.0 ( $\text{CH}_2\text{CH}_2$ ), 48.8 ( $\text{NCH}_2$ ), 122.2, 125.5, 128.7, 130.0, 134.4, 138.1, 147.3 (ArC), 151.6 ( $\text{N}_3\text{C}$ ) ppm. IR (KBr)  $\nu(\text{cm}^{-1})$ : 3375s (N-H), 2943m, 2927m, 2826m, 1623m, 1586m, 1407m, 1345m, 1281m, 1206m, 1069m, 975m, 780m, 761m. ESI-MS:  $m/z$  336.2 ( $\text{MH}^+$ ).

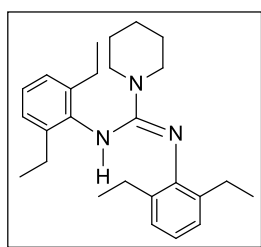
**(Z)-N,N'-bis(2,4,6-trimethylphenyl)piperidine-1-carboximidamide (8c):** Yield: 99%; oily.  $^1\text{H}$



NMR (400 MHz, 298K,  $\text{CD}_2\text{Cl}_2$ ):  $\delta = 1.31\text{-}1.36$  (m, 4H,  $\text{CH}_2\text{CH}_2$ ), 1.43-1.49 (m, 2H,  $\text{CH}_2\text{CH}_2$ ), 2.18 (s, 12H, *o*- $\text{CH}_3$ ), 2.21 (s, 6H, *p*- $\text{CH}_3$ ), 3.0-3.02 (m, 4H,  $\text{NCH}_2$ ), 4.94 (s, 1H, NH), 6.83 (br, 4H, ArH) ppm;  $^{13}\text{C}\{^1\text{H}\}$  NMR

(100 MHz, 298K,  $\text{CD}_2\text{Cl}_2$ ):  $\delta = 18.3, 19.1$  (*o*- $\text{CH}_3$ ), 20.8 (*p*- $\text{CH}_3$ ), 25.2 ( $\text{CH}_2\text{CH}_2$ ), 26.0 ( $\text{CH}_2\text{CH}_2$ ), 48.8 ( $\text{NCH}_2$ ), 129.3, 129.4, 129.7, 131.2, 134.2, 135.1, 135.5, 144.6 (ArC), 152.2 ( $\text{N}_3\text{C}$ ) ppm. IR (KBr)  $\nu(\text{cm}^{-1})$ : 3382s (N-H), 2933m, 2853m, 2166m, 1627m, 1603m, 1470m, 1393m, 1279m, 1256m, 1233m, 1212m, 1215m, 1072m, 975m, 852m. ESI-MS:  $m/z$  364.3 ( $\text{MH}^+$ ).

**(Z)-N,N'-bis(2,6-diethylphenyl)piperidine-1-carboximidamide (9c):** Yield: 99%; M.p. 119–



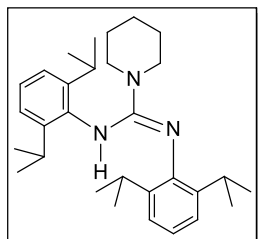
120 °C.  $^1\text{H}$  NMR (400 MHz, 298K,  $\text{CD}_2\text{Cl}_2$ ):  $\delta = 1.10\text{-}1.22$  (overlapping dd (br), 12H,  $\text{CH}_2\text{CH}_3$ ), 1.27-1.36 (m, 4H,  $\text{CH}_2\text{CH}_2$ ), 1.44-1.46 (m, 2H,  $\text{CH}_2\text{CH}_2$ ), 2.59-2.74 (m, br, 8H,  $\text{CH}_2\text{CH}_3$ ), 2.98-3.01 (m, 4H,  $\text{NCH}_2$ ), 5.03 (s, 1H, NH), 6.91-7.05 (m, 6H, ArH) ppm;  $^{13}\text{C}\{^1\text{H}\}$  NMR (100

MHz, 298K,  $\text{CD}_2\text{Cl}_2$ ):  $\delta = 14.4$  ( $\text{CH}_2\text{CH}_3$ ), 24.7 ( $\text{CH}_2\text{CH}_3$ ), 25.2 ( $\text{CH}_2\text{CH}_3$ ), 26.0 ( $\text{NCH}_2\text{CH}_2$ ), 48.8 ( $\text{NCH}_2\text{CH}_2$ ), 122.5, 126.4, 126.6, 135.8, 136.7, 140.1, 146.3 (ArC), 151.6 ( $\text{N}_3\text{C}$ ) ppm. IR

## Experimental Section

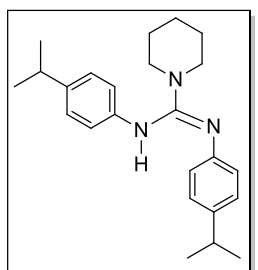
(KBr)  $\nu(\text{cm}^{-1})$ : 3387s (N-H), 2969m, 2940m, 1633m, 1586m, 1449m, 1392m, 1373m, 1280m, 1116m, 1070m, 1033m, 974m, 853m, 764m. ESI-MS:  $m/z$  392.3 ( $\text{MH}^+$ ).

**(Z)-N,N'-bis(2,6-diisopropylphenyl)piperidine-1-carboximidamide (10c):** Known



compound,<sup>19</sup> yield: 99%; M.p. 119–120 °C.  $^1\text{H}$  NMR (400 MHz, 298K,  $\text{CD}_2\text{Cl}_2$ ):  $\delta$  = 1.1-1.32 (br, 24H,  $\text{CH}(\text{CH}_3)_2$ ), 1.38-1.42 (m, 4H,  $\text{CH}_2\text{CH}_2$ ), 1.46-1.49 (m, 2H,  $\text{CH}_2\text{CH}_2$ ), 2.97-3.00 (m, 4H,  $\text{NCH}_2\text{CH}_2$ ), 3.16-3.21 (sept,  $J$  = 8.0 Hz, 4H,  $\text{CH}(\text{CH}_3)_2$ ), 5.02 (s, 1H,  $\text{NH}$ ), 6.96-7.16 (m,  $\text{ArH}$ ) ppm;  $^{13}\text{C}\{^1\text{H}\}$  NMR (100 MHz, 298K,  $\text{CD}_2\text{Cl}_2$ ):  $\delta$  = 22.3, 23.0 ( $\text{CH}(\text{CH}_3)_2$ ), 24.3, 25.2 ( $\text{CH}(\text{CH}_3)_2$ ), 25.4 ( $\text{CH}_2\text{CH}_2$ ), 25.7 ( $\text{NCH}_2\text{CH}_2$ ), 28.7 ( $\text{CH}(\text{CH}_3)_2$ ), 49.0 ( $\text{NCH}_2\text{CH}_2$ ), 122.7, 123.2, 124.0, 127.0, 134.8, 140.1, 145.1, 145.5 ( $\text{ArC}$ ), 151.4 ( $\text{N}_3\text{C}$ ) ppm. IR (KBr)  $\nu(\text{cm}^{-1})$ : 3393s (N-H), 2960m, 1629m, 1585m, 1407m, 1389m, 1111m, 1074m, 776m, 760m. MS/ESI:  $m/z$  448.7 ( $\text{MH}^+$ ).

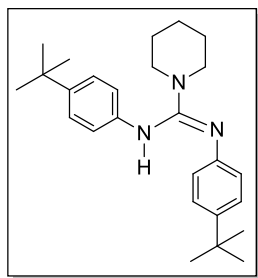
**(Z)-N,N'-bis(4-isopropylphenyl)piperidine-1-carboximidamide (11c):** Yield: 77%; oily.  $^1\text{H}$



NMR (400 MHz, 298K,  $\text{CDCl}_3$ ):  $\delta$  = 1.21-1.22 (d,  $J$  = 4.0 Hz, 12H,  $\text{CH}(\text{CH}_3)_2$ ), 1.53-1.55 (m, 6H,  $\text{CH}_2\text{CH}_2\text{CH}_2$ ), 2.79-2.89 (sept,  $J$  = 8.0 Hz, 2H,  $\text{CH}(\text{CH}_3)_2$ ), 3.28 (m, 4H,  $\text{NCH}_2\text{CH}_2$ ), 4.69 (1H,  $\text{NH}$ ), 6.86 (d,  $J$  = 8.0 Hz, 4H,  $\text{ArH}$ ) 7.09 (d,  $J$  = 8.0 Hz, 4H,  $\text{ArH}$ ) ppm;  $^{13}\text{C}\{^1\text{H}\}$  NMR (100 MHz, 298K,  $\text{CDCl}_3$ ):  $\delta$  = 24.1 ( $\text{CH}(\text{CH}_3)_2$ ), 24.7 ( $\text{CH}_2\text{CH}_2$ ), 25.3 ( $\text{NCH}_2\text{CH}_2$ ), 33.4 ( $\text{CH}(\text{CH}_3)_2$ ), 47.8 ( $\text{NCH}_2\text{CH}_2$ ), 120.7, 127.2, 142.8 ( $\text{ArC}$ ), 152.0, ( $\text{N}_3\text{C}$ ) ppm. IR (KBr)  $\nu(\text{cm}^{-1})$ : 3375s (N-H), 2959m, 1631m, 1579m, 1516m, 1447m, 1413m, 1287m, 1254m, 1121m, 825m, 549m. ESI-MS:  $m/z$  364.2 ( $\text{MH}^+$ ).



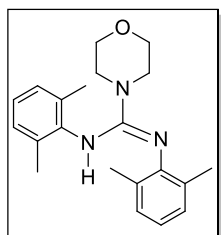
**(Z)-N,N'-bis(4-(tert-butyl)phenyl)piperidine-1-carboximidamide (12c):** Yield: 89%; oily.  $^1\text{H}$



NMR (400 MHz, 298K,  $\text{CD}_2\text{Cl}_2$ ):  $\delta$  = 1.28 (s, 18H,  $\text{C}(\text{CH}_3)_2$ ), 1.53-1.59 (m, 6H,  $\text{CH}_2\text{CH}_2$ ), 3.25-3.27 (m, 4H,  $\text{NCH}_2\text{CH}_2$ ), 6.82 (br, 4H,  $\text{ArH}$ ) 7.23-7.25 (d,  $J$  = 8.0 Hz, 4H,  $\text{ArH}$ ) ppm;  $^{13}\text{C}\{^1\text{H}\}$  NMR (100 MHz, 298K,  $\text{CD}_2\text{Cl}_2$ ):  $\delta$  = 24.7 ( $\text{CH}_2\text{CH}_2$ ), 25.3 ( $\text{NCH}_2\text{CH}_2$ ), 31.5 ( $\text{C}(\text{CH}_3)_3$ ), 34.2

( $\text{C}(\text{CH}_3)_3$ ), 47.8 ( $\text{NCH}_2\text{CH}_2$ ), 120.3, 126.0, 145.0 ( $\text{ArC}$ ), 151.9 ( $\text{N}_3\text{C}$ ) ppm. IR (KBr)  $\nu(\text{cm}^{-1})$ : 3382s (N-H), 2961m, 2859m, 1621m, 1515m, 1393m, 1269m, 1113m, 1072m, 978m, 825m, 837m, 824m, 548m. ESI-MS:  $m/z$  392.3 ( $\text{MH}^+$ ).

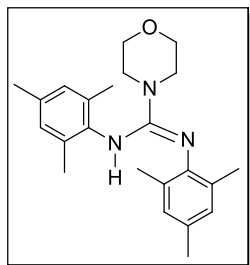
**(Z)-N,N'-bis(2,6-dimethylphenyl)morpholine-4-carboximidamide (13c):** Yield: 99%; M.p.



174–175 °C.  $^1\text{H}$  NMR (400 MHz, 298K,  $\text{CD}_2\text{Cl}_2$ ):  $\delta$  = 2.24 (s, 12H,  $o\text{-CH}_3$ ), 3.04-3.06 (m, 4H,  $\text{NCH}_2$ ), 3.45-3.47 (m, 4H,  $\text{OCH}_2$ ), 5.08 (s, 1H,  $\text{NH}$ ), 6.83-7.02 (m, 6H,  $\text{ArH}$ ) ppm;  $^{13}\text{C}\{^1\text{H}\}$  NMR (100 MHz, 298K,  $\text{CD}_2\text{Cl}_2$ ):  $\delta$  = 18.3 ( $\text{CH}_3$ ), 19.2 ( $\text{CH}_3$ ), 48.3 ( $\text{NCH}_2$ ), 66.9 ( $\text{OCH}_2$ ), 122.5, 126.1, 128.6, 128.9,

129.8, 134.5, 137.6, 146.7 ( $\text{ArC}$ ), 151.1 ( $\text{N}_3\text{C}$ ) ppm. IR (KBr)  $\nu(\text{cm}^{-1})$ : 3364s (N-H), 2942m, 1620m, 1587m, 1407m, 1345m, 1258m, 1215m, 1074m, 776m, 759m, 706m. ESI-MS:  $m/z$  338.5 ( $\text{MH}^+$ ).

**(Z)-N,N'-bis(2,4,6-trimethylphenyl)morpholine-4-carboximidamide (14c):** Yield: 98%; M.p.



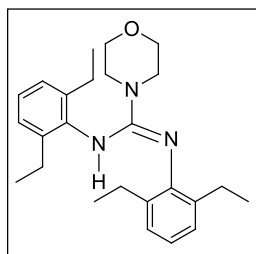
148–150 °C.  $^1\text{H}$  NMR (400 MHz, 298K,  $\text{CD}_2\text{Cl}_2$ ):  $\delta$  = 2.19 (s, 12H,  $o\text{-CH}_3$ ), 2.22 (s, 6H,  $p\text{-CH}_3$ ), 3.03-3.05 (m, 4H,  $\text{NCH}_2\text{CH}_2$ ), 3.44-3.47 (m, 4H,  $\text{OCH}_2\text{CH}_2$ ), 5.02 (s, 1H,  $\text{NH}$ ), 6.82-6.86 (m, 4H,  $\text{ArH}$ ) ppm;  $^{13}\text{C}\{^1\text{H}\}$

NMR (100 MHz, 298K,  $\text{CD}_2\text{Cl}_2$ ):  $\delta$  = 18.2 ( $o\text{-CH}_3$ ), 19.1 ( $o\text{-CH}_3$ ), 20.8 ( $p\text{-CH}_3$ ), 48.3 ( $\text{NCH}_2$ ), 66.9 ( $\text{OCH}_2$ ), 129.3, 129.6, 131.5, 134.3, 135.0, 135.6, 144.1 ( $\text{ArC}$ ), 151.5

## Experimental Section

(N<sub>3</sub>C) ppm. IR (KBr)  $\nu(\text{cm}^{-1})$ : 3364s (N-H), 2974m, 2917m, 2849m, 2373m, 1637m, 1458m, 1384m, 1305m, 1267m, 1113m, 1085m, 984m, 855m, 807s. ESI-MS:  $m/z$  366.2 (MH<sup>+</sup>).

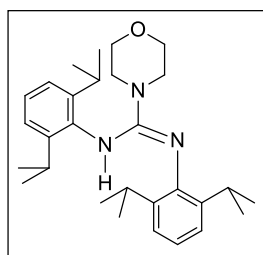
**(Z)-N,N'-bis(2,6-diethylphenyl)morpholine-4-carboximidamide (15c):** Known compound,<sup>20</sup>



Yield: 89%; M.p. 144–147 °C. <sup>1</sup>H NMR (400 MHz, 298K, CD<sub>2</sub>Cl<sub>2</sub>):  $\delta$  = 1.09-1.12 (t,  $J$  = 8.0, 4.0 Hz, 6H, CH<sub>2</sub>CH<sub>3</sub>), 1.22-1.25 (t,  $J$  = 8.0, 4.0 Hz, 6H, CH<sub>2</sub>CH<sub>3</sub>), 2.50-2.78 (m, 8H, CH<sub>2</sub>CH<sub>3</sub>), 3.02-3.04 (m, 4H, NCH<sub>2</sub>), 3.44-3.46 (m, 4H, OCH<sub>2</sub>), 5.11 (s, 1H, NH), 6.91-7.09 (m, 6H, ArH) ppm;

<sup>13</sup>C{<sup>1</sup>H} NMR (100 MHz, 298K, CD<sub>2</sub>Cl<sub>2</sub>):  $\delta$  = 14.3 (CH<sub>2</sub>CH<sub>3</sub>), 14.5 (CH<sub>2</sub>CH<sub>3</sub>), 24.7 (CH<sub>2</sub>CH<sub>3</sub>), 25.3 (CH<sub>2</sub>CH<sub>3</sub>), 48.3 (NCH<sub>2</sub>), 66.8 (OCH<sub>2</sub>), 122.8, 126.4, 126.6, 126.8, 135.6, 136.2, 140.3, 145.8 (ArC), 151.0 (N<sub>3</sub>C) ppm. IR (KBr)  $\nu(\text{cm}^{-1})$ : 3330s (N-H), 2969m, 2936m, 2858m, 2373m, 1638m, 1458m, 1381m, 1364m, 1273m, 1115m, 1084m, 982m, 855m, 809s. ESI-MS:  $m/z$  394.5 (MH<sup>+</sup>).

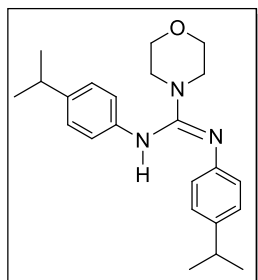
**(Z)-N,N'-bis(2,6-diisopropylphenyl)morpholine-4-carboximidamide (16c):** Yield: 99%; M.p.



134–135 °C. <sup>1</sup>H NMR (400 MHz, 298K, CD<sub>2</sub>Cl<sub>2</sub>):  $\delta$  = 0.99 (br, 6H, CH(CH<sub>3</sub>)<sub>2</sub>), 1.16-1.18 (d,  $J$  = 8.0 Hz, 6H, CH(CH<sub>3</sub>)<sub>2</sub>), 1.31-1.33 (d,  $J$  = 8.0 Hz, 12H, CH(CH<sub>3</sub>)<sub>2</sub>), 3.01-3.03 (m, 4H, NCH<sub>2</sub>CH<sub>2</sub>), 3.13-3.21 (sept,  $J$  = 8.0, 4.0 Hz, 4H, CH(CH<sub>3</sub>)<sub>2</sub>), 3.49-3.51 (m, 4H, OCH<sub>2</sub>CH<sub>2</sub>), 5.09 (s,

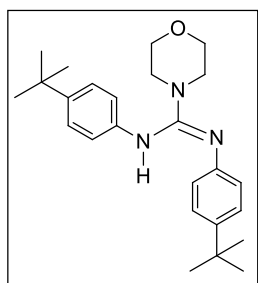
1H, NH), 6.96-7.20 (m, 6H, ArH) ppm; <sup>13</sup>C{<sup>1</sup>H} NMR (100 MHz, 298K, CD<sub>2</sub>Cl<sub>2</sub>):  $\delta$  = 22.3, 22.9 (CH(CH<sub>3</sub>)<sub>2</sub>), 24.3, 25.4 (CH(CH<sub>3</sub>)<sub>2</sub>), 28.8, 28.9 (CH(CH<sub>3</sub>)<sub>2</sub>), 48.6 (NCH<sub>2</sub>CH<sub>2</sub>), 66.6 (OCH<sub>2</sub>CH<sub>2</sub>), 123.0, 123.3, 124.2, 127.4, 134.2, 140.2, 144.5, 145.6 (ArC), 150.9 (N<sub>3</sub>C) ppm. IR (KBr)  $\nu(\text{cm}^{-1})$ : 3354s (N-H), 2968m, 2936m, 2858m, 2373m, 1638m, 1458m, 1381m, 1364m, 1273m, 1115m, 1084m, 982m, 855m, 809s. ESI-MS:  $m/z$  450.2 (MH<sup>+</sup>).

**(Z)-N,N'-bis(4-isopropylphenyl)morpholine-4-carboximidamide (17c):** Yield: 99%; oily.  $^1\text{H}$



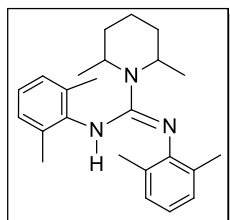
NMR (400 MHz, 298K,  $\text{CD}_2\text{Cl}_2$ ):  $\delta$  = 1.20-1.21 (d,  $J$  = 4.0 Hz, 12H,  $\text{CH}(\text{CH}_3)_2$ ), 2.78-2.89 (sept,  $J$  = 8.0 Hz, 2H,  $\text{CH}(\text{CH}_3)_2$ ), 3.27-3.29 (m, 4H,  $\text{NCH}_2$ ), 3.62-3.64 (m, 4H,  $\text{OCH}_2$ ), 5.52 (br, 1H,  $\text{NH}$ ), 6.80-7.11 (m, 8H,  $\text{ArH}$ ) ppm;  $^{13}\text{C}\{^1\text{H}\}$  NMR (100 MHz, 298K,  $\text{CD}_2\text{Cl}_2$ ):  $\delta$  24.2 ( $\text{CH}(\text{CH}_3)_2$ ), 33.8 ( $\text{CH}(\text{CH}_3)_2$ ), 47.4 ( $\text{NCH}_2$ ), 66.7 ( $\text{OCH}_2$ ), 119.0, 122.1, 127.5, 140.5, 143.2, 147.7 ( $\text{ArC}$ ), 151.4 ( $\text{N}_3\text{C}$ ) ppm. IR (KBr)  $\nu(\text{cm}^{-1})$ : 3330s (N-H), 2969m, 2936m, 2858m, 2373m, 1638m, 1458m, 1381m, 1364m, 1273m, 1115m, 1084m, 982m, 855m, 809s. ESI-MS:  $m/z$  366.2 ( $\text{MH}^+$ ).

**(Z)-N,N'-bis(4-tert-butylphenyl)morpholine-4-carboximidamide (18c):** Yield: 99%; M.p.



126–127 °C.  $^1\text{H}$  NMR (400 MHz, 298K,  $\text{CD}_2\text{Cl}_2$ ):  $\delta$  = 1.28 (s, 18H,  $\text{C}(\text{CH}_3)_3$ ), 3.27-3.30 (m, 4H,  $\text{NCH}_2\text{CH}_2$ ), 3.63-3.65 (m, 4H,  $\text{OCH}_2\text{CH}_2$ ), 5.52 (br, 1H,  $\text{NH}$ ), 6.78-7.27 (m, 8H,  $\text{ArH}$ ) ppm;  $^{13}\text{C}\{^1\text{H}\}$  NMR (100 MHz, 298K,  $\text{CD}_2\text{Cl}_2$ ):  $\delta$  = 31.6 ( $\text{C}(\text{CH}_3)_3$ ), 34.4 ( $\text{C}(\text{CH}_3)_3$ ), 47.4 ( $\text{NCH}_2$ ), 66.7 ( $\text{OCH}_2$ ), 118.6, 121.9, 126.5, 139.8, 145.4, 147.4, ( $\text{ArC}$ ), 151.4 ( $\text{N}_3\text{C}$ ) ppm. IR (KBr)  $\nu(\text{cm}^{-1})$ : 3382m (N-H), 3249m, 3162m, 2958m, 1627m, 1575m, 1513s, 1446s, 1427s, 1360m, 1364m, 1273m, 1115m, 1084m, 982m, 855m, 809s. ESI-MS:  $m/z$  394.6 ( $\text{MH}^+$ ).

**(Z)-N,N'-bis(2,6-dimethylphenyl)-2,6-dimethylpiperidine-1-carboximidamide (19c):** Yield:

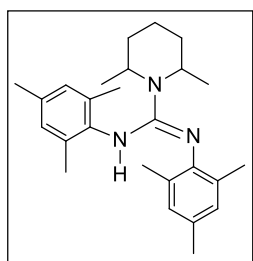


42%; oily.  $^1\text{H}$  NMR (400 MHz, 298K,  $\text{CDCl}_3$ ):  $\delta$  = 1.26 (d, 6H,  $J$  = 8.0 Hz,  $\text{CH}_3$ ), 1.35-1.85 (m, 6H,  $\text{CH}_2\text{CH}_2$ ), 2.24 (s, 6H,  $o\text{-CH}_3$ ), 2.29 (s, 6H,  $o\text{-CH}_3$ ), 3.90-3.97 (m, 2H,  $\text{NCH}$ ), 4.98 (s, 1H,  $\text{NH}$ ), 6.82-7.03 (m, 6H,  $\text{ArH}$ ) ppm;  $^{13}\text{C}\{^1\text{H}\}$  NMR (100 MHz, 298K,  $\text{CDCl}_3$ ):  $\delta$  14.5 ( $\text{CH}_2\text{CH}_2\text{CH}_2$ ), 18.5,

## Experimental Section

19.07 (*o*-CH<sub>3</sub>), 20.9 (NCHCH<sub>3</sub>), 30.3 (CHCH<sub>2</sub>CH<sub>2</sub>), 48.1 (NCH), 121.9, 125.2, 128.4, 128.7, 129.3, 133.7, 138.5, 147.5 (ArC), 150.4 (N<sub>3</sub>C) ppm. IR (KBr)  $\nu(\text{cm}^{-1})$ : 3373s (N-H), 2930m, 1619m, 1587m, 1469m, 1405m, 1367m, 1212m, 1148m, 1117m, 1037m, 974m, 894m, 774m, 766m. ESI-MS:  $m/z$  364.2 (MH<sup>+</sup>).

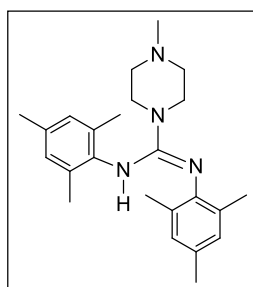
### (Z)-*N,N'*-bis(2,4,6-trimethylphenyl)-2,6-dimethylpiperidine-1-carboximidamide (20c):



Yield: 37%; oily. <sup>1</sup>H NMR (400 MHz, 298K, CDCl<sub>3</sub>):  $\delta$  = 1.25 (d, 6H, J = 8.0 Hz, CH<sub>3</sub>), 1.35-1.85 (m, 6H, CH<sub>2</sub>CH<sub>2</sub>CH<sub>2</sub>), 2.19-2.24 (m, 18H, *o,p*-CH<sub>3</sub>), 3.91-3.97 (m, 2H, NCH), 4.94 (s, 1H, NH), 6.79-6.85 (m, 4H, ArH) ppm; <sup>13</sup>C{<sup>1</sup>H} NMR (100 MHz, 298K, CDCl<sub>3</sub>):  $\delta$  = 14.6 (CH<sub>2</sub>CH<sub>2</sub>CH<sub>2</sub>),

18.5, 18.9 (*o*-CH<sub>3</sub>), 20.8 (*p*-CH<sub>3</sub>), 20.9 (NCHCH<sub>3</sub>), 30.3 (CHCH<sub>2</sub>CH<sub>2</sub>), 47.99 (NCH), 129.1, 129.3, 129.7, 130.8, 133.7, 134.6, 135.8, 144.8 (ArC), 150.9 (N<sub>3</sub>C) ppm. IR (KBr)  $\nu(\text{cm}^{-1})$ : 3375s (N-H), 2931m, 1621m, 1600m, 1478m, 1404m, 1368m, 1219m, 1146m, 1119m, 1036m, 888m, 852m. ESI-MS:  $m/z$  392.3 (MH<sup>+</sup>).

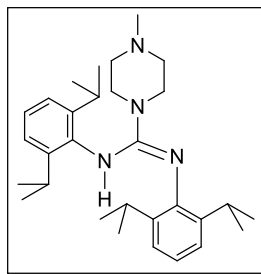
### (Z)-*N,N'*-bis(2,4,6-trimethylphenyl)-4-methylpiperazine-1-carboximidamide (21c):

 Yield:

92%; M.p. 129–131 °C. <sup>1</sup>H NMR (400 MHz, 298K, CDCl<sub>3</sub>):  $\delta$  = 2.17 (s, 6H, *o*-CH<sub>3</sub>), 2.22-2.23 (m, 19H, *o*-CH<sub>3</sub>, NCH<sub>3</sub>, CH<sub>3</sub>NCH<sub>2</sub>), 3.12 (br, 4H, NCH<sub>2</sub>), 5.00 (1H, NH), 6.80 (s, 2H, ArH), 6.85 (s, 2H, ArH) ppm; <sup>13</sup>C{<sup>1</sup>H} NMR (100 MHz, 298K, CDCl<sub>3</sub>):  $\delta$  = 18.2, 19.1 (*o*-CH<sub>3</sub>), 20.8,

20.9 (*p*-CH<sub>3</sub>), 46.2 (NCH<sub>3</sub>), 47.2 (NCH<sub>2</sub>), 54.9 (CH<sub>3</sub>NCH<sub>2</sub>), 129.1, 129.4, 129.7, 131.4, 133.8, 134.7, 135.2, 143.6, (ArC), 151.5 (N<sub>3</sub>C) ppm. IR (KBr)  $\nu(\text{cm}^{-1})$ : 3317m (N-H), 2915m, 2852m, 2797m, 1629m, 1600m, 1396m, 1368m, 1297m, 1266m, 1233m, 1214m, 1136m, 1006m, 989m, 857m, 546s. ESI-MS:  $m/z$  379.3 (MH<sup>+</sup>).

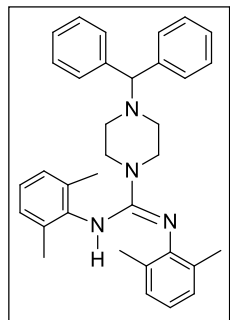
**(Z)-N,N'-bis(2,6-diisopropylphenyl)-4-methylpiperazine-1-carboximidamide (22c):** Yield:



89%; M.p. 147–149 °C.  $^1\text{H}$  NMR (400 MHz, 298K,  $\text{CDCl}_3$ ):  $\delta$  = 0.99-1.32 (br, dd, 24H,  $\text{CH}(\text{CH}_3)_2$ ), 2.22 (s, 3H,  $\text{NCH}_3$ ), 2.29 (br, 4H,  $\text{NCH}_2$ ), 3.09 (br, 4H,  $\text{CH}_3\text{NCH}_2$ ), 3.13 - 3.20 (sept,  $J$  = 8.0 Hz, 4H,  $\text{CH}(\text{CH}_3)_2$ ), 5.05 (s, 1H,  $\text{NH}$ ), 7.0-7.14 (m, 6H,  $\text{ArH}$ ) ppm;  $^{13}\text{C}\{^1\text{H}\}$  NMR (100 MHz,

298K,  $\text{CDCl}_3$ ):  $\delta$  = 22.3, 22.9, 24.2, 25.3 ( $\text{CH}(\text{CH}_3)_2$ ), 28.5, 28.6 ( $\text{CH}(\text{CH}_3)_2$ ), 46.3 ( $\text{NCH}_3$ ), 47.5 ( $\text{NCH}_2$ ), 54.5 ( $\text{CH}_3\text{NCH}_2$ ), 122.8, 123.0, 123.9, 126.9, 134.0, 139.7, 144.3, 145.0 ( $\text{ArC}$ ), 150.4 ( $\text{N}_3\text{C}$ ) ppm. IR (KBr)  $\nu$  ( $\text{cm}^{-1}$ ): 3391s (N-H), 2959m, 2841m, 2795s, 1626m, 1586m, 1394m, 1368m, 1267m, 1145m, 1079m, 989m, 805m, 762m. ESI-MS:  $m/z$  463.3 ( $\text{MH}^+$ ).

**(Z)-4-benzhydryl-N,N'-bis(2,6-dimethylphenyl)piperazine-1-carboximidamide (23c):** Yield:



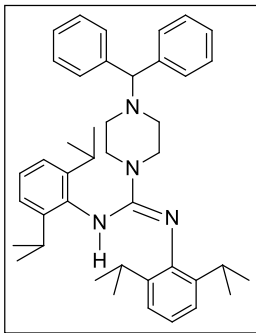
86%; M.p. 174–177 °C.  $^1\text{H}$  NMR (400 MHz, 298K,  $\text{CD}_2\text{Cl}_2$ ):  $\delta$  = 2.20 (s, 10H,  $\text{CH}_3$ (6H),  $\text{NCH}_2$ (4H)), 2.26 (s, 6H,  $\text{CH}_3$ ), 3.11-3.13 (m, 4H,  $\text{NCH}_2$ ), 4.12 (s, 1H,  $\text{CH}(\text{Ph})_2$ ), 5.02 (s, 1H,  $\text{NH}$ ), 6.83-7.05 (m, 6H,  $\text{ArH}$ ), 7.15 (m, 2H,  $\text{ArH}$ ), 7.24 (m, 4H,  $\text{ArH}$ ), 7.38 (m, 4H,  $\text{ArH}$ ) ppm;  $^{13}\text{C}\{^1\text{H}\}$  NMR (100 MHz, 298K,  $\text{CDCl}_3$ ):  $\delta$  = 18.2, 19.1 ( $\text{CH}_3$ ), 47.4 ( $\text{NCH}_2$ ), 51.8 ( $\text{CHNCH}_2$ ),

76.3 ( $\text{Ph}_2\text{CH}$ ), 122.4, 125.7, 127.0, 127.9, 128.4, 128.6, 128.7, 129.8, 133.9, 137.3, 142.8, 146.4 ( $\text{ArC}$ ), 151.1 ( $\text{N}_3\text{C}$ ) ppm. IR (KBr)  $\nu$ ( $\text{cm}^{-1}$ ): 3364s (N-H), 3027m, 2968m, 2915s, 2848s, 2821m, 1637m, 1587m, 1469m, 1451m, 1396m, 1305m, 1257m, 1214m, 1126m, 1080m, 991m, 784m, 764m, 705m. ESI-MS:  $m/z$  503.2 ( $\text{MH}^+$ ).

**(Z)-4-benzhydryl-N,N'-bis(2,6-diisopropylphenyl)piperazine-1-carboximidamide (24c):**

Yield: 76%; M.p. 154-157 °C.  $^1\text{H}$  NMR (400 MHz, 298K,  $\text{CDCl}_3$ ):  $\delta$  = 0.97-1.31 (d, 24H,  $\text{CH}(\text{CH}_3)_2$ ), 2.25 (m, 4H,  $\text{CHNCH}_2$ ), 3.06-3.08 (m, 4H,  $\text{NCH}_2$ ), 3.12-3.18 (sept, 4H,  $\text{CH}(\text{CH}_3)_2$ ),

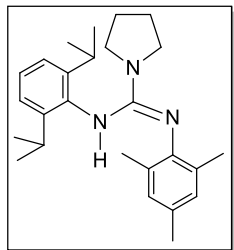
## Experimental Section



4.10 (s, 1H,  $CH(Ph)_2$ ), 5.02 (s, 1H,  $NH$ ), , 6.97-7.05 (m, 3H,  $ArH$ ), 7.10-7.16 (m, 5H,  $ArH$ ), 7.22-7.26 (m, 4H,  $ArH$ ), 7.38-7.39 (m, 4H,  $ArH$ ) ppm;  $^{13}C\{^1H\}$  NMR (100 MHz, 298K,  $CDCl_3$ ):  $\delta$  22.2, 22.9, 24.2, 25.4 ( $CH(CH_3)_2$ ), 28.4, 28.5 ( $CH(CH_3)_2$ ), 47.9 ( $NCH_2$ ), 51.6 ( $CHNCH_2$ ), 76.6 ( $NCH$ ), 122.5, 123.0, 123.7, 126.8, 127.0, 127.9, 128.6, 134.0, 139.7,

142.9, 144.4, 145.0 ( $ArC$ ), 150.7 ( $N_3C$ ) ppm. IR (KBr)  $\nu(cm^{-1})$ : 3394s ( $N-H$ ), 2960m, 2925m, 1582s, 1450m, 1423m, 1302m, 1138m, 977m, 805m, 706m. ESI-MS:  $m/z$  615.4 ( $MH^+$ ).

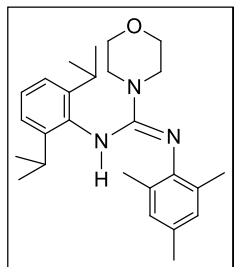
### (Z)-N'-(2,6-diisopropylphenyl)-N-(2,4,6-trimethylphenyl)pyrrolidine-1-carboximidamide



(**25c**): Yield: 99%; M.p. 120–123 °C.  $^1H$  NMR (400 MHz, 298K,  $CDCl_3$ ):  $\delta$  = 1.03-1.26 (m, 12H,  $CH(CH_3)_2$ ), 1.72 (b, 4H,  $CH_2CH_2$ ), 2.18-2.22 (br, 9H,  $o,p-CH_3$ ), 3.06 (br, 4H,  $NCH_2$ ), 3.30 (br, 2H,  $CH(CH_3)_2$ ), 5.09 (br, 1H,  $NH$ ), 6.80-7.15 (m, 5H,  $ArH$ ) ppm;  $^{13}C\{^1H\}$  NMR (100 MHz, 298K,  $CDCl_3$ ):  $\delta$

18.1, 19.0 ( $o-CH_3$ ), 20.8 ( $p-CH_3$ ), 22.4, 23.3, 24.4, 24.7 ( $CH(CH_3)_2$ ), 25.5 ( $NCH_2CH_2$ ), 28.09, 28.2 ( $CH(CH_3)_2$ ), 47.8 ( $NCH_2CH_2$ ), 122.4, 123.2, 123.4, 127.1, 129.1, 130.7, 134.4, 135.0, 141.2, 146.0 ( $Ar-C$ ), 148.2 ( $N_3C$ ) ppm. IR (KBr)  $\nu(cm^{-1})$ : 3380s ( $N-H$ ), 2960m, 2924m, 2876m, 1610m, 1584m, 1489m, 1418m, 1412m, 1231m, 1078m, 861m, 713m. ESI-MS:  $m/z$  391.9 ( $MH^+$ ).

### (Z)-N'-(2,6-diisopropylphenyl)-N-(2,4,6-trimethylphenyl)morpholine-4-carboximidamide



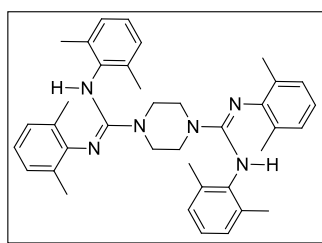
(**26c**): Yield: 93%; M.p. 131–133 °C.  $^1H$  NMR (400 MHz, 298K,  $CDCl_3$ ):  $\delta$  = 1.01-1.29 (m, 12H,  $CH(CH_3)_2$ ), 2.18-2.22 (2s, 9H,  $o-CH_3(6H)$ ,  $p-CH_3(3H)$ ), 3.09-3.10 (m, 4H,  $NCH_2$ ), 3.14-3.24 (sept, 2H,  $CH(CH_3)_2$ ), 3.51-3.54 (m, 4H,  $OCH_2$ ), 4.98, 5.10 (s, 1H,  $NH$ ), 6.81-6.87 (2s, 2H,  $ArH$ ), 6.99-

7.03 (m, 1H,  $ArH$ ), 7.08-7.17 (m, 2H,  $ArH$ ) ppm;  $^{13}C\{^1H\}$  NMR (100 MHz, 298K,  $CDCl_3$ ):  $\delta$  =

## Experimental Section

17.9, 19.1 (*o*-CH<sub>3</sub>), 20.8 (*p*-CH<sub>3</sub>), 22.5, 22.9 (CH(CH<sub>3</sub>)<sub>2</sub>), 24.3, 24.8 (CH(CH<sub>3</sub>)<sub>2</sub>), 28.1, 28.5 (CH(CH<sub>3</sub>)<sub>2</sub>), 47.9, 48.1 (NCH<sub>2</sub>), 66.5, 66.8 (OCH<sub>2</sub>), 122.9, 123.3, 123.8, 127.2, 129.2, 129.6, 131.6, 133.6, 134.1, 134.4, 135.0, 135.2, 140.0, 143.3, 143.8, 145.1 (ArC) 150.6, 152.0 (N<sub>3</sub>C) ppm. IR (KBr)  $\nu$ (cm<sup>-1</sup>): 3369s (N-H), 2963m, 2856m, 1621m, 1583m, 1486s, 1456s, 1399s, 1365s, 1231m, 1113s, 986m, 853m. ESI-MS:  $m/z$  408.59 (MH<sup>+</sup>).

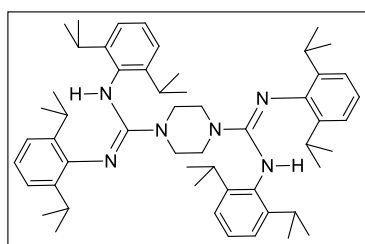
### (1*Z*,4*Z*)-*N*1,*N*'1,*N*4,*N*'4-tetrakis(2,6-dimethylphenyl)piperazine-1,4-bis(carboximidamide)



**(27c):** Yield: 90%; M.p. 246–249 °C. <sup>1</sup>H NMR (400 MHz, 298K, CDCl<sub>3</sub>):  $\delta$  = 2.2 (s, 12H, *o*-CH<sub>3</sub>), 2.24 (s, 12H, *o*-CH<sub>3</sub>), 2.94 (br, 8H, NCH<sub>2</sub>), 5.03 (s, 2H, NH), 6.83-7.05 (m, 12H, ArH) ppm; <sup>13</sup>C{<sup>1</sup>H} NMR (100 MHz, 298K, CDCl<sub>3</sub>):  $\delta$  = 18.2, 19.1 (CH<sub>3</sub>), 47.1 (NCH<sub>2</sub>),

122.5, 126.0, 128.4, 128.8, 129.7, 133.9, 137.0, 146.1 (ArC), 151.1 (N<sub>3</sub>C) ppm. IR (KBr)  $\nu$ (cm<sup>-1</sup>): 3376s (N-H), 2916s, 2848s, 1628m, 1588m, 1471m, 1395m, 1248m, 1290m, 1211m, 1085m, 989m, 778m, 767s. ESI-MS:  $m/z$  586.2 (MH<sup>+</sup>).

### (1*Z*,4*Z*)-*N*1,*N*'1,*N*4,*N*'4-tetrakis(2,6-diisopropylphenyl)piperazine-1,4-



**bis(carboximidamide) (28c):** Known compound,<sup>21</sup> Yield: 86%; M.p. 200–202 °C. <sup>1</sup>H NMR (400 MHz, 298K, CDCl<sub>3</sub>):  $\delta$  = 0.98-1.30 (m, 48H, CH(CH<sub>3</sub>)<sub>2</sub>), 2.97 (s, 8H, NCH<sub>2</sub>), 3.09-3.14 (sept, *J* = 8.0 Hz, 8H, CH(CH<sub>3</sub>)<sub>2</sub>), 5.03 (s, 2H, NH), 6.97-7.18 (m, 12H,

ArH) ppm; <sup>13</sup>C{<sup>1</sup>H} NMR (100 MHz, 298K, CDCl<sub>3</sub>):  $\delta$  = 22.5, 23.0 (CH(CH<sub>3</sub>)<sub>2</sub>), 24.2, 25.4 (CH(CH<sub>3</sub>)<sub>2</sub>), 28.4, 28.5 (CH(CH<sub>3</sub>)<sub>2</sub>), 46.9 (NCH<sub>2</sub>CH<sub>2</sub>), 122.7, 123.0, 123.9, 127.0, 133.8, 139.8, 144.1, 144.9 (ArC), 150.5 (N<sub>3</sub>C) ppm. IR (KBr)  $\nu$ (cm<sup>-1</sup>): 3391s (N-H), 2962m, 2868m, 2373m,

1623m, 1400m, 1384m, 1342m, 1326m, 1290m, 1259m, 1115m, 1084m, 990m, 758m. ESI-MS:  $m/z$  811.6 (MH<sup>+</sup>).

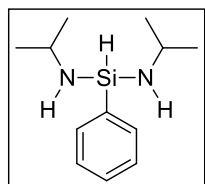
### 6B.3 General procedure for synthesis of aminosilanes from the reaction of amines with silanes catalyzed by [IMesMg(Mes)N(SiMe<sub>3</sub>)<sub>2</sub>]:

**6B.3.1 Typical procedure for the catalytic synthesis of aminosilanes:** In a glovebox, to a solution of IMesMg(Mes)N(SiMe<sub>3</sub>)<sub>2</sub> (0.05 equiv.) in 5 mL of benzene was added amines (1.2 equiv.) followed by PhSiH<sub>3</sub> (1 equiv). The mixture immediately began to effervesce. The resulting mixture was stirred at room temperature or heated at 60 °C for a fixed interval. The volatiles were removed under vacuum and the remaining residue was purified by distillation under vacuum to yield a colorless oil of the products.

**NMR scale reaction:** A sealed NMR tube is charged with IMesMg(Mes)N(SiMe<sub>3</sub>)<sub>2</sub> (0.05 equiv.), amines (1.2 equiv.) followed by PhSiH<sub>3</sub> (1 equiv) in benzene-d<sub>6</sub>. The reaction mixture was heated for fixed interval and the progress of the reaction was monitored on the basis of consumption of PhSiH<sub>3</sub> from integration of signals in the <sup>1</sup>H NMR spectra.

### 6B.3.2 Spectroscopic data for products 1d-18d:

**PhSiH(HN*i*Pr)<sub>2</sub> (1d).** Using PhSiH<sub>3</sub> (0.1g, 0.92 mmol, 1 equiv) and *i*PrNH<sub>2</sub> (0.114g, 1.94 mmol,



2.1equiv). Known compound,<sup>22</sup> colorless oil; yield: 0.155g (76%).<sup>1</sup>H NMR

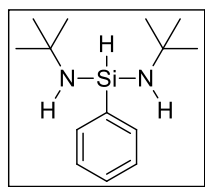
(C<sub>6</sub>D<sub>6</sub>, 400 MHz):  $\delta$  = 7.74 (m, 2H, *ortho*-C<sub>6</sub>H<sub>5</sub>), 7.26 (m, 3H, *meta*- and *para*-C<sub>6</sub>H<sub>5</sub>), 5.22 (s, 1H, SiH), 3.23 (m, <sup>3</sup>J<sub>HH</sub> = 5.6 z, 2H, CH(CH<sub>3</sub>)<sub>2</sub>), 1.03

(dd, <sup>3</sup>J<sub>HH</sub> = 8 Hz, 12 H, CH(CH<sub>3</sub>)<sub>2</sub>), 0.70 (br s, 2H, NH) ppm; <sup>13</sup>C{<sup>1</sup>H} NMR(C<sub>6</sub>D<sub>6</sub>, 100 MHz):  $\delta$  = 138.5 (*ipso*-C<sub>6</sub>H<sub>5</sub>), 134.5 (*ortho*-C<sub>6</sub>H<sub>5</sub>), 129.8 (*meta*-C<sub>6</sub>H<sub>5</sub>), 128.5 (*para*-C<sub>6</sub>H<sub>5</sub>), 43.1 (CH(CH<sub>3</sub>)<sub>2</sub>), 27.6 (CH(CH<sub>3</sub>)<sub>2</sub>) ppm; <sup>29</sup>Si NMR (C<sub>6</sub>D<sub>6</sub>, 80 MHz):  $\delta$  = -30.61 ppm.



## Experimental Section

**PhSiH(HN*t*Bu)<sub>2</sub> (2d).** Using PhSiH<sub>3</sub> (0.54g, 5 mmol, 1 equiv) and *t*BuNH<sub>2</sub> (0.914g, 12.5 mmol,

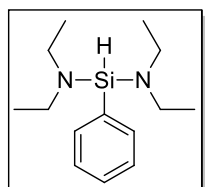


2.5 equiv). Known compound,<sup>23</sup> colorless liquid; yield: 0.975g (78%).<sup>1</sup>H

NMR (C<sub>6</sub>D<sub>6</sub>, 400 MHz):  $\delta$  = 7.78 (m, 2 H, *ortho*-C<sub>6</sub>H<sub>5</sub>), 7.26 (m, 3 H, *meta*- and *para*-C<sub>6</sub>H<sub>5</sub>), 5.47 (t, <sup>3</sup>J<sub>HH</sub> = 4 Hz, 1H, SiH), 1.18 (s, 18 H, CH<sub>3</sub>), 0.82 (b,

2H, NH) ppm; <sup>13</sup>C{<sup>1</sup>H} NMR (C<sub>6</sub>D<sub>6</sub>, 100MHz):  $\delta$  = 140.4 (*ipso*-C<sub>6</sub>H<sub>5</sub>), 134.4 (*ortho*-C<sub>6</sub>H<sub>5</sub>), 129.6 (*meta*-C<sub>6</sub>H<sub>5</sub>), 128.0 (*para*-C<sub>6</sub>H<sub>5</sub>), 49.4 (CMe<sub>3</sub>), 33.6 (CH<sub>3</sub>) ppm; <sup>29</sup>Si NMR (C<sub>6</sub>D<sub>6</sub>, 80 MHz):  $\delta$  = -37.32 ppm.

**PhSiH(NEt<sub>2</sub>)<sub>2</sub> (3d).** Using PhSiH<sub>3</sub> (0.25 g, 2.31 mmol, 1 equiv) and NHEt<sub>2</sub> (0.507 g, 6.94 mmol,

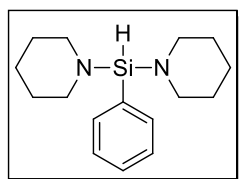


3 equiv). Known compound,<sup>23</sup> colorless liquid; yield: 0.525g (91%). <sup>1</sup>H NMR

(C<sub>6</sub>D<sub>6</sub>, 400 MHz):  $\delta$  = 7.73 (m, 2 H, *ortho*-C<sub>6</sub>H<sub>5</sub>) 7.25 (m, 3H, *meta*- and *para*-C<sub>6</sub>H<sub>5</sub>), 5.16 (s, 1H, SiH), 2.93 (q, <sup>3</sup>J<sub>HH</sub> = 8 Hz, 8H, CH<sub>2</sub>), 1.00 (t, <sup>3</sup>J<sub>HH</sub> =

8 Hz, 12H, CH<sub>3</sub>) ppm; <sup>13</sup>C{<sup>1</sup>H} NMR (C<sub>6</sub>D<sub>6</sub>, 100 MHz):  $\delta$  = 136.4 (*ipso*-C<sub>6</sub>H<sub>5</sub>), 135.2 (*ortho*-C<sub>6</sub>H<sub>5</sub>), 130.1 (*meta*-C<sub>6</sub>H<sub>5</sub>), 128.2 (*para*-C<sub>6</sub>H<sub>5</sub>), 44.4 (CH<sub>2</sub>), 27.3 (CCH<sub>3</sub>) ppm; <sup>29</sup>Si NMR (C<sub>6</sub>D<sub>6</sub>, 80 MHz):  $\delta$  = -19.28 ppm.

**PhSiH(NC<sub>5</sub>H<sub>10</sub>)<sub>2</sub> (4d).** Using PhSiH<sub>3</sub> (0.25g, 2.31 mmol, 1 equiv) and Piperidine (0.413g, 4.85

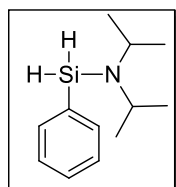


mmol, 2.1 equiv). Colorless liquid; yield: 0.57g (90%). <sup>1</sup>H NMR (C<sub>6</sub>D<sub>6</sub>,

400 MHz):  $\delta$  = 7.72 (m, 2H, *ortho*-C<sub>6</sub>H<sub>5</sub>), 7.26 (m, 3H, *meta*- and *para*-C<sub>6</sub>H<sub>5</sub>), 5.07 (s, 1H, SiH), 2.96 (m, 8H, NCH<sub>2</sub>CH<sub>2</sub>), 1.49 (m, 4H,

NCH<sub>2</sub>CH<sub>2</sub>CH<sub>2</sub>), 1.37 (m, 8H, NCH<sub>2</sub>CH<sub>2</sub>) ppm; <sup>13</sup>C{<sup>1</sup>H} NMR (C<sub>6</sub>D<sub>6</sub>, 100.64 MHz):  $\delta$  = 136.97 (*ipso*-C<sub>6</sub>H<sub>5</sub>), 135.04 (*ortho*-C<sub>6</sub>H<sub>5</sub>), 129.86 (*meta*-C<sub>6</sub>H<sub>5</sub>), 128.27 (*para*-C<sub>6</sub>H<sub>5</sub>), 46.81 (NCH<sub>2</sub>CH<sub>2</sub>), 28.09 (NCH<sub>2</sub>CH<sub>2</sub>), 25.95 (NCH<sub>2</sub>CH<sub>2</sub>CH<sub>2</sub>) ppm; <sup>29</sup>Si NMR (C<sub>6</sub>D<sub>6</sub>, 80 MHz):  $\delta$  = -19.95 ppm. IR (neat, cm<sup>-1</sup>): 3068 s, 3050 s, 2933 s, 2848 s, 2808 s, 2173, 2092 br s ( $\nu_{\text{SiH}}$ ), 1594 s, 1429 m, 1374 m, 1330 m, 1119 br m, 1059 br s, 954 s, 849 m, 736 s, 697 s, 491 m.

**PhSiH<sub>2</sub>(NiPr<sub>2</sub>) (5d).** Using PhSiH<sub>3</sub> (0.54g, 5 mmol, 1 equiv) and NiPr<sub>2</sub> (0.35g, 6 mmol, 1.2



equiv). Known compound,<sup>23</sup> colorless liquid; yield: 0.63g (77%). <sup>1</sup>H NMR

(C<sub>6</sub>D<sub>6</sub>, 400 MHz): δ = 7.68 (m, 2H, *ortho*-C<sub>6</sub>H<sub>5</sub>), 7.21 (m, 3H, *meta*- and *para*-

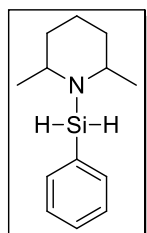
C<sub>6</sub>H<sub>5</sub>), 5.17 (s, 2H, SiH<sub>2</sub>), 3.08 (sept, <sup>3</sup>J<sub>HH</sub> = 8 Hz, 2H, CH(CH<sub>3</sub>)<sub>2</sub>), 1.05 (d, <sup>3</sup>J<sub>HH</sub>

= 4 Hz, 12H, CH(CH<sub>3</sub>)<sub>2</sub>) ppm; <sup>13</sup>C{<sup>1</sup>H} NMR (C<sub>6</sub>D<sub>6</sub>, 100 MHz): δ = 136.8 (*ipso*-C<sub>6</sub>H<sub>5</sub>), 134.9

(*ortho*-C<sub>6</sub>H<sub>5</sub>), 129.9 (*meta*-C<sub>6</sub>H<sub>5</sub>), 128.2 (*para*-C<sub>6</sub>H<sub>5</sub>), 47.6 (CH(CH<sub>3</sub>)<sub>2</sub>), 24.4 (CH(CH<sub>3</sub>)<sub>2</sub>) ppm;

<sup>29</sup>Si NMR (C<sub>6</sub>D<sub>6</sub>, 80 MHz): δ = -38.19 ppm.

**PhSiH<sub>2</sub>(NC<sub>7</sub>H<sub>14</sub>) (6d).** Using PhSiH<sub>3</sub> (0.25g, 2.31 mmol, 1 equiv) and 2,6-dimethyl Piperidine



(0.413g, 4.85 mmol, 2.1 equiv). Colorless liquid; yield: 0.41g (81%). <sup>1</sup>H NMR

(C<sub>6</sub>D<sub>6</sub>, 400 MHz): δ = 7.65 (m, 2H, *ortho*-C<sub>6</sub>H<sub>5</sub>), 7.21 (m, 3H, *meta*- and *para*-

C<sub>6</sub>H<sub>5</sub>), 5.19(s, 1H, SiH), 3.00(m, 2H, NCH), 1.65, 1.40, 1.30 (m, 4H,

CH<sub>2</sub>CH<sub>2</sub>CH<sub>2</sub>), 1.22 (d, <sup>3</sup>J<sub>HH</sub> = 8 Hz, NCH<sub>3</sub>), 1.15 (m, 2H, CH<sub>2</sub>CH<sub>2</sub>CH<sub>2</sub>) ppm;

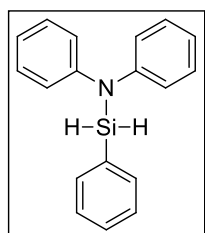
<sup>13</sup>C{<sup>1</sup>H} NMR (C<sub>6</sub>D<sub>6</sub>, 100MHz): δ = 137.7 (*ipso*-C<sub>6</sub>H<sub>5</sub>), 134.5 (*ortho*-C<sub>6</sub>H<sub>5</sub>), 129.7 (*meta*-C<sub>6</sub>H<sub>5</sub>),

128.3 (*para*-C<sub>6</sub>H<sub>5</sub>), 54.0 (NCH<sub>2</sub>CH<sub>2</sub>), 34.2 (NCH<sub>2</sub>CH<sub>2</sub>), 23.6 (CH<sub>3</sub>), 21.8 (NCH<sub>2</sub>CH<sub>2</sub>CH<sub>2</sub>) ppm;

<sup>29</sup>Si NMR (C<sub>6</sub>D<sub>6</sub>, 80 MHz): δ = -38.19 ppm. IR (neat, cm<sup>-1</sup>): 3073 s, 3051 s, 2958 s, 2929 s,

2170 br s (ν<sub>SiH</sub>), 1594 s, 1430 s, 1133 m, 1044 br, 850 s, 737 s, 697 s, 491 s.

**PhSiH<sub>2</sub>(NPh<sub>2</sub>) (7d).** Using PhSiH<sub>3</sub> (0.2g, 1.85 mmol, 1.1 equiv) and NPh<sub>2</sub> (0.284g, 1.68 mmol,



1 equiv) Colorless liquid; yield: 0.32g (63%). <sup>1</sup>H NMR (C<sub>6</sub>D<sub>6</sub>, 400 MHz): δ =

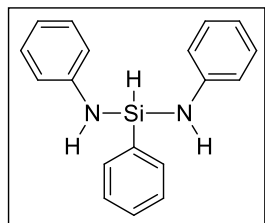
7.57 (m, 2H, *para*-C<sub>6</sub>H<sub>5</sub>), 7.11 (m, 4H, C<sub>6</sub>H<sub>5</sub>), 7.05 (m, 5H, C<sub>6</sub>H<sub>5</sub>), 6.84 (m,

4H, *ortho*-C<sub>6</sub>H<sub>5</sub>), 5.47 (s, 2H, SiH<sub>2</sub>) ppm; <sup>13</sup>C{<sup>1</sup>H} NMR (C<sub>6</sub>D<sub>6</sub>, 100 MHz): δ

= 148.8, 143.6, 134.8, 132.8, 130.5, 129.7, 129.5, 128.5, 124.0, 123.0, 121.2,

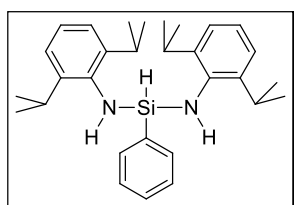
118.2 (ArC) ppm; <sup>29</sup>Si NMR (C<sub>6</sub>D<sub>6</sub>, 80 MHz): δ = -27.94 ppm.

**PhSiH(HNPh)<sub>2</sub> (8d).** Using PhSiH<sub>3</sub> (0.01g, 0.092 mmol, 1 equiv) and PhNH<sub>2</sub> (0.021g, 2.30



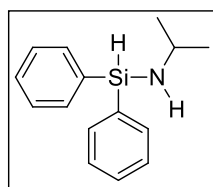
mmol, 2.5 equiv). Known compound,<sup>22</sup> <sup>1</sup>H NMR (C<sub>6</sub>D<sub>6</sub>, 400 MHz): δ = 7.59-7.62 (m, 2H, *ortho*-C<sub>6</sub>H<sub>5</sub>), 7.12-7.16 (m, 3H, *meta*- and *para*-C<sub>6</sub>H<sub>5</sub>), 7.03-7.07 (m, 4H, *meta*-C<sub>6</sub>H<sub>5</sub>), 6.72-6.77 (m, 2H, *para*-C<sub>6</sub>H<sub>5</sub>), 6.66-6.69 (m, 4H, *ortho*-C<sub>6</sub>H<sub>5</sub>), 5.61 (t, 1H, SiH), 3.44 (br, 2H, NH) ppm.

**PhSiH(HNDipp)<sub>2</sub> (9d).** Using PhSiH<sub>3</sub> (0.012g, 0.11 mmol, 1 equiv) and DippNH<sub>2</sub> (0.054g, 0.46



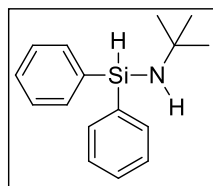
mmol, 4 equiv). Known compound,<sup>24</sup> <sup>1</sup>H NMR (C<sub>6</sub>D<sub>6</sub>, 400 MHz): δ = 7.77-7.79 (m, 2H, *ortho*-C<sub>6</sub>H<sub>5</sub>), 7.19-7.21 (m, 3 H, *meta*- and *para*-C<sub>6</sub>H<sub>5</sub>), 7.04-7.08 (m, 6H, *meta*- and *para*-C<sub>6</sub>H<sub>5</sub>), 5.67 (t, <sup>3</sup>J<sub>HH</sub> = 4.0 Hz, 1H, SiH), 3.31 (sept, <sup>3</sup>J<sub>HH</sub> = 8.0 Hz, 4H, CH(CH<sub>3</sub>)<sub>2</sub>), 3.06 (br, 2 H, NH), 1.12 (d, <sup>3</sup>J<sub>HH</sub> = 8.0 Hz, 12 H, CH<sub>3</sub>), 1.08 (d, <sup>3</sup>J<sub>HH</sub> = 8.0 Hz, 12 H, CH<sub>3</sub>) ppm.

**Ph<sub>2</sub>SiH(HN*i*Pr) (10d).** Using Ph<sub>2</sub>SiH<sub>2</sub> (0.25 g, 1.35 mmol, 1 equiv) and *i*PrNH<sub>2</sub> (0.088 g, 1.49



mmol, 1.1 equiv). Known compound,<sup>22</sup> colorless liquid; yield: 0.299g (92%). <sup>1</sup>H NMR (C<sub>6</sub>D<sub>6</sub>, 400 MHz): δ = 7.70 (m, 4H, *ortho*-C<sub>6</sub>H<sub>5</sub>), 7.21 (m, 6H, *meta*- and *para*-C<sub>6</sub>H<sub>5</sub>), 5.63 (d, 1H, SiH), 3.05 (*pseudo*-sextet, 1H, (CH(CH<sub>3</sub>)<sub>2</sub>), 0.98 (d, <sup>3</sup>J<sub>HH</sub> = 4 Hz, 6H, (CH(CH<sub>3</sub>)<sub>2</sub>), 0.66 (br s, 1H, NH) ppm; <sup>13</sup>C{<sup>1</sup>H} NMR (C<sub>6</sub>D<sub>6</sub>, 100 MHz): δ = 136.4 (*ipso*-C<sub>6</sub>H<sub>5</sub>), 135.2 (*ortho*-C<sub>6</sub>H<sub>5</sub>), 130.1 (*meta*-C<sub>6</sub>H<sub>5</sub>), 128.2 (*para*-C<sub>6</sub>H<sub>5</sub>), 44.4 (CH(CH<sub>3</sub>)<sub>2</sub>), 27.3 (CH(CH<sub>3</sub>)<sub>2</sub>) ppm; <sup>29</sup>Si NMR(C<sub>6</sub>D<sub>6</sub>, 80 MHz): δ = -20.26 ppm.

**Ph<sub>2</sub>SiH(HN*t*Bu) (11d).** Using Ph<sub>2</sub>SiH<sub>2</sub> (0.25g, 1.5 mmol, 1 equiv) and *t*BuNH<sub>2</sub> (0.128g, 1.76

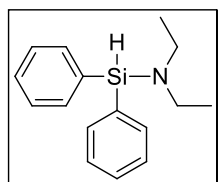


mmol, 1.3 equiv). Known compound,<sup>22</sup> colorless liquid; yield: 0.32g (96%). <sup>1</sup>H NMR (C<sub>6</sub>D<sub>6</sub>, 400 MHz): δ = 7.70 (m, 4 H, *ortho*-C<sub>6</sub>H<sub>5</sub>), 7.20 (m, 6H, *meta*- and *para*-C<sub>6</sub>H<sub>5</sub>), 5.72 (d, <sup>3</sup>J<sub>HH</sub> = 4 Hz, 1H, SiH), 1.12 (s, 9H, C(CH<sub>3</sub>)<sub>3</sub>,

## Experimental Section

0.94 (br, s, 1H, NH) ppm;  $^{13}\text{C}\{^1\text{H}\}$  NMR ( $\text{C}_6\text{D}_6$ , 100 MHz):  $\delta = 137.3$  (*ipso*- $\text{C}_6\text{H}_5$ ), 135.1 (*ortho*- $\text{C}_6\text{H}_5$ ), 129.9 (*meta*- $\text{C}_6\text{H}_5$ ), 128.2 (*para*- $\text{C}_6\text{H}_5$ ), 49.6 ( $\text{C}(\text{CH}_3)_3$ ), 33.3 ( $\text{C}(\text{CH}_3)_3$ ) ppm;  $^{29}\text{Si}$  NMR ( $\text{C}_6\text{D}_6$ , 80 MHz):  $\delta = -20.88$  ppm.

**$\text{Ph}_2\text{SiH}(\text{NEt}_2)$  (12d).** Using  $\text{Ph}_2\text{SiH}_2$  (0.25 g, 1.35 mmol, 1 equiv) and  $\text{NEt}_2$  (0.119 g, 1.62

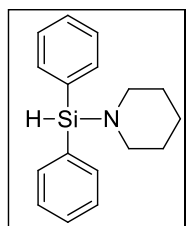


mmol, 1.2 equiv). Known compound,<sup>24</sup> colorless liquid; yield: 0.325g (94%).

$^1\text{H}$  NMR ( $\text{C}_6\text{D}_6$ , 400 MHz):  $\delta = 7.67$ -7.68 (m, 4 H, *ortho*- $\text{C}_6\text{H}_5$ ), 7.21 (m, 6H, *meta*- and *para*- $\text{C}_6\text{H}_5$ ), 5.60 (s, 1H, SiH), 2.90 (q,  $^3J_{\text{HH}} = 8$  Hz Hz, 4H,  $\text{CH}_2$ ),

0.95 (t,  $^3J_{\text{HH}} = 8$  Hz, 6H,  $\text{CH}_3$ ) ppm;  $^{13}\text{C}\{^1\text{H}\}$  NMR ( $\text{C}_6\text{D}_6$ , 100 MHz):  $\delta = 136.1$  (*ipso*- $\text{C}_6\text{H}_5$ ), 135.5 (*ortho*- $\text{C}_6\text{H}_5$ ), 130.0 (*meta*- $\text{C}_6\text{H}_5$ ), 128.3 (*para*- $\text{C}_6\text{H}_5$ ), 41.3 ( $\text{CH}_2$ ), 15.5 ( $\text{CH}_3$ ) ppm;  $^{29}\text{Si}$  NMR ( $\text{C}_6\text{D}_6$ , 80 MHz):  $\delta = -14.08$  ppm.

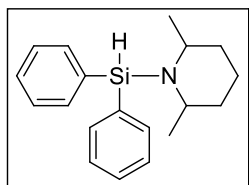
**$\text{Ph}_2\text{SiH}(\text{NC}_5\text{H}_{10})$  (13d).** Using  $\text{Ph}_2\text{SiH}_2$  (0.20g, 1.08 mmol, 1 equiv) and Piperidine (0.194g, 2.27



mmol, 2.1 equiv). Colorless liquid; yield: 0.25g (87%).  $^1\text{H}$  NMR ( $\text{C}_6\text{D}_6$ , 400

MHz): 7.69 (m, 4H, *ortho*- $\text{C}_6\text{H}_5$ ), 7.22 (m, 6H, *meta*- and *para*- $\text{C}_6\text{H}_5$ ), 5.55 (s, 1H, SiH), 2.92 (m, 4H,  $\text{NCH}_2\text{CH}_2$ ), 1.42 (m, 2H,  $\text{NCH}_2\text{CH}_2\text{CH}_2$ ), 1.32 (m, 4H,  $\text{NCH}_2\text{CH}_2$ ) ppm;  $^{13}\text{C}\{^1\text{H}\}$  NMR ( $\text{C}_6\text{D}_6$ , 100 MHz):  $\delta = 135.7$  (*ipso*- $\text{C}_6\text{H}_5$ ),

135.5 (*ortho*- $\text{C}_6\text{H}_5$ ), 130.0 (*meta*- $\text{C}_6\text{H}_5$ ), 128.3 (*para*- $\text{C}_6\text{H}_5$ ), 47.7 ( $\text{NCH}_2\text{CH}_2\text{CH}_2$ ), 27.9 ( $\text{NCH}_2\text{CH}_2\text{CH}_2$ ), 25.5 ( $\text{NCH}_2\text{CH}_2\text{CH}_2$ ) ppm;  $^{29}\text{Si}$  NMR ( $\text{C}_6\text{D}_6$ , 80 MHz):  $\delta = -13.84$  ppm. IR (neat,  $\text{cm}^{-1}$ ): 3070 s, 3049 s, 2934 s, 2852 s, 2134 br s ( $\nu_{\text{SiH}}$ ), 1591 s, 1429 s, 1119 br s, 1068 br m, 1035 s, 1014 s, 994 s, 822 s, 734 s, 717 s, 698 s, 514 s, 489 s.



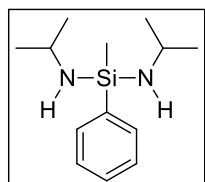
**$\text{Ph}_2\text{SiH}(\text{NC}_7\text{H}_{14})$  (14d).** Using  $\text{Ph}_2\text{SiH}_2$  (0.012g, 0.067 mmol, 1 equiv) and

2,6-dimethyl Piperidine (0.008g, 0.074 mmol, 1.1 equiv).  $^1\text{H}$  NMR ( $\text{C}_6\text{D}_6$ , 400 MHz):  $\delta = 7.73$ -7.75 (m, 2H, *ortho*- $\text{C}_6\text{H}_5$ ), 7.50-7.52 (m, 2H, *ortho*-

## Experimental Section

C<sub>6</sub>H<sub>5</sub>), 7.23 (m, 6H, *meta*- and *para*-C<sub>6</sub>H<sub>5</sub>), 5.08 (s, 1H, SiH), 2.44 (m, 2H, NCH), 1.67, 1.56, 1.43 (m, 4H, CH<sub>2</sub>CH<sub>2</sub>CH<sub>2</sub>), 1.29 (m, 2H, CH<sub>2</sub>CH<sub>2</sub>CH<sub>2</sub>), 1.15 (d, <sup>3</sup>J<sub>HH</sub> = 8.0 Hz, NCH<sub>3</sub>), 0.97 (d, <sup>3</sup>J<sub>HH</sub> = 8.0 Hz, NCH<sub>3</sub>) ppm.

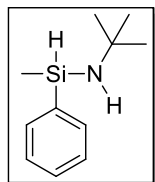
**PhMeSi(HN*i*Pr)<sub>2</sub> (15d).** Using PhMeSiH<sub>2</sub> (0.25 g, 2.03 mmol, 1 equiv) and *i*PrNH<sub>2</sub> (0.30g, 5.07



mmol, 2.5 equiv). Colorless liquid; yield: 0.202g (42%). <sup>1</sup>H NMR (C<sub>6</sub>D<sub>6</sub>, 400 MHz): δ = 7.72 (m, 2H, *ortho*-C<sub>6</sub>H<sub>5</sub>), 7.27 (m, 3H, *meta*- and *para*-C<sub>6</sub>H<sub>5</sub>), 3.16 (pseudo sept, 2H, CH(CH<sub>3</sub>)<sub>2</sub>), 1.03 (dd, <sup>3</sup>J<sub>HH</sub> = 4, 8 Hz, 12H, CH(CH<sub>3</sub>)<sub>2</sub>),

0.57 (br s, 2H, NH), 0.31 (s, 3H, SiCH<sub>3</sub>) ppm; <sup>13</sup>C{<sup>1</sup>H} NMR (C<sub>6</sub>D<sub>6</sub>, 100 MHz): δ = 140.5 (*ipso*-C<sub>6</sub>H<sub>5</sub>), 134.3 (*ortho*-C<sub>6</sub>H<sub>5</sub>), 129.3 (*meta*-C<sub>6</sub>H<sub>5</sub>), 127.9 (*para*-C<sub>6</sub>H<sub>5</sub>), 42.7 (CH(CH<sub>3</sub>)<sub>2</sub>), 28.14, 27.9 (CH(CH<sub>3</sub>)<sub>2</sub>), -1.3 (SiCH<sub>3</sub>) ppm; <sup>29</sup>Si NMR (C<sub>6</sub>D<sub>6</sub>, 80MHz): δ = -20.15 ppm.

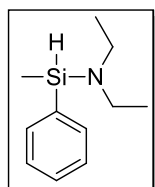
**PhMeSiH(HN*t*Bu) (16d).** Using PhMeSiH<sub>2</sub> (0.20 g, 1.62 mmol, 1 equiv) and *t*BuNH<sub>2</sub> (0.154 g,



2.11 mmol, 1.3 equiv). Known compound,<sup>22</sup> colorless liquid; yield: 0.274g (88%). <sup>1</sup>H NMR (C<sub>6</sub>D<sub>6</sub>, 400 MHz): δ = 7.65 (m, 2 H, *ortho*-C<sub>6</sub>H<sub>5</sub>), 7.23 (m, 3H, *meta*- and *para*-C<sub>6</sub>H<sub>5</sub>), 5.22 (m, 1H, SiH), 1.08 (s, 9H, C(CH<sub>3</sub>)<sub>3</sub>), 0.64 (br s, 2H,

NH), 0.30 (d, 3H, SiCH<sub>3</sub>) ppm; <sup>13</sup>C{<sup>1</sup>H} NMR (C<sub>6</sub>D<sub>6</sub>, 100 MHz): δ = 139.8 (*ipso*-C<sub>6</sub>H<sub>5</sub>), 134.3 (*ortho*-C<sub>6</sub>H<sub>5</sub>), 129.6 (*meta*-C<sub>6</sub>H<sub>5</sub>), 128.1 (*para*-C<sub>6</sub>H<sub>5</sub>), 49.4 (C(CH<sub>3</sub>)<sub>2</sub>), 33.3, (C(CH<sub>3</sub>)<sub>3</sub>), -0.9 (SiCH<sub>3</sub>) ppm; <sup>29</sup>Si NMR (C<sub>6</sub>D<sub>6</sub>, 80MHz): δ = -20.81 ppm.

**PhMeSi(H)NEt<sub>2</sub> (17d).** Using PhMeSiH<sub>2</sub> (0.25 g, 2.03 mmol, 1 equiv) and NEt<sub>2</sub> (0.178 g, 2.44



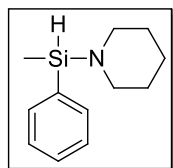
mmol, 1.2 equiv). Known compound,<sup>24</sup> colorless liquid; yield: 0.33g (84%). <sup>1</sup>H NMR (C<sub>6</sub>D<sub>6</sub>, 400 MHz): δ = 7.62 (m, 2H, *ortho*-C<sub>6</sub>H<sub>5</sub>), 7.23 (m, 3H, *meta* and *para*-C<sub>6</sub>H<sub>5</sub>), 5.12 (q, <sup>3</sup>J<sub>HH</sub> = 4 Hz, 1H, SiH), 2.81 (q, <sup>3</sup>J<sub>HH</sub> = 8 Hz, 4H, CH<sub>2</sub>), 0.94

(t, <sup>3</sup>J<sub>HH</sub> = 8 Hz, 6H, CH<sub>3</sub>), 0.35 (d, <sup>3</sup>J<sub>HH</sub> = 4 Hz, 3H, SiCH<sub>3</sub>) ppm; <sup>13</sup>C{<sup>1</sup>H} NMR (C<sub>6</sub>D<sub>6</sub>, 100

## Experimental Section

MHz):  $\delta = 138.5$  (*ipso*-C<sub>6</sub>H<sub>5</sub>), 134.5 (*ortho*-C<sub>6</sub>H<sub>5</sub>), 129.7 (*meta*-C<sub>6</sub>H<sub>5</sub>), 128.2 (*para*-C<sub>6</sub>H<sub>5</sub>), 41.4 (CH<sub>2</sub>), 15.8 (CH<sub>3</sub>), -2.8 (SiCH<sub>3</sub>) ppm; <sup>29</sup>Si NMR (C<sub>6</sub>D<sub>6</sub>, 80 MHz):  $\delta = -11.17$  ppm.

**PhMeSiH(NC<sub>5</sub>H<sub>10</sub>) (18d).** Using PhMeSiH<sub>2</sub> (0.20 g, 1.62 mmol, 1 equiv) and NHEt<sub>2</sub> (0.152 g,



1.77 mmol, 1.1 equiv). Colorless liquid; yield: 0.272g (82%). <sup>1</sup>H NMR (C<sub>6</sub>D<sub>6</sub>,

400 MHz):  $\delta = 7.61$  (m, 4H, *ortho*-C<sub>6</sub>H<sub>5</sub>), 7.24 (m, 6H, *meta*- and *para*-C<sub>6</sub>H<sub>5</sub>),

5.07 (q, <sup>3</sup>J<sub>HH</sub> = 4 Hz, 1H, SiH), 2.84 (m, 4H, NCH<sub>2</sub>CH<sub>2</sub>), 1.43 (m, 2H,

NCH<sub>2</sub>CH<sub>2</sub>CH<sub>2</sub>), 1.31 (m, 4H, NCH<sub>2</sub>CH<sub>2</sub>), 0.33 (d, <sup>3</sup>J<sub>HH</sub> = 4 Hz, 3H, SiCH<sub>3</sub>) ppm; <sup>13</sup>C{<sup>1</sup>H} NMR

(C<sub>6</sub>D<sub>6</sub>, 100 MHz):  $\delta = 138.0$  (*ipso*-C<sub>6</sub>H<sub>5</sub>), 134.5 (*ortho*-C<sub>6</sub>H<sub>5</sub>), 129.7 (*meta*-C<sub>6</sub>H<sub>5</sub>), 128.2 (*para*-

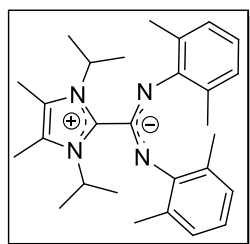
C<sub>6</sub>H<sub>5</sub>), 47.5 (NCH<sub>2</sub>CH<sub>2</sub>CH<sub>2</sub>), 27.9 (NCH<sub>2</sub>CH<sub>2</sub>CH<sub>2</sub>), 25.6 (NCH<sub>2</sub>CH<sub>2</sub>CH<sub>2</sub>), -3.4 (SiCH<sub>3</sub>) ppm;

<sup>29</sup>Si NMR (C<sub>6</sub>D<sub>6</sub>, 80 MHz):  $\delta = -10.66$  ppm. IR (neat, cm<sup>-1</sup>): 3070 s, 3051 s, 3011 s, 2960 s,

2131 br s ( $\nu_{\text{SiH}}$ ), 1428 s, 1254 s, 1121 s, 1063 br s, 881 s, 844 s, 722 s, 699 s, 470 s.

## 6B.4 Synthetic procedure and characterization of NHC-CDI adducts (1e-31e).

**[1,3-diisopropyl-4,5-dimethylimidazolium-2-{N,N'-bis(2,6-dimethylphenyl)amidinate}](1e):**



In the glovebox, 1,3-diisopropyl-4,5-dimethylimidazol-2-ylidene (144 mg,

0.8 mmol, 1 equiv.) and 1,3-di-(2,6-dimethylphenyl) carbodiimide (200

mg, 0.8 mmol, 1 equiv.) are mixed together in a Schlenk tube. The reaction

tube is then connected to the Schlenk line and added toluene (5 mL). The

reaction mixture is stirred at room temperature for 1 h. The crude reaction mixture is dried under

high vacuum and washed with anhydrous hexane (2 × 5 mL) and dried under high *vacuo*. The

white solid is recrystallized from hexane/dichloromethane (1:1) mixture to get colorless crystals

that are suitable for X-ray diffraction studies. Finally, isolated desired compound **1e**, yield: 306

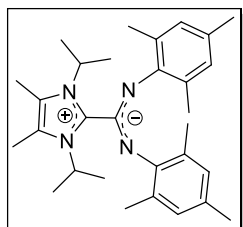
mg (89%); M.p. 163–167 °C. <sup>1</sup>H NMR (400 MHz, CDCl<sub>3</sub>)  $\delta = 6.59$  (d, *J* = 8.0 Hz, 4H, *m*-ArH),

## Experimental Section

6.44 (m, 2H, *p*-ArH), 5.89 (br, 2H, CH(CH<sub>3</sub>)<sub>2</sub>), 2.33(s, 6H, imidazole CH<sub>3</sub>), 2.15(s, 6H, CH<sub>3</sub>Ar), 1.68 (d, *J* = 8.0 Hz, 12H, CH(CH<sub>3</sub>)<sub>2</sub>) ppm; <sup>13</sup>C{<sup>1</sup>H} NMR (101 MHz, CDCl<sub>3</sub>) δ = 148.2 (NCN), 140.4, 128.7, 126.7, 123.6, 119.6, 51.1, 21.7, 19.9, 10.3 ppm. HRMS (ESI) *m/z*: calcd for C<sub>28</sub>H<sub>38</sub>N<sub>4</sub> [M + H]<sup>+</sup>, 431.3169; found 431.3195.

**Note:** All compounds (**2e-31e**) were synthesized by using a similar procedure to that employed for the preparation **1e** and using appropriate NHC and *N,N'*-diaryl CDI precursors.

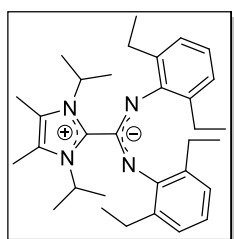
### [1,3-diisopropyl-4,5-dimethylimidazolium-2-{*N,N'*-bis(2,4,6-trimethylphenyl)amidinate}]



**(2e):** White solid; yield: 89%; M.p. 162–164 °C. <sup>1</sup>H NMR (400 MHz, CDCl<sub>3</sub>) δ = 6.39 (s, 4H, *m*-ArH), 5.79 (br, 2H, CH(CH<sub>3</sub>)<sub>2</sub>), 2.31 (s, 6H, imidazole CH<sub>3</sub>), 2.10 (s, 12H, *o*-CH<sub>3</sub>), 2.06 (s, 6H, *p*-CH<sub>3</sub>), 1.65 (d, *J* = 8.0 Hz, 12H, CH(CH<sub>3</sub>)<sub>2</sub>) ppm; <sup>13</sup>C{<sup>1</sup>H} NMR (101 MHz, CDCl<sub>3</sub>) δ = 145.1

(NCN), 140.9, 128.4, 127.4, 123.8, 121.5, 51.3, 21.6, 20.5, 19.7, 10.3 ppm. HRMS (ESI) *m/z*: calcd. for C<sub>30</sub>H<sub>42</sub>N<sub>4</sub> [M + H]<sup>+</sup>, 459.3482; found 459.3546.

### [1,3-diisopropyl-4,5-dimethylimidazolium-2-{*N,N'*-bis(2,6-diethylphenyl)amidinate}] (**3e**):



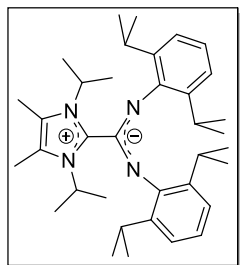
Off white solid; yield: 90%; M.p. 142–145 °C. <sup>1</sup>H NMR (400 MHz, CDCl<sub>3</sub>) δ = 6.55 (m, 6H, *m,p*-ArH), 5.83 (sept, 2H, CH(CH<sub>3</sub>)<sub>2</sub>), 2.71 (m, 4H, CH<sub>2</sub>CH<sub>3</sub>), 2.39 (m, 4H, CH<sub>2</sub>CH<sub>3</sub>), 2.35 (s, 6H, , imidazole CH<sub>3</sub>), 1.68 (d, *J* = 8.0 Hz, 12H, CH(CH<sub>3</sub>)<sub>2</sub>), 1.07 (t, *J* = 8.0 Hz, 4 Hz, 12H, CH<sub>2</sub>CH<sub>3</sub>) ppm;

<sup>13</sup>C{<sup>1</sup>H} NMR (101 MHz, CDCl<sub>3</sub>) δ = 148.2 (NCN), 147.4, 140.2, 134.4, 123.5, 123.4, 119.7, 51.3, 25.3, 21.7, 14.1, 10.3 ppm. HRMS (ESI) *m/z*: calcd. for C<sub>32</sub>H<sub>46</sub>N<sub>4</sub> [M + H]<sup>+</sup>, 487.3795; found 487.3762.

### [1,3-diisopropyl-4,5-dimethylimidazolium-2-{*N,N'*-bis(2,6-diisopropylphenyl)amidinate}]

**(4e):** light yellow solid; yield: 95%; M.p. 155–158 °C. <sup>1</sup>H NMR (400 MHz, CDCl<sub>3</sub>) δ = 6.92 (d, *J*

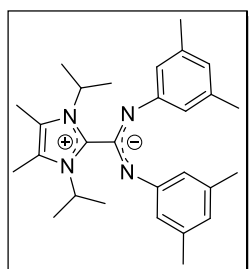
## Experimental Section



= 8.0 Hz, 4H, *m*-ArH), 6.75 (t,  $J = 8.0$  Hz, 2H, *p*-ArH), 5.45 (m, 2H, CH(CH<sub>3</sub>)<sub>2</sub>), 3.21 (m, 2H, CH(CH<sub>3</sub>)<sub>2</sub>), 2.29 (s, 6H, imidazoleCH<sub>3</sub>), 1.36 (d,  $J = 8.0$  Hz, 12H, CH(CH<sub>3</sub>)<sub>2</sub>), 1.03 (s, 24H, CH(CH<sub>3</sub>)<sub>2</sub>) ppm; <sup>13</sup>C{<sup>1</sup>H} NMR (101 MHz, CDCl<sub>3</sub>)  $\delta = 148.3$ (NCN), 146.9, 139.7, 124.1, 122.0, 119.3,

51.6, 28.9, 23.5, 23.1, 21.1, 10.5 ppm. HRMS (ESI)  $m/z$ : calcd. for C<sub>36</sub>H<sub>54</sub>N<sub>4</sub> [M + H]<sup>+</sup>, 543.4421; found 543.4428.

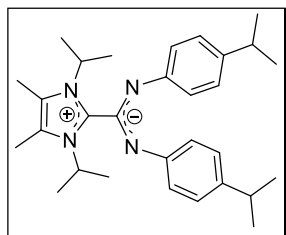
### [1,3-diisopropyl-4,5-dimethylimidazolium-2-]{*N,N'*-bis(3,5-dimethylphenyl)amidinate}]



(**5e**): Yellow solid; yield: 89%; M.p. 172–175 °C. <sup>1</sup>H NMR (400 MHz, CDCl<sub>3</sub>)  $\delta = 6.72$  (br, 4H, *o*-ArH), 6.43 (s, 2H, *p*-ArH), 5.01 (m, 2H, CH(CH<sub>3</sub>)<sub>2</sub>), 2.25 (s, 6H, imidazole CH<sub>3</sub>), 2.16 (s, 12H, *o*-CH<sub>3</sub>), 1.49 (d,  $J = 8.0$  Hz, 12H, CH(CH<sub>3</sub>)<sub>2</sub>) ppm; <sup>13</sup>C{<sup>1</sup>H} NMR (101 MHz, CDCl<sub>3</sub>)  $\delta =$

147.7(NCN), 138.3, 137.4, 127.0, 125.2, 118.9, 117.8, 53.1, 21.3, 21.2, 10.4 ppm. HRMS (ESI)  $m/z$ : calcd. for C<sub>28</sub>H<sub>38</sub>N<sub>4</sub> [M + H]<sup>+</sup>, 431.3169; found 431.3200.

### [1,3-diisopropyl-4,5-dimethylimidazolium-2-]{*N,N'*-bis(4-isopropylphenyl)amidinate}] (**6e**):



Light yellow solid; yield: 94 %; M.p. 155–160 °C. <sup>1</sup>H NMR (400 MHz, CDCl<sub>3</sub>)  $\delta = 7.15$ – $7.26$  (m, 4H, ArH), 7.00 (d,  $J = 4.0$  Hz, 4H, ArH), 4.91 (br, 2H, CH(CH<sub>3</sub>)<sub>2</sub>), 2.78 (sept,  $J = 8.0$  Hz, 4.0 Hz, 2H, CH(CH<sub>3</sub>)<sub>2</sub>), 2.27 (s, 6H, imidazole CH<sub>3</sub>), 1.44 (br, 12H, CH(CH<sub>3</sub>)<sub>2</sub>),

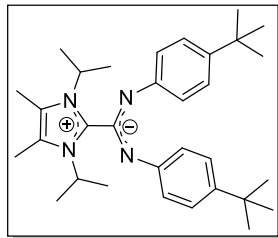
1.17 (d,  $J = 4.0$  Hz, 12H, CH(CH<sub>3</sub>)<sub>2</sub>) ppm; <sup>13</sup>C{<sup>1</sup>H} NMR (101 MHz, CDCl<sub>3</sub>)  $\delta = 141.8$  (NCN), 137.9, 129.1, 128.3, 126.4, 125.3, 121.7, 52.3, 33.57, 24.3, 21.1, 10.4 ppm. HRMS (ESI)  $m/z$ : calcd. for C<sub>30</sub>H<sub>42</sub>N<sub>4</sub> [M + H]<sup>+</sup>, 459.3482; found 459.3479.

### [1,3-diisopropyl-4,5-dimethylimidazolium-2-]{*N,N'*-bis(4-*t*-butylphenyl)amidinate}] (**7e**):

light yellow solid; yield 90 %; Mp: 195–200 °C. <sup>1</sup>H NMR (400 MHz, CDCl<sub>3</sub>)  $\delta = 7.10$  (m, 8H,

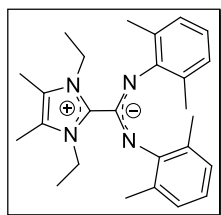


## Experimental Section



ArH), 5.06 (m, 2H,  $CH(CH_3)_2$ ), 2.25 (s, 6H, imidazole  $CH_3$ ), 1.39 (br, 12H,  $CH(CH_3)_2$ ), 1.24 (s, 18H,  $C(CH_3)_3$ ) ppm;  $^{13}C\{^1H\}$  NMR (101 MHz,  $CDCl_3$ )  $\delta$  = 149.4 (NCN), 142.4, 125.0, 121.9, 51.7, 34.1, 31.6, 21.2, 10.3 ppm. HRMS (ESI)  $m/z$ : calcd. for  $C_{32}H_{46}N_4$   $[M + H]^+$ , 487.3795; found 487.3766.

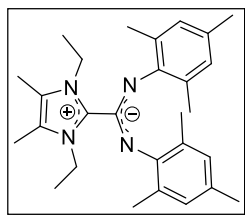
### [1,3-diethyl-4,5-dimethylimidazolium-2-]{*N,N'*-bis(2,6-dimethylphenyl)amidinate}] (8e):



white solid; yield: 85%; M.p. 155–159 °C.  $^1H$  NMR (400 MHz,  $CDCl_3$ )  $\delta$  = 6.62 (d,  $J$  = 8.0 Hz, 4H, *m*-ArH), 6.48 (t,  $J$  = 8.0 Hz, 2H, *p*-ArH), 4.54 (q,  $J$  = 8.0 Hz, 4 Hz, 4H), 2.22 (s, 6H, imidazole  $CH_3$ ), 2.16 (s, 12H, *o*- $CH_3$ ), 1.53 (t,  $J$  = 8.0 Hz, 6H) ppm;  $^{13}C\{^1H\}$  NMR (101 MHz,  $CDCl_3$ )  $\delta$  = 147.4 (NCN),

139.9, 129.1, 126.9, 123.5, 120.2, 41.3, 20.0, 15.7, 8.6 ppm. HRMS (ESI)  $m/z$ : calcd. for  $C_{26}H_{34}N_4$   $[M + H]^+$ , 403.2856; found 403.2856.

### [1,3-diethyl-4,5-dimethylimidazolium-2-]{*N,N'*-bis(2,4,6-trimethylphenyl)amidinate}] (9e):



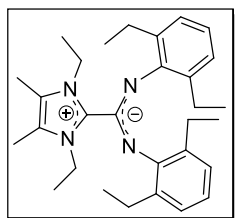
White solid; yield: 81%; M.p. 160–164 °C.  $^1H$  NMR (400 MHz,  $CDCl_3$ )  $\delta$  = 6.42 (s, 4H, *m*-ArH), 4.48 (br, 4H,  $CH_2CH_3$ ), 2.19 (s, 6H, imidazole  $CH_3$ ), 2.11 (s, 12H, *o*- $CH_3$ ), 2.06 (s, 6H, *p*- $CH_3$ ), 1.50 (m, 6H,  $CH_2CH_3$ ) ppm;  $^{13}C\{^1H\}$  NMR (101 MHz,  $CDCl_3$ )  $\delta$  = 145.2(NCN), 144.0, 140.2,

129.5, 128.9, 127.5, 123.8, 41.4, 20.5, 19.8, 15.5, 8.5 ppm. HRMS (ESI)  $m/z$ : calcd. for  $C_{28}H_{38}N_4$   $[M + H]^+$ , 431.3169; found 431.3196.

### [1,3-diethyl-4,5-dimethylimidazolium-2-]{*N,N'*-bis(2,6-diethylphenyl)amidinate}] (10e):

Yellow solid; yield: 91%; M.p. 173–178 °C.  $^1H$  NMR (400 MHz,  $CDCl_3$ )  $\delta$  = 6.52–6.60 (m, 6H, *m,p*-ArH), 4.62 (q, 6H,  $J$  = 8.0 Hz, ArH), 2.72 (br, 4H,  $CH_2CH_3$ ), 2.43 (br, 4H,  $CH_2CH_3$ ), 2.23

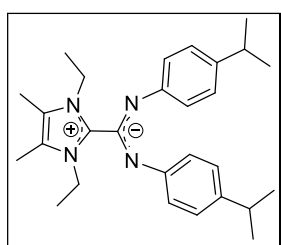
## Experimental Section



(s, 6H, imidazole  $CH_3$ ), 1.58 (t,  $J = 8.0, 4.0$  Hz, 6H,  $CH_2CH_3$ ), 1.07 (t,  $J = 8.0$  Hz, 12H,  $CH_2CH_3$ ) ppm;  $^{13}C\{^1H\}$  NMR (101 MHz,  $CDCl_3$ )  $\delta = 146.9$ (NCN), 139.8, 134.4, 123.6, 123.0, 119.9, 41.4, 25.2, 15.7, 14.2, 8.5 ppm. HRMS (ESI)  $m/z$ : calcd. for  $C_{30}H_{42}N_4$   $[M + H]^+$ , 459.3482; found

459.3519.

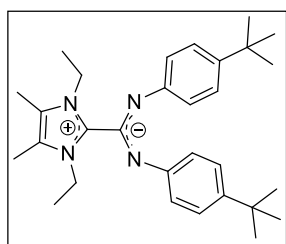
### [1,3-diethyl-4,5-dimethylimidazolium-2-ylidene- $\{N,N'$ -bis(4-isopropylphenyl)amidinate}] (11e):



Yellow solid; yield: 80%; M.p. 166–169 °C.  $^1H$  NMR (400 MHz,  $CDCl_3$ )  $\delta = 6.86$  (m, 8H,  $o,m$ -ArH), 4.23 (q,  $J = 8.0, 4.0$  Hz, 4H,  $CH_2CH_3$ ), 2.72 (sept,  $J = 8.0, 4.0$  Hz, 2H,  $CH(CH_3)_2$ ), 2.19 (s, 6H, imidazole  $CH_3$ ), 1.39 (t,  $J = 8.0$  Hz, 6H,  $CH_2CH_3$ ), 1.14 (d,  $J = 8.0$  Hz,

12H,  $CH(CH_3)_2$ ) ppm;  $^{13}C\{^1H\}$  NMR (101 MHz,  $CDCl_3$ )  $\delta = 140.2$  (NCN), 129.1, 128.3, 125.9, 123.9, 123.0, 121.6, 41.5, 33.5, 24.3, 14.9, 8.6 ppm. HRMS (ESI)  $m/z$ : calcd. for  $C_{28}H_{38}N_4$   $[M + H]^+$ , 431.3169; found 431.3167.

### [1,3-diethyl-4,5-dimethylimidazolium-2-ylidene- $\{N,N'$ -bis(4-*t*-butylphenyl)amidinate}] (12e):



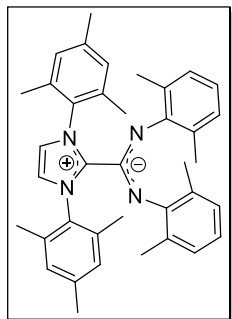
Light yellow solid; yield: 84%; M.p. 155–158 °C.  $^1H$  NMR (400 MHz,  $CDCl_3$ )  $\delta = 7.01$  (d,  $J = 8.0$  Hz, 4H, ArH), 6.82 (br, 4H, ArH), 4.24 (q,  $J = 8.0$  Hz, 4H, ArH), 2.18 (s, 6H, imidazole  $CH_3$ ), 1.38 (t,  $J = 8.0$  Hz, 6H,  $CH_2CH_3$ ), 1.21 (s, 18H,  $C(CH_3)_3$ ) ppm;  $^{13}C\{^1H\}$  NMR (101 MHz,

$CDCl_3$ )  $\delta = 148.2$  (NCN), 142.2, 126.1, 124.7, 123.7, 121.2, 115.0, 41.4, 34.0, 31.6, 14.9, 8.6 ppm. HRMS (ESI)  $m/z$ : calcd. for  $C_{30}H_{42}N_4$ ,  $[M + H]^+$ , 459.3482; found 459.3496.

### [1,3-bis(2,4,6-trimethylphenyl)imidazolium-2-ylidene- $\{N,N'$ -bis(2,6-dimethylphenyl)amidinate}]

(13e): White solid; yield: 92%; M.p. 172–176 °C.  $^1H$  NMR (400 MHz,  $CDCl_3$ )  $\delta = 7.05$ (s, 2H,

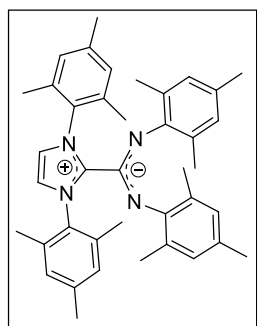
## Experimental Section



imidazole *CH*), 6.97 (s, 4H, *m*-ArH), 6.31 (d, 4H,  $J = 8.0$  Hz, *m*-ArH), 6.22 (t, 2H, *p*-ArH), 2.40 (s, 12H, *o*-CH<sub>3</sub>), 2.32 (s, 6H, *p*-CH<sub>3</sub>), 1.46 (s, 12H, *o*-CH<sub>3</sub>) ppm; <sup>13</sup>C{<sup>1</sup>H} NMR (101 MHz, CDCl<sub>3</sub>)  $\delta = 149.2$  (NCN), 148.9, 140.2, 137.1, 136.2, 132.7, 129.28, 128.4, 125.92, 120.2, 118.1, 21.2, 19.2, 18.4 ppm HRMS (ESI)  $m/z$ : calcd. for C<sub>38</sub>H<sub>42</sub>N<sub>4</sub> [M + H]<sup>+</sup>, 555.3482; found

555.3499.

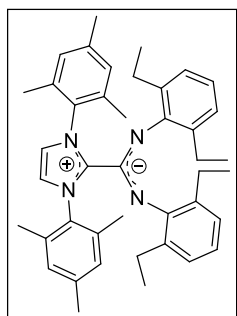
### [1,3-bis(2,4,6-trimethylphenyl)imidazolium-2-ylidenebis(2,4,6-trimethylphenyl)amidine]



(**14e**): Light yellow solid; yield: 88%; M.p. 186–189 °C. <sup>1</sup>H NMR (400 MHz, CDCl<sub>3</sub>)  $\delta = 7.04$  (br, 2H, imidazole *CH*), 6.95 (s, 4H, *m*-ArH), 6.10 (s, 4H, *m*-ArH), 2.39 (s, 12H, *o*-CH<sub>3</sub>), 2.32 (s, 6H, *p*-CH<sub>3</sub>), 1.92 (s, 6H, *p*-CH<sub>3</sub>), 1.42 (s, 12H, *o*-CH<sub>3</sub>) ppm; <sup>13</sup>C{<sup>1</sup>H} NMR (101 MHz, CDCl<sub>3</sub>)  $\delta = 149.4$  (NCN), 146.5, 140.1, 137.6, 136.3, 132.8, 129.4, 129.2, 127.9, 126.9,

126.4, 119.9, 21.2, 20.4, 19.0, 18.4 ppm. HRMS (ESI)  $m/z$ : calcd. for C<sub>40</sub>H<sub>46</sub>N<sub>4</sub> [M + H]<sup>+</sup>, 583.3795; found 583.3834.

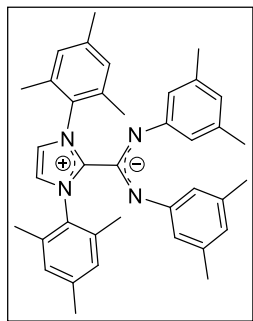
### [1,3-bis(2,4,6-trimethylphenyl)imidazolium-2-ylidenebis(2,6-diethylphenyl)amidine]



(**15e**): Off white solid; yield: 92%; M.p. 185–190 °C. <sup>1</sup>H NMR (400 MHz, CDCl<sub>3</sub>)  $\delta = 7.04$  (s, 6H, imidazole *CH*(2H), *m*-ArH(4H)), 6.33 (s, 6H, *m,p*-ArH), 2.42 (s, 12H, *o*-CH<sub>3</sub>), 2.39 (s, 6H, *p*-CH<sub>3</sub>), 1.87 (m, 4H, CH<sub>2</sub>CH<sub>3</sub>), 1.77 (m, 4H, CH<sub>2</sub>CH<sub>3</sub>), 0.77 (t, 12H,  $J = 8.0$  Hz, CH<sub>2</sub>CH<sub>3</sub>) ppm; <sup>13</sup>C{<sup>1</sup>H} NMR (101 MHz, CDCl<sub>3</sub>)  $\delta = 149.3$  (NCN), 147.9, 140.3, 137.2, 136.4,

133.5, 132.6, 129.2, 122.6, 120.1, 118.4, 23.8, 21.2, 18.4, 13.6 ppm. HRMS (ESI)  $m/z$ : calcd. for C<sub>42</sub>H<sub>50</sub>N<sub>4</sub> [M + H]<sup>+</sup>, 611.4108; found 611.4086.

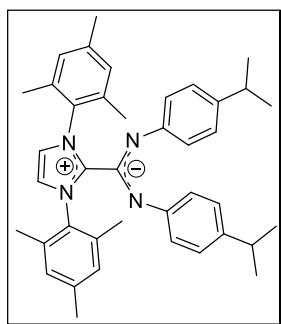
**[1,3-bis(2,4,6-trimethylphenyl)imidazolium-2- $\{N,N'$ -bis(3,5-dimethylphenyl) amidinate}]**



**(16e):** White solid; yield: 86%; M.p. 200–206 °C.  $^1\text{H}$  NMR (400 MHz,  $\text{CDCl}_3$ )  $\delta$  = 7.07 (s, 2H, imidazole *CH*), 7.03 (s, 4H, *m*-ArH), 5.97 (s, 2H, *p*-ArH), 5.57 (s, 4H, *m*-ArH), 2.39 (s, 6H, *p*- $\text{CH}_3$ ), 2.35 (s, 12H, *o*- $\text{CH}_3$ ), 1.87 (s, 12H, *p*- $\text{CH}_3$ ) ppm;  $^{13}\text{C}\{^1\text{H}\}$  NMR (101 MHz,  $\text{CDCl}_3$ )  $\delta$  = 152.2 (NCN), 149.1, 141.9, 139.8, 135.9, 135.7, 132.4, 129.0, 120.1, 120.0,

119.3, 21.2, 21.0, 18.1 ppm. HRMS (ESI)  $m/z$ : calcd. for  $\text{C}_{38}\text{H}_{42}\text{N}_4$   $[\text{M} + \text{H}]^+$ , 555.3482; found 555.3512.

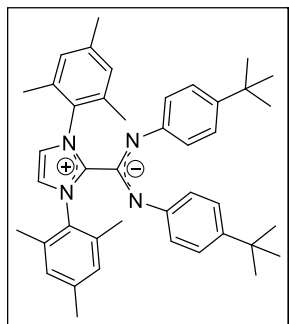
**[1,3-bis(2,4,6-trimethylphenyl)imidazolium-2- $\{N,N'$ -bis(4-isopropylphenyl)amidinate}]**



**(17e):** Yellow solid; yield: 84%; M.p. 195–200 °C.  $^1\text{H}$  NMR (400 MHz,  $\text{CDCl}_3$ )  $\delta$  = 7.05 (s, 2H, imidazole *CH*), 7.03 (s, 4H, ArH), 6.48 (d,  $J$  = 8.0 Hz, 4H, ArH), 5.86 (d,  $J$  = 8.0 Hz, 4H, ArH), 2.55 (sept,  $J$  = 8.0, 4.0 Hz, 2H,  $\text{CH}(\text{CH}_3)_2$ ), 2.41 (s, 6H, *p*- $\text{CH}_3$ ), 2.32 (s, 12H, *o*- $\text{CH}_3$ ), 1.03 (d,  $J$  = 8.0 Hz, 12H,  $\text{CH}(\text{CH}_3)_2$ ) ppm;  $^{13}\text{C}\{^1\text{H}\}$  NMR (101 MHz,  $\text{CDCl}_3$ )  $\delta$

= 150.1 (NCN), 149.5, 141.3, 139.8, 137.8, 135.9, 132.8, 128.9, 124.5, 120.9, 119.9, 33.3, 24.4, 21.3, 18.1 ppm. HRMS (ESI)  $m/z$ : calcd. for  $\text{C}_{40}\text{H}_{46}\text{N}_4$   $[\text{M} + \text{H}]^+$ , 583.3795; found 583.3759.

**[1,3-bis(2,4,6-trimethylphenyl)imidazolium-2- $\{N,N'$ -bis(4-*t*-butylphenyl)amidinate}] (18e):**

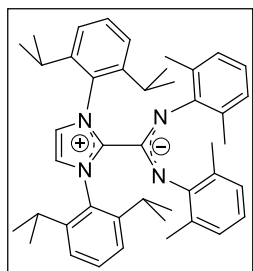


Orange solid; yield: 96%; M.p. 194–198 °C.  $^1\text{H}$  NMR (400 MHz,  $\text{CDCl}_3$ )  $\delta$  = 7.05 (s, 2H, imidazole *CH*), 7.03 (s, 4H, *m*-ArH), 6.65 (d,  $J$  = 8.0 Hz, 4H, ArH), 5.87 (d,  $J$  = 8.0 Hz, 4H, ArH), 2.41 (s, 6H, *o*- $\text{CH}_3$ ), 2.30 (s, 12H, *p*- $\text{CH}_3$ ), 1.09 (s, 18H,  $\text{C}(\text{CH}_3)_3$ ) ppm;  $^{13}\text{C}\{^1\text{H}\}$  NMR (101 MHz,  $\text{CDCl}_3$ )  $\delta$  = 149.6 (NCN), 141.2, 139.9, 139.8, 135.9, 132.9,

## Experimental Section

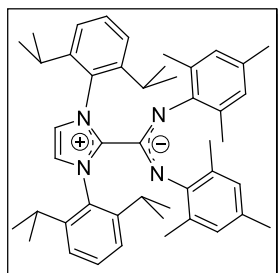
128.9, 123.4, 120.6, 119.9, 33.7, 31.7, 21.3, 18.1 ppm. HRMS (ESI)  $m/z$ : calcd. for  $C_{42}H_{50}N_4$  [ $M + H$ ]<sup>+</sup>, 611.4108; found 611.4131.

### [1,3-bis(2,6-diisopropylphenyl)imidazolium-2- $\{N,N'$ -bis(2,6-dimethylphenyl)amidinate}]



**(19e)**: Off white solid; yield: 84%; M.p. 225–228 °C. <sup>1</sup>H NMR (400 MHz, CDCl<sub>3</sub>)  $\delta$  = 7.38 (t,  $J$  = 8.0 Hz, 2H,  $p$ -ArH), 7.23 (d,  $J$  = 8.0 Hz, 4H,  $m$ -ArH), 7.08 (s, 2H, imidazole CH), 6.28 (d,  $J$  = 4.0 Hz, 4H,  $m$ -ArH), 6.17 (t,  $J$  = 8.0, 4.0 Hz, 2H,  $p$ -ArH), 3.17 (sept,  $J$  = 8.0, 4.0 Hz, 4H, CH(CH<sub>3</sub>)<sub>2</sub>), 1.51 (s, 12H,  $o$ -CH<sub>3</sub>), 1.47 (s, 12H,  $o$ -CH<sub>3</sub>), 1.30 (d,  $J$  = 4.0 Hz, CH(CH<sub>3</sub>)<sub>2</sub>), 1.19 (d,  $J$  = 8.0 Hz, CH(CH<sub>3</sub>)<sub>2</sub>) ppm; <sup>13</sup>C{<sup>1</sup>H} NMR (101 MHz, CDCl<sub>3</sub>)  $\delta$  = 149.9 (NCN), 148.4, 145.9, 137.0, 133.9, 130.4, 127.7, 125.6, 124.1, 122.0, 117.7, 29.4, 25.6, 22.8, 19.2 ppm. HRMS (ESI)  $m/z$ : calcd. for  $C_{44}H_{54}N_4$  [ $M + H$ ]<sup>+</sup>, 639.4421; found 639.4443.

### [1,3-bis(2,6-diisopropylphenyl)imidazolium-2- $\{N,N'$ -bis(2,4,6-trimethylphenyl)amidinate}]

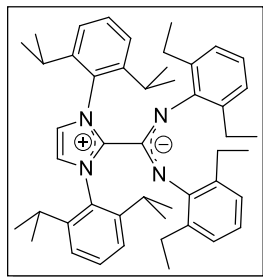


**(20e)**: Yellow solid; yield: 83%; M.p. 187–190 °C. <sup>1</sup>H NMR (400 MHz, CDCl<sub>3</sub>)  $\delta$  = 7.55 (t,  $J$  = 8.0 Hz, 2H,  $p$ -ArH), 7.40–7.43 (m, 6H, imidazole CH(2H),  $m$ -ArH(4H)), 6.25 (s, 4H,  $m$ -ArH), 3.36 (m, 4H, CH(CH<sub>3</sub>)<sub>2</sub>), 2.09 (s, 6H,  $p$ -CH<sub>3</sub>), 1.65 (s, 12H,  $o$ -CH<sub>3</sub>), 1.50 (d,  $J$  = 8.0 Hz, 12H, CH(CH<sub>3</sub>)<sub>2</sub>), 1.38 (d,  $J$  = 8.0 Hz, 12H, CH(CH<sub>3</sub>)<sub>2</sub>) ppm; <sup>13</sup>C{<sup>1</sup>H} NMR (101 MHz, CDCl<sub>3</sub>)  $\delta$  = 150.0 (NCN), 146.2, 145.8, 137.6, 133.9, 130.3, 127.2, 126.5, 126.1, 124.0, 29.4, 25.5, 22.8, 20.4, 19.1 ppm. HRMS (ESI)  $m/z$ : calcd. for  $C_{46}H_{58}N_4$  [ $M + H$ ]<sup>+</sup>, 667.4734; found 667.4738.

### [1,3-bis(2,6-diisopropylphenyl)imidazolium-2- $\{N,N'$ -bis(2,6-diethylphenyl)amidinate}]

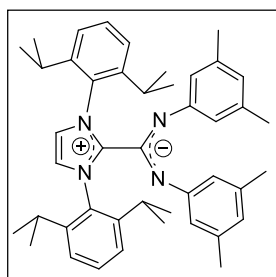
**(21e)**: Light yellow solid; yield: 81%; M.p. 173–176 °C. <sup>1</sup>H NMR (400 MHz, CDCl<sub>3</sub>)  $\delta$  = 7.62 (t,  $J$  = 8.0 Hz, 2H), 7.52–7.46 (m, 6H, imidazole CH(2H), ArH(4H)), 6.51 (br, 6H, ArH), 3.37 (sept,

## Experimental Section



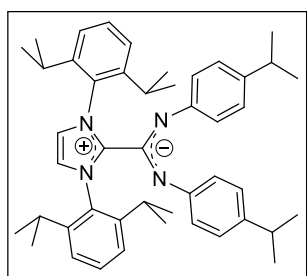
4H,  $\text{CH}(\text{CH}_3)_2$ ), 2.12 (m, 4H,  $\text{CH}_2\text{CH}_3$ ), 1.99 (m, 4H, m, 4H,  $\text{CH}_2\text{CH}_3$ ), 1.54 (d,  $J = 4.0$  Hz, 12H,  $\text{CH}(\text{CH}_3)_2$ ), 1.42 (d,  $J = 8.0$  Hz, 12H), 0.92 (t,  $J = 8.0$  Hz, 12H) ppm;  $^{13}\text{C}\{^1\text{H}\}$  NMR (101 MHz,  $\text{CDCl}_3$ )  $\delta = 150.0$  (NCN), 147.6, 145.5, 137.4, 134.5, 133.0, 130.4, 124.2, 122.3, 122.0, 118.2, 29.5, 25.6, 23.5, 23.0, 13.6 ppm. HRMS (ESI)  $m/z$ : calcd. for  $\text{C}_{48}\text{H}_{62}\text{N}_4$   $[\text{M} + \text{H}]^+$ , 695.5047; found 695.5044.

### [1,3-bis(2,6-diisopropylphenyl)imidazolium-2- $\{N,N'$ -bis(3,5-dimethylphenyl)amidinate}]



**(22e)**: Light yellow solid; yield: 89%; M.p. 182–184 °C.  $^1\text{H}$  NMR (400 MHz,  $\text{CDCl}_3$ )  $\delta = 7.48$  (t,  $J = 8.0$  Hz, 2H,  $p$ -ArH), 7.30 (d,  $J = 8.0$  Hz, 4H,  $m$ -ArH), 7.10 (s, 2H, imidazole CH), 5.89 (s, 2H,  $p$ -ArH), 5.44 (s, 4H,  $m$ -ArH), 2.92 (sept,  $J = 8.0, 4.0$  Hz, 4H,  $\text{CH}(\text{CH}_3)_2$ ), 1.80 (s, 12H,  $o$ -CH<sub>3</sub>), 1.35 (d,  $J = 8.0$  Hz, 12H,  $\text{CH}(\text{CH}_3)_2$ ), 1.22 (d,  $J = 8.0$  Hz, 12H,  $\text{CH}(\text{CH}_3)_2$ ) ppm;  $^{13}\text{C}\{^1\text{H}\}$  NMR (101 MHz,  $\text{CDCl}_3$ )  $\delta = 152.3$  (NCN), 150.8, 145.8, 141.3, 139.4, 135.2, 132.9, 130.3, 128.4, 127.4, 123.9, 122.0, 121.1, 119.1, 118.9, 29.4, 25.2, 23.2, 21.1 ppm. HRMS (ESI)  $m/z$ : calcd. for  $\text{C}_{44}\text{H}_{54}\text{N}_4$   $[\text{M} + \text{H}]^+$ , 639.4421; found 639.4450.

### [1,3-bis(2,6-diisopropylphenyl)imidazolium-2- $\{N,N'$ -bis(4-isopropylphenyl)amidinate}]

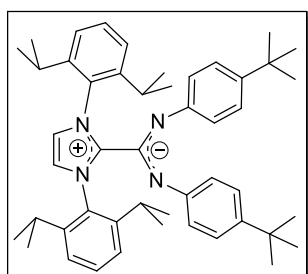


**(23e)**: Yellow solid; yield: 81%; M.p. 188–190 °C.  $^1\text{H}$  NMR (400 MHz,  $\text{CDCl}_3$ )  $\delta = 7.49$  (t,  $J = 8.0$  Hz, 4 Hz, 2H,  $p$ -ArH), 7.30 (dd,  $J = 8.0$  Hz, 4 Hz, 4H,  $m$ -ArH), 7.11 (s, 2H, imidazole CH), 6.38 (d,  $J = 8.0$  Hz, 4H, ArH), 5.69 (d,  $J = 8.0$  Hz, 4H, ArH), 2.90 (sept, 4H,  $\text{CH}(\text{CH}_3)_2$ ), 2.52 (sept, 4H,  $\text{CH}(\text{CH}_3)_2$ ), 1.32 (d,  $J = 4.0$  Hz, 12H,  $\text{CH}(\text{CH}_3)_2$ ), 1.22, 1.21, 1.02, 1.00. 6.38 (d,  $J = 6.6$  Hz, 2H), 5.69 (d,  $J = 6.3$  Hz, 2H), 2.90 (td,  $J = 12.3, 6.7$  Hz, 2H), 2.52 (sept,  $J = 6.9$  Hz, 1H), 1.32 (d,  $J = 5.3$  Hz, 6H), 1.22 (d,  $J = 5.8$  Hz, 6H), 1.01 (d,  $J = 6.9$  Hz, 6H)

## Experimental Section

ppm;  $^{13}\text{C}\{^1\text{H}\}$  NMR (101 MHz,  $\text{CDCl}_3$ )  $\delta = 150.9$  (NCN), 149.8, 145.7, 140.5, 137.2, 133.2, 130.2, 124.0, 123.8, 121.0, 120.7, 33.2, 29.4, 25.2, 24.4, 23.2 ppm. HRMS (ESI)  $m/z$ : calcd. for  $\text{C}_{46}\text{H}_{58}\text{N}_4$   $[\text{M} + \text{H}]^+$ , 667.4734; found 667.4740.

### [1,3-bis(2,6-diisopropylphenyl)imidazolium-2- $\{N,N'$ -bis(4-



tbtylphenyl)amidinate}] (24e): Yellow solid; yield: 93%; M.p.

208–210 °C.  $^1\text{H}$  NMR (400 MHz,  $\text{CDCl}_3$ )  $\delta = 7.49$  (t,  $J = 8.0$  Hz, 2H,  $p$ -ArH), 7.31 (d,  $J = 8.0$  Hz, 4H,  $m$ -ArH), 7.10 (s, 2H, imidazole CH),

6.54 (d,  $J = 8.0$  Hz, 4H, ArH), 5.70 (d,  $J = 8.0$  Hz, 2H, ArH), 2.89

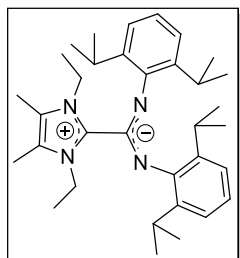
(sept,  $J = 8.0$  Hz, 4.0 Hz, 2H), 1.31 (d,  $J = 4.0$  Hz, 12H,  $\text{CH}(\text{CH}_3)_2$ ), 1.21 (d,  $J = 8.0$  Hz, 12H,

$\text{CH}(\text{CH}_3)_2$ ), 1.07 (s, 18H,  $\text{C}(\text{CH}_3)_3$ ) ppm;  $^{13}\text{C}\{^1\text{H}\}$  NMR (101 MHz,  $\text{CDCl}_3$ )  $\delta = 150.9$  (NCN),

149.2, 145.7, 140.3, 139.4, 133.3, 130.2, 123.8, 122.9, 121.0, 120.5, 33.7, 31.7, 29.4, 25.2, 23.2

ppm. HRMS (ESI)  $m/z$ : calcd. for  $\text{C}_{48}\text{H}_{62}\text{N}_4$   $[\text{M} + \text{H}]^+$ , 695.5047; found 695.5056.

### [1,3-diethylimidazolium-4,5-dimethyl-2- $\{N,N'$ -(2,6-diisopropylphenyl)amidinate}] (25e):



Light yellow solid; yield: 71%; M.p. 186–190 °C.  $^1\text{H}$  NMR (400 MHz,

$\text{CDCl}_3$ )  $\delta = 6.96$  (d,  $J = 8.0$  Hz, 4H,  $m$ -ArH), 6.79 (t,  $J = 8.0, 4.0$  Hz, 2H,  $p$ -

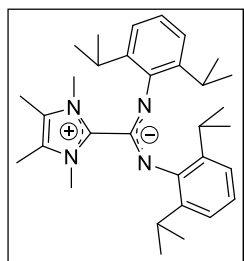
ArH), 4.12 (m, 4H,  $\text{CH}_2\text{CH}_3$ ), 3.34 (m, 2H,  $\text{CH}(\text{CH}_3)_2$ ), 2.14 (s, 6H,

imidazole  $\text{CH}_3$ ), 1.38 (t,  $J = 8.0, 4.0$  Hz, 6H,  $\text{CH}_2\text{CH}_3$ ), 1.08 (s, 24H,

$\text{CH}(\text{CH}_3)_2$ );  $^{13}\text{C}\{^1\text{H}\}$  NMR (101 MHz,  $\text{CDCl}_3$ )  $\delta = 148.8$  (NCN), 146.4, 141.2, 139.8, 123.5,

122.0, 119.1, 41.4, 28.6, 23.7, 14.9, 8.7 ppm. ESI-MS for  $\text{C}_{36}\text{H}_{54}\text{N}_4$ ,  $[\text{M} + \text{H}]^+$ ,  $m/z = 514.40$ .

### [1,3-dimethylimidazolium-4,5-dimethyl-2- $\{N,N'$ -(2,6-diisopropylphenyl)amidinate}] (26e):



Light yellow solid; yield: 77%; M.p. 156 – 160 °C.  $^1\text{H}$  NMR (400 MHz,

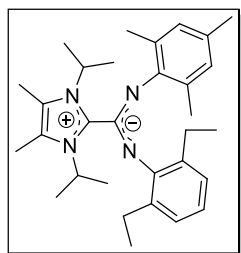
$\text{CDCl}_3$ )  $\delta = 6.84$ – $6.97$  (m, 6H, ArH), 3.64 (s, 6H, imidazole  $\text{NCH}_3$ ), 3.36

(m, 2H,  $\text{CH}(\text{CH}_3)_2$ ), 2.10 (s, 6H, imidazole  $\text{CCH}_3$ ), 1.08 (br, 24H,

## Experimental Section

$\text{CH}(\text{CH}_3)_2$ );  $^{13}\text{C}\{^1\text{H}\}$  NMR (101 MHz,  $\text{CDCl}_3$ )  $\delta$  = 141.0, 129.0, 128.2, 123.2, 122.7, 122.4, 33.2, 33.0, 28.8, 28.6, 23.9, 23.2, 8.8, 8.7. ESI-MS for  $\text{C}_{36}\text{H}_{54}\text{N}_4$ ,  $[\text{M} + \text{H}]^+$ ,  $m/z$  = 486.37.

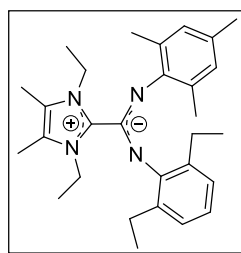
**[1,3-diisopropyl-4,5-dimethylimidazolium-2- $\{N$ -2,6-diethylphenyl- $N'$ -(2,4,6-trimethylphenyl)amidinate}] (27e):** White solid; yield: 82%; M.p. 140–145 °C.  $^1\text{H}$  NMR (400 MHz,



$\text{CDCl}_3$ )  $\delta$  =  $^1\text{H}$  NMR (400 MHz,  $\text{CDCl}_3$ )  $\delta$  = 6.64 (m, 3H,  $m,p$ -ArH), 6.40 (s, 2H,  $m$ -ArH), 5.59 (br, 2H,  $\text{CH}(\text{CH}_3)_2$ ), 2.66 (m, 2H,  $\text{CH}_2\text{CH}_3$ ), 2.43 (m, 2H,  $\text{CH}_2\text{CH}_3$ ), 2.35 (s, 6H, imidazole  $\text{CH}_3$ ), 2.06 (s, 6H,  $o$ - $\text{CH}_3$ ), 2.05 (s, 3H,  $p$ - $\text{CH}_3$ ), 1.65 (d,  $J$  = 4.0 Hz, 12H,  $\text{CH}(\text{CH}_3)_2$ ), 1.08 (t,  $J$  = 8.0 Hz, 6H,

$\text{CH}_2\text{CH}_3$ ) ppm;  $^{13}\text{C}\{^1\text{H}\}$  NMR (101 MHz,  $\text{CDCl}_3$ )  $\delta$  = 140.7 (NCN), 134.5, 128.8, 128.4, 127.4, 127.2, 126.0, 125.6, 123.7, 119.8, 51.3, 25.4, 21.7, 20.5, 19.7, 14.2, 10.3 ppm. HRMS (ESI)  $m/z$ : calcd. for  $\text{C}_{31}\text{H}_{44}\text{N}_4$   $[\text{M} + \text{H}]^+$ , 473.3639; found 473.3605.

**[1,3-diethyl-4,5-dimethylimidazolium-2- $\{N$ -2,6-diethylphenyl- $N'$ -(2,4,6-trimethylphenyl)amidinate}] (28e):** Off white solid; yield: 91%; M.p. 150–155 °C.  $^1\text{H}$  NMR



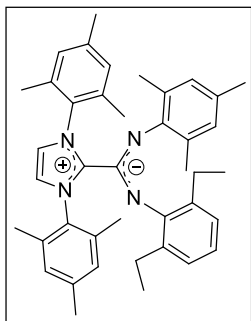
(400 MHz,  $\text{CDCl}_3$ )  $\delta$  = 6.66–6.50 (m, 3H,  $m,p$ -ArH), 6.36 (s, 2H,  $m$ -ArH), 4.56 (q, 4H,  $J$  = 8.0 Hz), 2.71 (br, 2H,  $\text{CH}_2\text{CH}_3$ ), 2.49 (br, 2H,  $\text{CH}_2\text{CH}_3$ ), 2.21 (s, 6H, imidazole  $\text{CH}_3$ ), 2.08 (s, 6H,  $o$ - $\text{CH}_3$ ), 2.03 (s, 3H,  $p$ - $\text{CH}_3$ ), 1.55 (t,  $J$  = 8.0 Hz, 4.0 Hz, 6H), 1.08 (t,  $J$  = 8.0 Hz, 6H) ppm;  $^{13}\text{C}\{^1\text{H}\}$  NMR (101

MHz,  $\text{CDCl}_3$ )  $\delta$  = 146.4 (NCN), 140.2, 134.6, 128.5, 127.4, 123.7, 123.2, 119.9, 77.4, 77.3, 77.1, 76.7, 41.2, 25.2, 20.4, 19.8, 15.6, 14.2, 8.5 ppm. HRMS (ESI)  $m/z$ : calcd. for  $\text{C}_{29}\text{H}_{40}\text{N}_4$   $[\text{M} + \text{H}]^+$ , 445.3326; found 445.3327.

**[1,3-bis(2,4,6-trimethylphenyl)imidazolium-2- $\{N$ -2,6-diethylphenyl- $N'$ -(2,4,6-trimethylphenyl)amidinate}] (29e):** White solid; yield: 83%; M.p. 195–201 °C.  $^1\text{H}$  NMR (400 MHz,



## Experimental Section

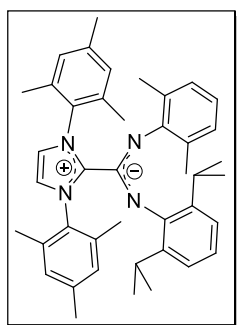


$\text{CDCl}_3$   $\delta$  = 7.04 (s, 2H, imidazole CH), 6.98 (s, 4H, ArH), 6.33 (s, 3H, *m,p*-ArH), 6.06 (s, 2H, *m*-ArH), 2.40 (s, 12H, *o*-CH<sub>3</sub>), 2.34 (s, 6H, *p*-CH<sub>3</sub>), 1.89 (s, 3H, *p*-CH<sub>3</sub>), 1.80 (m, 4H, CH<sub>2</sub>CH<sub>3</sub>), 1.38 (s, 6H, *p*-CH<sub>3</sub>), 0.76 (t, *J* = 8.0 Hz, 6H, CH<sub>2</sub>CH<sub>3</sub>) ppm; <sup>13</sup>C{<sup>1</sup>H} NMR (101 MHz, CDCl<sub>3</sub>)  $\delta$  = 148.4 (NCN), 146.9, 145.6, 139.2, 136.5, 135.4, 132.7,

131.7, 128.2, 126.8, 126.0, 125.6, 121.5, 119.1, 117.1, 22.9, 20.2, 19.4, 17.9, 17.4, 12.6 ppm.

HRMS (ESI) *m/z*: calcd. for C<sub>41</sub>H<sub>48</sub>N<sub>4</sub> [M + H]<sup>+</sup>, 597.3952; found 597.3925.

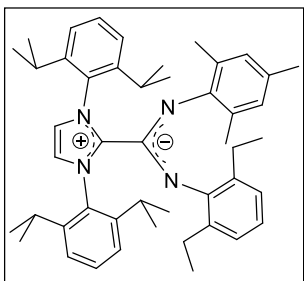
**[1,3-bis(2,4,6-trimethylphenyl)imidazolium-2-{N-2,6-diisopropylphenyl-N'-2,6-dimethylphenyl}amidinate]] (30e):** Off white solid; yield: 91%; M.p. 152–156 °C. <sup>1</sup>H NMR (400 MHz,



$\text{CDCl}_3$ )  $\delta$  = 7.02 (s, 4H, *m*-ArH), 7.00 (s, 2H, imidazole CH), 6.40 (s, 3H, *m,p*-ArH), 6.31 (d, *J* = 4.0 Hz, 2H, *m*-ArH), 6.21 (t, *J* = 8.0 Hz, 1H, *p*-ArH), 2.63 (sept, *J* = 8.0, 4.0 Hz, 2H, CH(CH<sub>3</sub>)<sub>2</sub>), 2.41 (s, 12H, *o*-CH<sub>3</sub>), 2.38 (s, 6H, *p*-CH<sub>3</sub>), 1.45 (s, 6H, *o*-CH<sub>3</sub>), 0.81 (d, *J* = 4.0 Hz, 6H, CH(CH<sub>3</sub>)<sub>2</sub>), 0.61 (d, *J* = 8.0 Hz, 6H, CH(CH<sub>3</sub>)<sub>2</sub>) ppm; <sup>13</sup>C{<sup>1</sup>H} NMR (101 MHz, CDCl<sub>3</sub>)  $\delta$  =

149.4 (NCN), 149.2, 146.3, 140.1, 139.4, 136.6, 136.2, 133.0, 129.3, 128.1, 126.2, 120.4, 119.6, 119.1, 117.9, 27.8, 26.0, 21.2, 20.7, 19.5, 18.5 ppm. HRMS (ESI) *m/z*: calcd. for C<sub>44</sub>H<sub>54</sub>N<sub>4</sub> [M + H]<sup>+</sup>, 639.4421; found 639.4450.

**[1,3-bis(2,6-diisopropylphenyl)imidazolium-2-{N-2,6-diethylphenyl-N'-2,4,6-trimethylphenyl}amidinate]] (31e):** Orange solid; yield: 85%; M.p. 167–171 °C. <sup>1</sup>H NMR (400 MHz,



$\text{CDCl}_3$ )  $\delta$  = 7.41 (t, *J* = 8.0 Hz, 2H, *p*-ArH), 7.27 (d, *J* = 8.0 Hz, 4H, *m*-ArH), 7.08 (s, 2H, imidazole CH), 6.33 (br, 3H, *m,p*-ArH), 6.05 (s, 2H, *m*-ArH), 3.18 (sept, *J* = 8.0, 4.0 Hz, 4H, CH(CH<sub>3</sub>)<sub>2</sub>), 2.06–1.97(m, 2H, CH<sub>2</sub>CH<sub>3</sub>), 1.91 (s, 3H, *p*-CH<sub>3</sub>), 1.87–1.80 (m, 1H), 1.41

## Experimental Section

(s,6H, *o*-CH<sub>3</sub>), 1.32 (d, *J* = 8.0 Hz, 12H, CH(CH<sub>3</sub>)<sub>2</sub>), 1.23 (d, *J* = 8.0 Hz, 12H, CH(CH<sub>3</sub>)<sub>2</sub>), 0.75 (t, *J* = 8.0 Hz, 6H, CH<sub>2</sub>CH<sub>3</sub>) ppm; <sup>13</sup>C{<sup>1</sup>H} NMR (101 MHz, CDCl<sub>3</sub>) δ = 150.0 (NCN), 147.5, 146.2, 145.72, 137.6, 134.3, 133.1, 130.3, 126.9, 126.5, 126.2, 124.1, 122.1, 122.0, 117.9, 29.4, 25.6, 23.5, 22.9, 20.5, 19.0, 13.6 ppm. HRMS (ESI) *m/z*: calcd. for C<sub>47</sub>H<sub>60</sub>N<sub>4</sub> [M + H]<sup>+</sup>, 681.4891; found 681.4890.

## References:

- (1) SAINT+, Bruker AXS Inc., Madison, Wisconsin, USA, **1999** (Program for Reduction of Data collected on Bruker CCD Area Detector Diffractometer V. 6.02).
- (2) SADABS, Bruker AXS, Madison, Wisconsin, USA, **2004**.
- (3) Sheldrick, G. M., *Acta Crystallogr. Sect. A* **2008**, *64*, 112-122.
- (4) Kuhn, N.; Kratz, T. *Synthesis*, **1993**, *6*, 561-562.
- (5) Raynaud, J.; Liu, N.; Gnanou, Y.; Taton, D. *Macromolecules*, **2010**, *43*, 8853-8861.
- (6) Bantreil, X.; Nolan, S. P. *Nat. Protocols*, **2011**, *6*, 69-77.
- (7) Westerhausen, M.; Schwarz, W. Z. *Anorg. Allg. Chem.*, **1992**, *609*, 39-44.
- (8) Chai, J.-D.; Head-Gordon, M. *Phys. Chem. Chem. Phys.*, **2008**, *10*, 6615-6620.
- (9) (a) Lee, C.; Yang, W.; Parr, R. G. *Phys. Rev. B*, **1988**, *37*, 785-789; (b) Becke, A. D. *J. Chem. Phys.*, **1993**, *98*, 5648-5652.
- (10) (a) Perdew, J. P. *Phys. Rev. B*, **1986**, *33*, 8822-8824; (b) Becke, A. D. *Phys. Rev. A*, **1988**, *38*, 3098-3100.
- (11) Weigend, F.; Ahlrichs, R. *Phys. Chem. Chem. Phys.*, **2005**, *7*, 3297-3305.
- (12) Shen, H.; Chan, H.-S.; Xie, Z. *Organometallics*, **2006**, *25*, 5515-5517.

*Experimental Section*

- (13) Zhou, S.; Wang, S.; Yang, G.; Li, Q.; Zhang, L.; Yao, Z.; Zhou, Z.; Song, H.-b. *Organometallics*, **2007**, *26*, 3755-3761.
- (14) Ong, T.-G.; O'Brien, J. S.; Korobkov, I.; Richeson, D. S. *Organometallics*, **2006**, *25*, 4728-4730.
- (15) Ong, T.-G.; Yap, G. P. A.; Richeson, D. S. *J. Am. Chem. Soc.*, **2003**, *125*, 8100-8101.
- (16) Zhang, W.-X.; Nishiura, M.; Hou, Z. *Chem. -Eur. J.*, **2007**, *13*, 4037-4051.
- (17) Thomas, E. W.; Nishizawa, E. E.; Zimmermann, D. C.; Williams, D. J. *J. Med. Chem.*, **1989**, *32*, 228-236.
- (18) Zhu, X.; Du, Z.; Xu, F.; Shen, Q. *J. Org. Chem.*, **2009**, *74*, 6347-6349.
- (19) Noor, A.; Bauer, T.; Todorova, T. K.; Weber, B.; Gagliardi, L.; Kempe, R. *Chem. -Eur. J.*, **2013**, *19*, 9825-9832.
- (20) Srinivasan, N.; Ramadas, K. *Tetrahedron Lett.*, **2001**, *42*, 343-346.
- (21) Jin, G.; Jones, C.; Junk, P. C.; Lippert, K.-A.; Rose, R. P.; Stasch, A. *New J. Chem.*, **2009**, *33*, 64-75.
- (22) Dunne, J. F.; Neal, S. R.; Engelkemier, J.; Ellern, A.; Sadow, A. D. *J. Am. Chem. Soc.*, **2011**, *133*, 16782-16785.
- (23) Xie, W.; Hu, H.; Cui, C. *Angew. Chem. Int. Ed.*, **2012**, *51*, 11141-11144.
- (24) Hill, M. S.; Liptrot, D. J.; MacDougall, D. J.; Mahon, M. F.; Robinson, T. P. *Chem. Sci.*, **2013**, *4*, 4212-4222.